Universitat de Girona

EXPLORING THE REACTIVITY OF IN SITU GENERATED METAL VINYLCARBENES

Àlex Díaz Jiménez

Universitat de Girona

DOCTORAL THESIS

EXPLORING THE REACTIVITY OF *IN SITU* GENERATED METAL VINYLCARBENES

Àlex Díaz Jiménez

2024

Universitat de Girona

DOCTORAL THESIS

EXPLORING THE REACTIVITY OF *IN SITU* GENERATED METAL VINYLCARBENES

Àlex Díaz Jiménez

2024

DOCTORAL PROGRAMME IN CHEMISTRY

Supervised by:

Dr. Anna Pla-Quintana

Prof. Anna Roglans Ribas

Tutor:

Prof. Anna Roglans Ribas

Presented to obtain the degree of PhD at the Universitat de Girona

Universitat de Girona

Dr. Anna Pla-Quintana and Prof. Anna Roglans Ribas, from the Universitat de Girona,

WE DECLARE:

That this thesis entitled **"Exploring the reactivity of *in situ* generated metal vinylcarbenes"** presented by **Àlex Díaz Jiménez** to obtain the doctoral degree has been completed under our supervision and meets the requirements to opt for an International Doctorate.

For all intents and purposes, we hereby sign this document

Dr. Anna Pla-Quintana

Prof. Anna Roglans

Girona, 3rd June 2024

Acknowledgements

Aquesta tesi doctoral hauria estat impossible sense el suport i l'ajuda de moltes persones. Per aquest motiu, m'agradaria agrair a tothom que m'ha acompanyat en aquest camí, tant a nivell personal com professional. En aquest sentit, i sense cap mena de dubte, les dues persones que han contribuït més en el desenvolupament d'aquesta tesi són les meves supervisores: la doctora Anna Pla-Quintana i la professora Anna Roglans. Sóc perfectament conscient que els inicis no van ser fàcils, que hem hagut de picar molta pedra per poder arribar al punt on ens trobem avui, i això hauria estat impossible sense la seva ajuda. A nivell científic, m'han aportat una infinitat de coneixements, idees per provar, nous projectes, han escoltat les meves propostes i m'han ajudat en qualsevol cosa que he necessitat. A nivell personal, van confiar en mi quan els resultats no sortien, fins i tot quan començava a dubtar de mi mateix, elles no van perdre la fe en mi. Tot això en global ha culminat en aquesta tesi i en els resultats que hem obtingut i publicat, dels quals em sento increïblement orgullós. No hi ha prou paraules per expressar el meu agraïment cap a vosaltres, moltes gràcies per tot, Annes. M'agradaria també expandir els meus agraïments a tots els col·laboradors amb els quals he tingut l'oportunitat de treballar: al doctor Albert Poater, al professor Miquel Solà i al Roger Monreal per les col·laboracions computacionals que han complementat tots els resultats experimentals. També agrair al doctor Albert Poater i al professor Miquel Solà per l'ajuda i la supervisió dels càlculs computacionals que he fet durant tota la tesi. Al professor Pedro Pérez i a la doctora Ana Caballero, per la col·laboració al llarg de tota la tesi i l'oportunitat de treballar amb catalitzadors de plata. A més a més, agrair l'oportunitat de fer una estada als seus laboratoris a Huelva. A la doctora Anna Company juntament amb l'Andrea Álvarez per la caracterització dels vinilcarbens de plata. Al professor Miquel Costas per obrir-me les portes al món dels carbens de ferro i per l'oportunitat de treballar al seu grup durant els últims mesos de la tesi. Agrair també al professor Jeremy May per acollir-me al seu grup a la Universitat de Houston, on vaig poder realitzar una estada de 3 mesos. Finalment, agrair també als doctors Sergio Braulio, la doctora Lluïsa Matas, Anna Costa, la doctora Laura Rodríguez, el doctor Àngel Oliveras i en Xavier Fontrodona dels Serveis Tècnics de recerca de la unitat de Girona pels anàlisis de RMN, HPLC, MS i XRD.

M’agradaria agrair també a tots els companys de laboratori amb els quals he coincidit al llarg del temps al METSO i amb els quals he compartit la majoria del temps, i amb els que, més enllà de la ciència, hem pogut forjar una amistat: el doctor Albert Artigas, el doctor Jordi Vila, la Cristina Castanyer, en Ricard López, el doctor Rubén Álvarez, en Nil Insa, en Roger Monreal, el doctor Stuart Kennington i l’Elías Romero. Afegir també a tots els membres del QBIS-CAT amb els quals he coincidit els últims mesos i que m'han ajudat en tot el que he necessitat. Dins de l’IQCC, especial menció al doctor Martí Gimferrer i al Sergi Danés, amb els quals hem pogut establir una gran amistat i amb els quals espero que puguem seguir comentant (i criticant) cada article i cada estrelleta de Twitter que ens trobem.

Més enllà de la ciència, m’agradaria agrair també a tots els que han estat allà per mi i m’han acompanyat durant aquest camí, tant escoltant les meves queixes com alegrant-se pels meus èxits. En aquest sentit, destacar en Laura, en Borja, en Paulí i la Núria. Per molts més retrobaments, cafès a la Tasca i caps de setmana de caminades pels cims de Catalunya. Moltes gràcies per tot, guapos 2.0.

Agradeceros también a vosotros: Ruben, Joel Artacho, Sergi, Joel Santoro y Xela por estar todos estos años a mi lado. Por estar siempre juntos, por todos los viajes, por todos los Lux que se han convertido en Papillon, por nuestras discusiones eternas y recurrentes y principalmente por apoyarnos en todo. Muchas gracias, amigos.

Por último, agradecer a los más importantes, a mi familia: Lidia, Papa y Mama. Gracias a vosotros estoy donde estoy, sin vuestro apoyo no hubiese llegado nunca hasta aquí. Esta tesis es para vosotros. Muchas gracias por todo.

Additionally, financial support is greatly acknowledged from: Ministerio de Ciencia, Innovación y Universidades del Gobierno de España for Predoctoral FPU grant (ref. FPU18/02912) and for mobility fellowships (EST19/00712 and EST23/00525); and for CTQ2017-85341-P and PID2020-113711GB-I00 projects and to the Agència de Gestió d'Ajuts Universitaris i de Recerca de la Generalitat de Catalunya for Project 2017SGR39 and 2021SGR623 projects.

Full list of publications

This doctoral thesis resulted in the following publications:

À. Díaz-Jiménez, R. Monreal-Corona, A. Poater, M. Álvarez, E. Borrego, P.J. Pérez, A. Caballero, A. Roglans and A. Pla-Quintana. Intramolecular Interception of the Remote Position of Vinylcarbene Silver Complex Intermediates by C(sp^3)−H Bond Insertion*. Angew. Chem. Int. Ed.* **2023***, 62,* e202215163.

(IF: 16.6; JCR Ranking: 13/178 (2022); 1st quartile Chemistry, Multidisciplinary)

À. Díaz-Jiménez, R. Monreal-Corona, M.Solà, A. Poater, A. Roglans and A. Pla-Quintana. Synthesis of 1*H*-Isoindole-Containing Scaffolds Enabled by a Nitrile Trifunctionalization*. ACS Catal.* **2024,** *14***,** 10, 7381–7388.

(IF: 12.9, JCR Ranking: 22/161 (2022); 1st quartile Chemistry, Physical)

Other publications not included in this thesis:

Ò. Torres, M. Fernàndez, À. Díaz-Jiménez, A. Pla-Quintana, A. Roglans and M. Solà. Examining the Factors That Govern the Regioselectivity in Rhodium-Catalyzed Alkyne Cyclotrimerization. *Organometallics.* **2019**, *38*, 14, 2853–2862

(IF: 3.804; JCR Ranking: 6/45 (2019); 1st quartile Chemistry, Inorganic & Nuclear)

R. Monreal-Corona, [+] À. Díaz-Jiménez, [+] A. Roglans, A. Poater and A. Pla-Quintana. Indolizine Synthesis through Annulation of Pyridinium 1,4-Thiolates and Copper Carbenes: A Predictive Catalysis Approach. *Adv. Synth. Catal.* **2023**, *365*, 760-766.

(IF: 5.4; JCR Ranking: 4/52 (2022); 1st quartile Chemistry, Organic)

[+] These authors contributed equally to this work.

À. Díaz-Jiménez, S.C.D Kennington, A. Roglans, and A. Pla-Quintana. Copper(I) Iodide Catalyzed [3 + 3] Annulation of Iodonium Ylides with Pyridinium 1,4-Zwitterionic Thiolates for the Synthesis of 1,4-Oxathiin Scaffolds. *Org. Lett.* **2023**, *25*, 26, 4830-4834.

(IF: 5.2; JCR Ranking: 6/52 (2022); 1st quartile Chemistry, Organic)

À. Díaz-Jiménez, A. Roglans, Miquel Solà and A. Pla-Quintana. Mechanistic insights into the rhodium catalysed dehydrogenative cycloaddition of cyano-yne-allene substrates. *Org. Chem. Front.* **2024.** DOI: 10.1039/D4QO00378K.

(IF: 5.4; JCR Ranking: 4/52 (2022); 1st quartile Chemistry, Organic)

Glossary of abbreviations

General abbreviations

°C	Degrees Celsius
Å	Angstrom
Ac	Acetyl
AcOEt	Ethyl acetate
AcN	Acetonitrile
ACS	American Chemical Society
Ar	Aryl
B3LYP	Becke, three parameter, Lee-Yang-Parr
BINAP	2,2′-Bis(diphenylphosphino)-1,1′-binaphthalene
Bn	Benzyl
Bu	Butyl
Bz	Benzoyl
COD	1,5-Cyclooctadiene
Cp*	1,2,3,4,5-pentamethylcyclopentadienyl
D3	D3 Grimme's dispersion model
DBU	1,8-Diazabiciclo[5.4.0]undec-7-eno
DCE	1,2-Dichloroethane
DCC	*N*,*N*′-Dicyclohexylcarbodiimide
DCM	Dichloromethane
DFT	Density Functional Theory
DMAP	*p*-(Dimethylamino)pyridine
DMSO	Dimethyl sulfoxide
E	Electronic energy
EDG	Electron-donating group
e.e	Enantiomeric excess
eq.	Equivalent/s
ESI	Electrospray ionization
Et	Ethyl
et al.	from latin 'et alia', which means 'and others'
EWG	Electron-withdrawing group
G	Gibbs energy
g	Grams
h	Hours
K	Degrees Kelvin
kcal	Kilocalories
L	Ligand

M	Molar (unless otherwise noted)
m-	Meta-
Me	Methyl
mg	Miligram/s
mL	Mililiter/s
mM	Milimolar
MS	Mass Spectrometry
NHC	*N*-Heterocyclic carbene
NMR	Nuclear Magnetic Resonance
o-	Ortho-
p-	Para-
p-ABSA	*p*-Acetamidobenzenesulfonyl azide
PES	Potential energy surface
Ph	Phenyl
Pic	Dichloro(2-pyridinecarboxylato)
RSC	Royal Society of Chemistry
r.t	Room temperature
$[Rh_2(esp)_2]$	Bis[rhodium(α,α,α′,α′-tetramethyl-1,3-benzenedipropionic acid)]
$[Rh_2(OAc)_4]$	Rhodium(II) acetate
$[Rh_2(OOCH_3)_4]$	Rhodium(II) formate
$[Rh_2(OOct)_4]$	Rhodium(II) octanoate
$[Rh_2(OAc)_4]$	Rhodium(II) pivalate
$[Rh_2(PFB)_4]$	Rhodium(II) perfluorobutyrate
$[Rh_2(S\text{-BTPCP})_4]$	Dirhodium tetrakis[(*S*)-1-(4-bromophenyl)-2,2- diphenylcyclopropane carboxylate]
$[Rh_2(S\text{-DOSP})_4]$	Tetrakis[(*S*)-(-)-N-(p-dodecylphenylsulfonyl)prolinato]dirhodium(II)
$[Rh_2(S\text{-NTTL})_4]$	Dirhodium(II,II) tetrakis[N-(1,2-naphthaloyl)-(*S*)-tert-Leucinate]
$[Rh_2(S\text{-PTAD})_4]$	Tetrakis[(*S*)-(+)-(1-adamantyl)-(N-phthalimido)acetato]dirhodium(II)
$[Rh_2(S\text{-PTTL})_4]$	Tetrakis[N-phthaloyl-(S)-tert-leucinate]dirhodium(II)
$[Rh_2(S\text{-TBSP})_4]$	Tetrakis[1-[(4-tert-butylphenyl)sulfonyl]-(2*S*)-pyrrolidinecarboxylate]dirhodium(II)
$[Rh_2(S\text{-TFPTTL})_4]$	Tetrakis[N-tetrafluorophthaloyl-(*S*)-tert-leucinato]dirhodium
$[Rh_2(TFA)_2]$	Rhodium(II) trifluoroacetate
SMD	Continuum model based on density
SPE	Single-point energy
T	Temperature
*t*Bu	Tert-butyl
TDI	TOF determining intermediate
TDTS	TOF determining transition state
THF	Tetrahydrofuran
TLC	Thin layer chromatography
TM	Transition metal
TOF	Turnover frequency

Tol	Tolyl
TS	Transition state

Abbreviations used in compound characterization

^{13}C NMR	Carbon nuclear magnetic resonance
^{1}H NMR	Proton nuclear magnetic resonance
1D	Monodimensional
2D	Bidimensional
$CDCl_3$	Deuterated chloroform
cm^{-1}	Reciprocal centimeters
COSY	Proton-proton correlation spectroscopy
d	Doublet
ESI-HRMS	Electrospray ionization high resolution mass spectrometry
HMBC	Heteronuclear multiple-bond correlation spectroscopy
HSQC	Heteronuclear single-quantum correlation spectroscopy
Hz	Hertz
IR (ATR)	Infrared spectroscopy (attenuated total reflectance)
m	Multiplet
M.P.	Melting point
m/z	Mass to charge ratio
MHz	Megahertz
MW	Molecular weight
ppm	Parts per million
q	Quadruplet
quint	Quintuplet
Rf	Retention factor
s	Singlet
sept	Heptuplet or septet
t	Triplet
δ	Chemical shift

Table of Contents

List of Figures 1

List of Schemes 3

List of Tables 8

Summary 9

Resum 10

Resumen 11

Chapter 1. Introduction 13

1.1. Carbenes and metal carbenes in organic synthesis 15

1.1.1. Carbenes: historical context 15

1.1.2. Metal carbenes: historical context and classifications 17

1.2. Metal vinylcarbenes 21

1.2.1. Catalytic generation of metal vinylcarbenes: historical perspective 21

1.2.2. Reactivity of metal vinylcarbenes 22

Chapter 2. General objectives 63

Chapter 3. Synthesis of 1*H*-Isoindole-Containing Scaffolds Enabled by a Nitrile Trifunctionalization 67

Chapter 4. Intramolecular Interception of the Remote Position of Vinylcarbene Silver Complex Intermediates by Csp^3−H Bond Insertion 79

Chapter 5. Concerted or stepwise carbene transfer reactions to Csp^2-H bonds? A mechanistic insight 89

Chapter 6. Mechanistic insights into metal-dependent vinylcarbene generation via carbene/alkyne metathesis of terminal diazoalkynes 101

Chapter 7. General conclusions 111

Chapter 8. Methods 115

Supplementary material for Chapter 3 117

Supplementary material for Chapter 4 139

Supplementary material for Chapter 5 158

Supplementary material for Chapter 6 169

References 175

List of Figures

Figure 1.1. Initially proposed and then corrected structure for the Chugaev's salt 17

Figure 1.2. First metal-carbenes reported by Fischer and Schrock 17

Figure 1.3. Bonding scheme in Fischer and Schrock carbenes 18

Figure 1.4. Classification of carbene species based on their substitution pattern.....18

Figure 3.1. Scope of the reaction.....73

Figure 3.2. Gibbs energy for the first carbene formation and carbene-alkyne metathesis, nitrile ylide formation and 1,7-electrocyclization of **4a**. Gibbs energies (298 K) relative to 4a and [$Rh_2(OOCH)_4$] are shown in kcal/mol ([Rh] = [$Rh_2(OOCH)_4$]). 74

Figure 3.3. Gibbs energy for the second carbene formation and carbene-alkyne metathesis. Gibbs energies (298 K) relative to 4a and [$Rh_2(OOCH)_4$] are shown in kcal/mol ([Rh] = [$Rh_2(OOCH)_4$]). 75

Figure 3.4. Gibbs energy for the electrocyclization, isoindole formation, 1,5-H shift and proton catalyzed ring contraction for the formation of **5a**. Gibbs energies (298 K) relative to 4a and [$Rh_2(esp)_2$] are shown in kcal/mol ([Rh] = [$Rh_2(esp)_2$]). 76

Figure 3.5. Gibbs energy for the mechanism involving two units of vinylcarbene **D.** Gibbs energies (298 K) relative to **4a** and [$Rh_2(OOCH)_4$] are shown in kcal/mol ([Rh] = [$Rh_2(OOCH)_4$]). 77

Figure 4.1. General structure of trispyrazolyl borate ligands and Tp^x ligands used in this study. 80

Figure 4.2. Scope of the reaction.....84

Figure 4.3. Gibbs energy profile (in kcal/mol) of the silver-catalyzed CAM reaction ([Ag] = $Tp^{(CF3)2,Br}Ag$). 87

Figure 5.1. Selectivity observed for *o*-substituted substrates. 92

Figure 5.2. Gibbs energy profile (in kcal/mol) of the silver-catalyzed CAM reaction of **13a** ([Ag] = $Tp^{(CF3)2,Br}Ag$). 94

Figure 5.3. ^{1}H-NMR spectrum recorded every 10 minutes for the detection of the silver vinylcarbene. 98

Figure 5.4. 1H-NMR spectra for the starting material **13a** and final product **14a**. 98

Figure 5.5. HMBC correlation experiment for the detection of the silver vinylcarbene. 99

Figure 6.1. Gibbs energy comparison for diazo-yne reaction and carbene formation mechanism. (Ag=$Tp^{(CF3)2,Br}Ag$(THF)).....106

Figure 6.2. Gibbs energy profile for the silver catalyzed CAM leading to the 6-endo vinylcarbene and 2-pyrone formation. Energies are relative to A. (Ag=$Tp^{(CF3)2,Br}Ag$(THF)).....107

Figure 6.3. Gibbs energy profile for the silver catalyzed CAM leading to the 5-exo vinylcarbene. Energies are relative to **C_Me**. (Ag=$Tp^{(CF3)2,BrAg}$(THF)).....108

Figure 6.4. Gibbs energy profile for the rhodium catalyzed CAM leading to the 5-exo vinylcarbene. Energies are relative to **A**. ([Rh]=[$Rh_2(HCOOH)_4$]).....109

Figure 8.1. Previously reported diazo compounds 13a, 13d, 13f-13l.....160

Figure 8.2. Previously reported diazo compounds 15a-15e and 15g.....169

List of Schemes

Scheme 1.1. General reactivity of metal carbenes. 15

Scheme 1.2. Formation of dichlorocarbene by base-mediated hydrolysis of chloroform (a) and subsequent reaction with pyrrole (b). 16

Scheme 1.3. Reactivity of ethyl diazoacetate with benzene and styrene reported by Buchner. 16

Scheme 1.4. Synthesis of the first isolated carbene by Arduengo. 17

Scheme 1.5. Generation of metal carbenes from diazo compounds. 19

Scheme 1.6. Generation of metal carbenes from N-sulfonylhydrazones. 19

Scheme 1.7. Generation of metal carbenes from a) sulfoxonium and b) iodonium ylides. 20

Scheme 1.8. Generation of metal carbenes from triazole derivatives. 20

Scheme 1.9. Generation of metal carbenes via retro-Buchner reaction. 20

Scheme 1.10. Generation of metal carbenes via 1,2-shift of propargyl esters. 20

Scheme 1.11. Generation of metal carbenes via ring opening of cyclopropenes. 21

Scheme 1.12. Early examples of reactions involving catalytically generated vinylcarbenes. 22

Scheme 1.13. Rhodium (II) catalyzed [3+4] cycloaddition of vinyl diazo compound and furan. 22

Scheme 1.14. Rhodium (II) catalyzed [3+4] cycloaddition of vinyl diazo compounds and cyclopentadiene. ..23

Scheme 1.15. Rhodium (II) catalyzed intermolecular [3+4] cycloaddition of vinyl diazo compounds and acyclic dienes. 23

Scheme 1.16. Rhodium (II) catalyzed [3+4] cycloaddition of vinyl diazo compounds and pyrroles. 23

Scheme 1.17. Rhodium (II) catalyzed intramolecular reaction of pyrroles and substituted vinyl diazo derivatives. 24

Scheme 1.18. Rhodium catalyzed enantioselective [3+4] cycloadditions of vinydiazo compounds. 25

Scheme 1.19. Rhodium catalyzed [3+4] cycloadditions of styryl diazo derivatives and conjugated aldehydes or imines. 26

Scheme 1.20. Intramolecular rhodium catalyzed [3+4] for the preparation of bicyclononatrienes. 27

Scheme 1.21. Rhodium catalyzed [3+4] cycloaddition between enoldiazo compounds and dienes with complete reversal of reactivity. 27

Scheme 1.22. Gold catalyzed [3+4] cycloaddition between propargyl esters and imino dienes. 28

Scheme 1.23. Platinum catalyzed [3+4] cycloaddition using o-anilines and dienes. 28

Scheme 1.24. Gold catalyzed intramolecular [*3+4*] cycloaddition of cyclopropenes and furans. 29

Scheme 1.25. Rhodium (II) catalyzed [3+4] cycloaddition between enynals and dienes. 29

Scheme 1.26. Silver catalyzed [3+4] cycloaddition between *N*-triftosylhydrazones and dienes/furans. 32

Scheme 1.27. Rhodium catalyzed [2+1] cycloaddition between vinyldiazo compounds and alkenes. 30

Scheme 1.28. Intermolecular [2+1] cycloaddition between alkenes and propargyl esters. 31

Scheme 1.29. Gold catalyzed intramolecular cyclopropanation of olefins using cyclopropenes as carbene precursors. 31

Scheme 1.30. Silver catalyzed cyclopropanation of olefins using N-triftosylhydrazones. 32

Scheme 1.31. Gold catalyzed cyclopropanation of olefins using cycloheptatrienes as vinylcarbene precursors. 32

Scheme 1.32. Rhodium catalyzed [2+1] cycloaddition between N-sulfonylhydrazone sodium salts and aldehydes. 32

Scheme 1.33. Rhodium catalyzed enantioselective cyclopropenation of alkynes using styryl diazoacetates. 33

Scheme 1.34. Silver catalyzed cyclopropanation of indoles using vinyldiazo compounds. 33

Scheme 1.35. Rhodium catalyzed cyclopropanation of benzofurans and indoles. 33

Scheme 1.36. Rhodium catalyzed [3+2] cycloaddition between vinyldiazo compounds and vinyl ethers. 34

Scheme 1.37. [3+2] cycloaddition reactions involving alkenes and non-diazo carbene precursors. 35

Scheme 1.38. Gold catalyzed [3+2] cycloaddition between vinylcarbenes and ynamides. 35

Scheme 1.39. Regiodivergent gold catalyzed [3+2] cycloaddition of vinyldiazo compounds and allenes. 36

Scheme 1.40. Gold catalyzed [3+2] cycloaddition between allenes and cycloheptatrienes. 36

Scheme 1.41. Rhodium catalyzed [3+2] cycloaddition between indoles and vinyldiazo compounds. 37

Scheme 1.42. Rhodium and gold catalyzed [3+3] cycloaddition between vinylcarbenes and azomethyl ylides. 38

Scheme 1.43. Platinum and rhodium catalyzed [3+3] cycloaddition between vinylcarbenes and nitrones. 38

Scheme 1.44. Rhodium catalyzed [3+3] cycloaddition using enoldiazo compounds. 39

Scheme 1.45. Copper catalyzed [3+3] cycloaddition between vinyl sulfoxonium ylides and cyclopropenones. 39

Scheme 1.46. Copper catalyzed [3+1] cylcloaddition between enoldiazo compounds and sulfur ylides. 40

Scheme 1.47. Rhodium catalyzed [5+3] cycloaddition between enoldiazo compounds and 1,5-dipole equivalents. 41

Scheme 1.48. Rhodium catalyzed [5+2] cycloaddition between diazo succinimides and nitriles and aldehydes. 42

Scheme 1.49. Rhodium catalyzed Csp^3-H bond insertion of *in situ* generated vinylcarbenes 43

Scheme 1.50. Rhodium catalyzed C-H activation of vinyldiazoacetates and cyclohexadiene. 43

Scheme 1.51. Silver catalyzed vinylcarbene insertion into Csp^3-H bonds. 44

Scheme 1.52. Rhodium catalyzed intramolecular Csp^3-H insertion of cyclopropenes. 44

Scheme 1.53. Rhodium catalyzed intramolecular Csp^3-H insertion of enoldiazoacetamides. 44

Scheme 1.54. Ruthenium catalyzed gem-hydrogenation of enynes followed by Csp^3-H insertion. 45

Scheme 1.55. Gold catalyzed intramolecular vinylogous Csp^3-H insertion. 45

Scheme 1.56. Silver catalyzed Csp^2-H insertion using cyclopropenes as carbene precursors. 46

Scheme 1.57. Intramolecular platinum catalyzed Csp^2-H insertion. 46

Scheme 1.58. Rhodium catalyzed intermolecular vinyldiazo Csp^2-H insertion. 47

Scheme 1.59. Intermolecular rhodium catalyzed vinylogous Csp^2-H functionalization of indoles or pyrroles. 47

Scheme 1.60. Intermolecular gold catalyzed vinylogous Csp^2-H functionalization of benzene derivatives. ... 48

Scheme 1.61. Intermolecular rhodium catalyzed vinylogous Csp^2-H functionalization of aniline derivatives. 48

Scheme 1.62. Rhodium catalyzed O-H and Si-H insertion of vinyldiazo compounds. 49

Scheme 1.63. Molibdenum catalyzed vinylogous OH insertion using vinyldiazo compounds. 49

Scheme 1.64. Rhodium and silver divergent selectivity in the intermolecular X-H insertion of vinyldiazo compounds. 50

Scheme 1.65. Gold and silver divergent selectivity in the intermolecular O-H insertion of vinyldiazo compounds and 2-pyridones. 50

Scheme 1.66. Intermolecular X-H insertion reaction using cyclopropenes as carbene precursors. 51

Scheme 1.67. Intermolecular Si-H insertion on vinylcarbenes *in situ* generated from cycloheptatrienes and triftosylhydrazones. 51

Scheme 1.68. Copper catalyzed intermolecular B-H insertion. 52

Scheme 1.69. General scheme for the CAM process. 53

Scheme 1.70. First report of the Dötz reaction. 53

Scheme 1.71. First examples of catalytic CAM reactions terminated with [2+1] cycloaddition. 54

Scheme 1.72. Rhodium catalyzed CAM reactions terminated with [3+4] or C-H insertions. 55

Scheme 1.73. Rhodium catalyzed CAM terminated with Csp^3-H insertion. 56

Scheme 1.74. Rhodium catalyzed catalyst-controlled CAM terminated with Csp^3-H insertion. 56

Scheme 1.75. Enantioselective rhodium(I) catalyzed double CAM reaction. 57

Scheme 1.76. Enantioselective rhodium (I) catalyzed CAM reactions reported by our group. 57

Scheme 1.77. Copper catalyzed divergent outcomes of CAM reactions with aryls. 58

Scheme 1.78. Rhodium catalyzed enantioselective double CAM terminated with Csp^2-H insertion. 58

Scheme 1.79. Metal catalyzed CAM reactions reported by Xu. 59

Scheme 1.80. Intramolecular rhodium catalyzed CAM reactions. 60

Scheme 1.81. Intermolecular ruthenium catalyzed CAM reported by Dixneuf. 60

Scheme 1.82. Ruthenium catalyzed intermolecular CAM reported by Saá. 61

Scheme 2.1. Plausible outcomes for the rhodium catalyzed intermolecular trapping of vinylcarbenes with nitriles. 64

Scheme 2.2. Plausible outcomes for the silver catalyzed intramolecular CAM. 65

Scheme 3.1. Rhodium catalyzed intermolecular trapping of vinylcarbenes with nitriles reported by Krasavin. 68

Scheme 3.2. Rhodium catalyzed intermolecular trapping of *in situ* generated vinylcarbenes with nitriles. 69

Scheme 3.3 Initial results for the synthesis of 1*H*-isoindole-containing scaffolds via rhodium catalyzed cascade reaction. 69

Scheme 3.4. Synthesis of cyano propargyl diazoacetates **4a**-**4l**. 72

Scheme 3.5. Deuterium labelling experiment. 77

Scheme 4.1. CAM reaction terminated with C-H bond functionalization: carbenic vs vinylogous reactivity. 81

Scheme 4.2. Synthesis of dimethyl-aniline propargyl diazoacetates **10a**-**10j.** 83

Scheme 4.3. Deuterium labelling experiment. 85

Scheme 4.4. Plausible mechanistic pathways for the silver-catalyzed CAM. 85

Scheme 5.1. Conventional proposed mechanism for metal carbene Csp^2-H bond insertion. 90

Scheme 5.2. General scheme for the CAM terminated in Csp^2-H bond insertion. 90

Scheme 5.3. Synthesis of phenyl propargyl diazoacetates **13a-13m.** 91

Scheme 5.4. Scope of the transformation. 93

Scheme 5.5. Resonance structures for the Wheland intermediate. 95

Scheme 6.1. Divergent vinylcarbene generation in CAM reactions. 102

Scheme 6.2. Synthesis of propargyl diazoacetates **15a-15i.** 104

Scheme 6.3. Scope of the transformation 105

Scheme 7.1. Summary of all carbene/alkyne metathesis reactions developed in this thesis. 113

Scheme 8.1. Synthesis of propagyl alcohol **S1a**. 117

Scheme 8.2. General procedure for the preparation of propargyl alcohols **S2a** and **S3a**. 117

Scheme 8.3. General procedure for the preparation of propargyl esters **S4a-S4l**. 118

Scheme 8.4. General procedure for the preparation of diazo compounds **4a-4l**. 123

Scheme 8.5. General procedure for the rhodium-catalyzed intermolecular carbene/alkyne metathesis adding external nitriles. 129

Scheme 8.6. General procedure for the rhodium-catalyzed carbene/alkyne metathesis tandem reaction. 131

Scheme 8.7. Experimental procedure for the synthesis of propargyl alcohol **S5a**. 139

Scheme 8.8. General procedure for the synthesis of propargyl alcohols **S6a-6ad**. 139

Scheme 8.9. General procedure for the synthesis of propargyl esters **S7a-S7j**. 141

Scheme 8.10. General procedure for the synthesis of diazo compounds **10a-10j.**.....145

Scheme 8.11. Experimental procedure for the alkyne **S3-d_6.**.....150

Scheme 8.12. General procedure for the silver carbene/alkyne metathesis tandem reaction terminated in vinylogous Csp^3-H insertion.....152

Scheme 8.13. Experimental procedure for the synthesis of propargyl alcohol **S8a**. 158

Scheme 8.14. General procedure for the preparation of propargyl esters **S9a-S9d**. 158

Scheme 8.15. General procedure for the preparation of diazo compounds **13b, 13c, 13e and 13m**. 161

Scheme 8.16. General procedure for the silver catalyzed carbene/alkyne metathesis tandem reaction terminated in Csp^2-H insertion. 163

Scheme 8.17. General procedure for the preparation of diazo compounds **15f-15h**. 169

Scheme 8.18. General procedure for the silver-catalyzed 6-endo carbene/alkyne metathesis tandem reaction. 171

Scheme 8.19. General procedure for the rhodium-catalyzed 5-exo carbene/alkyne metathesis tandem reaction. 174

List of Tables

Table 3.1. Optimization of the reaction conditions for the metal catalyzed nitrile trifunctionalization reaction. 71

Table 4.1. Initial screening of silver-based catalysts for the CAM-cascade reaction. 81

Table 4.2. Optimization of the reaction conditions. 83

Table 5.1. Obtained $\Delta G^{\#}$ values for the TS leading to concerted and stepwise Csp^2-H insertion. 96

Table 5.2. Obtained $\Delta G^{\#}$ values for the TS leading to concerted and stepwise Csp^2-H insertion using $[Tp^{Br3}Ag]_2$. 97

Table 6.1. Optimization of the reaction conditions. 103

Summary

One of the primary objectives in organic synthesis is to devise novel methods for converting simple and readily available compounds into more complex and functionalized structures. In this regard, transition metal-catalyzed transformations have gained significant attention in recent years, with metal carbenes emerging as particularly valuable intermediates due to their unique structure and versatile reactivity. Among these, metal vinylcarbene complexes stand out due to the presence of an alkenyl unit within their structure, which enables a diverse array of novel transformations, including functionalization at the carbenic or at the vinylogous position, as well as cycloaddition reactions in a (3+n) fashion.

Among various catalytic methods for generating vinylcarbenes, the carbene/alkyne metathesis (CAM) method represents an exceptionally powerful strategy for accessing polycyclic compounds in a one-pot manner. Our group has developed several rhodium-catalyzed CAM reactions and has contributed significantly to understanding their mechanisms through DFT calculations and experimental techniques. However, most CAM-related transformations occur intramolecularly and rely on internal alkynes. Furthermore, despite the demonstrated utility of silver complexes as catalysts in vinylcarbene chemistry, their use in CAM transformations has not been documented. Motivated by these considerations and our ongoing interest in carbene-related reactions, we sought to develop processes that address these limitations encountered in CAM transformations.

In Chapter 3, we have successfully intercepted intermolecularly a CAM generated rhodium vinylcarbene with a nitrile, leading to the synthesis of 1*H*-isoindole derivatives. By incorporating a nitrile group into the initial diazo compound, we achieved an extended cascade reaction that produced polycyclic products in a completely diastereoselective manner, formally yielding the trifunctionalization of a nitrile. Moving forward to the use of silver as a catalyst in CAM transformations, in chapter 4, we have accomplished the objective of developing a platform for the efficient generation of silver vinylcarbenes via intramolecular CAM. Upon vinylcarbene formation, selective vinylogous Csp^3-H insertion led to the synthesis of benzoazepine derivatives. Expanding on the outcome of the previous chapter, Chapter 5 detailed the synthesis of indene derivatives using a silver catalyst via CAM terminated in Csp^2-H bond insertion. Additionally, we have unraveled the possibility of a concerted Csp^2-H bond insertion mechanism, distinct from previously described carbene Csp^2-H functionalization pathways. Moreover, we have experimentally detected the *in situ* generated silver vinylcarbene using spectroscopic techniques. Finally, in Chapter 6, we have overcome the limitation of employing internal alkynes in intramolecular CAM reactions by developing an efficient method for generating 6-endocyclic vinylcarbenes using terminal diazo alkynes under silver catalysis. Conversely, the use of rhodium catalysts results in the exclusive formation of the 5-exocyclic vinylcarbene. Detailed DFT calculations have been employed to elucidate the divergent selectivity observed upon switching the catalyst used for the transformation.

Resum

Un dels objectius principals de la química orgànica és el desenvolupament de noves metodologies per transformar compostos simples i fàcilment disponibles en estructures molt més complexes i funcionalitzades. En aquest sentit, el camp de les transformacions basades en metalls de transició ha experimentat un creixement exponencial en els darrers anys. En aquestes transformacions, els carbens metàl·lics destaquen com a intermedis extremadament valuosos, gràcies a la seva estructura única i la seva reactivitat versàtil. Dins de la família dels carbens metàl·lics, els complexos de vinilcarbè ressalten especialment, degut a la presència d'una unitat vinílica en la seva estructura, que permet una àmplia gamma de noves transformacions químiques. Això inclou la monofuncionalització en la posició carbènica o remota, així com el seu ús com a sintons de tres carbonis en reaccions de cicloadició (3+n).

Dels diversos mètodes existents per a generar vinilcarbens, el procés de metàtesi carbè/alquí (CAM) emergeix com una estratègia excepcionalment potent per accedir a compostos policíclics en un sol pas de reacció. En aquest sentit, el nostre grup ha desenvolupat una sèrie de reaccions CAM utilitzant catalitzadors de rodi i ha contribuït significativament a comprendre el mecanisme d'aquestes transformacions mitjançant càlculs computacionals DFT i tècniques experimentals. No obstant, la majoria de les reaccions CAM es produeixen de manera intramolecular i requereixen l'ús d'alquins interns. D'altra banda, tot i que l'ús de catalitzadors de plata en l'àmbit dels vinilcarbens és conegut, no hi ha exemples de l'ús de complexos de plata com a catalitzadors de reaccions del tipus CAM. Considerant aquests fets, juntament amb el nostre coneixement en la química dels carbens metàl·lics, vam concebre la possibilitat de desenvolupar processos que superessin aquestes limitacions habituals en les transformacions basades en CAM.

En el Capítol 3, hem capturat de manera intermolecular un vinilcarbè de rodi generat per una transformació CAM, utilitzant compostos de tipus nitril, i produint derivats de 1*H*-isoindole en el procés. A través de la incorporació d'aquesta unitat de nitril en el compost diazo inicial, hem desenvolupat una reacció en cascada que genera productes policíclics de manera totalment diastereoselectiva, en un procés que formalment involucra la trifuncionalització d'un nitril. Respecte a l'ús de catalitzadors de plata en reaccions CAM, al Capítol 4, hem establert una plataforma eficient per a la generació de vinilcarbens de plata mitjançant un procés de CAM intramolecular. Després de la CAM, el vinilcarbè generat s'insereix de manera selectiva en un enllaç Csp^3-H en la posició remota del vinilcarbè, produint derivats de benzoazepina. Expandint els coneixements obtinguts anteriorment, en el Capítol 5 hem detallat la síntesi de derivats d'indè mitjançant un procés CAM que finalitza amb una inserció Csp^2-H. Addicionalment, mitjançant càlculs DFT, hem proposat la possibilitat d'una inserció Csp^2-H que es produeix de manera concertada, en contraposició als processos reportats prèviament per inserció de carbens en enllaços Csp^2-H. A més, hem identificat experimentalment el vinilcarbè de plata generat *in situ* mitjançant tècniques espectroscòpiques. Finalment, en el Capítol 6, hem superat la limitació de l'ús d'alquins interns en les reaccions CAM. Utilitzant diazocompostos amb alquins terminals, hem aconseguit la generació selectiva de vinilcarbens 6-endocíclics. D'altra banda, l'ús de catalitzadors de rodi produeix exclusivament vinilcarbens 5-exocíclics. Els estudis DFT realitzats ens han permès racionalitzar les diferències de selectivitat observades experimentalment en canviar el catalitzador de la reacció.

Resumen

Uno de los principales objetivos de la química orgánica es desarrollar nuevas metodologías para transformar compuestos simples y fácilmente disponibles en estructuras mucho más complejas y funcionalizadas. En este contexto, el campo de las transformaciones basadas en metales de transición ha experimentado un crecimiento exponencial en los últimos años. En estas transformaciones, los carbenos metálicos han surgido como intermedios de gran valor gracias a su estructura única y su reactividad versátil. Dentro de la familia de los carbenos metálicos, los complejos de vinilcarbeno destacan especialmente debido a la presencia de una unidad vinílica en su estructura, que abre la puerta a una amplia gama de nuevas transformaciones químicas. Estas reacciones incluyen la monofuncionalización en la posición carbénica o remota, así como el uso de los vinilcarbenos como sintones de tres carbonos en cicloadiciones del tipo (3+n). Entre los diversos métodos existentes para generar vinilcarbenos, el proceso de metátesis carbeno/alquino (CAM) se destaca como una estrategia excepcional para acceder a compuestos policíclicos en un solo paso de reacción. En este contexto, nuestro grupo ha desarrollado una serie de reacciones CAM utilizando catalizadores de rodio, contribuyendo significativamente a la comprensión del mecanismo de estas transformaciones mediante cálculos computacionales DFT y técnicas experimentales. Sin embargo, la mayoría de las reacciones CAM se producen de manera intramolecular y requieren el uso de alquinos internos. A pesar de que el uso de catalizadores de plata en el ámbito de los vinilcarbenos es conocido, no existen ejemplos del uso de complejos de plata como catalizadores en reacciones de tipo CAM. Considerando estos hechos junto con nuestro conocimiento en la química de los carbenos metálicos, concebimos la posibilidad de desarrollar procesos que superaran estas limitaciones habituales en las transformaciones basadas en CAM.

En el Capítulo 3, hemos capturado de manera intermolecular un vinilcarbeno de rodio generado mediante una transformación CAM, utilizando compuestos de tipo nitrilo y produciendo derivados de 1*H*-isoindol en el proceso. Incorporando la unidad nitrilo en el compuesto diazo inicial, hemos desarrollado una reacción en cascada que genera productos policíclicos de manera totalmente diastereoselectiva, en un proceso que formalmente implica la trifuncionalización de un nitrilo. Respecto al uso de catalizadores de plata en reacciones CAM, en el Capítulo 4 hemos desarrollado una plataforma eficiente para la generación de vinilcarbenos de plata mediante una CAM intramolecular. Después de la CAM, el vinilcarbeno inserta selectivamente en un enlace Csp^3-H en la posición remota del vinilcarbeno, produciendo los productos finales de benzoazepina. Ampliando los conocimientos obtenidos, en el Capítulo 5 hemos detallado la síntesis de derivados de indeno mediante un proceso CAM que concluye con una inserción Csp^2-H. Además, mediante cálculos DFT, hemos sugerido la posibilidad de una inserción Csp^2-H concertada, en contraposición a los procesos reportados previamente para la inserción de carbenos en enlaces Csp^2-H. También hemos identificado experimentalmente el carbeno de plata generado *in situ* mediante técnicas espectroscópicas. Finalmente, en el Capítulo 6, hemos superado la limitación del uso de alquinos internos en las reacciones CAM. Utilizando compuestos diazo con alquinos terminales, hemos logrado la generación selectiva de vinilcarbenos 6-endocíclicos. Por otro lado, el uso de catalizadores de rodio produce exclusivamente vinilcarbenos 5-exocíclicos. Los estudios DFT realizados nos han permitido explicar las diferencias de selectividad observadas experimentalmente al cambiar el catalizador de la reacción

Chapter 1. Introduction

1.1. Carbenes and metal carbenes in organic synthesis

One of the primary objectives in organic synthesis is to develop novel methods for transforming simple and readily available compounds into much more complex and functionalized structures, particularly when these transformations can proceed with high levels of chemo-, stereo-, and enantioselectivity. Moreover, these new developments should ideally be more efficient in terms of steps and atom economy compared to traditional synthetic approaches. In this regard, transition metal-catalyzed transformations have gathered significant attention and have been extensively explored in recent years,[1] with metal carbenes being one of the most valued intermediates due to their unique structure and wide range of reactivity (**Scheme 1.1**). Metal carbenes exhibit versatile reactivity, engaging in cycloaddition reactions with unsaturated compounds to furnish three-membered ring products. Beyond cycloaddition, they show the capability to insert into both carbon-hydrogen and heteroatom-hydrogen bonds. Furthermore, reaction with ethers, thioethers, or secondary amines leads to the formation of ylides, which in turn can participate in subsequent reactions.

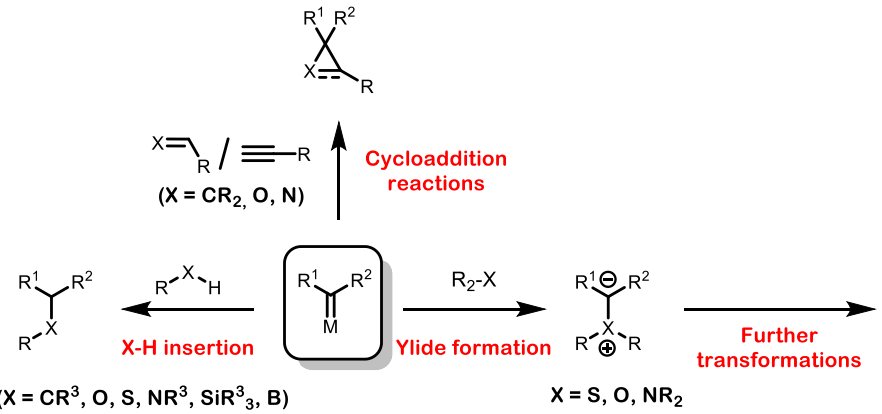

Scheme 1.1. General reactivity of metal carbenes.

1.1.1. Carbenes: historical context

Carbenes are defined as compounds containing a neutral divalent carbon atom with six electrons in its valence shell.[2] They were initially regarded only as intermediates in organic transformations, with the first postulation of their existence made by Geuther and Hermann back in 1855. They suggested that hydrolysis of chloroform in basic media occurred through a divalent carbon intermediate, which was named dichlorocarbene.[3] The same reaction intermediate was proposed by Nef for the Reimer-Tiemann reaction of pyrrole to chloropyridine in 1897 (**Scheme 1.2**).[4]

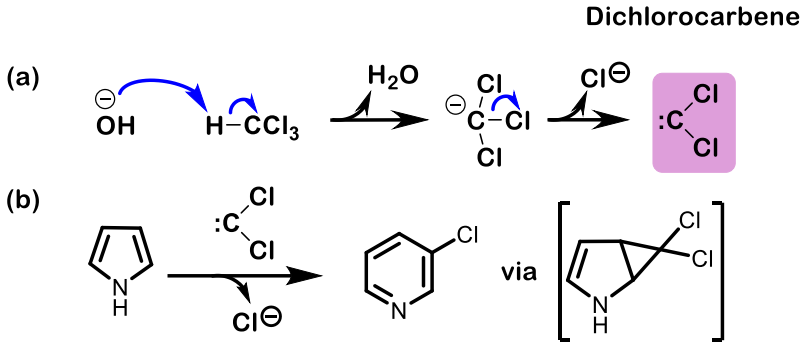

Scheme 1.2. Formation of dichlorocarbene by base-mediated hydrolysis of chloroform (a) and subsequent reaction with pyrrole (b).

Building upon these discoveries, the synthetic organic community capitalized on the versatility of carbenes and their use as intermediates in organic transformations. Early examples of these contributions are the ones reported by Buchner et al., where they demonstrated the potential of ethyl diazoacetate as a carbene source in the synthesis of cycloheptatriene derivatives from benzene (in the so-called Buchner reaction)[5] or for the cyclopropanation of styrene[6] (**Scheme 1.3**). It is important to note that these reactions required high temperatures, resulting in low yields and lacking selectivity. These inherent disadvantages could be overcome by employing metals to modulate the reactions (*vide infra*).

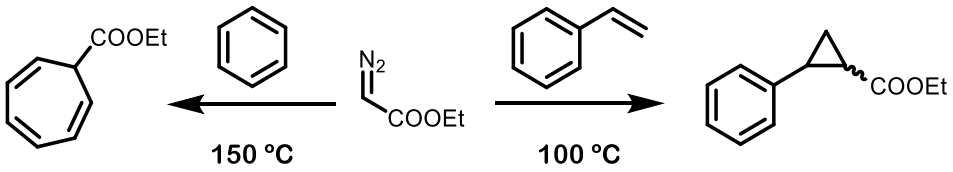

Scheme 1.3. Reactivity of ethyl diazoacetate with benzene and styrene reported by Buchner.

Doering and *et al.* also contributed to the field by describing the preparation of tropolones via the Buchner reaction of diazomethane to arenes under photochemical conditions,[7] and reporting the cyclopropanation of cyclohexene using chloroform and bromoform, indirectly confirming the formation of dihalocarbenes in the reaction.[8]

Carbenes were only regarded as elusive reaction intermediates until 1991, when Arduengo et al. reported the first isolable and crystallizable free carbene.[9] By deprotonating an imidazolium salt using a strong base, the corresponding carbene could be isolated (**Scheme 1.4**). Further studies on the features of this class of carbenes showed that the nitrogen-based ring, along with proper substitution in both the carbon backbone and the N atom, could lead to the formation of much more stable carbenic structures. These discoveries led to the definition of a new carbene family, the N-Heterocyclic Carbenes.

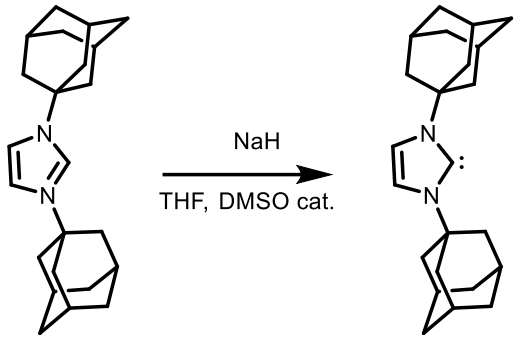

Scheme 1.4. Synthesis of the first isolated carbene by Arduengo.

1.1.2. Metal carbenes: historical context and classifications

The presence of two unshared electrons in the carbenic carbon could potentially lead to bond formation with transition metals. The first metal carbene complex was prepared in 1925 by Chugaev, upon reaction of a methyl isocyanate platinum complex with hydrazine.[10] However, the obtained product was incorrectly formulated (**Figure 1.1a**). It was not until 1970 that Shaw realized the correct existence of a metal carbene structure in Chugaev's salt (**Figure 1.1b**).[11]

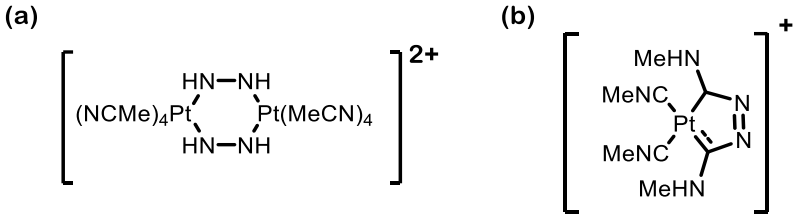

Figure 1.1. Initially proposed and then corrected structure for the Chugaev's salt.

In 1965, prior to the correction of the Chugaev's salt structure, Fischer reported the existence of a transition metal carbene for the first time. The structure consisted of a penta(carbon monoxide) tungsten complex containing a methoxymethylcarbene unit coordinated to the metal (**Figure 1.2a**).[12] Five years later, Schrock published the first example of a high oxidation state metal carbene, involving tantalum as the metal center (**Figure 1.2b**).

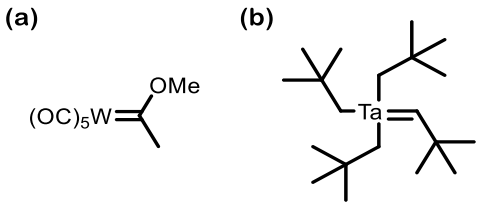

Figure 1.2. First metal-carbenes reported by Fischer and Schrock.

These two works paved the way for the discovery of new metal carbenes, which, depending on the metal and substituents, could exhibit different structures, bonding, or reactivity. This led to the establishment of two classes of metal carbenes: the Fischer and the Schrock-type metal carbenes.

1.1.2.1. Fischer and Schrock metal carbenes

Fischer-type carbenes (**Figure 1.3a**) consist of 18-electron complexes with the carbenic carbon bonded to heteroatoms or electron-withdrawing substituents. They are associated with a low oxidation state metal with strong π-acceptor ligands. Fischer-type carbenes are derived from singlet carbenes, and the bonding between the metal and the carbene involves a strong σ-donation from the carbene sp^2 orbital to the empty *d* orbital of the metal and a weak π-backbonding from the metal to the empty p_z carbene orbital.[13] The metal-to-carbon bond of Fischer carbenes is typically shorter than the one found in the Schrock ones, and the electron density is located in the metal center, causing the carbene to behave as an electrophile. Schrock-type carbenes (**Figure 1.3b**), on the other hand, are derived from triplet carbenes, possessing less than 18 valence electrons and typically with poor π-acceptor ligands. The bonding in this class of carbenes is better described as a covalent interaction between the carbene ligand and the metal, with the bonds polarized towards the carbon rendering the metal center nucleophilic.

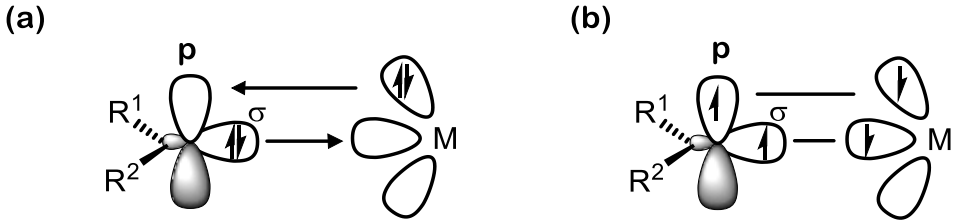

Figure 1.3. Bonding scheme in Fischer and Schrock carbenes.

1.1.2.2. Davies carbene classification

To understand and predict the reactivity of metal carbenes in organic transformations, Davies proposed in 2003 a classification based on the substituents present in the carbene.[14] Although initially proposed for copper and rhodium complexes, the community embraced this categorization, and it has become a widely used approach to understand and predict the reactivity of metal carbenes in organic transformations (**Figure 1.4**).

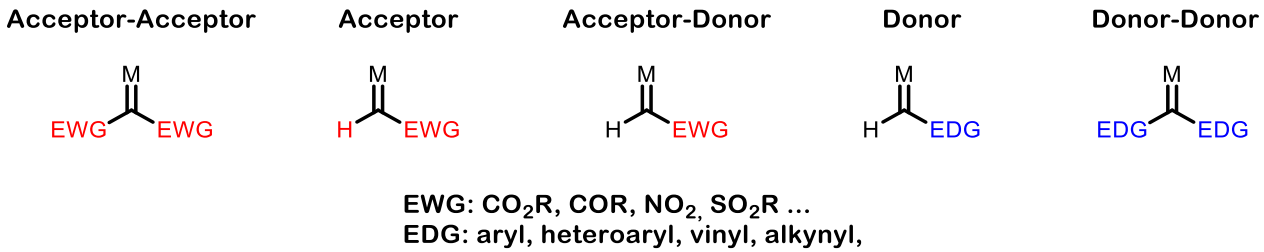

Figure 1.4. Classification of carbene species based on their substitution pattern.

Acceptor/acceptor carbenes contain two strong electron-withdrawing groups. This substitution pattern yields highly reactive intermediates due to the increased electron-deficient nature of the metal center. The high reactivity of these carbenes leads to decreased selectivity whenever they are involved in common carbene transfer reactions. To mitigate, to some extent, these selectivity issues, the removal of one electron-withdrawing group yields acceptor carbenes. Although still highly reactive, their selectivity is improved compared to acceptor/acceptor carbenes. The last type of carbenes that Davies disclosed is known as donor/acceptor carbenes. As the name implies, one of the electron-withdrawing groups is replaced by an electron-donating group, typically an aryl or a vinyl functionality. This imparts the metal carbene with a balance

in terms of reactivity and selectivity. Although not included in the original work, two novel types of carbenes have been studied more recently: the donor carbenes and the donor/donor carbenes. Following the trend mentioned previously, the neighboring electron-donating group should confer more stability and less reactivity to the carbene. However, their use has been limited due to the inherent instability of the corresponding diazocompounds, generally used as their precursors (*vide infra*).[15]

1.1.2.3. Metal carbene generation

Among the various methods for generating metal carbenes, the decomposition of diazo compounds stands out as the most prevalent. Diazo compounds feature a dinitrogen unit bonded to a carbon atom. When they are reacted with a metal catalyst, dediazoniation occurs, leading to the formation of the desired metal carbene through the extrusion of dinitrogen—the driving force of the reaction (**Scheme 1.5**). However, diazo compounds are commonly regarded as unstable and potentially explosive, thereby limiting their applicability in large-scale reactions. It is worth noting that, contrary to the observed trend for metal carbenes, diazo precursors become increasingly unstable with the introduction of more electron-donating substituents adjacent to the diazo group.

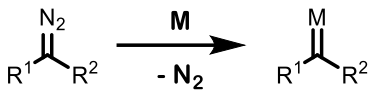

Scheme 1.5. Generation of metal carbenes from diazo compounds.

To address the potential hazards associated with handling diazo compounds, the synthetic chemistry community has developed a range of non-diazo compounds capable of catalytically generating metal carbenes.[16] The most prevalent non-diazo carbene precursors will be summarized herein.

N-sulfonylhydrazones emerge as a prominent method for accessing metal carbenes through *in situ* generation of diazo compounds.[17] *N*-sulfonylhydrazones are easily synthesized from the corresponding aldehydes or ketones and, under basic conditions, undergo a sulfinate elimination reaction generating the diazo compound *in situ*. This diazo compound can then be intercepted by a metal catalyst present in the reaction media, avoiding its accumulation and leading to the formation of the desired metal carbene (**Scheme 1.6**).

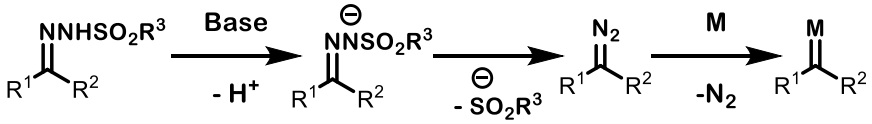

Scheme 1.6. Generation of metal carbenes from *N*-sulfonylhydrazones.

Sulfoxonium[18, 19] and iodonium ylides[19] have recently emerged as powerful carbene precursors. These species are crystalline, bench stable solids that can be easily prepared on a gram scale. When treated with a metal, they generate metalcarbenes upon dimethylsulfoxide (**Scheme 1.7a**) or iodoarene (**Scheme 1.b**) extrusion, respectively. Sulfoxonium ylides can accommodate both electron-donating and electron-withdrawing groups adjacent to the carbon that will be converted to the carbenic carbon upon reaction. Conversely, iodonium ylides require the presence of neighboring electron-withdrawing substituents.

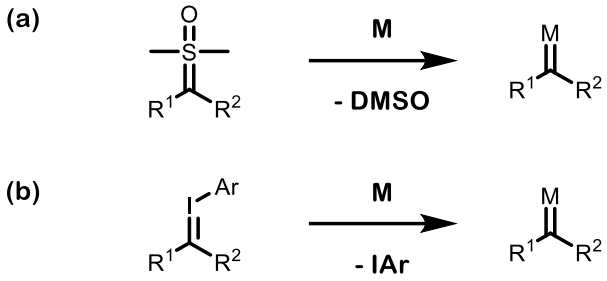

Scheme 1.7. Generation of metal carbenes from a) sulfoxonium and b) iodonium ylides.

Triazoles and their analogues exist in an equilibrium with their ring-opened α-imino diazo isomer.[20] While this equilibrium generally favors the closed triazole form, strategic substituent tuning can enhance the prevalence of the diazo isomer. Finally, following the same principle as illustrated in **Scheme 1.5**, the presence of a metal catalyst generates the corresponding α-imino carbene upon dinitrogen extrusion (**Scheme 1.8**).

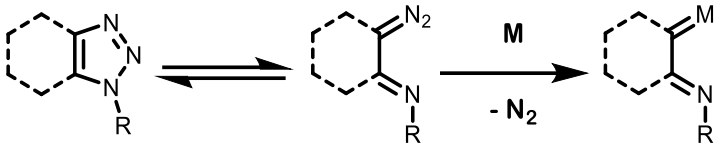

Scheme 1.8. Generation of metal carbenes from triazole derivatives.

Similarly to triazoles, cycloheptatrienes exist in equilibrium with their corresponding bicyclic norcaradiene derivatives. Through careful tuning of substituents, the norcaradiene form can predominate, enabling a retro-Buchner reaction in the presence of a metal catalyst. This reaction results in the extrusion of an arene and the formation of the desired carbene (**Scheme 1.9**).[21] While reports of cycloheptatrienes as carbene precursors have been limited, their use has been increasingly reported in recent literature, indicating a growing interest in their application.

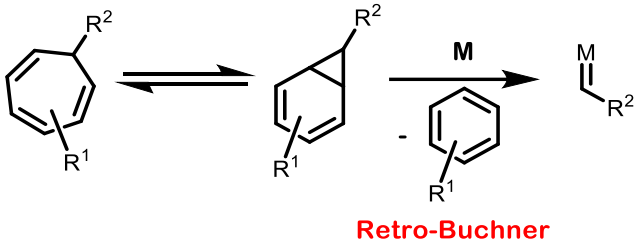

Scheme 1.9. Generation of metal carbenes via retro-Buchner reaction.

Thanks to the capability of various metals to activate alkynes through coordination, metallocarbenes can be generated via isomerization reactions, a transformation that we exemplify herein with the reaction of propargyl esters. The mechanism underlying carbene generation involves coordination at the alkyne group, followed by a 1,2-migration from the ester moiety, leading to the formation of the metal carbene (**Scheme 1.10**).[22]

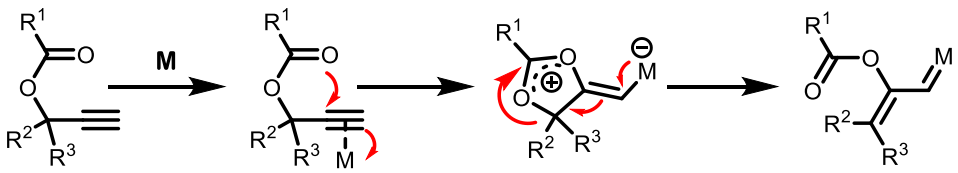

Scheme 1.10. Generation of metal carbenes via 1,2-shift of propargyl esters.

In addition to alkynes, highly strained cyclopropenes can serve as carbene precursors through a mechanism also reliant on metal coordination. In these cases, metal coordination facilitates the ring opening of the three-membered ring, resulting in the formation of the corresponding carbene, a process driven by the release of ring strain (**Scheme 1.11**).[23] This process generates a metal vinylcarbene with increased reactivity potential (*vide infra*).

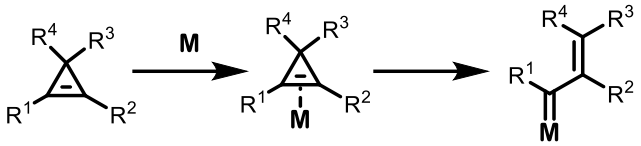

Scheme 1.11. Generation of metal carbenes via ring opening of cyclopropenes.

1.2. Metal vinylcarbenes

Metal vinylcarbene complexes are a particularly interesting class of carbenes due to the presence of a vinylic unit embedded in their structure. This extra functionality gives rise to a wide array of novel transformations, as both the carbenic site and the remote (or vinylogous) positions can be functionalized. Besides the conventional monofunctionalization of both positions (the vinylcarbene acting as a C1 synthon), the extra conjugation around the carbene unit allows for the development of cycloaddition reactions in a (3+n) fashion (vinylcarbene acting as a C3 synthon).

1.2.1. Catalytic generation of metal vinylcarbenes: historical perspective

The first examples of catalytic generation of vinylcarbenes date back to the 1970s when cyclopropenes were employed as precursors for vinylcarbenes. In 1972, Gil-Av reported the conversion of cyclopropene derivatives to dienes under silver perchlorate catalysis.[24] Presumably, the cyclopropene ring opening leads to the formation of a silver vinylcarbene *in situ*, which subsequently undergoes a 1,2-H shift to yield the final product (**Scheme 1.12a**). In 1974, McMeeking utilized $Ni(COD)_2$ as a catalyst for intermolecular cyclopropanation of olefins using 3,3-dimethylcyclopropene (**Scheme 1.12b**).[25] Later studies reported similar outcomes when $Ni(CO)_4$ was employed as the catalyst.[26]

The first example of using diazo compounds as precursors for vinylcarbenes was documented in 1975 by Salomon. By reacting vinyldiazomethane under copper catalysis in the presence of various olefins, the cyclopropanation adduct could be obtained (**Scheme 1.12c**).[27] Although the yields for the reactions were low, this served as a proof of concept for using vinyldiazo compounds as vinylcarbene precursors.

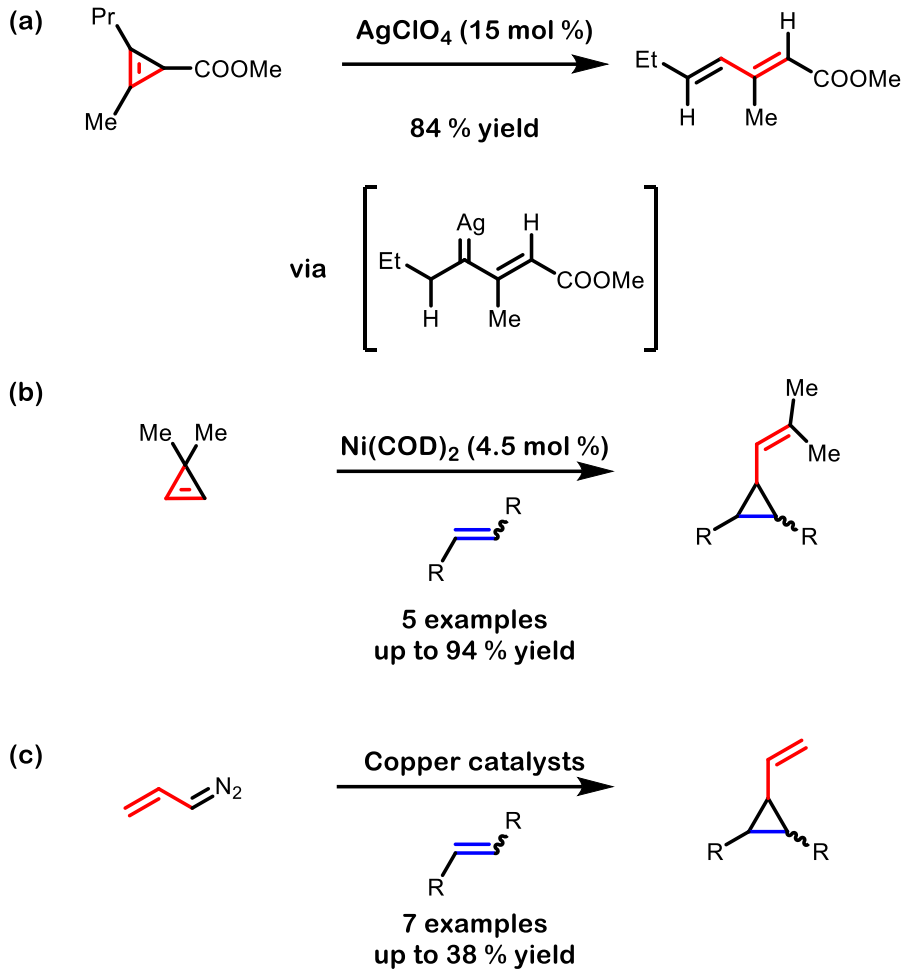

Scheme 1.12. Early examples of reactions involving catalytically generated vinylcarbenes.

1.2.2. Reactivity of metal vinylcarbenes

These early examples proved the utility of vinylcarbenes as versatile intermediates and paved the way for the development of its chemistry. In this regard, in 1985 Davies realized the potential of using rhodium (II) catalysts to capitalize on the versatility of the *in situ* generated metal vinylcarbene.[28] By reacting a vinyl diazo with furan in the presence of $[Rh_2(OAc)_4]$, the corresponding seven-membered ring cycloadduct arising from a formal [3+4] cycloaddition could be isolated in 45% yield with complete selectivity to the *endo* isomer (**Scheme 1.13**).

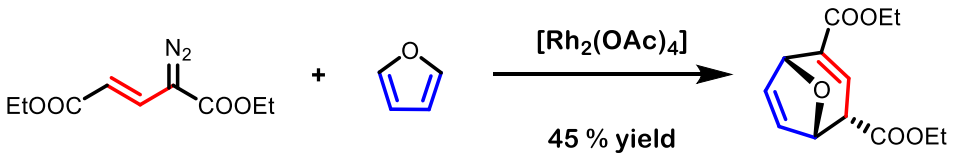

Scheme 1.13. Rhodium (II) catalyzed [3+4] cycloaddition of vinyl diazo compound and furan.

The reaction was not limited just to the use of furan as later studies by the same group reported that several substituted furans were tolerated in the reaction.[29] These pioneering studies by Davies incorporated the vinyl unit of the vinylcarbene into the final product, laying the groundwork for uncovering new reactions inaccessible through conventional metal carbenes. All the efforts done by Davies,[30] as well as others in the field of

vinylcarbene chemistry, will be summarized in this thesis organized by type of reaction, highlighting the cases in which the reactivity is different to the one that would be observed with pristine carbenes.

1.2.2.1. Cycloaddition reactions

1.2.2.1.1. [3+4] Cycloadditions

Following their first study, the group of Davies expanded the scope of the reaction to cyclopentadiene and unraveled the mechanism underlying the formal [3+4] cycloaddition reaction.[31] By tuning the substituents in the diazo group, they could isolate the products arising from a cyclopropanation reaction, which upon heating isomerized towards the expected cycloheptadienes by means of a Cope rearrangement. These findings established that the reaction mechanism proceeds through a tandem process instead of a concerted [3+4] cycloaddition (**Scheme 1.14**). Analogous to the previous report, Wulff described similar results reacting an isolated chromium vinylcarbene and Danishefsky's diene to obtain either de [2+1] or the [3+4] adduct.[32]

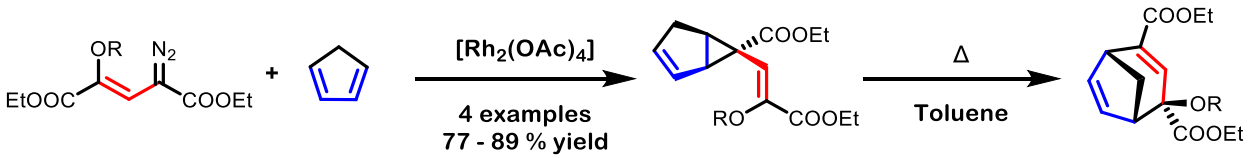

Scheme 1.14. Rhodium (II) catalyzed [3+4] cycloaddition of vinyl diazo compounds and cyclopentadiene.

Following work by Davies showed the versatility of the intermolecular [3+4] reaction using this time acyclic dienes as the four-carbon partner. By tuning the initial vinyl diazo compound, a series of novel hydroazulenes could be prepared with moderate to good yields (**Scheme 1.15**).[33] Although initially envisioned as an intermolecular reaction, several reports by Davies confirmed also that the reaction could proceed intramolecularly by embedding the vinyldiazo and the diene units in the same starting material.[34]

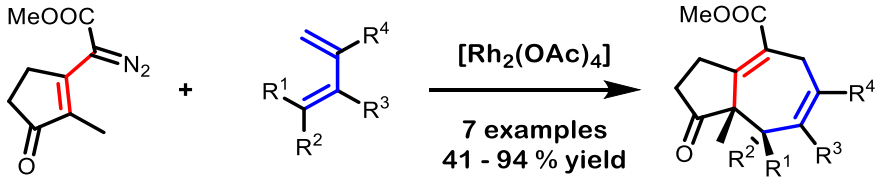

Scheme 1.15. Rhodium (II) catalyzed intermolecular [3+4] cycloaddition of vinyl diazo compounds and acyclic dienes.

Similar to furans and cyclopentadienes, pyrroles could also be tolerated in the tandem reaction.[35] While unprotected pyrroles failed to furnish the desired product, introducing an ester group in the N atom proved to be key for the formation of the corresponding nitrogenated bicyclic adducts (**Scheme 1.16**).

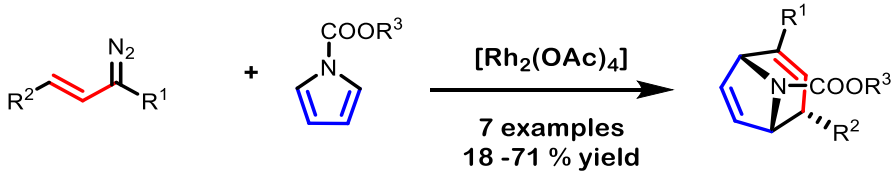

Scheme 1.16. Rhodium (II) catalyzed [3+4] cycloaddition of vinyl diazo compounds and pyrroles.

The outcome of the intramolecular reaction with pyrroles was found to be dependent on the substitution pattern in the vinyl group of the vinyldiazo moiety.[36] Whereas silyl enol ethers yielded a formal [3+4] adduct (in

analogous way to the intermolecular reaction), unsubstituted vinylcarbenes produced azetidine derivatives (**Scheme 1.17**). In both cases the authors postulated the formation of a common zwitterionic intermediate by nucleophilic attack by C2 of the pyrrole to the rhodium vinyl carbene. Depending on the substituent, this intermediate evolves towards different products. These findings clearly demonstrate how the substitution pattern in the diazo compound can modulate the reactivity of the generated vinylcarbene. From this moment onward, vinyl diazo derivatives containing silyl enol ethers will be referred as enoldiazo compounds, a term widely utilized by Doyle in describing these substrates.[37]

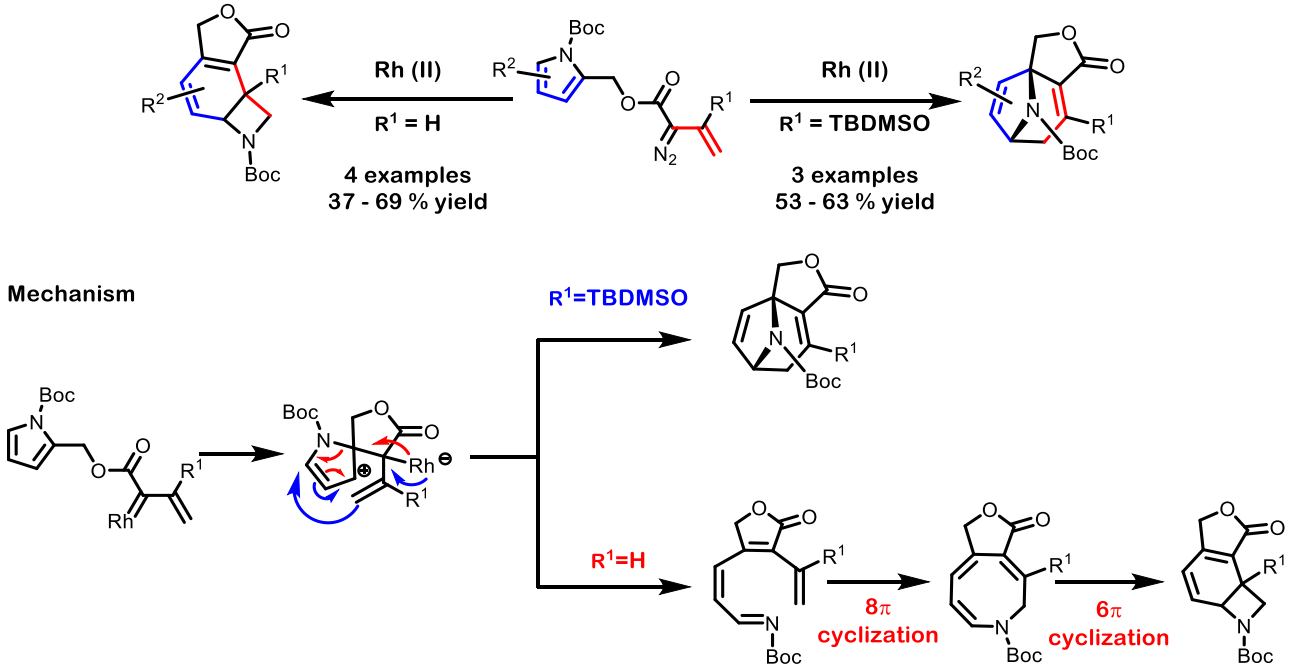

Scheme 1.17. Rhodium (II) catalyzed intramolecular reaction of pyrroles and substituted vinyl diazo derivatives.

While all the previous reports afforded racemic products, the development of chiral rhodium (II) catalysts marked a turning point. The group of Davies capitalized on their developed [3+4] cycloadditions to achieve the desired 7-membered-ring products in an enantioselective fashion. In 1994, they reported the enantioselective transformation with dienes and furan (**Scheme 1.18a**) using [Rh_2(*S*-TBSP)$_4$] as the chiral catalyst.[38] Nonetheless, pyrroles proved to be more challenging, and it was not until 2007 than the same group reported the desired reaction, using enoldiazo compounds in the presence of [Rh_2(*S*-PTAD)$_4$] catalyst (**Scheme 1.18b**).[39]

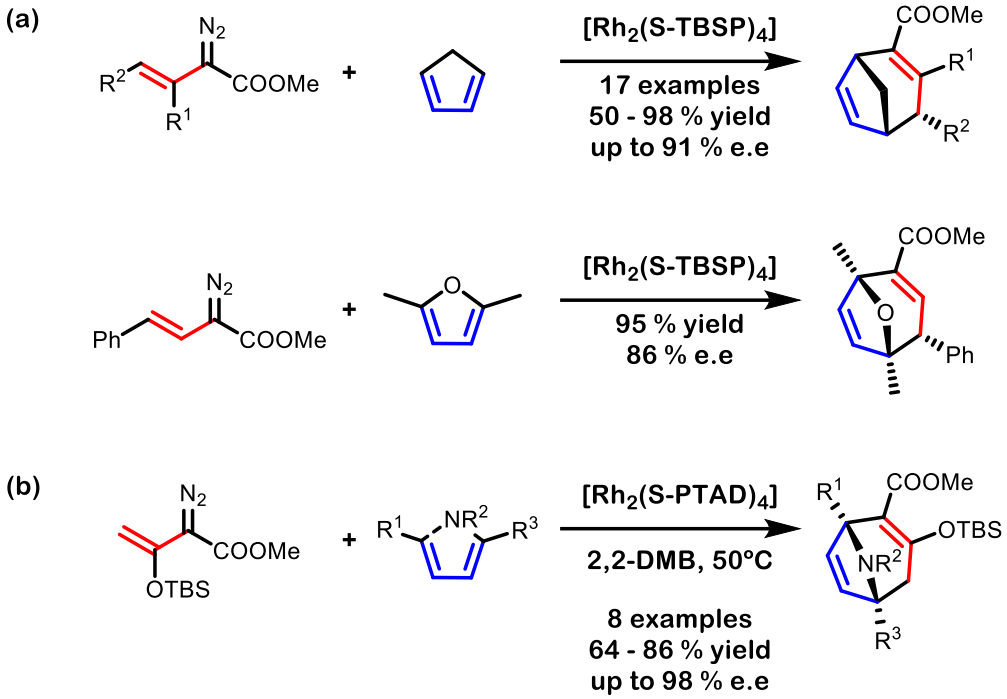

Scheme 1.18. Rhodium catalyzed enantioselective [3+4] cycloadditions of vinydiazo compounds.

Up to that point, all examples reported relied in the use of conjugated carbon-based double bonds. However, the Doyle group recognized the potential of employing conjugated imines or aldehydes as substrates for the transformation.[40] Just by subjecting these hetero-dienes to styryl diazo compounds under rhodium catalysis, they successfully isolated the corresponding seven-member ring, albeit alongside undesired [2+1] and [3+2] adducts. Despite the obtained product being the same as for the [2+1]/Cope mechanism, the pathway for this transformation is based on the formation of an initial imino/carbonyl-ylide that collapses with itself furnishing the corresponding dihydro-azepines or dihydro-oxepines (**Scheme 1.19**). Expanding on these initial discoveries, the same group subsequently reported the exclusive formation of the [3+4] cycloadduct by utilizing enoldiazo compounds.[41]

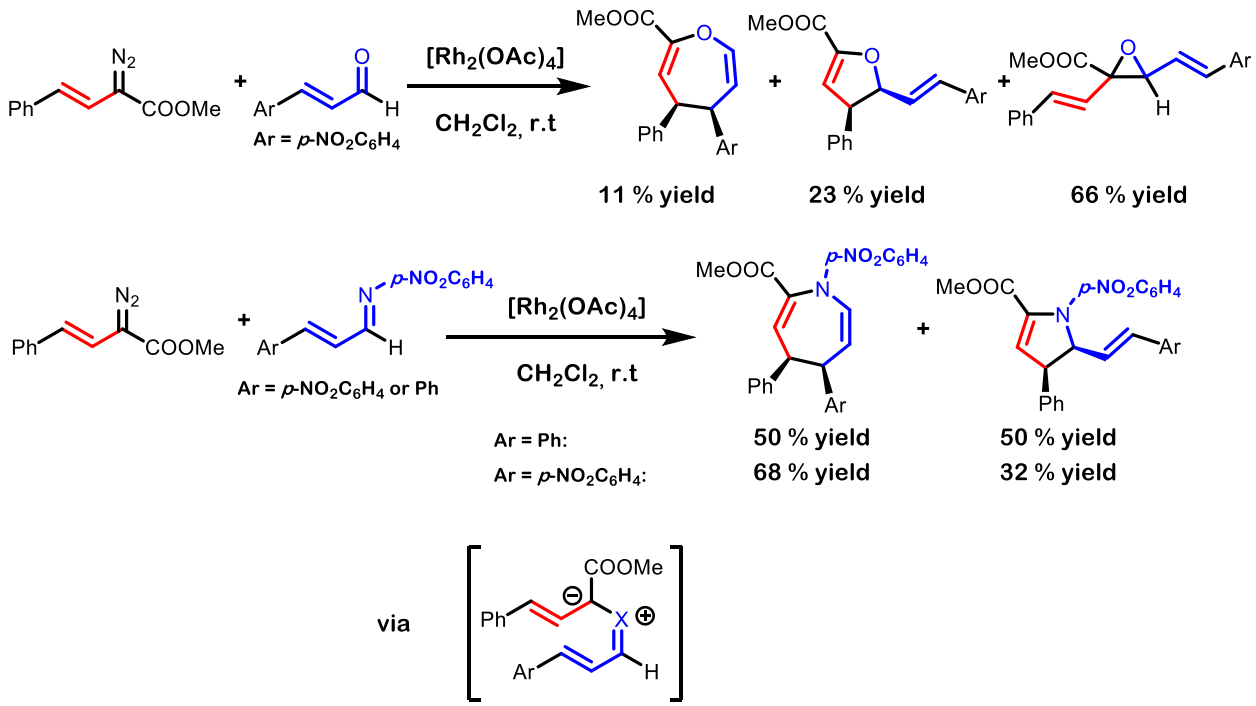

Scheme 1.19. Rhodium catalyzed [3+4] cycloadditions of styryl diazo derivatives and conjugated aldehydes or imines.

To expand the pool of substrates able to engage in the cycloaddition, the Doyle group introduced an intramolecular reaction employing aryls as diene surrogates.[42] While Davies had hinted at this reactivity's potential in 1992, only limited examples were reported, with low yields and unstable products.[43] In contrast, by incorporating a benzyl unit into enoldiazo compounds, the cyclopropanation of the phenyl moiety leads to the formation of the corresponding norcaradiene. This intermediate does not undergo expansion toward the corresponding cycloheptatriene (Buchner reaction) but instead undergoes a Cope rearrangement with the alkene moiety of the initial diazo compound, yielding bicyclononatriene scaffolds in good to moderate yields. Moreover, the reaction can be conducted in an enantioselective fashion by using a chiral rhodium catalyst (**Scheme 1.20**).

While all the examples reported so far capitalized in initial reactivity at the carbenic site of the vinylcarbene, one could envision that initiating the reaction at the vinylogous site might lead to a [3+4] cycloaddition with a complete reversal of regioselectivity. In this context, the Davies group disclosed this transformation by reacting enoldiazo compounds with silyl enol-containing dienes in the presence of their highly constrained cyclopropyl-based [Rh_2(*S*-BTPCP)$_4$] catalyst[44] yielding the reversed cycloheptatriene with high levels of regio-, diastereo- and enantioselectivity **(Scheme 1.21)**.[45] The postulated mechanism for the reaction is based on an initial nucleophilic attack by one alkene of the diene toward the vinylogous position, followed by an intramolecular ring closing to furnish the corresponding cycloheptadienes.

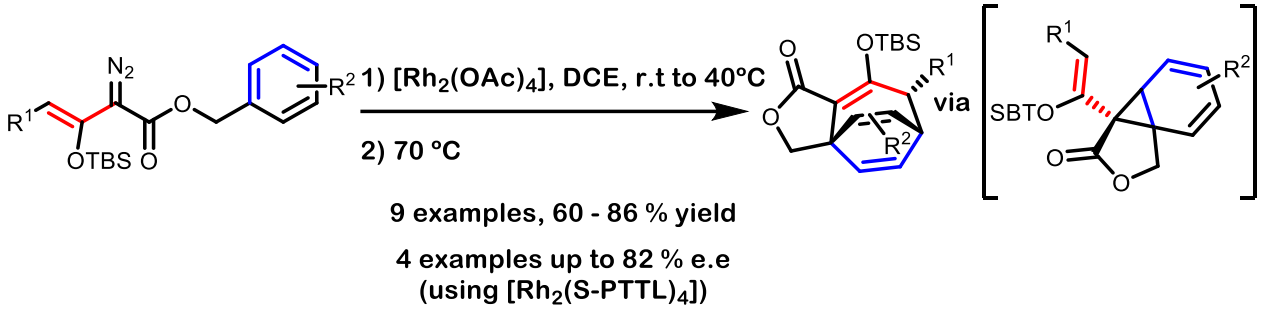

Scheme 1.20. Intramolecular rhodium catalyzed [3+4] for the preparation of bicyclononatrienes.

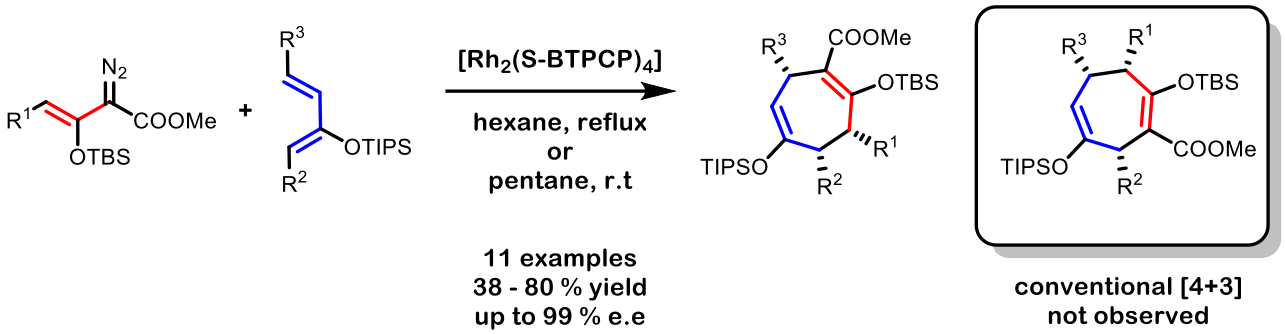

Scheme 1.21. Rhodium catalyzed [3+4] cycloaddition between enoldiazo compounds and dienes with complete reversal of reactivity.

The combination of rhodium (II) and vinyldiazo compounds had dominated the field so far. However, the scientific community started to invest in the exploration of novel vinylcarbene precursors and the development of catalytic systems centered around other metals. The first example of a non-rhodium based [3+4] cycloaddition was reported by Toste in 2008. Propargyl esters were treated with a gold catalyst to generate *in situ* a gold vinylcarbene, which was intermolecularly trapped by a conjugated imine (**Scheme 1.22**).[46] From this point onward, the [3+4] cycloaddition with the hetero-diene proceeds in a manner analogous to the reaction with rhodium and imines/aldehydes (*vide supra*). Expanding on these findings, other research groups have reported the analogous trapping of the *in situ* generated gold vinylcarbene with dienes[47, 48] or furans.[49] Taking advantage from the π-activation of alkynes strategy, the Tang group demonstrated the generation of platinum vinylcarbenes using ortho-propargyl aniline derivatives.[50] In this case, alkyne activation by the π-acidic platinum center, followed by nucleophilic addition of the pending amino group, ultimately leads to the formation of the vinylcarbene. Subsequent intermolecular [3+4] cycloaddition with an external diene result in the formation of the final cyclohepta[b]indole products. Given the regioselectivity of the cycloaddition, the authors postulate an initial addition of the diene at the vinylogous site of the vinylcarbene (**Scheme 1.23**). Interestingly, for some examples within the scope, the authors disclosed that rhodium (I) catalysts perform better than platinum complexes. Notably, furans are also tolerated in this transformation.

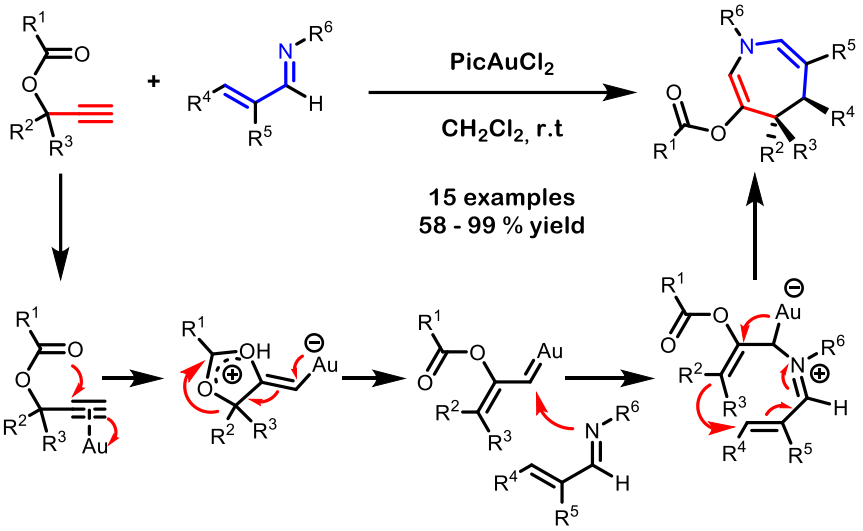

Scheme 1.22. Gold catalyzed [3+4] cycloaddition between propargyl esters and imino dienes.

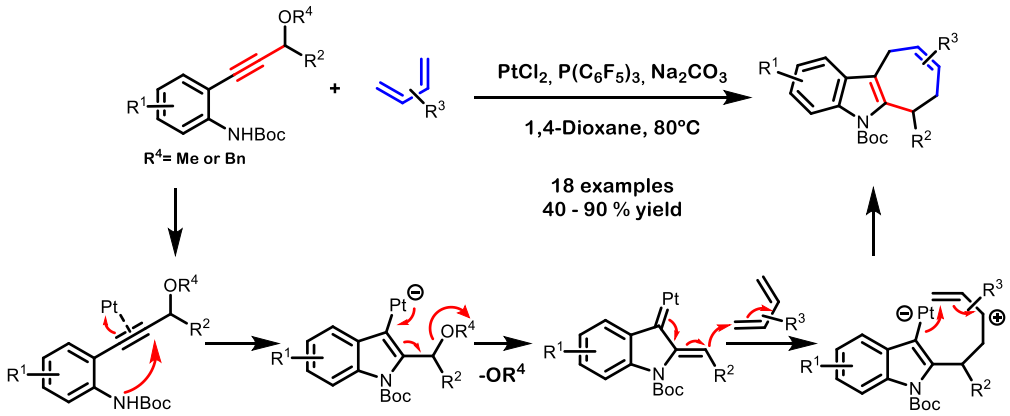

Scheme 1.23. Platinum catalyzed [3+4] cycloaddition using o-anilines and dienes.

The research groups led by Hashmi and Hyland reported an intramolecular gold-catalyzed [3+4] reaction by linking a furan with a cyclopropene as carbene precursor (**Scheme 1.24**).[51] The authors propose two potential mechanisms, both centered around the ring opening of the cyclopropene from the less substituted site, leading to the desired gold vinylcarbene. The first proposed mechanism envisions a direct concerted [3+4] cycloaddition with the furan. On the other hand, a stepwise [3+4] cycloaddition could be considered. Given the observed regioselectivity in the reaction, the authors suggest that the initial nucleophilic addition from the C2 of the heterocycle must occur at the vinylogous site of the gold carbene. Remarkably, when the authors conducted the reaction using pyrrole or indole derivatives, [3+4] adducts were not observed. Instead, Csp^2-H insertion at the C3 position was reported as the outcome for the reaction involving nitrogen-based heterocycles.

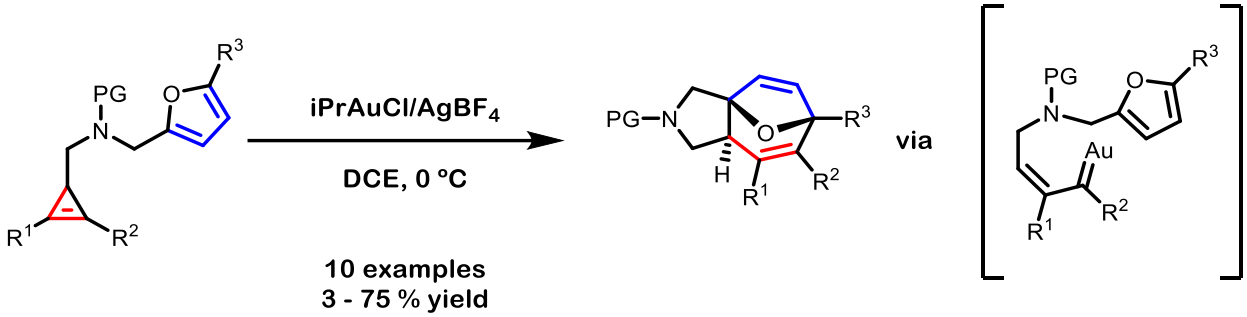

Scheme 1.24. Gold catalyzed intramolecular [3+4] cycloaddition of cyclopropenes and furans.

More recently, Zhu *et al.* reported an unconventional approach to produce endocyclic rhodium (II) vinylcarbenes using enynals as precursors (**Scheme 1.25**).[52] This methodology exploits the previous reports by the same group for carbene generation through isomerization reactions.[53] In this specific case, rhodium coordination to the alkyne initiates a concerted [3+2] cycloaddition, involving the terminal aldehyde and a pending alkene. The resulting vinylcarbene can then undergo intermolecular reaction with a diene, yielding the final tetracyclic fused adducts. While the authors predominantly explore the racemic version of the transformation, they also present several examples where the reaction can be conducted in an enantioselective manner using the [Rh_2(*S*-NTTL)$_4$] catalyst.

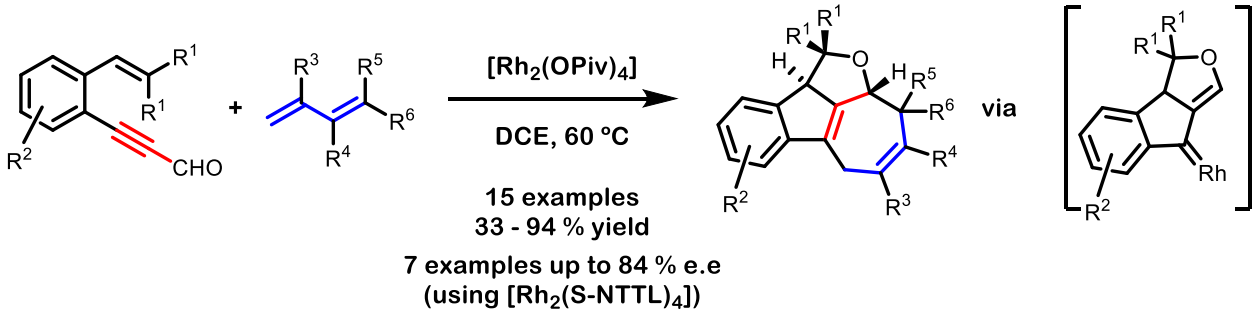

Scheme 1.25. Rhodium (II) catalyzed [3+4] cycloaddition between enynals and dienes.

One of the main limitations in the use of vinyldiazo compounds for carbene generation arises from the need for an acceptor group adjacent to the diazo moiety. Apart from the stabilization of the precursor diazo compound, this necessity arises from the propensity of unsubstituted vinyldiazo compounds to undergo intramolecular thermal isomerization, resulting in pyrazole products.[54] To overcome this limitation, the group of Bi recently introduced a novel strategy, employing a silver trispyrazolyl-based catalyst in combination with vinyl-*N*-triftosylhydrazones. This approach serves as an excellent platform for the generation of both unsubstituted and alkyl-substituted silver vinylcarbenes. Exploiting the reactivity of these carbenes, they demonstrated their efficacy in [3+4] cycloadditions with dienes[55] and furans[56] (**Scheme 1.26**). They also perform DFT calculations for both reactions, revealing divergent reaction pathways. While dienes undergo a conventional [2+1]/Cope rearrangement, furans engage in a direct concerted [3+4] cycloaddition with the silver vinylcarbene. These findings showcase the versatility of mechanisms involved in [3+4] cycloadditions with vinylcarbenes.

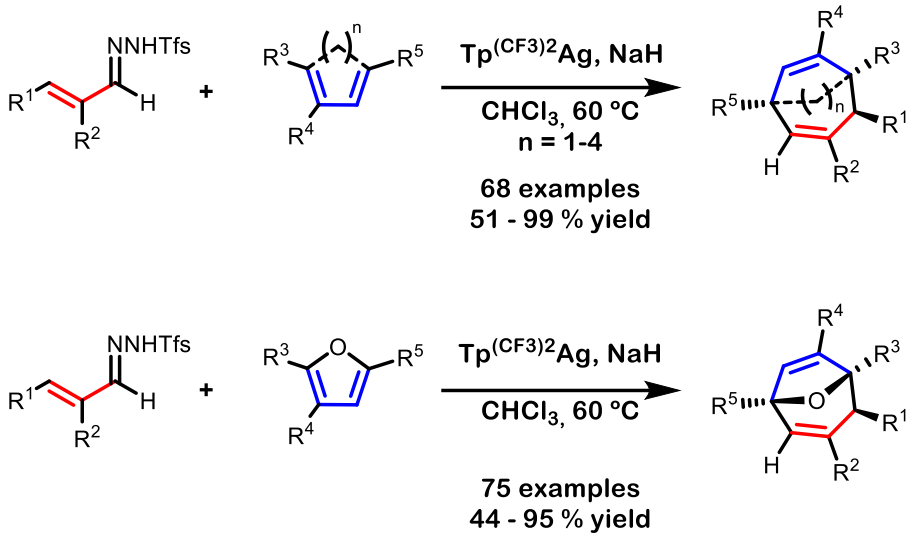

Scheme 1.26. Silver catalyzed [3+4] cycloaddition between *N*-triftosylhydrazones and dienes/furans.

1.2.2.1.2. [2+1] Cycloadditions

As expected, when alkenyl diazo compounds were reacted with simple alkenes in the presence of rhodium acetate, the corresponding cyclopropane could be isolated with high yields and good to excellent diastereoselectivity (**Scheme 1.27a**).[57] Conducting the same reaction but using enol ethers as the olefin and rhodium octanoate as the catalyst, the newly formed cyclopropanes could undergo rearrangement upon treatment with Et_2AlCl. The resulting cyclopentenes would be the products arising from a formal [3+2] cycloaddition between the vinylcarbene and the alkene (**Scheme 1.27b**).[58] Several years later, the reactions were performed using chiral rhodium catalysts, achieving the transformations in an enantioselective fashion.[59]

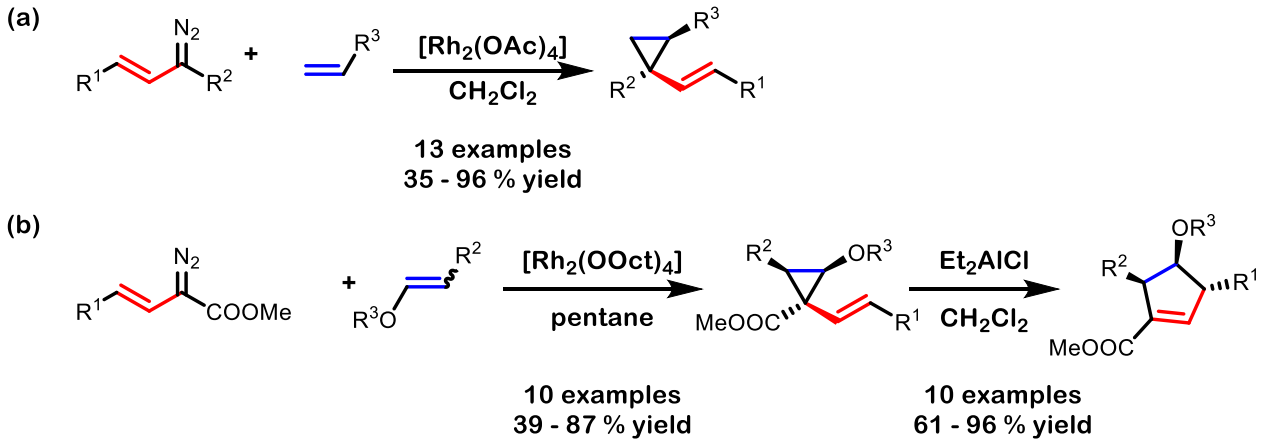

Scheme 1.27. Rhodium catalyzed [2+1] cycloaddition between vinyldiazo compounds and alkenes.

Similarly to [3+4] cycloaddition reactions, alternative vinylcarbene precursors can be employed for the cyclopropanation of olefins. Recognizing this potential, the Ohe group employed propargyl esters for this purpose, and reported a [2+1] cycloaddition under ruthenium catalysis (**Scheme 1.28a**).[60] Two years later, Toste published the enantioselective version of this transformation using chiral gold catalysts (**Scheme 1.28b**).[61]

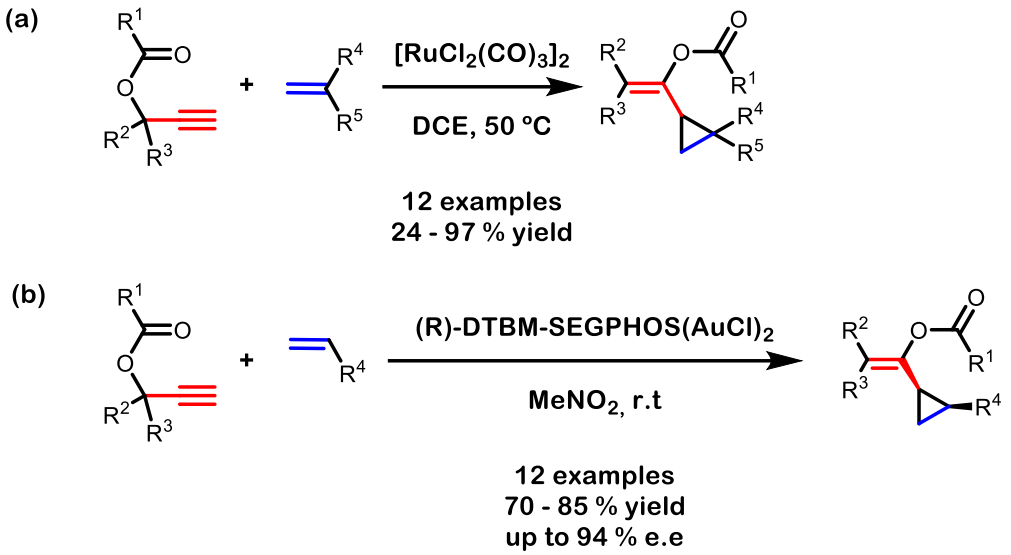

Scheme 1.28. Intermolecular [2+1] cycloaddition between alkenes and propargyl esters.

The intramolecular version of this kind of reactivity is particularly interesting due to the potential to generate bicyclic compounds. In this regard, the Cossy group using cyclopropenes as the source for the vinyl carbene detailed a series of intramolecular [2+1] cycloadditions involving alkenes tethered to cyclopropene units (**Scheme 1.29**).[62] Although their initial studies were conducted under gold catalysis,[63] rhodium (II) could also be efficient in the reaction.[64]

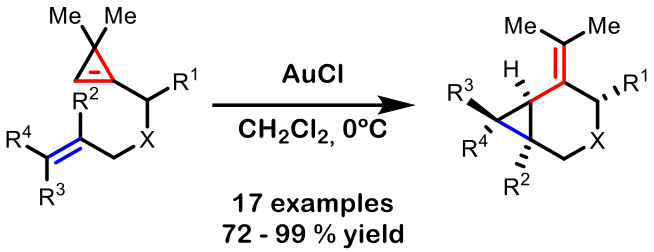

Scheme 1.29. Gold catalyzed intramolecular cyclopropanation of olefins using cyclopropenes as carbene precursors.

Recently, the group of Bi capitalized once again in the potential of their vinyl-N-triftosylhydrazones in conjunction with silver catalysts for the intermolecular cyclopropanation of alkenes (**Scheme 1.30**).[65] Notably, their approach is not the sole method to access unsubstituted vinylcarbenes, as the Echavarren group uncovered the capability of alkenyl cycloheptatrienes to generate vinylcarbenes through a gold catalyzed retro-Buchner reaction. The resultant vinylcarbene can then cyclopropanate an external olefin (**Scheme 1.31**).[66] This mechanistic hypothesis was corroborated by means of DFT calculations. Notably, the Echavarren group continued their efforts in this field, just modifying the cycloheptatriene moiety to enable the reaction under milder conditions, using zinc[67] and later rhodium (II) catalysts.[68]

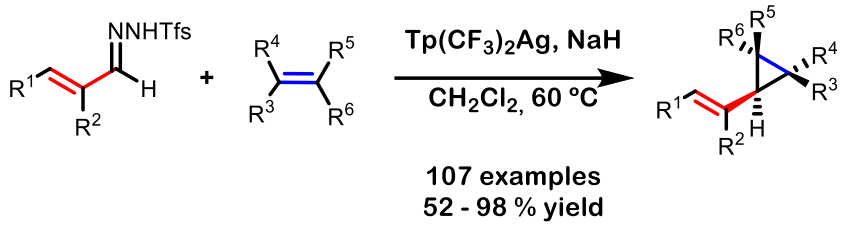

Scheme 1.30. Silver catalyzed cyclopropanation of olefins using N-triftosylhydrazones.

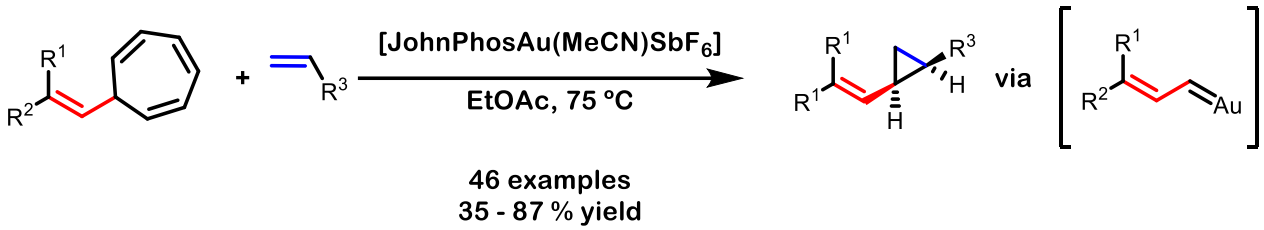

Scheme 1.31. Gold catalyzed cyclopropanation of olefins using cycloheptatrienes as vinylcarbene precursors.

Similar to the [3+4] cycloaddition, other substrates can be accommodated in the [2+1] reaction to yield three-membered heterocycles. Initial studies by Hamaguchi demonstrated the use of aldehydes [69] and thioketones [70] albeit with product mixtures containing [2+1] and [3+2] adducts. Improved results in the [2+1] cycloaddition with aldehydes were reported by the group of Aggarwal, when using N-sulfonylhydrazone sodium salts as diazo precursors in combination with rhodium (II) catalysts in presence of sulfides (**Scheme 1.32**).[71]

According to their proposed mechanism, the *in situ* formed vinylcarbene is trapped by the sulfide, generating a sulfur ylide. Subsequent reaction with the external aldehyde yields the corresponding betaine intermediate, which evolves into the desired oxirane. When chiral sulfides are employed, good enantiomeric excesses are achievable in certain examples. Regarding thioketones, the Feng group addressed selectivity issues by utilizing cobalt catalysts to achieve the corresponding thiiranes in excellent yields and enantioselectivities.[72]

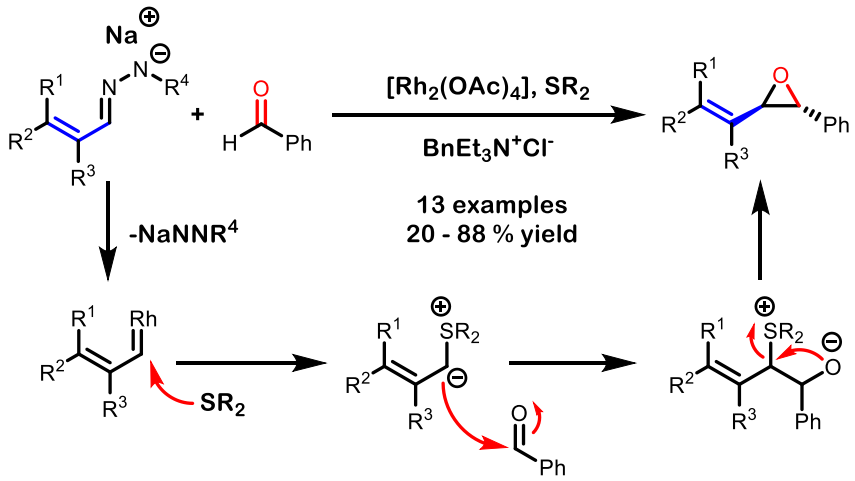

Scheme 1.32. Rhodium catalyzed [2+1] cycloaddition between N-sulfonylhydrazone sodium salts and aldehydes.

Beyond alkenes and carbonyl-related compounds, alkynes are also amenable to [2+1] cycloaddition. The first example on the cyclopropenation reaction using vinyldiazo compounds was reported by Davies in 2010.[73] When styryl diazoacetates were reacted with terminal alkynes in the presence of [Rh_2(*S*-DOSP)$_4$], the

corresponding cyclopropenes could be isolated in high yields and with excellent enantioselectivity (**Scheme 1.33**). This reactivity extends beyond phenyl-substituted vinyldiazo compounds, as the same group reported a year later on the reaction employing enoldiazo compounds.[74]

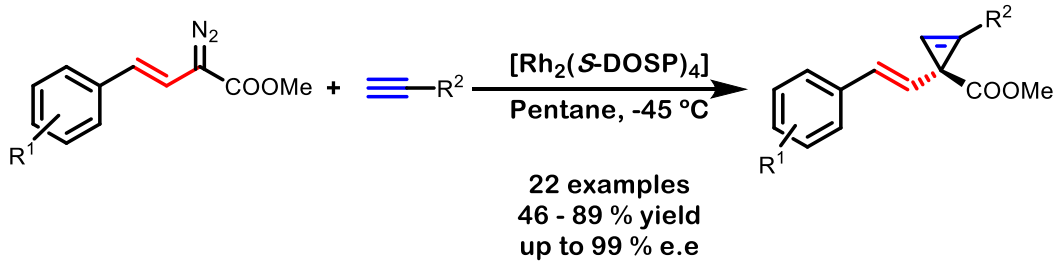

Scheme 1.33. Rhodium catalyzed enantioselective cyclopropenation of alkynes using styryl diazoacetates.

Heterocyclic compounds are among the other interesting substrates that can undergo cyclopropanation reactions. Furans and pyrroles have shown their propensity to yield the [3+4] adduct (*vide supra*). However, this reactivity is suppressed when working with their benzo derivatives, specifically indoles and benzofurans. The Sun group was the first to report on this type of reactivity, showcasing the reaction between vinyldiazo compounds and indoles under silver catalysis (**Scheme 1.34**).[75] The mechanism for the transformation was later studied through DFT calculations by the Yang group.[76]

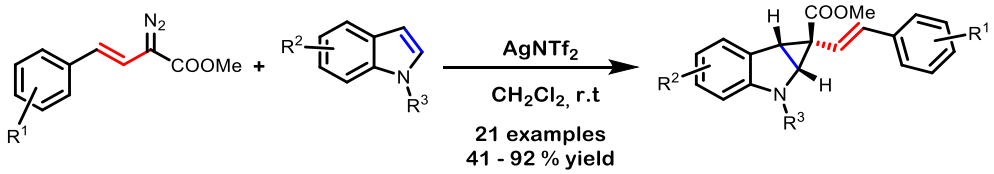

Scheme 1.34. Silver catalyzed cyclopropanation of indoles using vinyldiazo compounds.

In addition to vinyldiazo compounds, cyclopropenes have been found to participate in the same reaction under rhodium (II) catalysis. Two articles, published nearly simultaneously, capitalized on this reactivity: the Lautens group focused on the cyclopropanation of benzofurans (**Scheme 1.35a**) [77] while the Jiang group primarily reported the reaction with indoles (**Scheme 1.35b**). [78]

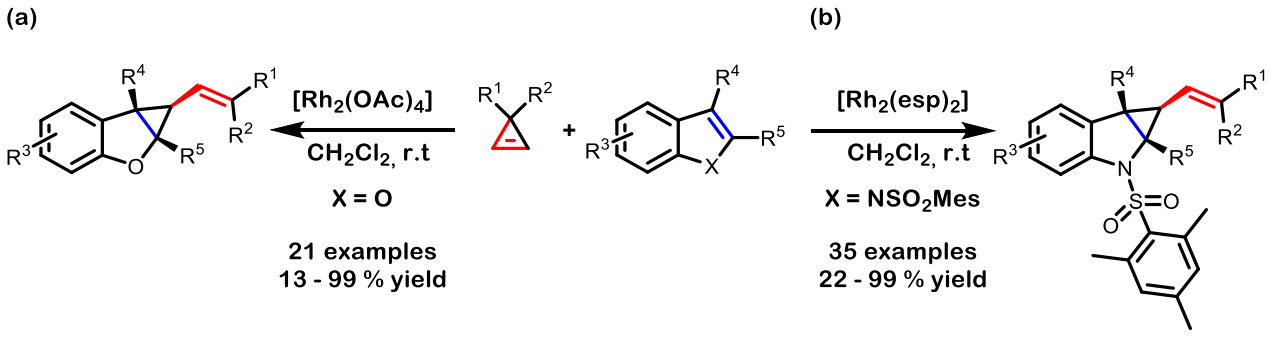

Scheme 1.35. Rhodium catalyzed cyclopropanation of benzofurans and indoles.

1.2.2.1.3. [3+2] Cycloadditions

Given the prevalence of the alkene unit, vinylcarbenes can also serve as three-carbon synthons for constructing 5-membered carbo- or heterocyclic rings. The first group to realize this potential was the one by Davies in 1992. While studying the previously commented reactivity of vinyldiazo compounds and vinyl ethers

(**Scheme 1.27b)** the authors realized that by adjusting the reaction conditions, cyclopentene scaffolds could be obtained (**Scheme 1.36**).[79] Furthermore, based on the regioselectivity of the reaction, the mechanism of the transformation should involve an initial nucleophilic addition at the vinylogous site followed by ring closing. This made this work the first report based on fully selective vinylogous functionalization of a vinylcarbene. The same authors, nine years later, reported the enantioselective version of this transformation using [Rh_2(*S*-DOSP)$_4$] as the catalyst.[80]

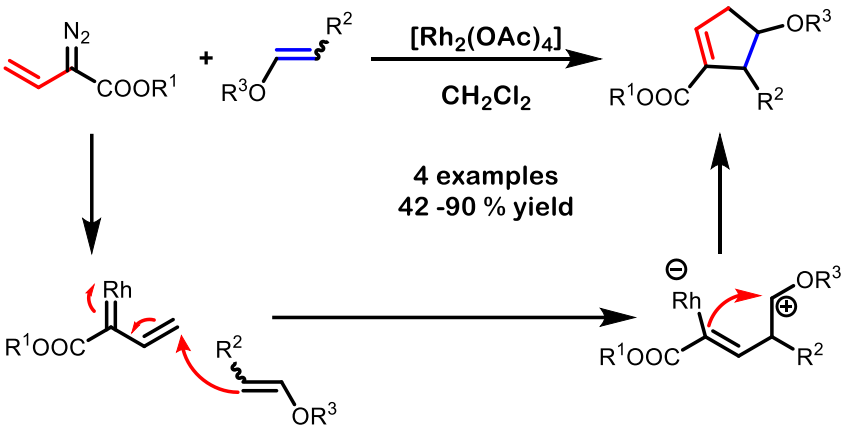

Scheme 1.36. Rhodium catalyzed [3+2] cycloaddition between vinyldiazo compounds and vinyl ethers.

The Davies group further explored the versatility of this reaction by reporting the same transformation using enoldiazo compounds.[81] More notably, they published the enantioselective version of the reaction with chiral gold catalysts.[82] Similarly, the López group reported a gold-catalyzed [3+2] cycloaddition between vinyldiazo compounds and styrenes[83] or pinacol alkenylboronates.[84] More recently, Feng introduced an enantioselective nickel-catalyzed version of this transformation.[85]

To widen the applicability of this reaction, several studies involving alternative vinylcarbene precursors emerged. The Nevado group moved from vinyldiazo compounds to propargyl esters under gold catalysis (**Scheme 1.37a**).[48] They proposed a mechanism involving initial cyclopropanation of the olefin followed by gold-catalyzed isomerization toward the final cyclopentene. Furthermore, when dienes were employed as reaction partners, only the [3+4] cycloadduct was observed. On the other hand, Iwasawa et al. employed their method based on the isomerization of ortho-propargyl anilines. In the presence of platinum, the generated vinylcarbene was trapped by an external vinyl ether in a [3+2] fashion, yielding the corresponding tricyclic scaffolds (**Scheme 1.37b**).[86] Similarly to the early works in the field, the proposed mechanism involved initial nucleophilic addition at the vinylogous position followed by ring closing. This proposal was later substantiated by Zhang through DFT calculations.[87]

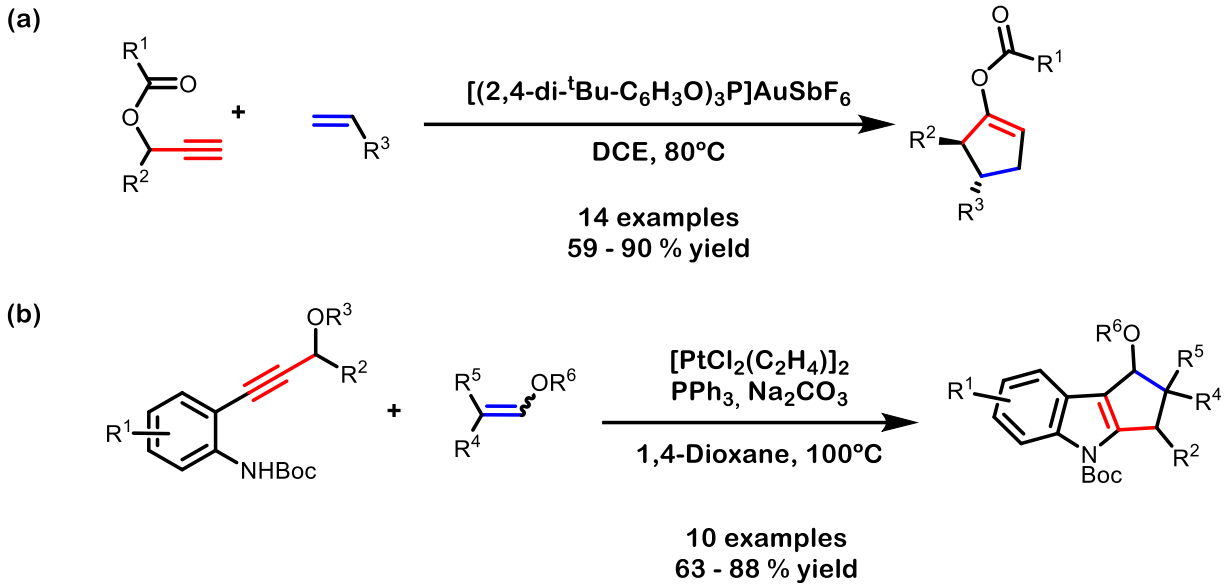

Scheme 1.37. [3+2] cycloaddition reactions involving alkenes and non-diazo carbene precursors.

Besides altering the carbene precursor, modifying the 2-atom synthon can yield a variety of 5-membered ring structures. By employing alkynes, for instance, cyclopentadiene products could be obtained. The first example of this chemistry was reported by Hashmi et al.[88] They reacted propargyl acetates and ynamides in the presence of gold to produce the corresponding amino-substituted cyclopentadienes (**Scheme 1.38a**). This same reactivity was later reported by Huang, although they used cyclopropenes as starting materials (**Scheme 1.38b**).[89]

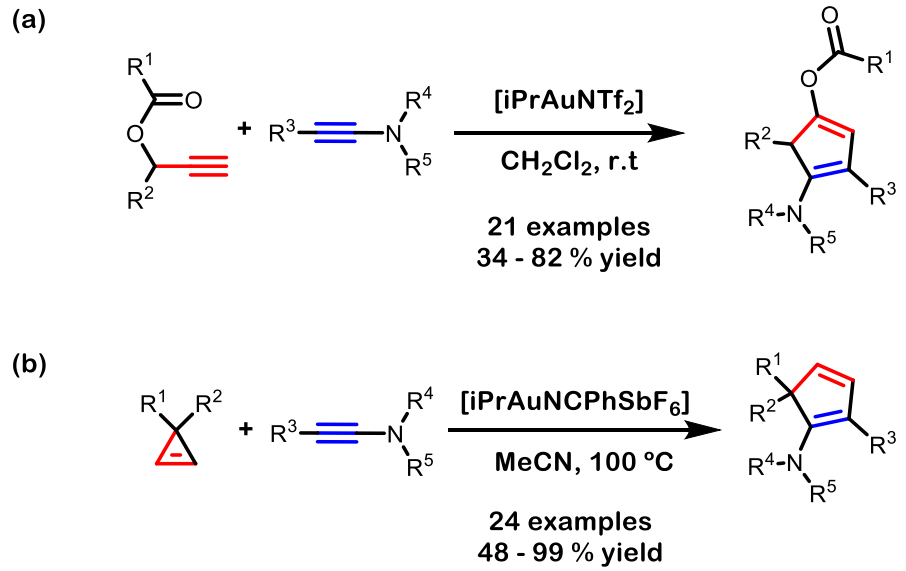

Scheme 1.38. Gold catalyzed [3+2] cycloaddition between vinylcarbenes and ynamides.

The inclusion of allenes in the reaction is also well-tolerated, resulting in cyclopentenes with an additional external double bond. In continuation of their work in gold catalysis and vinyldiazo compounds, the López group reported a regiodivergent [3+2] cycloaddition with allenes. When unbiased substituted allenes were employed, the [3+2] cycloaddition occurred with the external double bond of the allene (**Scheme 1.39a**).[90] On the contrary, when the reaction was conducted with N-allenamides, the reactivity shifted towards the double

bond directed linked to the nitrogen (**Scheme 1.39b**).[91] In both cases, the formation of an initial zwitterionic intermediate takes place upon the addition of the central carbon of the allene at the vinylogous position of the carbene. Depending on the substituents, the reaction evolves towards the formation of one or the other regioisomer. A complementary reactivity is observed when the carbene precursor is a cycloheptatriene, as reported by Echavarren (**Scheme 1.40**).[92] In this scenario, the gold vinylcarbene reacts at the carbenic position, subsequently closing with the internal alkene. The cyclopentene resulting from this step then undergoes isomerization, ultimately yielding the isolated cyclopentadiene products.

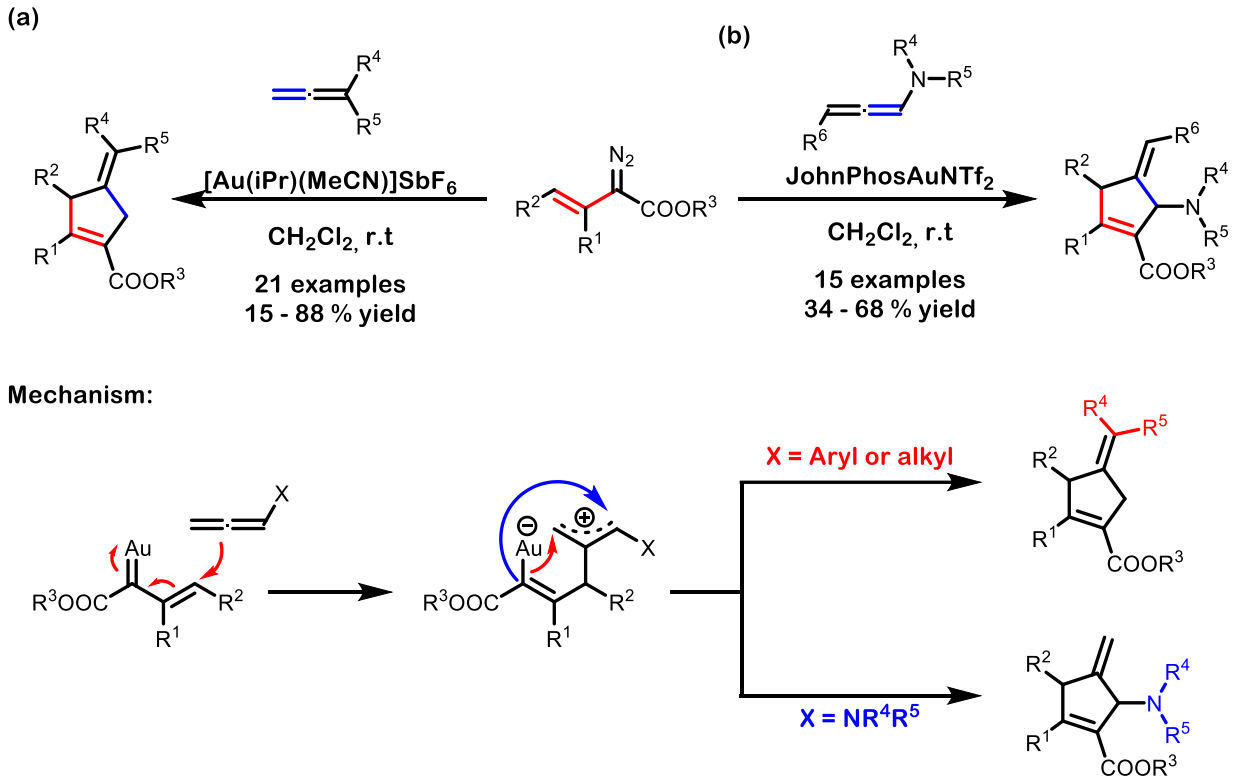

Scheme 1.39. Regiodivergent gold catalyzed [3+2] cycloaddition of vinyldiazo compounds and allenes.

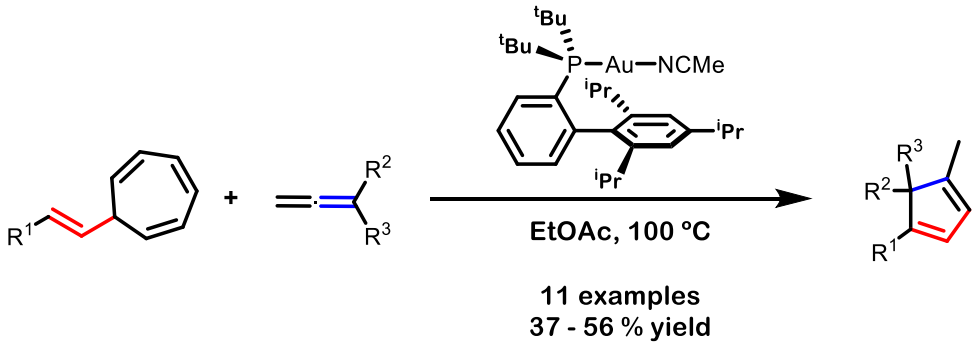

Scheme 1.40. Gold catalyzed [3+2] cycloaddition between allenes and cycloheptatrienes.

Expanding the range of alkenes tolerated in this cycloaddition, the groups of Davies and Doyle independently reported a rhodium-catalyzed [3+2] cycloaddition involving indoles and vinyldiazo compounds. Two complementary reactivities were observed just by working with different starting materials. Davies employed conventional styryl diazo derivatives, proposing an initial addition of the indole into the carbenic position (**Scheme 1.41a**).[93] Optimal regioselectivities were achieved with substituted indoles at either the C2 or C3

positions. On the other hand, Doyle's study focused on the use of enoldiazo compounds, proposing a mechanism based on indole addition at the vinylogous site of the vinyl carbene (**Scheme 1.41b**).[94] Notably, the reaction tolerated unsubstituted indoles without sacrificing regioselectivity. In both examples chiral rhodium catalysts were evaluated, yielding tricyclic indole derivatives with excellent levels of enantioselectivity.

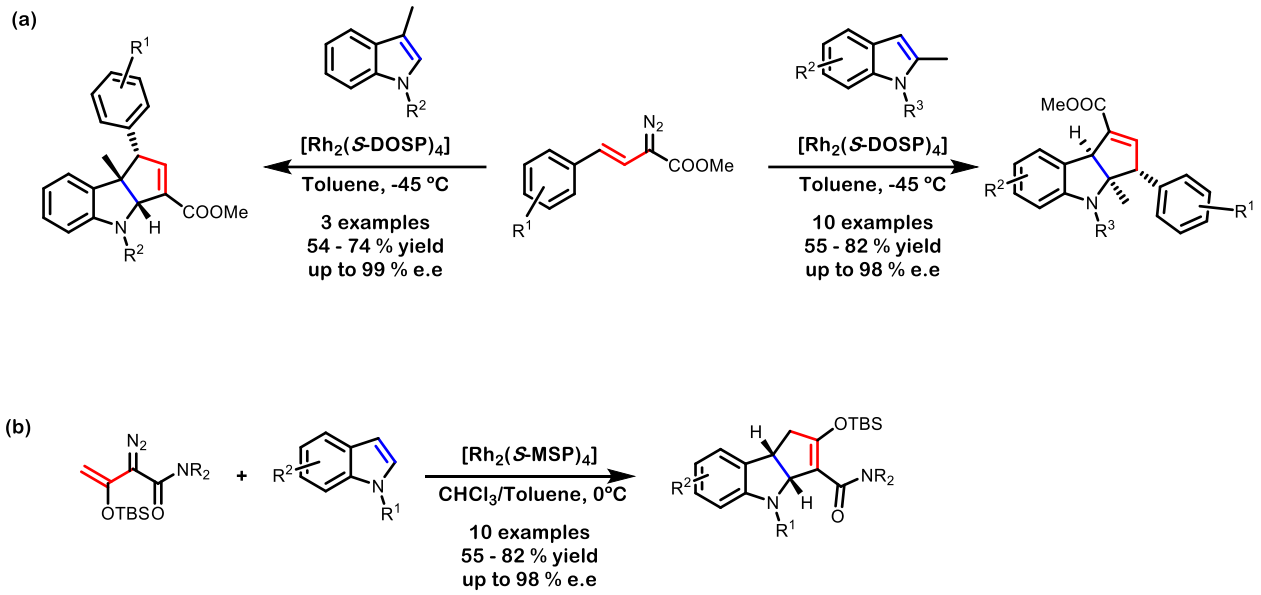

Scheme 1.41. Rhodium catalyzed [3+2] cycloaddition between indoles and vinyldiazo compounds.

1.2.2.1.4. [3+3] Cycloadditions

All the examples presented so far, relied in the use of unsaturated compounds as partners for the cycloaddition reactions. Nevertheless, the synthetic chemistry community has increasingly recognized the potential of ylides in reacting with vinylcarbenes. The inherent nucleophilicity arising from the negative charge in ylides, coupled with the electrophilic nature of metal carbenes, renders ylides exceptionally well-suited partners for engaging in reactions with vinylcarbenes.

The pioneering work in this chemistry was carried out by the Toste group. In 2008, they reported a gold-catalyzed [3+3] cycloaddition between propargyl acetates and azomethyl ylides, yielding bicyclic compounds (**Scheme 1.42a**).[95] Four years later, the Doyle group demonstrated the use of enoldiazo compounds in a similar reaction with azomethyl ylides (**Scheme 1.42b**) under rhodium catalysis.[96] It is noteworthy to highlight the mechanistic differences between these examples. When propargyl esters are employed, the initial addition of the negatively charged nitrogen from the ylide occurs at the carbenic position. Conversely, when enoldiazo compounds are utilized, the addition takes place at the vinylogous site, as confirmed by DFT calculations by the Xue group.[97]

In addition to azomethyl ylides, various other ylides have been explored for this transformation. Simply by substituting the negatively charged nitrogen with an oxygen, and employing nitrones, the corresponding azaoxacyclic scaffolds could be obtained. Notably, the Hashmi group reported a platinum-catalyzed [3+3] cycloaddition involving ortho-propargyl anilines and nitrones, yielding indolyl derivatives (**Scheme 1.43a**).[98] On the other hand, the Doyle group capitalized on enoldiazo compounds under rhodium catalysis for the

enantioselective synthesis of oxazine derivatives (**Scheme 1.43b**).[99] In both cases, the initial nucleophilic addition of the nitrone takes place at the remote position of the vinylcarbene.

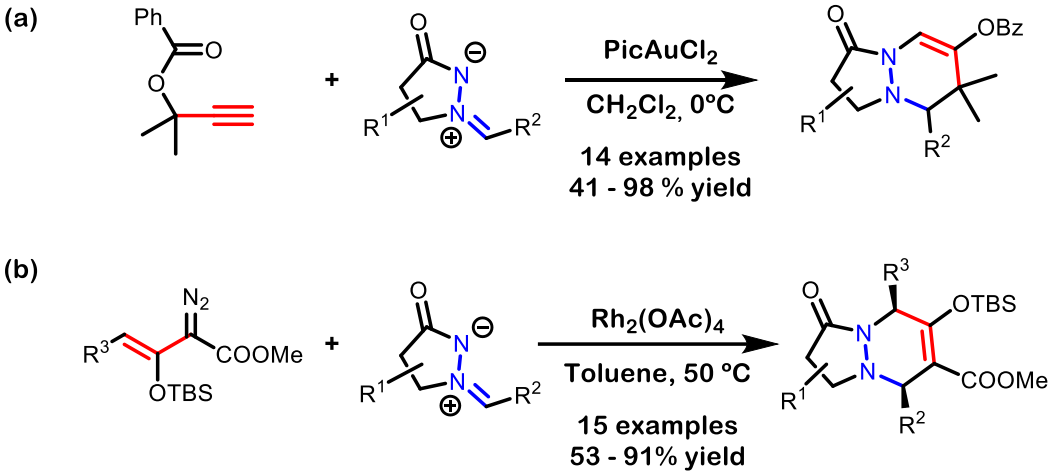

Scheme 1.42. Rhodium and gold catalyzed [3+3] cycloaddition between vinylcarbenes and azomethyl ylides.

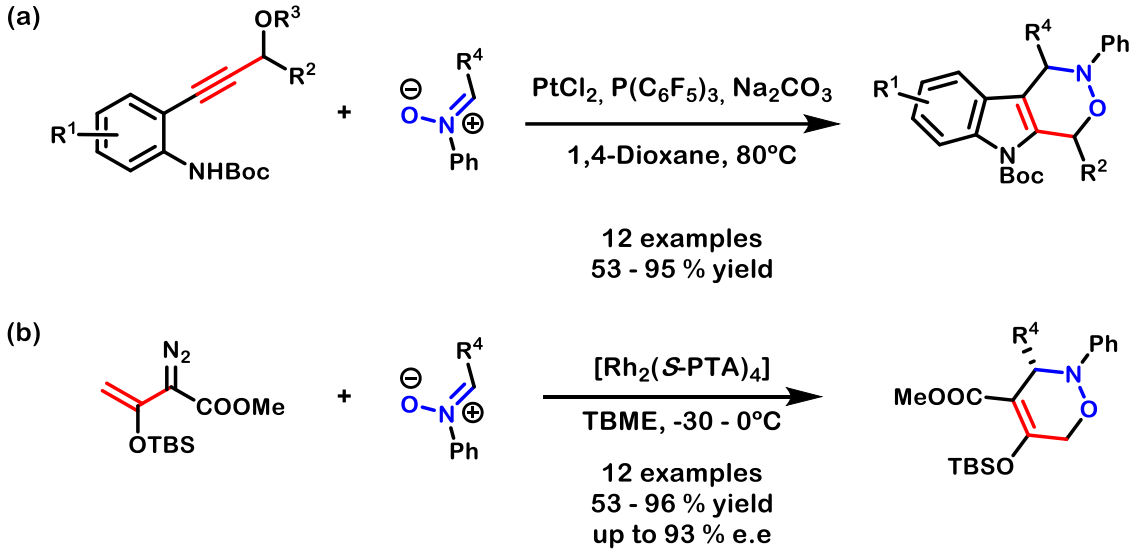

Scheme 1.43. Platinum and rhodium catalyzed [3+3] cycloaddition between vinylcarbenes and nitrones.

The Doyle group continued to broaden the range of ylides compatible with rhodium-catalyzed [3+3] cycloaddition reactions involving enoldiazo compounds. *N*-acyliminopyridinium ylides proved effective for the synthesis of tetrahydropyridazines with high yields and enantioselectivities (**Scheme 1.44a**).[100] Additionally, they explored the utility of isoquinolinium/pyridinium methylides as ylides for this transformation (**Scheme 1.44b**).[101] As anticipated from prior findings, the reaction initiated at the vinylogous position, as confirmed by DFT calculations.[102]

More recently the group of Zhang reported the copper catalyzed [3+3] cycloaddition between vinylsulfoxonium ylides and cyclopropenones for the preparation of substituted phenols (**Scheme 1.45**).[103] The generated copper vinylcarbene was trapped by an *in situ* formed ylide from cyclopropenone. The final step involves the aromatization of the newly formed cyclohexanone, ultimately yielding the phenol derivatives.

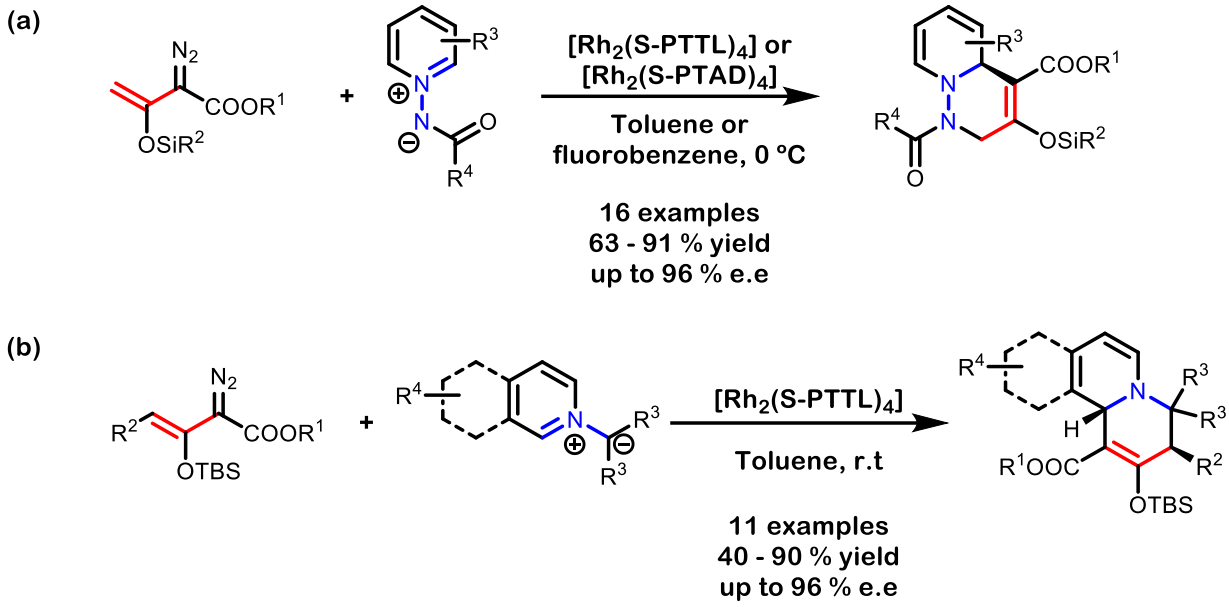

Scheme 1.44. Rhodium catalyzed [3+3] cycloaddition using enoldiazo compounds.

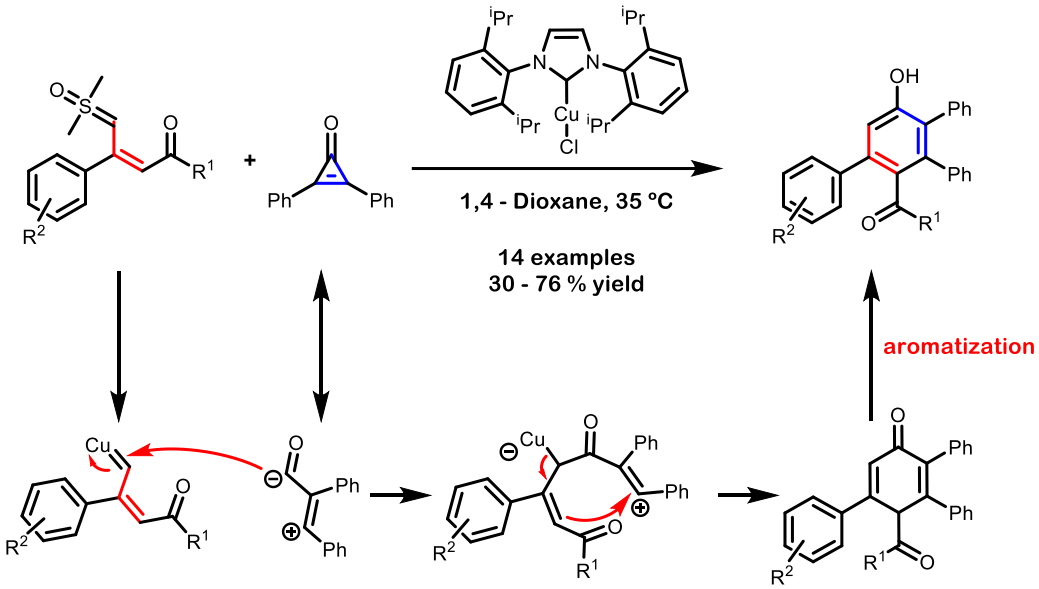

Scheme 1.45. Copper catalyzed [3+3] cycloaddition between vinyl sulfoxonium ylides and cyclopropenones.

1.2.2.1.5. [3+1] Cycloadditions

Building on their contributions to the field of [3+3] cycloadditions, the Doyle group recognized that modifying the ylide structure could open avenues for diverse cycloaddition reactions. In this context, sulfur ylides emerged as excellent partners, serving as a one-carbon synthon for the synthesis of four-membered-ring compounds through [3+1] cycloadditions involving the alkenyl unit of the vinylcarbene.

The first example of this chemistry in 2017 focused on the enantioselective synthesis of cyclobutenes by employing enoldiazo compounds and carbonyl-derived sulfur ylides under copper catalysis (**Scheme 1.46a**).[104] Expanding on this work, the same group demonstrated that modifying the carbonyl unit of the sulfur ylide with an N-arylamino group resulted in the synthesis of chiral azetidines with high yields and enantiomeric excesses (**Scheme 1.46b**).[105] Subsequent investigations in a later study further explored the potential applications of

these azetidine compounds.[106] The mechanism of the reaction is initiated by the addition of the nucleophilic nitrogen of the ylide into the vinylogous position of the copper carbene. In contrast to the previously reported [3+2] and [3+3] cycloaddition, the subsequent step involves the addition of the double bond of the vinylcopper intermediate, followed by the loss of SPh_2. The mechanism is completed by the extrusion of the copper catalyst, ultimately yielding the azetidine derivatives.

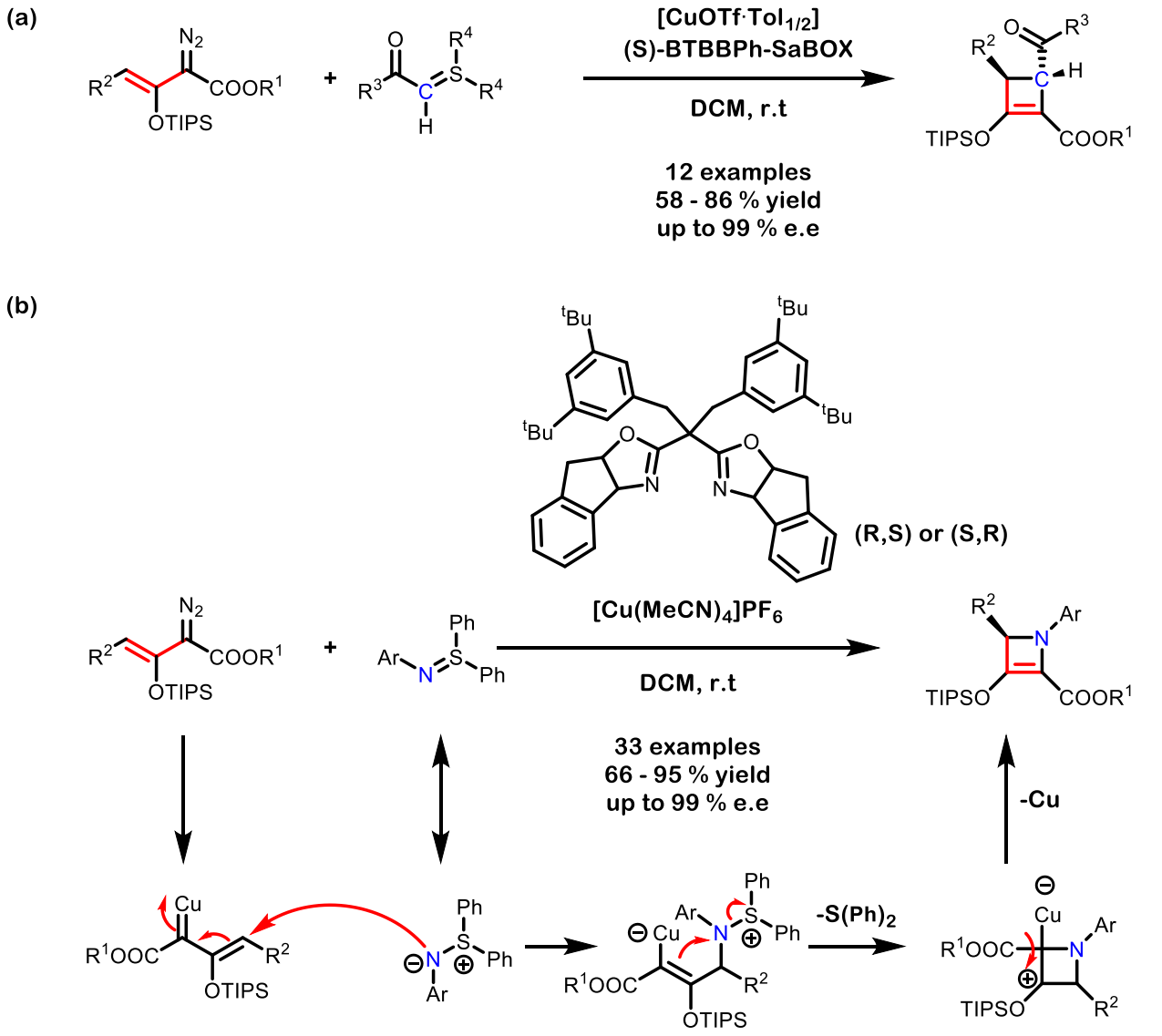

Scheme 1.46. Copper catalyzed [3+1] cylcloaddition between enoldiazo compounds and sulfur ylides.

1.2.2.1.6. Higher order cycloadditions

Recent reports have emerged involving vinylcarbenes in higher order cycloadditions. These transformations rely on either extending the ylide used in the process or elongating the conjugation in the vinylcarbene precursor. Notably, Yoo's group reported a [3+5] cycloaddition involving enoldiazo compounds and 1,5-dipole equivalents under rhodium catalysis (**Scheme 1.47**).[107] The proposed mechanism for this transformation involves the initial addition of the negatively charged nitrogen into the vinylogous position of the vinylcarbene. Subsequently, the newly formed ylide collapses into the 2-position of the pending positively charged pyridine,

resulting in the formation of the final six-eight fused bicyclic compounds. DFT calculations carried out by the same group proved the validity of the initial mechanistic hypothesis.[108]

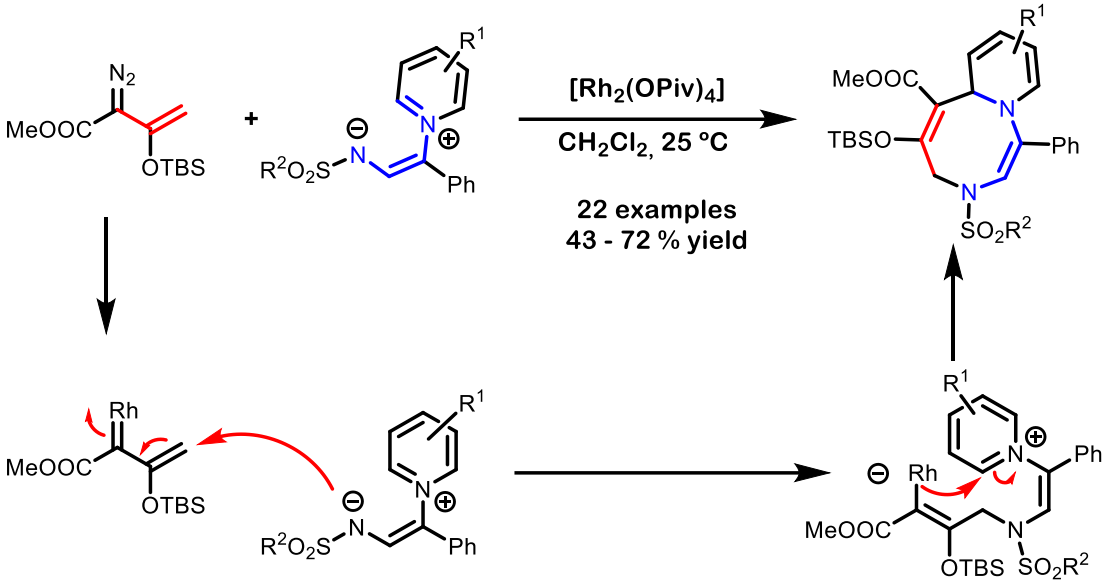

Scheme 1.47. Rhodium catalyzed [3+5] cycloaddition between enoldiazo compounds and 1,5-dipole equivalents.

In 2021, the group of Krasavin introduced a novel class of vinyl diazo compounds based on a succinimide scaffold.[109] While exploring the reactivity of these new carbene precursors, they discovered that the aryl substituent in the vinyl moiety facilitates the participation of the product in [5+2] cycloadditions. Indeed, the reaction of nitriles with diazo succinimides under rhodium catalysis resulted in the synthesis of benzoazepine derivatives (**Scheme 1.48a**).[110] The proposed mechanism involves the addition of the nitrile into the carbenic carbon, leading to the formation of the corresponding nitrile ylide. This intermediate undergoes a 1,7-electrocyclization, followed by a 1,5-hydrogen shift, resulting in the generation of benzazepines derivatives. Based on this report, the same group continued to expand the boundaries of this chemistry and demonstrated analogous behavior with aldehydes[111] and ketones[112] (**Scheme 1.48b**).

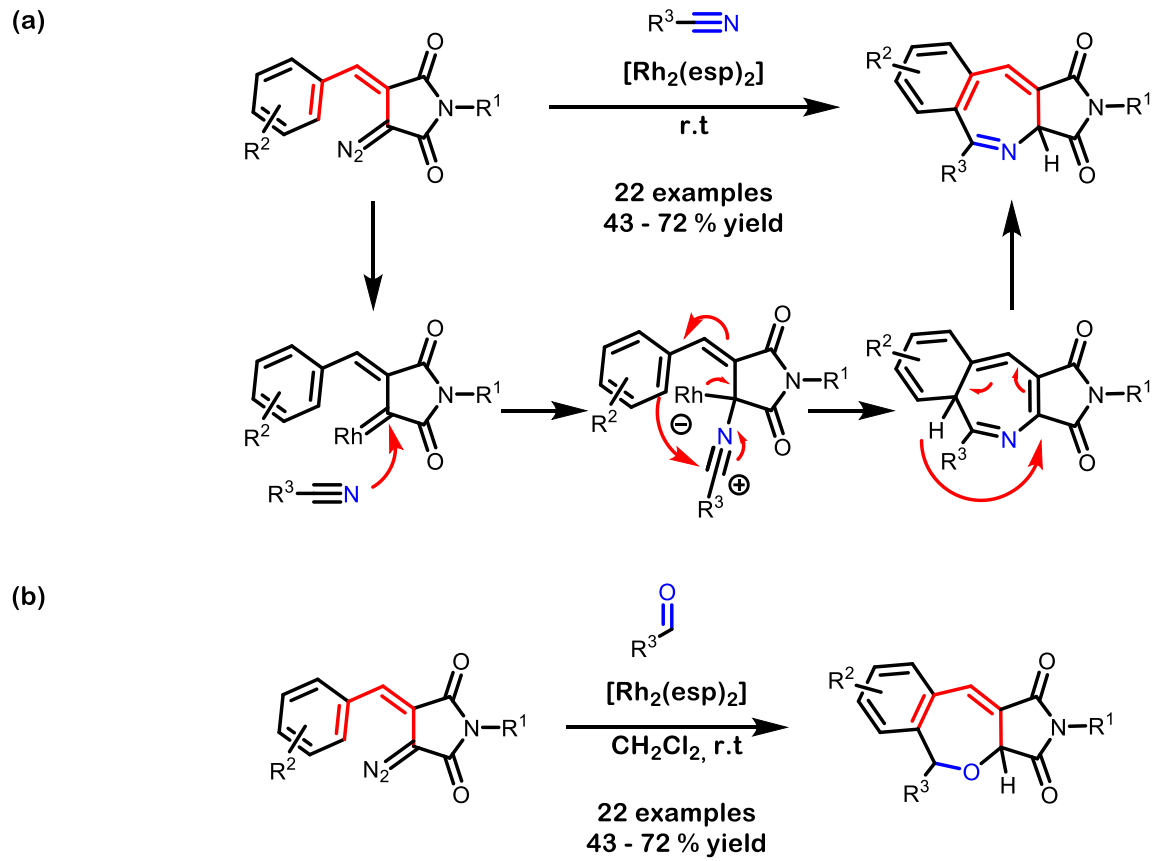

Scheme 1.48. Rhodium catalyzed [5+2] cycloaddition between diazo succinimides and nitriles and aldehydes.

1.2.2.2. C-H Insertion reactions

1.2.2.2.1. C*sp*^{3}-H Insertion

All the examples so far have predominantly explored the cycloaddition reactions of metal vinylcarbenes. However, metal vinylcarbenes can also undergo insertion reactions into C-H bonds. The efficacy of metal carbenes in C*sp*^{3}-H bond insertion is well-established,[113] and by extrapolating this reactivity to the vinylcarbene family, allyl substituted products can be successfully obtained. The first examples of this chemistry were reported in the early 1990s by the group of Muller, who used cyclopropenes as the carbene precursors (**Scheme 1.49**).[114] In their approach, the rhodium vinylcarbene, *in situ* generated by heating a cyclopropene decorated with an alkyl chain in the presence of rhodium perfluorobutyrate, inserted into the pending C*sp*^{3}-H bond. Although the reported yields were modest, these findings served as a proof of concept, highlighting the potential of vinylcarbenes to participate in C*sp*^{3}-H bond functionalization.

The group of Davies expanded their work in the vinylcarbene realm studying the potential of vinyl diazo compounds in C*sp*^{3}-H insertion reactions. While exploring the C-H insertion of donor-acceptor and acceptor-acceptor carbenes into cyclohexane, they reported one example of vinyldiazoacetate insertion into the cyclohexane ring.[115] Surprisingly, when the reaction was carried out using cyclohexadienes, an isomerized product was observed (**Scheme 1.50**).[116] The resulting product required the involvement of the alkenyl unit of the carbene, underscoring the remarkable versatility of vinylcarbenes in developing novel transformations that would otherwise remain beyond the scope of conventional carbene chemistry. Although the reaction scope

was limited, several vinyldiazo compounds were tested and the reactions could be enantioselectively carried out using [Rh_2(*S*-DOSP)$_4$] as the catalyst. The proposed mechanism for this transformation was based on a concerted yet asynchronous process involving hydride-transfer and C−C bond-formation as corroborated by DFT calculations.[117] Moreover, the same group exploited this chemistry for the preparation of several natural products.[118]

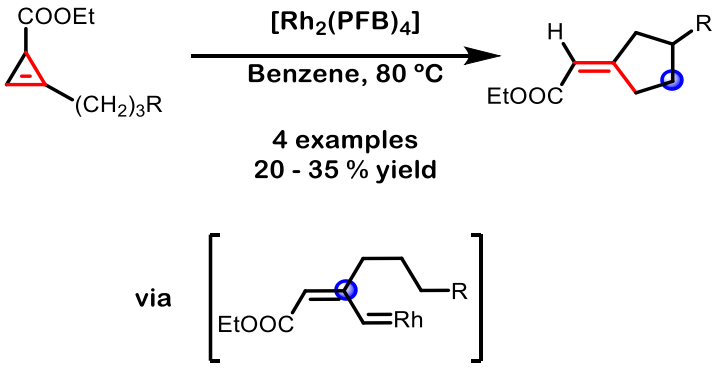

Scheme 1.49. Rhodium catalyzed C*sp*^{3}-H bond insertion of *in situ* generated vinylcarbenes.

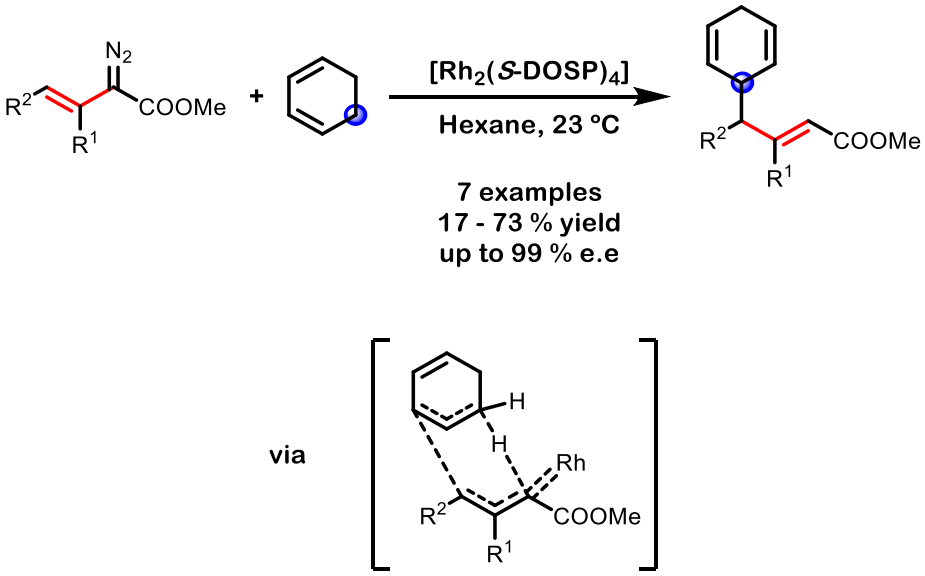

Scheme 1.50. Rhodium catalyzed C-H activation of vinyldiazoacetates and cyclohexadiene.

While the field of C*sp*^{3}-H insertion of vinylcarbenes has predominantly been dominated by rhodium,[119] copper and gold catalysts,[120] several groups have explored the potential of other metals in this domain. Notably, in 2008, the group of Dias reported the first instance of silver-catalyzed vinylcarbene insertion into C*sp*^{3}-H bonds. The process involved the reaction of methyl styryldiazoacetate with alkanes in the presence of trispyrazolyl-based silver catalysts, yielding insertion into the carbenic carbon (**Scheme 1.51a**).[121] More recently, the Bi group presented analogous findings employing *N*-triftosylhydrazones as carbene precursors for the allylic functionalization of alkanes (**Scheme 1.51b**).[122]

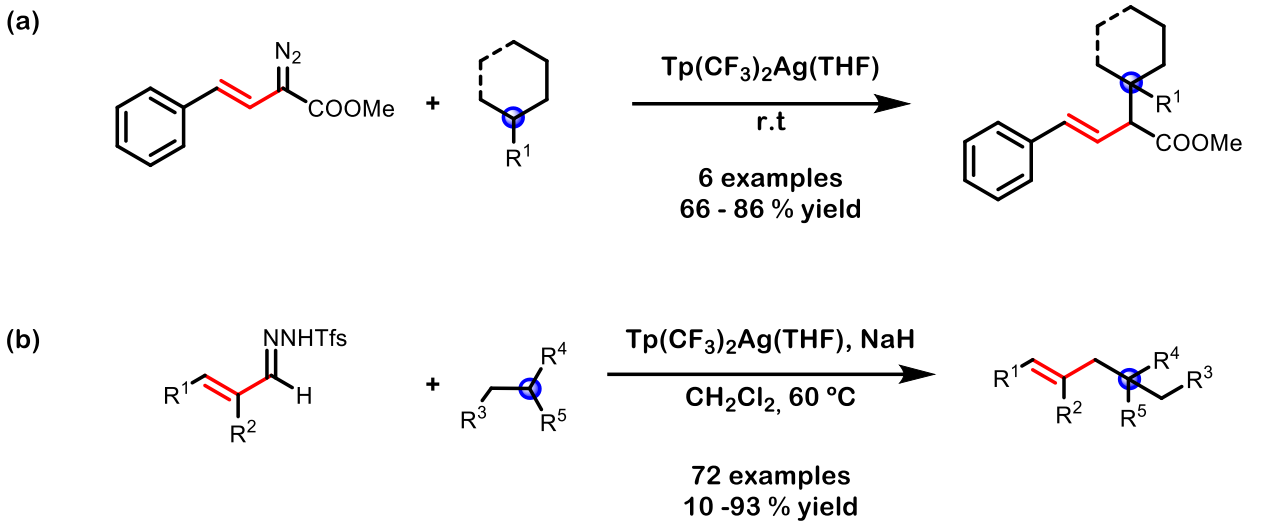

Scheme 1.51. Silver catalyzed vinylcarbene insertion into C*sp*^{3}-H bonds.

In addition to intermolecular reactions, several reports have studied the intramolecular C*sp*^{3}-H insertions. The group of Cossy draw inspiration from the initial reports from Muller and explored the reactivity of cyclopropenes with pendant alkyl moieties. Their approach involved the reaction of these derivatives in the presence of rhodium acetate, leading to the formation of C-H insertion adducts with both high yields and diastereoselectivities (**Scheme 1.52**).[123] Three years later the group of Doyle, reported the use of enoldiazoacetamides as excellent substrates for the enantioselective preparation of β-lactam derivatives in the presence of rhodium catalysts (**Scheme 1.53**).[124]

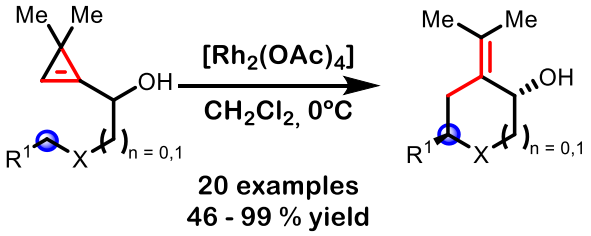

Scheme 1.52. Rhodium catalyzed intramolecular C*sp*^{3}-H insertion of cyclopropenes.

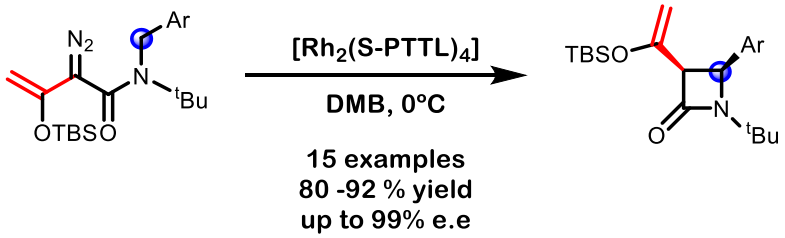

Scheme 1.53. Rhodium catalyzed intramolecular C*sp*^{3}-H insertion of enoldiazoacetamides.

The Fürstner group recently disclosed an innovative approach to carbene generation through the gem-hydrogenation of alkynes. In this ruthenium-catalyzed process two hydrogen atoms of a hydrogen molecule are effectively transferred to one carbon of an alkyne, resulting in the formation of a ruthenium carbene on the remaining carbon of the triple bond.[125]

Extending the application of this methodology, the same research group demonstrated the gem-hydrogenation of enynes, leading to the generation of a ruthenium vinylcarbene that undergoes intramolecular insertion into a Csp^3-H bond yielding tetrahydrofuran compounds (**Scheme 1.54**).[126]

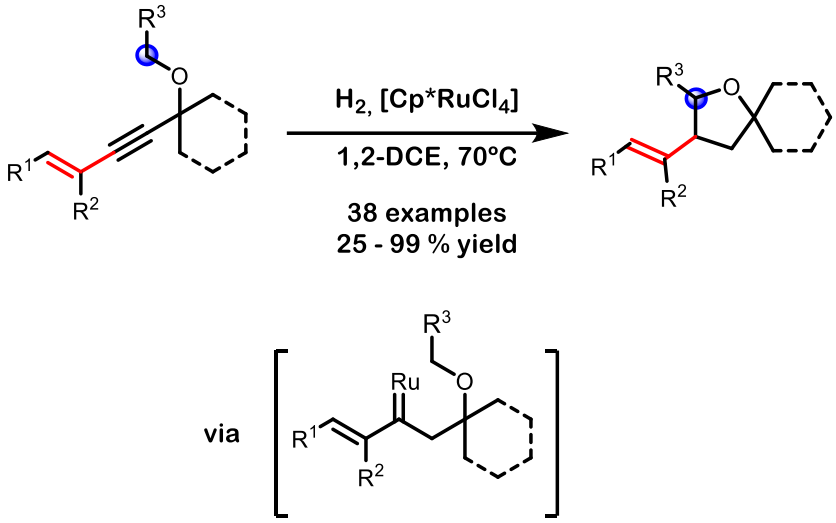

Scheme 1.54. Ruthenium catalyzed gem-hydrogenation of enynes followed by Csp^3-H insertion.

All the reactions so far have relied on the Csp^3-H insertion into the carbenic position of the vinylcarbene. To the best of our knowledge, only one instance in the literature has explored the insertion at the vinylogous position. The group of Liu reported the intramolecular insertion of a Csp^3-H bond from an acetal group into the remote position of a gold vinylcarbene, formed through the isomerization of an allenene group (**Scheme 1.55**).[127] The proposed mechanism for this transformation initiates with the gold catalyst coordinating to the allene moiety. Subsequent cyclization with the alkene unit results in the generation of the gold vinylcarbene. Instead of a concerted CH insertion, an hydride shift to the carbenic position takes place. Following this, S_E2' addition at the vinylogous position yields the ultimate tricyclic scaffold. Upon acid work-up, the tricyclic structure undergoes hydrolysis, ultimately leading to the formation of the ketone derivative.

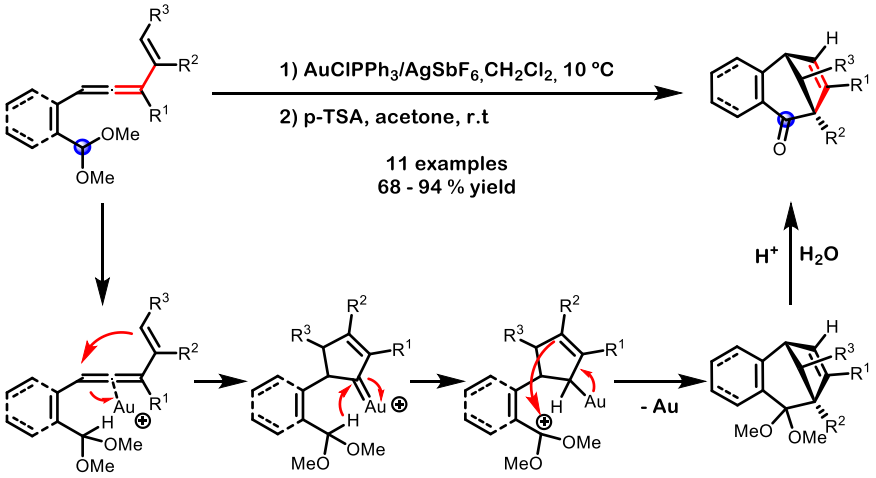

Scheme 1.55. Gold catalyzed intramolecular vinylogous Csp^3-H insertion.

1.2.2.2.2. Csp^2-H Insertion

In addition to the early examples of Csp^3-H insertion using cyclopropenes, the potential functionalization of Csp^2-H bonds can be envisioned by strategically introducing an aryl moiety. This reactivity was initially revealed by Padwa et al. in 1982.[128] When a cyclopropene with a pending phenyl group was reacted in the presence of silver perchlorate, the formation of the corresponding indene product was observed, entailing a Csp^2-H insertion (**Scheme 1.56**). Although the examples were limited, these findings laid the ground for vinylcarbene insertion into Csp^2-H bonds. Subsequently, various groups reported improved results using diverse metals as catalysts, including gold,[129] palladium,[130] and copper.[131]

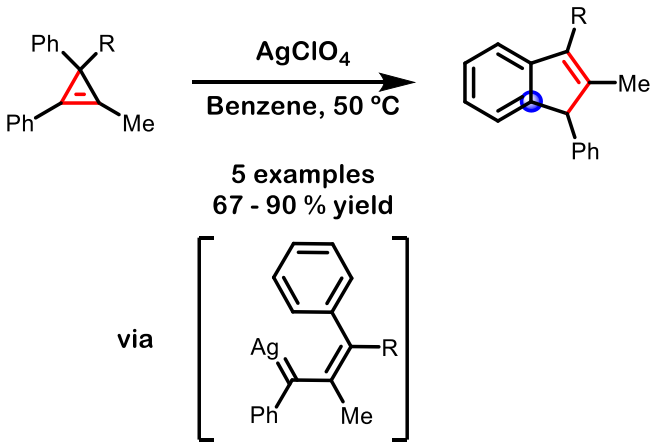

Scheme 1.56. Silver catalyzed Csp^2-H insertion using cyclopropenes as carbene precursors.

Furthermore, the identical reaction pattern could be observed upon carbene precursor modification. In this context, Sarpong harnessed the ability of propargyl esters to generate vinylcarbenes and reported a platinum-catalyzed intramolecular Csp^2-H insertion using this kind of vinylcarbene precursor. (**Scheme 1.57**).[132] Notably, the versatility of this reaction extends beyond benzene derivatives, as the reaction scope includes functionalization of a pendant pyrrole and indole rings as well.

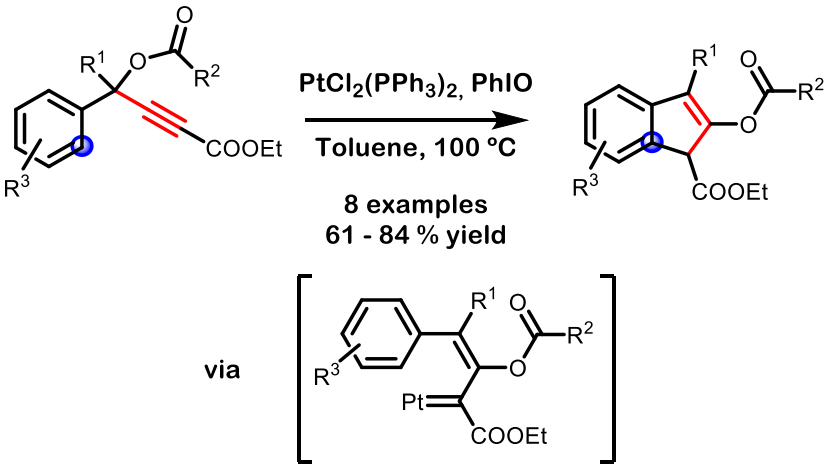

Scheme 1.57. Intramolecular platinum catalyzed Csp^2-H insertion.

Given the success in the intramolecular Csp^2-H insertion, the group of Davies reported the first example of the intermolecular version of the reaction (**Scheme 1.58**).[43] Through the reaction of vinyldiazo compounds with arene derivatives under rhodium catalysis, the resulting Csp^2-H insertion product was observed. Nonetheless, the reaction suffered limitations due to the formation of Buchner adducts under the reaction conditions, highlighting the challenge of achieving selective intermolecular Csp^2-H insertion into benzene derivatives.

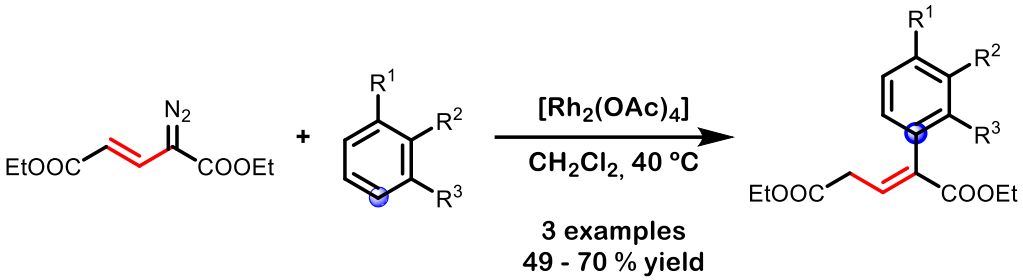

Scheme 1.58. Rhodium catalyzed intermolecular vinyldiazo Csp^2-H insertion.

To overcome these challenges, the same group transitioned from benzene to pyrrole and indole derivatives. In this scenario, employing a slightly modified vinyldiazo compound in the presence of $[Rh_2(esp)_2]$ and C_1 or C_2 methyl-substituted indoles or pyrroles resulted in the formation of the corresponding vinylogous Csp^2-H insertion adduct (**Scheme 1.59**).[133] Intriguingly, the removal of the methyl group led to carbenic functionalization as the primary product, emphasizing the key role of increased steric bulkiness attributed to the methyl group in the reaction selectivity. Two years later the same group reported the enantioselective version of the reaction using the $[Rh_2(S\text{-biTISP})_2]$ catalyst. [134]

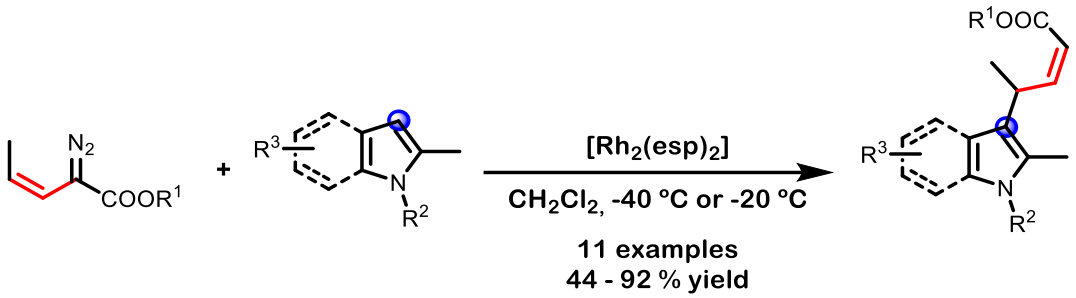

Scheme 1.59. Intermolecular rhodium catalyzed vinylogous Csp^2-H functionalization of indoles or pyrroles.

The synthetic community sought also to achieve selective functionalization of benzene derivatives, with vinyl diazo compounds employing alternative catalytic systems. Notably, in 2012, the López group reported the selective gold-catalyzed vinylogous Csp^2-H insertion of aryls with vinyldiazo compounds (**Scheme 1.60**).[135] Building upon these findings, they subsequently extended the same reactivity into ferrocene and ruthenocene functionalization.[136]

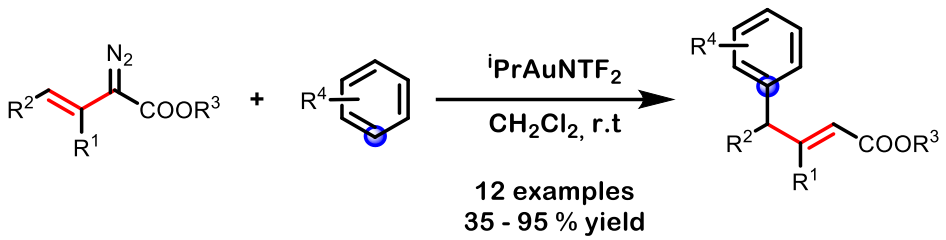

Scheme 1.60. Intermolecular gold catalyzed vinylogous Csp^2-H functionalization of benzene derivatives.

More recently, Xu improved even further this reactivity and unveiled the enantioselective version of the aryl vinylogous Csp^2-H insertion. In this instance, the reaction employed aniline derivatives as the arene unit, utilizing a catalytic system based on the combination of rhodium(I) with chiral cyclic dienes as ligands (**Scheme 1.61a**).[137] Notably, the reaction showed tolerance to the presence of hydroxyl groups in the aniline derivative, without the formation of the corresponding OH-insertion adduct. Subsequently, the same group conducted the reaction in the presence of chiral cinchona alkaloids, resulting in the formation of dihydrobenzofurans in a one-pot reaction, involving a cascade vinylcarbene Csp^2-H insertion followed by an oxa-Michael addition (**Scheme 1.61b**).[138] The success of this reactivity motivated the same group to report the intermolecular Csp^2-H insertion using a similar catalytic system, this time with pyrroles and indoles.[139]

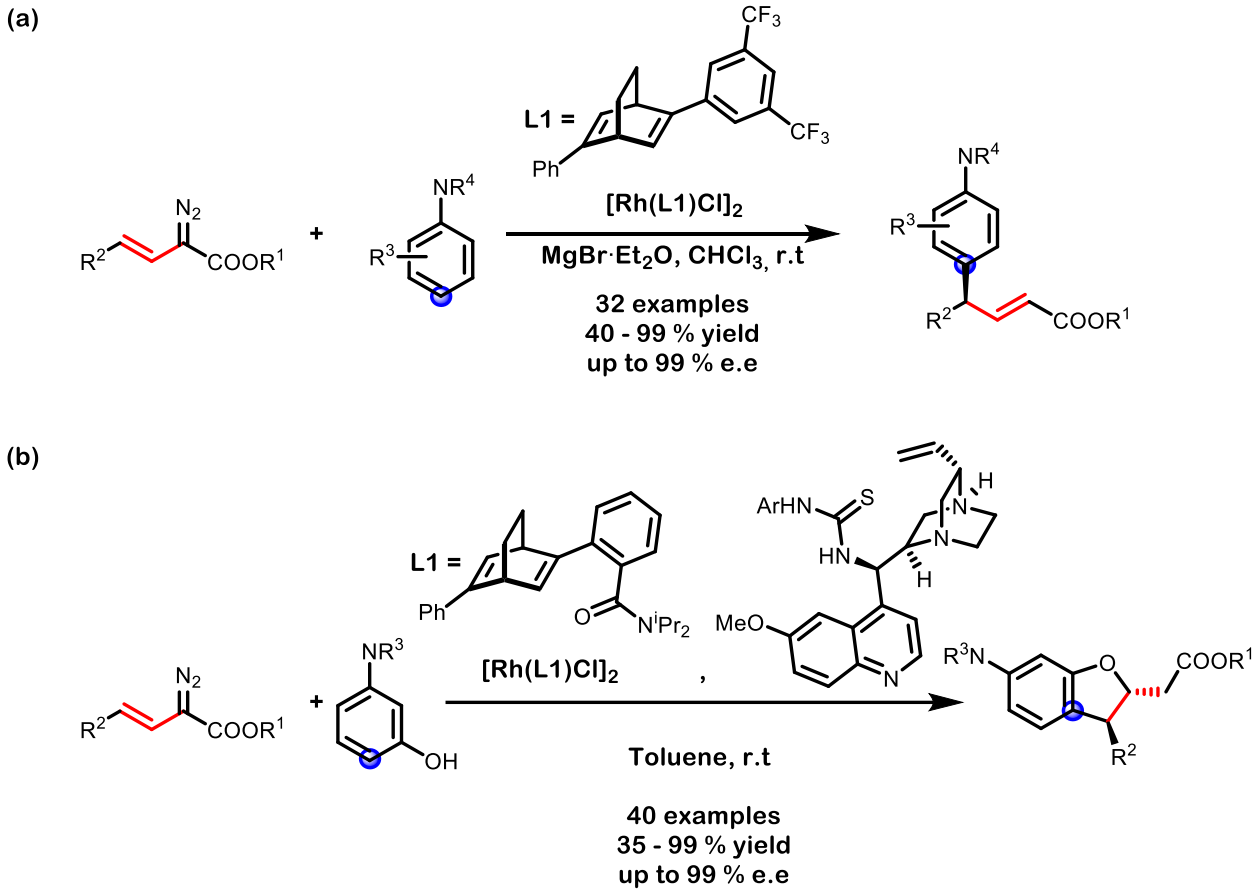

Scheme 1.61. Intermolecular rhodium catalyzed vinylogous Csp^2-H functionalization of aniline derivatives.

1.2.2.3. X-H insertion reactions

The insertion reactions involving vinylcarbenes extend beyond C-H bonds. Due to the lower bond dissociation energy of heteroatom-hydrogen (X-H) bonds compared to C-H bonds, the insertion of carbenes into X-H bonds is easier. Extensive documentation supports the ability of carbenes to insert into a diverse range of X-H bonds, suggesting a similar reactivity for vinylcarbenes.[140]

The first example of this reactivity dates to 1987 by the Davies group. By reacting vinyldiazo compounds with several alcohols in presence of rhodium acetate, vinyl ethers could be obtained in good yields upon O-H insertion and double-bond isomerization (**Scheme 1.62a**). [31] In continuation of this results, the group of Landais reported the Si-H insertion using the same catalytic system (**Scheme 1.62b**). [141] The enantioselective version of this Si-H insertion was disclosed later by the group of Davies, using the [Rh_2(*S*-DOSP)$_4$] catalyst.[142]

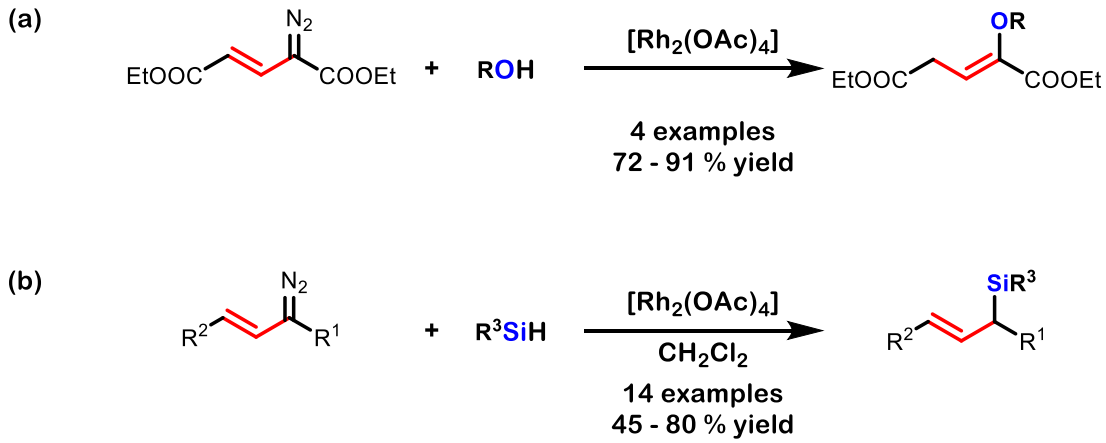

Scheme 1.62. Rhodium catalyzed O-H and Si-H insertion of vinyldiazo compounds.

After these pioneering examples, the Davies group began exploring the regioselectivity of the reaction using catalysts based on other metals. In their initial findings, they demonstrated that a molybdenum-based catalyst selectively promoted the insertion of methanol at the remote position (as a mixture of Z/E isomers) (**Scheme 1.63**), whereas rhodium predominantly yielded the carbenic product.[143] Just as observed with molybdenum catalysts, the same research group later reported that when employing ruthenium paddlewheel complexes, vinylogous O-H insertion emerged as the major product.[144]

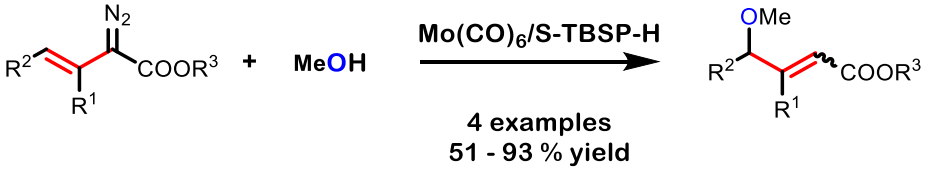

Scheme 1.63. Molibdenum catalyzed vinylogous OH insertion using vinyldiazo compounds.

After these proof of concept studies, research was centered on improving the yield, scope, and selectivity, particularly regarding Z/E isomerism in the vinylogous product. Initial findings by Hu showed that the use of a silver catalyst provided highly selective reactions, although the scope of the study was limited to just two examples.[145] In 2011, Davies presented a comprehensive comparative study on the rhodium- and silver-catalyzed O-H and N-H insertion of vinyldiazo compounds.[146] Under rhodium catalysis, functionalization at the carbenic site prevailed as the major product (**Scheme 1.64a)**. In contrast, treatment with silver triflate

resulted in the corresponding vinylogous product with complete regiocontrol (**Scheme 1.64b**). Seven years later, the Nemoto group reached similar conclusions, employing silver tetrafluoroborate as the catalyst in this case.[147]

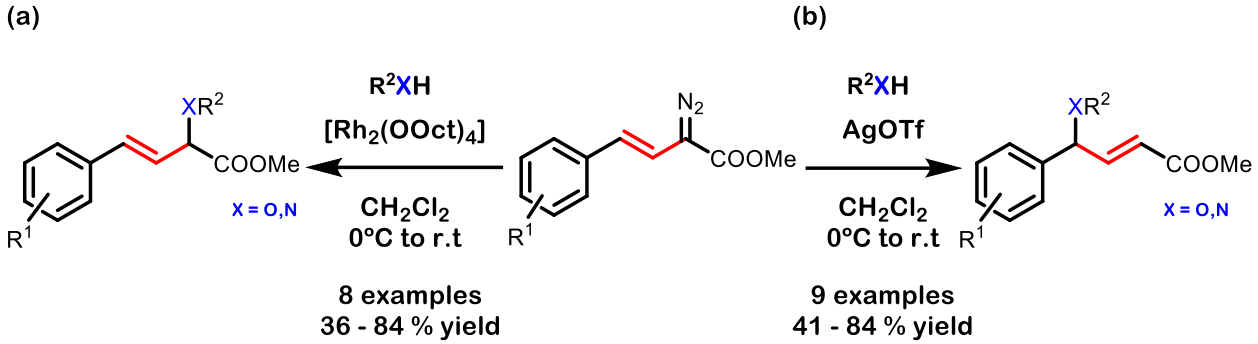

Scheme 1.64. Rhodium and silver divergent selectivity in the intermolecular X-H insertion of vinyldiazo compounds.

The Sun group further expanded this chemistry by employing 2-pyridones as the O-H bond source.[148] As expected, the use of silver as the catalyst exclusively provided the vinylogous product **(Scheme 1.65a)**. Conversely, employing a gold source as the catalyst allowed for the selective generation of the carbenic product (**Scheme 1.65b**). The enantioselective version of this carbenic reactivity was later reported by the same group using chiral gold catalysts.[149]

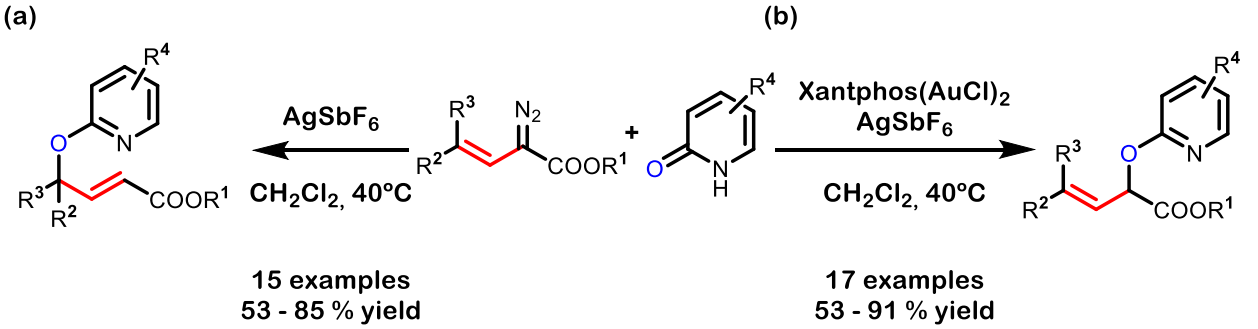

Scheme 1.65. Gold and silver divergent selectivity in the intermolecular O-H insertion of vinyldiazo compounds and 2-pyridones.

Following the success achieved in X-H insertion reactions with vinyldiazo compounds, various reports appeared employing alternative carbene sources for this transformation. The Lee group, reported the gold-catalyzed intermolecular functionalization of cyclopropenes using alcohols, yielding exclusively the vinylogous product (**Scheme 1.66a**).[150] Similar outcomes were reported by Dong *et al.*, using secondary amines for the corresponding N-H insertion (**Scheme 1.66b**).[151] Conversely, the Vicente group detailed the synthesis of allylsilanes through a zinc-catalyzed Si-H insertion,[152] through a reaction that selectively takes place at the carbenic position (**Scheme 1.66c**). The same group extended on this work by reporting similar reactivity using rhodium catalysts.[153]

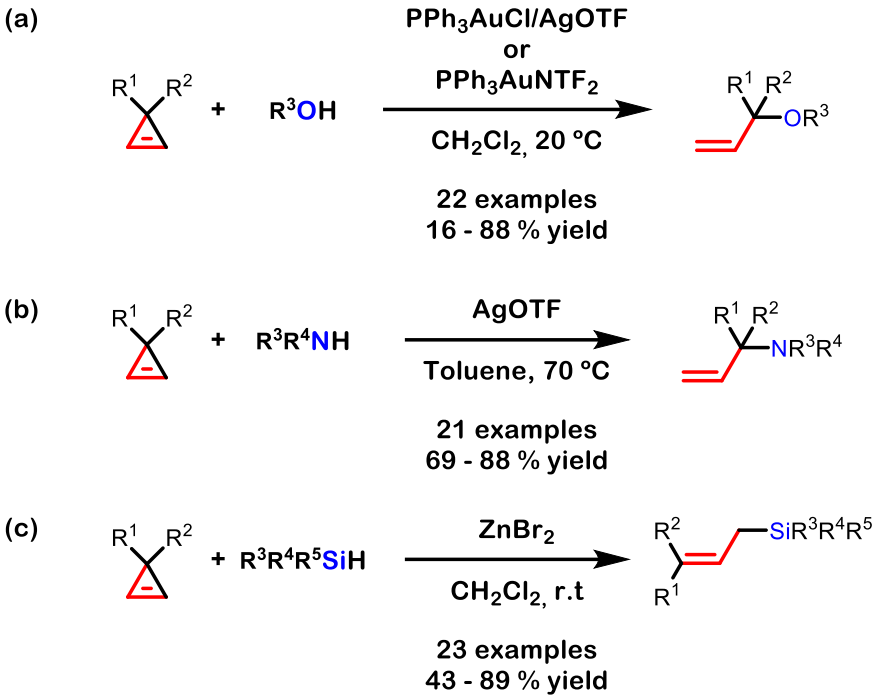

Scheme 1.66. Intermolecular X-H insertion reaction using cyclopropenes as carbene precursors.

The Echavarren group also evaluated the reactivity of vinylcarbenes in X-H insertions employing their well-established retro-Buchner strategy for vinyl carbene *in situ* generation. Upon reacting cycloheptatriene derivatives in the presence of silanes under rhodium catalysis, they successfully obtained the corresponding allyl silanes through carbenic functionalization (**Scheme 1.67a**).[68] The Bi group expanded their work using vinyl-N-triftosylhydrazones under silver catalysis and reported the corresponding carbenic Si-H insertion (**Scheme 1.67b**).[154]

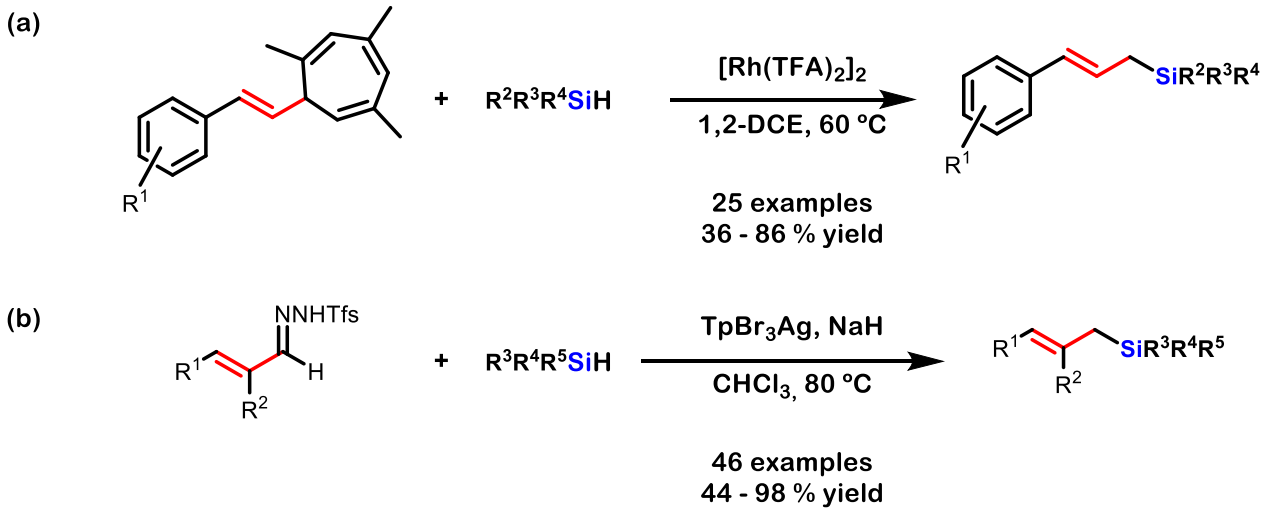

Scheme 1.67. Intermolecular Si-H insertion on vinylcarbenes *in situ* generated from cycloheptatrienes and triftosylhydrazones.

In addition to silanes, amines, and alcohols, other types of X-H bonds can participate in carbene insertion reactions. B-H bonds have recently emerged as candidates for such transformations.[155] In the field of vinylcarbene chemistry, the first example of a B-H insertion was reported in 2020 by Vilotijevic. In this study, the authors employed borane–phosphine adducts, reacting them with vinyldiazo compounds in the presence of a copper catalyst, yielding the corresponding phosphine-protected allylboranes (**Scheme 1.68a**).[156] More recently, the Zhu group expanded on this chemistry by utilizing cyclopropenes as carbene precursors and borane-amino adducts as the B-H source to synthesize the desired borane derivatives (**Scheme 1.68b**).[157] Additionally, the same group reported the enantioselective version of this transformation, employing a chiral copper catalyst.[158] In all these examples the reaction takes place selectively on the carbenic site.

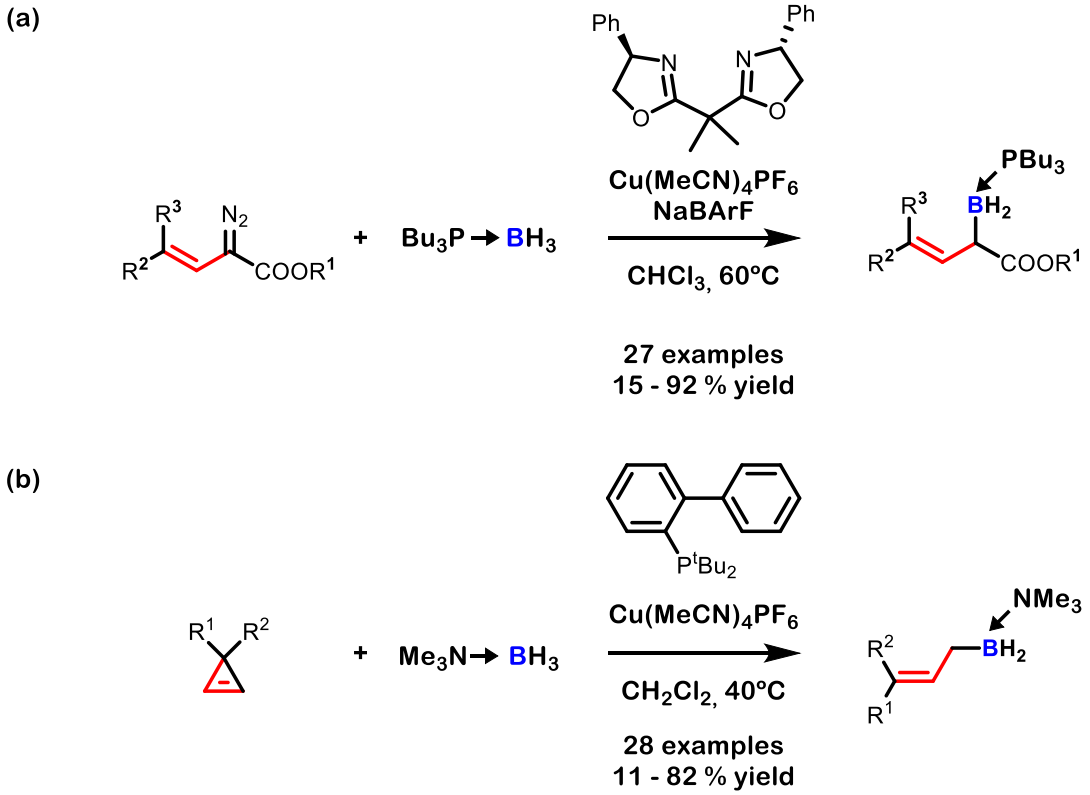

Scheme 1.68. Copper catalyzed intermolecular B-H insertion.

1.2.2.4. Carbene/Alkyne metathesis

The examples shown so far have highlighted the remarkable versatility of vinylcarbenes, both in terms of their reactivity and the diverse range of precursors employed for their generation. However, it is worth noting that in these reports, the vinylcarbene is directly formed from the precursor, which subsequently engages in the intended reactivity. Among various catalytic methods for generating vinylcarbenes, the carbene/alkyne metathesis (CAM) method stands out as an extremely powerful strategy for accessing polycyclic compounds in a one-pot fashion.[159] This transformation relies on the reaction between a metal carbene and an alkyne, leading to the generation of a vinylcarbene. This occurs through the transfer of carbene character to the β-carbon of the alkyne, coupled with the formation of a double bond between the carbenic carbon and the α-carbon of the alkyne (**Scheme 1.69**). This CAM strategy has been employed as the key method to access vinylcarbenes in this thesis. Therefore, the pivotal contributions on this field are summarized herein.

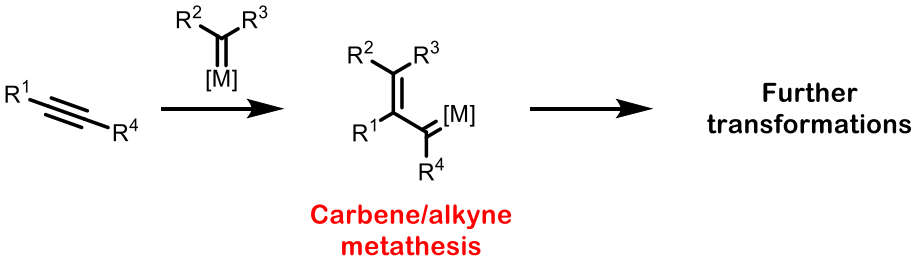

Scheme 1.69. General scheme for the CAM process.

The initial instances of this reactivity were reported by Dötz et al. in 1975. In their seminal work, they described the reaction between an isolated chromium Fisher-type carbene and diphenylacetylene, resulting in the formation of a naphthol derivative (**Scheme 1.70**).[160] The proposed mechanism involves the generation of a chromium vinylcarbene through a carbene/alkyne metathesis, that upon insertion of one carbonyl ligand from the metal, gives rise to a ketene. Subsequent electrocyclization and aromatization leads to the ultimate formation of the naphthol. Although the reaction is not catalytic, the carbonylation strategy emerged as an outstanding platform for synthesizing naphthol and phenol derivatives, eventually earning recognition as the Dötz reaction.[161]

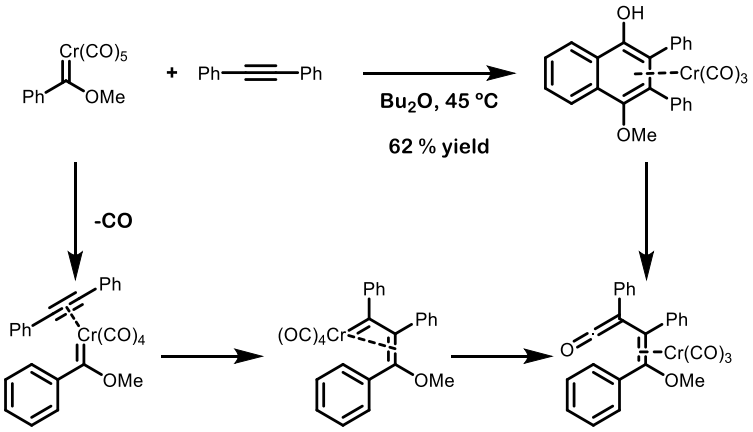

Scheme 1.70. First report of the Dötz reaction.

This pioneering work established the potential for generating vinylcarbenes through the reaction of carbenes and alkynes. Subsequently, several research groups capitalized on this chemistry and reported the successful trapping of the vinylcarbene with olefins, resulting in the formation of the corresponding cyclopropane adducts.[162]

While these studies served as proof of concept for the reaction, a notable limitation was the necessity of using stoichiometric quantities of the initial isolated metal carbene. Recognizing the potential of diazo compounds to generate carbenes in a catalytic manner and the ability of isolated carbenes to react with alkynes, the groups of Padwa and Hoye independently reported the first examples of a catalytic version of the CAM process. By tethering an initial diazo moiety to an internal alkyne with a pendant alkene, an *in situ* generated vinylcarbene could engage in a [2+1] cycloaddition with the remaining olefin generating three cycles in just one reaction step. In Padwa's study, rhodium was employed as the catalyst (**Scheme 1.71a**),[163] while in Hoye's one, palladium emerged as the metal of choice (**Scheme 1.71b**).[164]

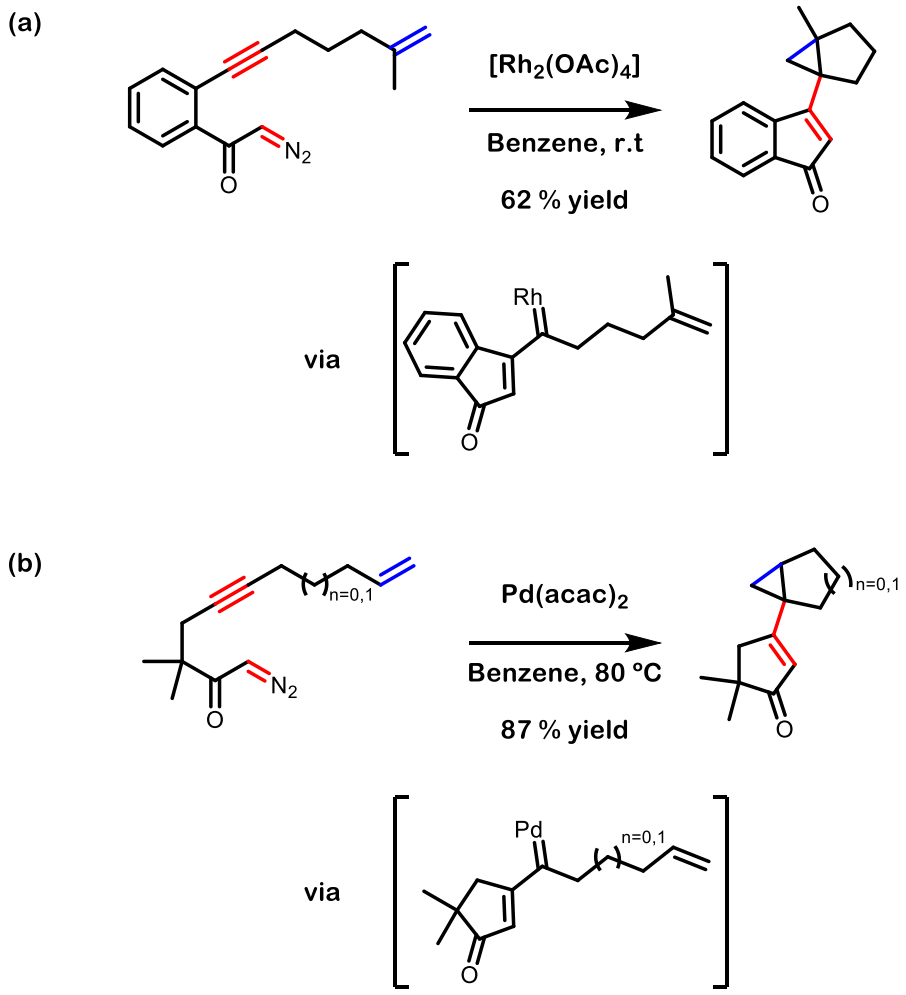

Scheme 1.71. First examples of catalytic CAM reactions terminated with [2+1] cycloaddition.

Building on the success of their respective reports, both groups dominated the field for the subsequent decade, exploring the chemistry of CAM-generated vinylcarbenes. Their investigations included further exploration of [2+1] cycloaddition reactions with alkenes and alkynes,[165] [3+4] cycloadditions (**Scheme 1.72a**),[166] Csp^3-H insertions (**Scheme 1.72b**),[167] and Csp^2-H insertions (**Scheme 1.72c**),[168, 169] both of the latter exclusively on the carbenic site.

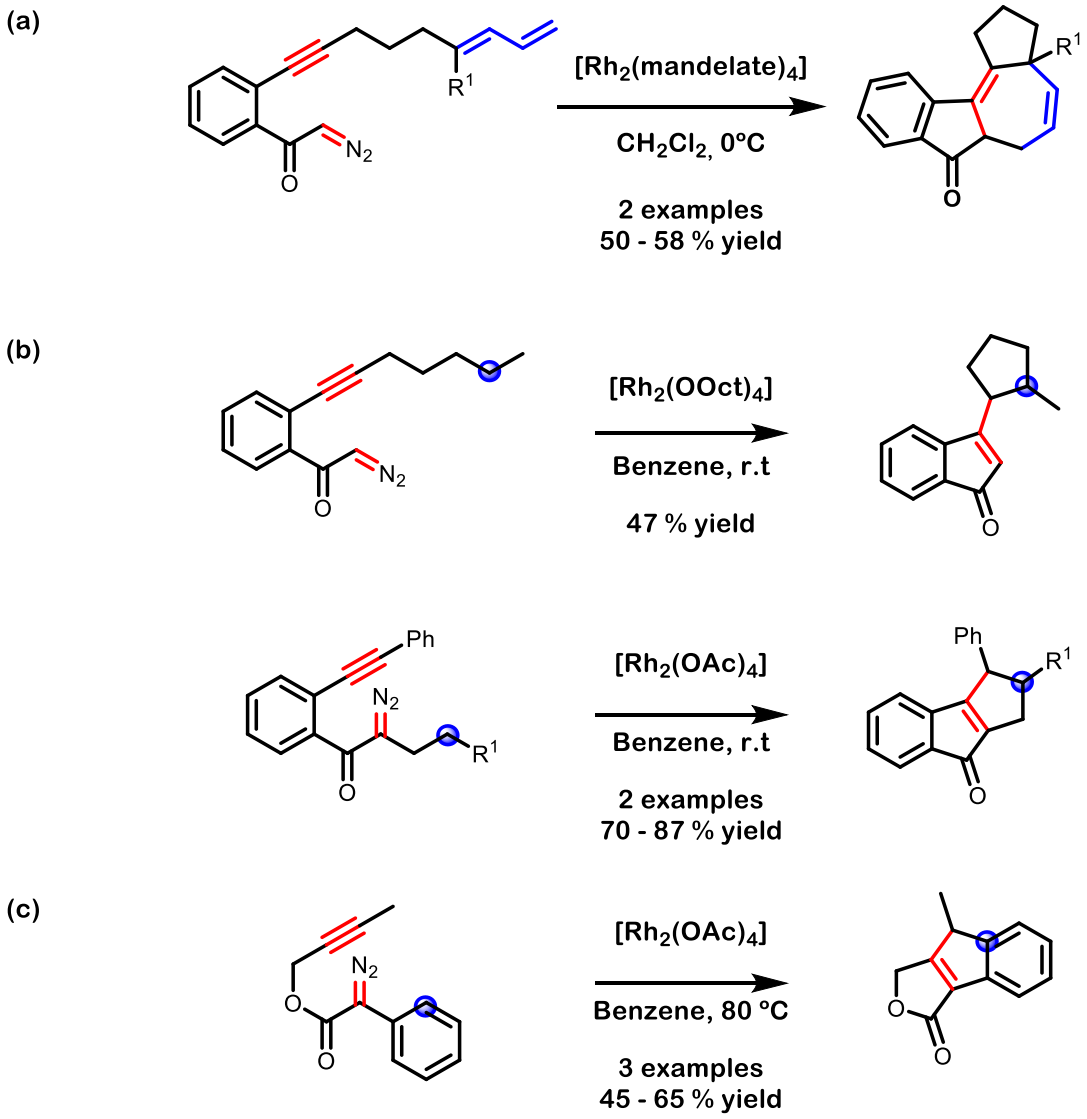

Scheme 1.72. Rhodium catalyzed CAM reactions terminated with [3+4] or C-H insertions.

The versatility of the cyclizations comprising the generation of a metal vinyl carbene through a CAM and subsequent reactivity was demonstrated, although the examples presented were somewhat limited in scope and did not involve stereoselective transformations.

Other research groups drew inspiration from the reports by Padwa and Hoye, embarking on efforts to broaden the chemistry of CAM processes. The May group, for instance, delved deeper into the potential of vinylcarbene Csp^3-H insertion. They developed a diazo alkynyl substrate with an embedded aliphatic-cyclic scaffold in the propargyl position. Upon treating the initial diazo compound with a rhodium catalyst, the desired vinylcarbene is formed and inserts into the pending Csp^3-H bond, resulting in the formation of bridged polycyclic compounds (**Scheme 1.73a**).[170] Expanding on their research, they exchanged the diazo group with a *N*-tosylhydrazone (**Scheme 1.73b**),[171] and in 2017, they reported a novel chiral rhodium (II) catalyst able of performing the reaction in an enantioselective fashion.[172]

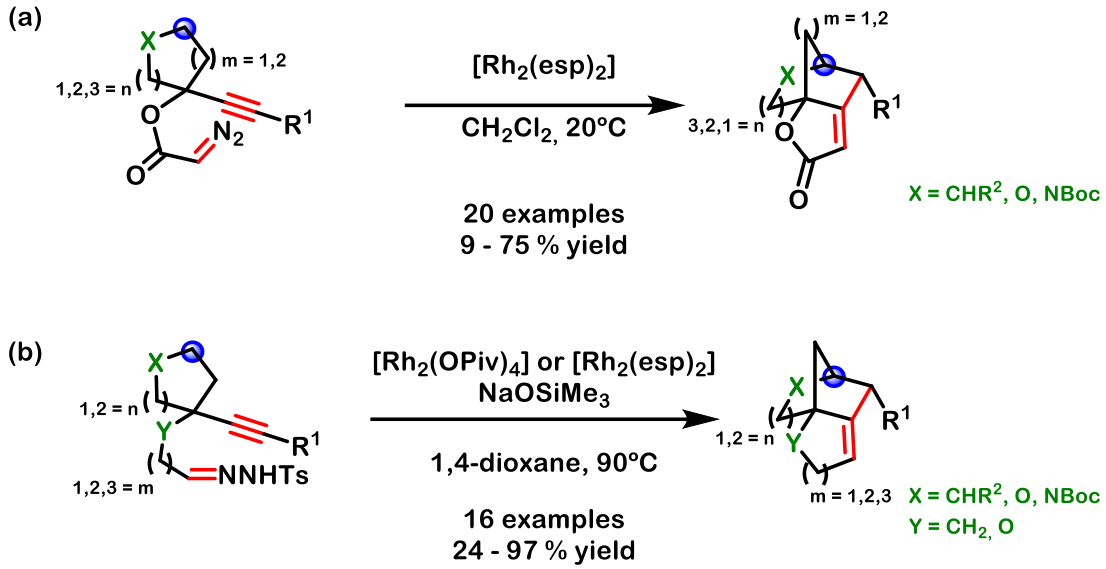

Scheme 1.73. Rhodium catalyzed CAM terminated with C*sp*^{3}-H insertion.

Building on this chemistry, in 2019 the groups of Xu and Doyle reported the synthesis of chiral dihydroindole derivatives via a CAM cascade of propargyl diazoacetates terminated with C*sp*^{3}-H bond insertion.[173] Through the modification of ligands on the dirhodium complex, they achieved selective insertion into either a primary C-H bond or a secondary or tertiary C-H bond (**Scheme 1.74**).

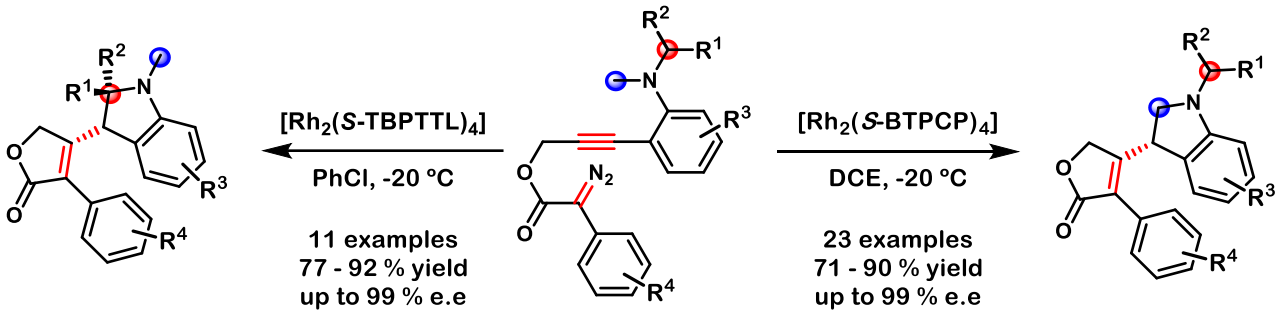

Scheme 1.74. Rhodium catalyzed catalyst-controlled CAM terminated with C*sp*^{3}-H insertion.

Before these two examples by May and Xu, there were no instances of enantioselective carbene/alkyne metathesis reactions documented in the literature. Recognizing this gap, our group seized the opportunity and reported the first example of an enantioselective CAM cascade. This was achieved using a rhodium (I)/chiral biphosphine catalytic system and *N*-sulfonylhydrazones as carbene precursors (**Scheme 1.75**).[174] Upon heating in dichloroethane, the initial carbene underwent a double CAM with both alkynes present in the molecule. Finally, an enantioselective nucleophilic addition from the sulfinate, released upon the initial carbene formation, yielded chiral sulfone derivatives.

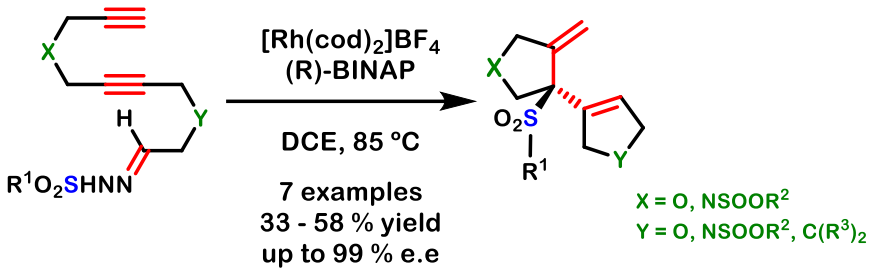

Scheme 1.75. Enantioselective rhodium(I) catalyzed double CAM reaction.

Realizing the potential of this catalytic system, our group continued exploring the chemistry of *N*-sulfonylhydrazone substrates by modifying the terminal alkyne and replaced it with other unsaturations. Initially, the alkyne was exchanged with an olefin, and as expected, the corresponding cyclopropanation occurred, yielding the desired vinylcyclopropanes in good yields and excellent enantioselectivities (**Scheme 1.76a**).[175] Finally, introducing an allene as the terminal unsaturation resulted in the obtention of methylenetetrahydropyran derivatives with excellent levels of enantioselectivity (**Scheme 1.76b**).[176]

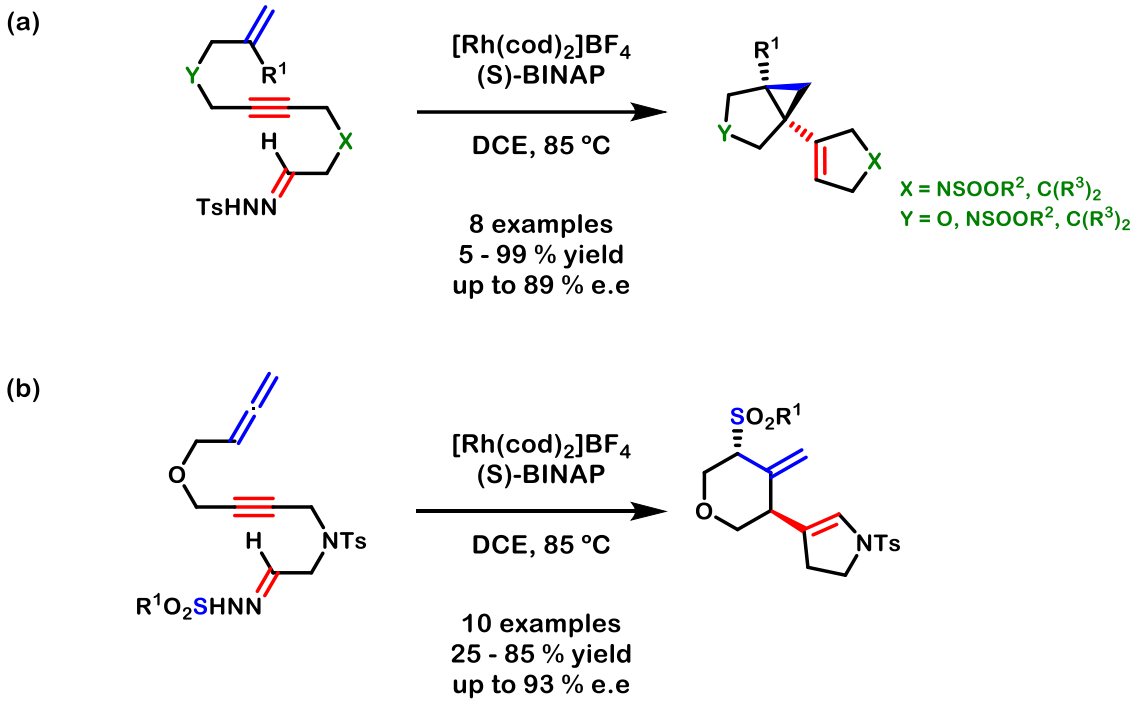

Scheme 1.76. Enantioselective rhodium (I) catalyzed CAM reactions reported by our group.

As demonstrated earlier, the Padwa group had already showcased the potential for C*sp*^{2}-H functionalization under rhodium catalysis. Seeking alternative catalytic systems based on different metals, the Doyle group revisited this reactivity in 2017. In their findings, they identified a copper-based system as the optimal catalyst for the transformation and explored the scope of the intramolecular C*sp*^{2}-H insertion for the preparation of tricyclic lactones (**Scheme 1.77a**).[177] In light of copper's success as a potential catalyst for reacting with aryls, the Xu group extended on this chemistry and reported the copper-catalyzed Buchner reaction of diazo derivatives bearing an *o*-aniline moiety at the terminal aryl group of the alkyne. Upon CAM, the *in situ* generated copper vinylcarbene undergoes a [2+1] cycloaddition with the pending aniline, suppressing any potential C*sp*^{2}-H insertion reaction, leading to the formation of cycloheptatriene derivatives (**Scheme 1.77b**).[178]

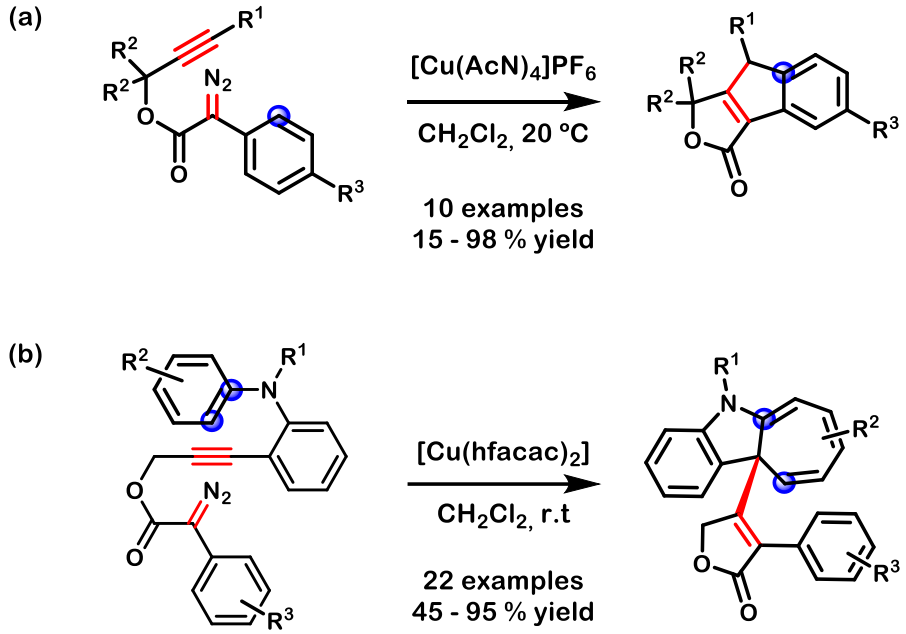

Scheme 1.77. Copper catalyzed divergent outcomes of CAM reactions with aryls.

The group of Xu advanced even further in this chemistry and reported in 2020 the first example of an enantioselective CAM process terminated with a C*sp*^{2}-H insertion (**Scheme 1.78**). Employing chiral rhodium catalysis and utilizing diazo compounds with two alkyne units, a double CAM took place. The resultant vinylcarbene then inserted into the pending aryl moiety in an enantioselective manner, yielding chiral fluorenes with excellent yields and e.e values.

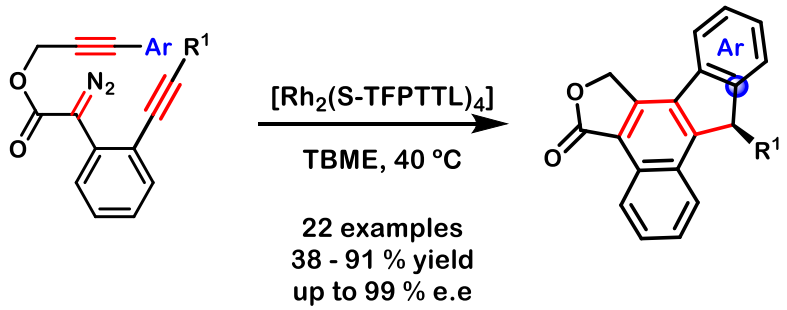

Scheme 1.78. Rhodium catalyzed enantioselective double CAM terminated with C*sp*^{2}-H insertion.

The Xu's group has not only explored the conventional reactivity of carbenes but has also recognized the diverse potential of various functional groups capable of trapping vinylcarbenes. Throughout their investigations, they have successfully generated a broad spectrum of distinct scaffolds by using the CAM strategy. Introducing an o-azido substituent in the α-aryl group to the diazo moiety, resulted in the efficient trapping of the vinylcarbene by the azide, leading to the synthesis of quinolines derivatives (**Scheme 1.79a**).[179] Further diversifying their approach, the group replaced the entire α-aryl group with an alkene, leading to an intramolecular [3+2] cycloaddition between the vinylcarbene and the olefin. This strategy yielded cyclopentadiene-derived structures. Interestingly, utilizing a phenyl-substituted alkene induced a [1,5]-H shift, producing achiral cyclopentadienes (**Scheme 1.79b**).[180]

Conversely, the introduction of a silyl group in the alkene suppressed the hydrogen shift, allowing for the generation of chiral cyclopentadienes in enantioenriched form when the reaction was conducted with a chiral

rhodium catalyst. These chiral cyclopentadienes were subsequently trapped *in situ* with maleimide derivatives, resulting in the isolation of the final bridged products (**Scheme 1.79c**).[181]

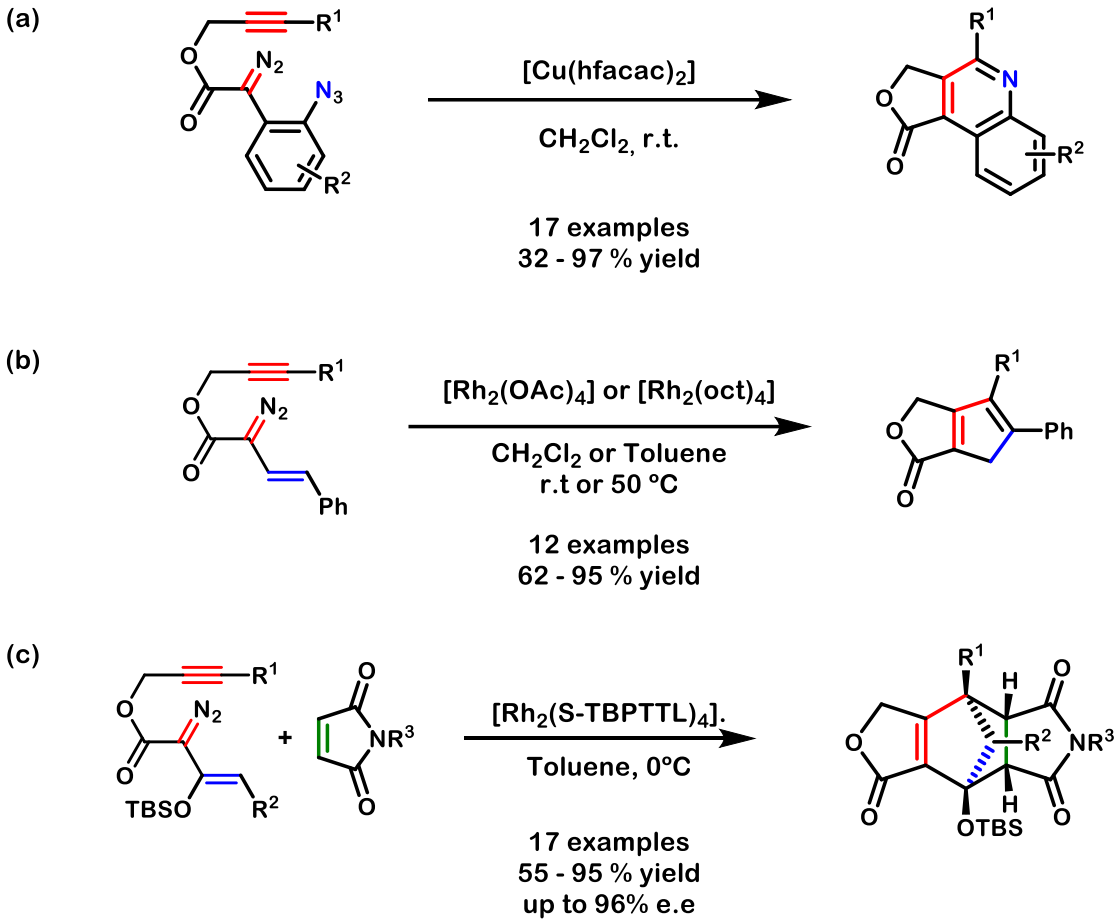

Scheme 1.79. Metal catalyzed CAM reactions reported by Xu.

Based on the reports by Xu and Doyle, the group of Hu synthesized a substrate bearing an acylated 2-aminophenyl group. Upon rhodium catalysis the intermediate rhodium vinylcarbene was captured by the carbonyl moiety, yielding 3*H*-indol-3-ol derivatives (**Scheme 1.80a**).[182] Building upon this concept, the Song group replaced the amide with a thiacarbamate leading to the formation of 2-aminobenzofurans upon sulfur extrusion (**Scheme 1.80b**).[183]

The intermolecular version of the reaction has also been explored in the literature, with the first example reported by Dixneuf in 2000. In their study, monosubstituted diazo compounds were subjected to ruthenium catalysis, leading to the formation of the corresponding carbene. This carbene subsequently reacted intermolecularly with an alkyne via CAM, resulting in the desired vinylcarbene. Ultimately, coupling of the vinylcarbene with another equivalent of the diazoalkane, yielded diene derivatives (**Scheme 1.81a**).[184] The same research group continued to explore the potential of this platform for intermolecular CAM and, three years later, they reported the intermolecular reaction of diazoalkanes with enynes (**Scheme 1.81b**).[185] As anticipated, the resultant vinylcarbene from the CAM underwent cyclopropanation of the pending olefin, leading to the formation of the corresponding bicyclic compounds. The authors subsequently widened the scope of the reaction and improved its functional group tolerance.[186] Additionally, the Zeng group achieved similar results

but employed rhodium (I) catalysts instead of ruthenium.[187] Notably, the Dixneuf group expanded the application of this reaction to allenynes, yielding the corresponding vinylcyclopropanes in the process.[188]

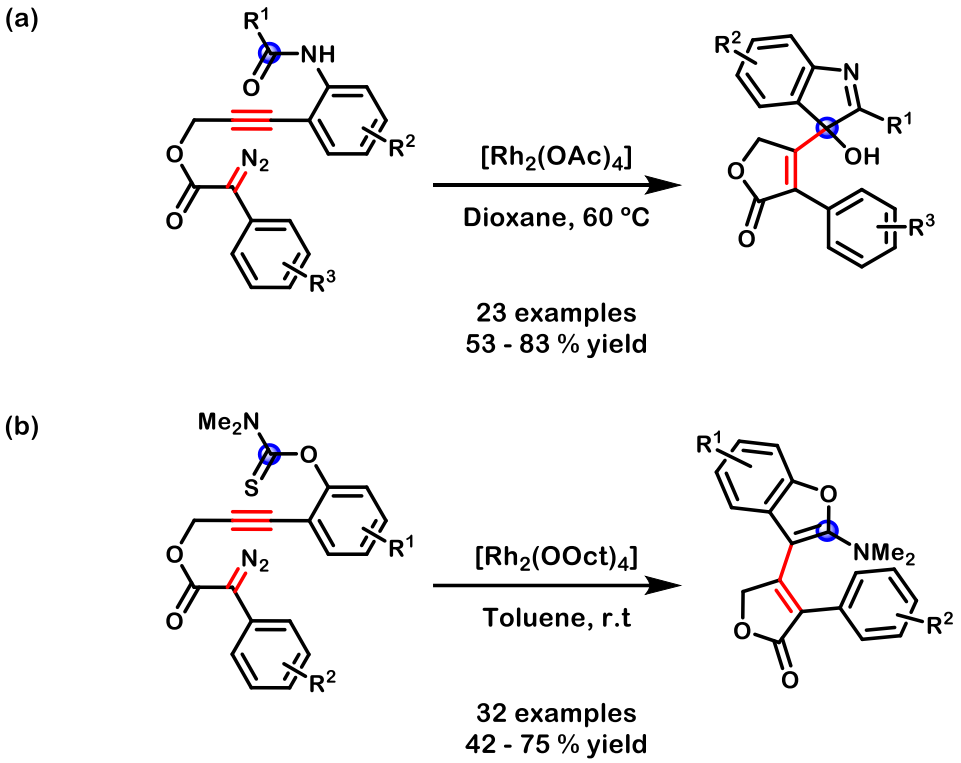

Scheme 1.80. Intramolecular rhodium catalyzed CAM reactions.

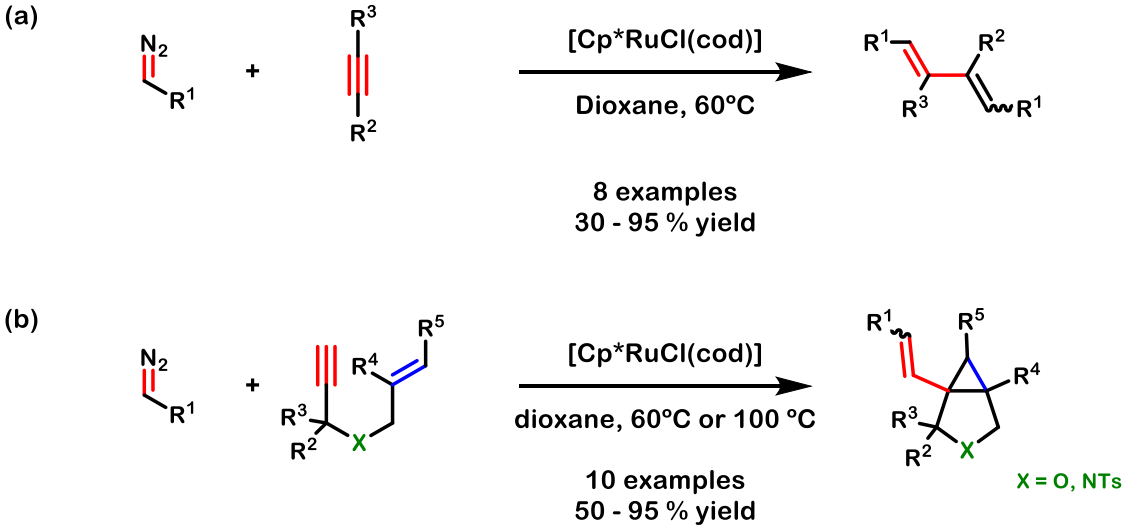

Scheme 1.81. Intermolecular ruthenium catalyzed CAM reported by Dixneuf.

Inspired by Dixneuf's seminal works, the Saá's group leveraged the established conditions for ruthenium vinylcarbene generation to set up diverse cascade processes. In their initial work, they attached an alkyl chain to the alkyne. Consequently, upon vinylcarbene formation, insertion into a neighboring C*sp*^{3}-H bond occurred (**Scheme 1.82a**).[189] Building upon this work, the group delved further into this chemistry, investigating the reaction of diazoalkanes with alkynals. Under the reaction conditions, the vinylcarbene was effectively trapped by the carbonyl group, ultimately yielding 2-vinyldihydropyrans and dihydro-1,4-oxazines (**Scheme 1.82b,**

left).[190] Intriguingly, the introduction of substituents adjacent to the carbonyl group induced a complete switch in reactivity, resulting in the exclusive formation of vinyl epoxypyrrolidines (**Scheme 1.82b, right**).[191]

Finally, the same group decided to explore the potential of vinylcarbene insertion into N-H bonds. Through the strategic tethering of an aniline group to an alkynyl chain, the anticipated N-H insertion adduct was successfully obtained (**Scheme 1.82c, left**).[192] However, with a subtle modification of the substrate, anchoring a benzylamine group instead of an aniline moiety, the N-H insertion reaction was entirely suppressed, unveiling 1,3-benzoxazines as the solitary product of the reaction (**Scheme 1.82c, right**).[193]

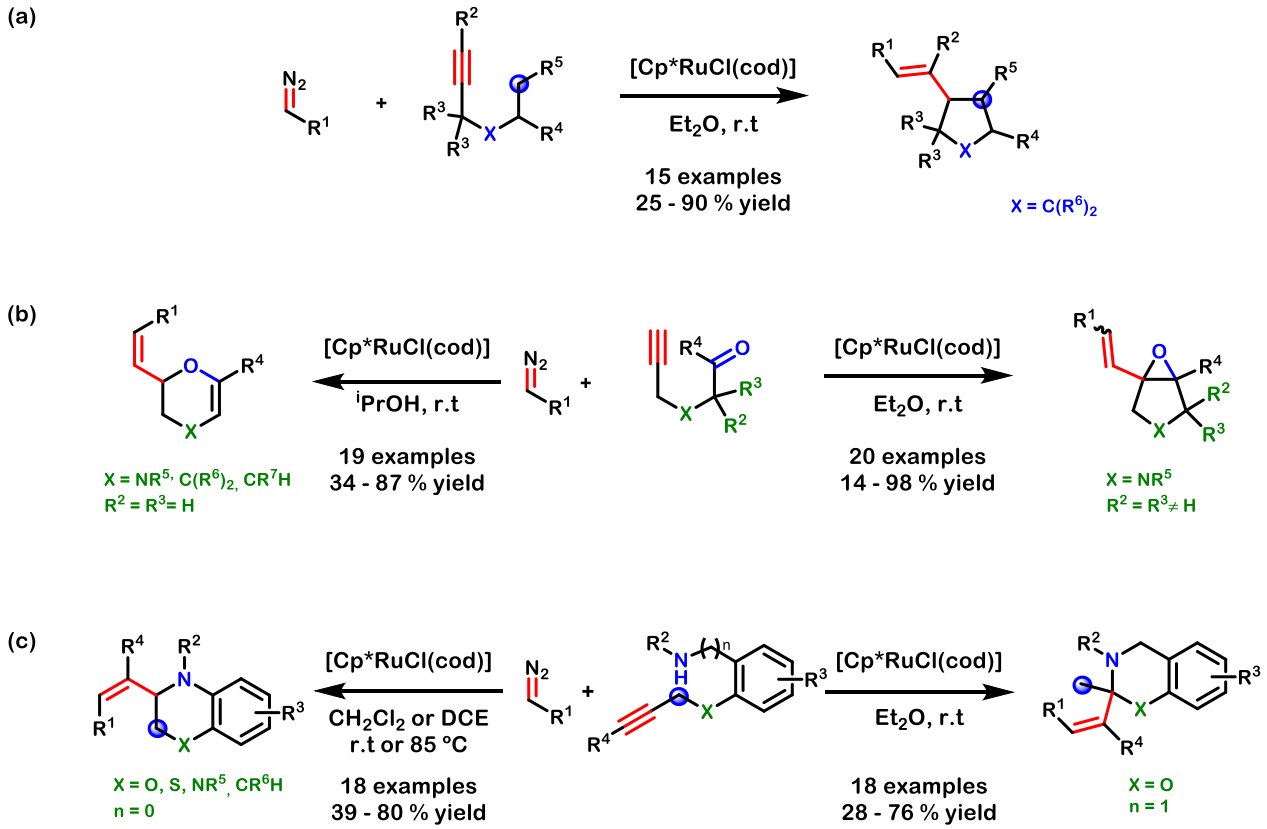

Scheme 1.82. Ruthenium catalyzed intermolecular CAM reported by Saá.

Chapter 2. General objectives

Metal vinylcarbenes have demonstrated a remarkable ability to generate a diverse range of products through various reactivity pathways. Among the available methodologies available for catalytically accessing metal vinylcarbenes, carbene/alkyne metathesis (CAM) stands out as a powerful transformation for their *in situ* generation. Additionally, the construction of complex polycyclic frameworks can be efficiently achieved through cascade reactions involving CAM, where the terminating reaction of the metal vinylcarbene can be fine-tuned. However, the majority of CAM-related transformations occur intramolecularly and rely on internal alkynes. Furthermore, although the utility of silver complexes as catalysts in vinylcarbene chemistry has been demonstrated, their use in CAM transformations remains notably absent.

Hence, from a broader perspective, the goal of this thesis is to develop novel transformations utilizing CAM for the *in situ* generation of the metal vinylcarbene. Our focus is on reactions that significantly enhance molecular complexity, particularly by extending cascade reactions, and establishing conditions to control selectivity, while concurrently delving into the factors governing this selectivity. For greater clarity, the objectives of this thesis are categorized into two main sections.

Rhodium (II) catalyzed intermolecular trapping of CAM generated vinylcarbenes.

The **first objective** of this thesis is to study the intermolecular reactivity between rhodium vinylcarbenes generated from CAM. Capitalizing on the recent research work by the Krasavin group,[110] we postulated that the vinylcarbene could potentially react with an external nitrile, leading to the formation of the corresponding nitrile ylide (**Scheme 2.1**). Then, the presence of an aryl group in the remote position of the vinylcarbene could trigger a 1,7-electrocyclization, followed by a 1,5-H shift, resulting in the synthesis of benzoazepine derivatives. Furthermore, by incorporating the nitrile group into the diazo compound utilized as the carbene precursor, we aimed to facilitate more prolonged cascade reactions through the reaction of a second carbene with the generated benzoazepine moiety.

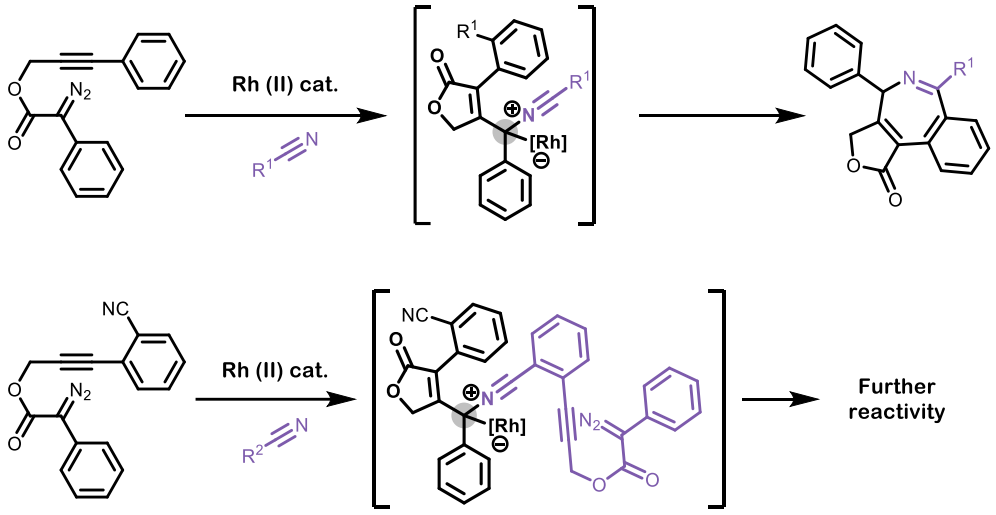

Scheme 2.1. Plausible outcomes for the rhodium catalyzed intermolecular trapping of vinylcarbenes with nitriles.

Silver catalyzed intramolecular CAM.

The **second objective** of this thesis is to establish a platform for the efficient generation of silver vinylcarbenes via intramolecular CAM (**Scheme 2.2**). Subsequently, we will explore the ability of these silver vinylcarbenes to engage in C-H bond activation. As outlined in the introduction, silver has demonstrated superior selectivity in functionalizing the vinylogous position in X-H insertion reactions compared to rhodium catalysts. Furthermore, only one example has been reported by Liu for vinylogous Csp^3-H bond insertion using gold.[127] Building upon these precedents, we hypothesize that the silver vinylcarbene produced through CAM could undergo selective vinylogous Csp^3-H insertion with an strategically placed *o*-dimethylamino unit in the aryl group at the terminal position of the alkyne. The **third objective** of this thesis it to capitalize on the developed platform and study the reactivity of this vinylcarbene with Csp2-H bonds. By simply removing the *o*-dimethylamino we envision the reaction to undergo C-H insertion with the pending aryl group. Besides insertion into CH bonds, our **last objective** in this thesis is to explore the possibility of overcoming the limitation of using internal alkynes in intramolecular CAM reactions. In this context we envision the possibility of using silver catalysts to selectively generate a 6-endocyclicic vinylcarbene. This newly formed carbene could then react further yielding the final cascade process.

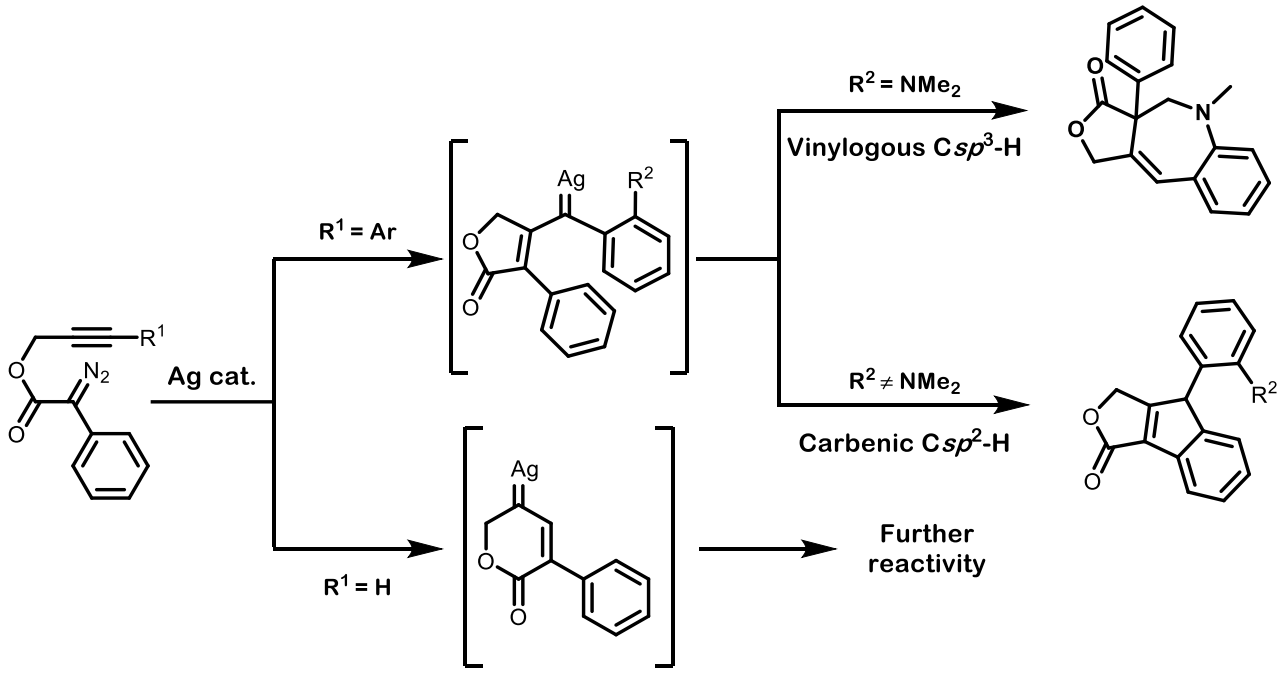

Scheme 2.2. Plausible outcomes for the silver catalyzed intramolecular CAM.

Chapter 3. Synthesis of 1*H*-Isoindole-Containing Scaffolds Enabled by a Nitrile Trifunctionalization

Nitrile ylides are intriguing chemical compounds that play a crucial role as powerful intermediates in organic chemistry [194] and they rank among the most reactive dipoles known.[195] These versatile compounds engage in 1,3-dipolar cycloadditions with a range of multiple bonds, including CC-, CN-, CO-, CS-, NN-, and NO-groups, leading to the formation of diverse N-heterocyclic compounds. Beyond their intermolecular reactivity, nitrile ylides, when conveniently functionalized with multiple bonds, readily give rise to heterocyclic molecules through 1,5-electrocyclization. Expanding the scope, extended conjugation can induce 1,7-electrocyclization, followed by a 1,5-H shift. This less-explored but highly efficient pathway offers a unique route to access benzoazepine scaffolds.[196] Notably, as mentioned in the introduction (see **Scheme 1.48**), the Krasavin group provided the lone example of a 1,7-electrocyclization involving a nitrile ylide generated by the reaction of a nitrile with a diazo compound followed by a 1,5-H shift (**Scheme 3.1**).[110]

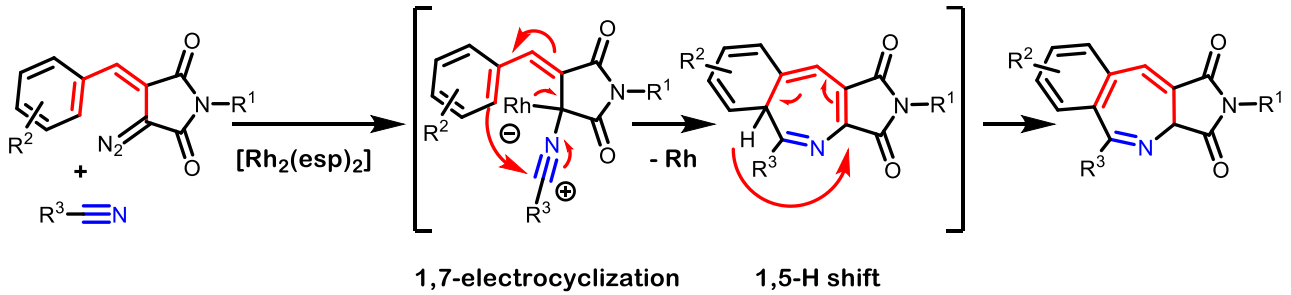

Scheme 3.1. Rhodium catalyzed intermolecular trapping of vinylcarbenes with nitriles reported by Krasavin.

In the course of our project aimed at the development of molecular complexity through the reaction of *in situ* generated vinyl metal carbenes, we decided to explore whether a simple propargyl diazoacetate model was amenable to a CAM / nitrile ylide formation / 1,7-electrocyclization reaction. The exploration posed numerous challenges, including the intricate control of cascade events and the preference for intramolecular reactivity.

We initiated our investigation by exploring the reaction between propargyl diazoacetate **1** and benzonitrile (10 equivalents) in the presence of 2 mol% of $[Rh_2(esp)_2]$ in dichloromethane at room temperature (**Scheme 3.2**). Under the reaction conditions, two products were isolated. Firstly, the *in situ* generated donor-donor rhodium vinyl carbene inserted into the Csp^2-H bond, affording compound **2** with a yield of 66%. Simultaneously, the anticipated cascade reaction led to the formation of the benzoazepine derivative **3a**, obtained in a 33% yield. The structural confirmation of **3a** was unambiguously established through X-ray diffraction analysis.

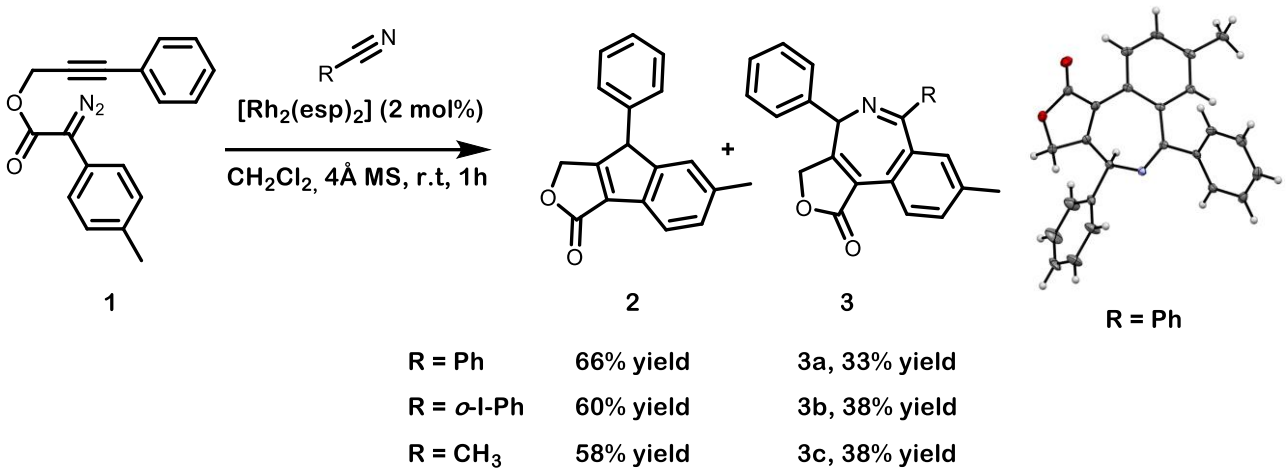

Scheme 3.2. Rhodium catalyzed intermolecular trapping of *in situ* generated vinylcarbenes with nitriles.

In an effort to improve the ratio between **3** and **2** the variation at the nitrile component of the reaction was explored. However, whether using *o*-iodobenzonitrile or acetonitrile, yielded similar results. From the obtained results, it was clear that the intramolecular Csp^2-H insertion was hampering the benzoazepine formation. To address this challenge and to advance towards a process with increased molecular complexity, we conceived the idea of synthesizing a propargyl diazoacetate conveniently functionalized with a nitrile group in a position where the formation of the nitrile ylide was not favored intramolecularly. Our intention was to promote intermolecular reactions to enable a more prolonged cascade. Thus, we synthesized propargyl diazoacetate **4a** (see below for the synthesis) and investigated its reactivity. When diazo **4a** was reacted in presence of [Rh_2(esp)$_2$] in dichloromethane at room temperature a complex mixture of unidentified products was obtained. However, by conducting the reaction at -40ºC, we successfully isolated and characterized compound **5a** with a yield of 29% (**Scheme 3.3**). Of note, the formation of the Csp^2-H insertion product analogous to **2** was not observed.

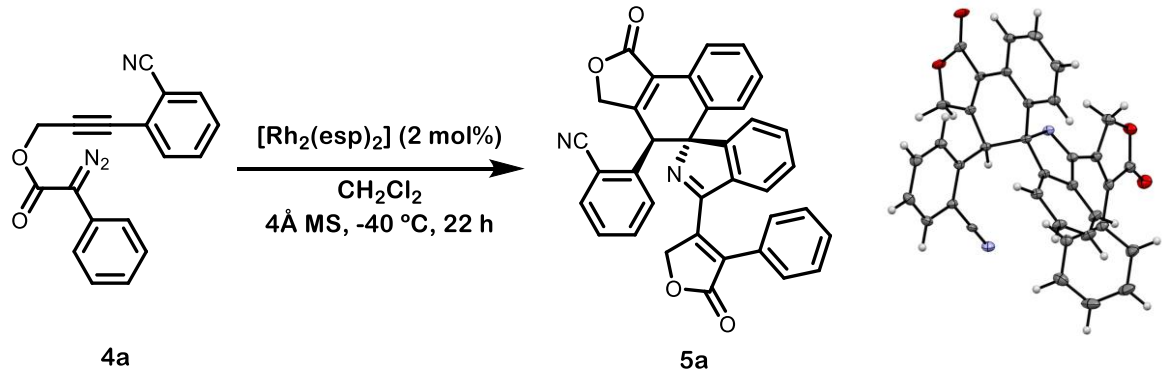

Scheme 3.3 Initial results for the synthesis of 1*H*-isoindole-containing scaffolds via rhodium catalyzed cascade reaction.

The resulting product is a dimer constructed through the formation of up to five new bonds, including two C=C, one C=N, and two C-C bonds. This intricate process generates four new cycles in one reaction step, showcasing a remarkable increase in molecular complexity. Notably, among the five newly formed bonds, three are established within one of the nitrile units of the initial material, formally triggering a nitrile trifunctionalization process. Furthermore, the synthesis of the 1*H*-isoindole core, an essential component of the obtained product, poses challenges due to its inherent tendency to undergo isomerization, leading to the

formation of aromatic isoindoles.[197] Notably, this core structure is a key motif in AZD3839,[198] a potent and selective inhibitor of human BACE1 that advanced to clinical trials for Alzheimer's disease treatment as part of AstraZeneca's development. Given the inherent interest and relevance of the product containing the 1*H*-isoindole core, particularly in light of its potential applications, and considering that its formation deviates from the expected outcome in a reaction involving a nitrile and a metal vinylcarbene, we embarked on optimizing the reaction conditions (**Table 3.1**).

Initially, we explored alternative catalytic systems that had previously demonstrated efficiency in CAM reactions. As demonstrated by Xu et al., copper catalysis proved effective for their CAM process.[178] Regrettably, our attempt to utilize $[Cu(MeCN)]_4(PF_6)_2$ (**entry 1**) in our system failed to initiate any reaction. Subsequently, we explored conditions similar to those reported by our group, employing a Rh(I)/biphosphine catalytic system.[174, 175, 176] However, no consumption of the starting material was observed (**entry 2**). Consequently, we made the decision to revert to Rh(II)-derived catalysts. The use of $[Rh_2(OAc)_4]$ and $[Rh_2(S\text{-BTPCP})_4]$ only yielded complex mixtures of unidentified products (**entries 3-4**). In contrast, the use of $[Rh_2(S\text{-PTTL})_4]$ and $[Rh_2(S\text{-PTAD})_4]$ resulted in the formation of the desired product with yields of 48% and 50%, respectively (**entries 5-6**). In pursuit of an enantioselective reaction, we attempted running the reaction with $[Rh_2(S\text{-PTAD})_4]$ using different solvents (**entries 7-11**). In all cases, the yields decreased, and meaningful enantiomeric excess (e.e.) values were not obtained. Consequently, we reverted to the $[Rh_2(esp)_2]$ catalyst. Running the reaction at -25 ºC resulted in a drastic increase in the yield, isolating the spirocyclic product **5a** in a 75 % yield (**Entry 12**). Recognizing the temperature sensitivity of the process, we conducted the reaction at a slightly higher temperature, yielding a decreased 62% yield (**entry 13**). Adjusting the concentration of the reaction provided **5a** in a 53% yield (**entry 14**), while a reduction in led to a final product yield of 40% (**entry 15**). Finally, we explored modifying the catalyst loading, but neither an increase nor a decrease improved the process yield (**entries 16-18**). Considering the results of the optimization, we identified entry 12 as the optimal reaction conditions for the nitrile trifunctionalization reaction.

Upon optimizing the reaction conditions, a series of diverse cyano propargyl diazoacetates (**4a-4l**) were successfully synthesized (**Scheme 3.4)** and tested to evaluate the scope of the transformation (**Figure 3.1**). The selection of the 12 initial diazo compounds (**4a-4l**) was aimed to analyze the electronic effects of various substituents in both the *para* and *meta*-position of the 2-diazo-2-phenylacetate scaffold and the benzonitrile ring. These compounds were prepared following the conditions shown in **Scheme 3.4** (for experimental details see **Supplementary Material**). Starting from commercially available *ortho*-bromo/iodo benzonitriles, Sonogashira coupling with propargyl alcohol was conducted to produce the corresponding aryl-substituted propargyl alcohol. Subsequently, coupling of this alcohol with the desired phenylacetic acid was carried out in the presence of DCC. Finally, by reacting the prepared esters with p-ABSA as the diazo transfer reagent and DBU as the base, the desired diazo compounds (**4a-4l**) were obtained.

Table 3.1. Optimization of the reaction conditions for the metal catalyzed nitrile trifunctionalization reaction. [a]

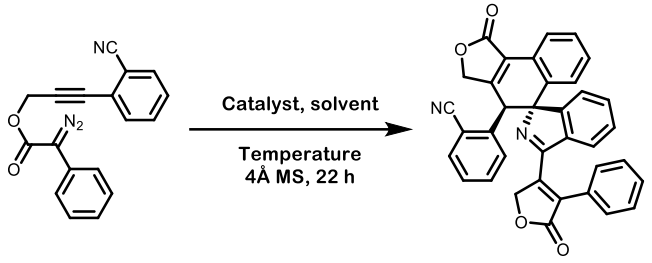

4a **5a**

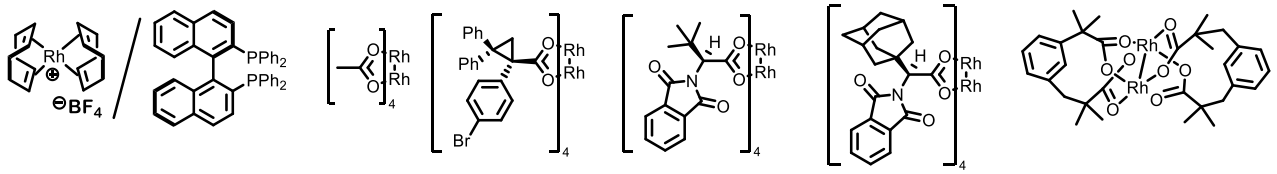

[Rh(COD)$_2$]BF$_4$ (R)-BINAP [Rh$_2$(OAc)$_4$] [Rh$_2$(S-BTPCP)$_4$] [Rh$_2$(S-PTTL)$_4$] [Rh$_2$(S-PTAD)$_4$] [Rh$_2$(esp)$_2$]

Entry	Catalyst	Solvent	T (ºC)	[4a] (M)	Yield (%)[b]
1	[Cu(MeCN)$_4$](PF$_6$)$_2$	CH_2Cl_2	-25	0.035	No reaction
2	[Rh(COD)$_2$]BF$_4$ / (*R*)-BINAP (5 mol%)	CH_2Cl_2	-25	0.035	No reaction
3	[Rh$_2$(OAc)$_4$]	CH_2Cl_2	-25	0.035	Complex mixture
4	[Rh$_2$(*S*-BTPCP)$_4$]	CH_2Cl_2	-25	0.035	Complex mixture
5	[Rh$_2$(*S*-PTTL)$_4$]	CH_2Cl_2	-25	0.035	48
6	[Rh$_2$(*S*-PTAD)$_4$]	CH_2Cl_2	-25	0.035	50
7	[Rh$_2$(*S*-PTAD)$_4$]	THF	-25	0.035	0
8	[Rh$_2$(*S*-PTAD)$_4$]	Toluene	-25	0.035	32
9	[Rh$_2$(*S*-PTAD)$_4$]	Hexane/CH_2Cl_2	-25	0.035	6
10	[Rh$_2$(*S*-PTAD)$_4$]	$CHCl_3$	-25	0.035	11
11	[Rh$_2$(*S*-PTAD)$_4$]	PhCl	-25	0.035	18
12	**[Rh$_2$(esp)$_2$]**	**CH_2Cl_2**	**-25**	**0.035**	**75**
13	[Rh$_2$(esp)$_2$]	CH_2Cl_2	-20	0.035	62
14	[Rh$_2$(esp)$_2$]	CH_2Cl_2	-25	0.160	53
15	[Rh$_2$(esp)$_2$]	CH_2Cl_2	-25	0.007	40
16	[Rh$_2$(esp)$_2$] (3 mol%)	CH_2Cl_2	-25	0.035	67
17	[Rh$_2$(esp)$_2$] (1 mol%)	CH_2Cl_2	-25	0.035	69
18	[Rh$_2$(esp)$_2$] (0.05 mol%)	CH_2Cl_2	-25	0.035	35

[a] Standard conditions (unless otherwise noted): 0.11 mmol of **4a** (at the indicated concentration), 2 mol% of the indicated metal catalyst at the indicated solvent and temperature for 22h. [b] All yields reported correspond to isolated yields.

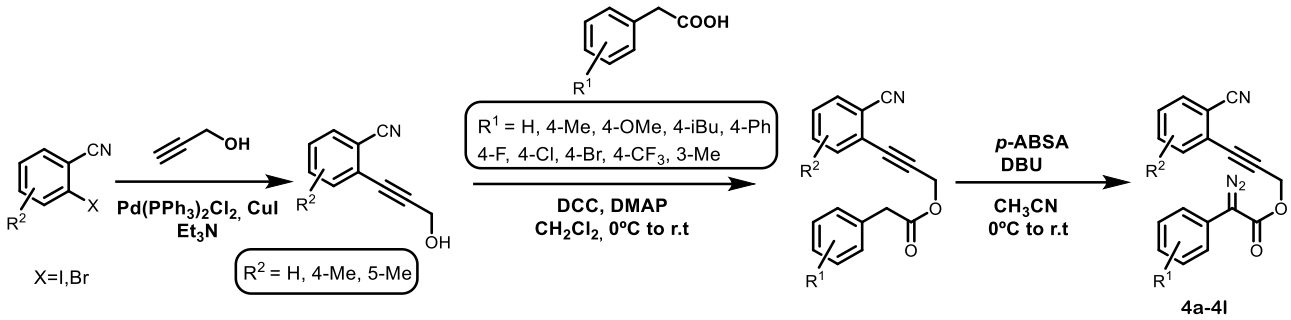

Scheme 3.4. Synthesis of cyano propargyl diazoacetates **4a**-**4l.**

Introduction of electron-withdrawing groups (F. Cl, Br and CF_3) in the *para* position of the 2-diazo-2-phenylacetate moiety allowed for the efficient preparation of the corresponding products **5b-e** (**Figure 3.1**). While the inclusion of a fluorine atom had a negligible impact on the yield of **5b**, the incorporation of chlorine, bromine, or trifluoromethyl groups resulted in an overall reduction in yield to the range of 54-57%. Conversely, the introduction of a methyl group in the same position yielded **5f** with a comparable yield to the unsubstituted substrate **5a**, while the addition of an iso-butyl group slightly diminished the yield of **5g** to 65%. To assess the influence of an aromatic ring, a phenyl group was introduced in the *para* position of substrate **4h**, resulting in a reaction with an improved 82% yield. The introduction of a methoxy group, with increased electron-donating character, led to the formation of **5i** with an excellent 86 % yield. In summary, the yield of the reaction exhibits an upward trend with the incorporation of electron-donating groups. At this point, it was also decided to analyze the effect of introducing substituents to the benzonitrile ring in a substrate already containing a methoxy group in the 2-diazo-2-phenylacetate moiety. Introducing a methyl ring in the *para* position to the cyano moiety significantly decreased the yield (compare the results of **5i** to **5j**). Surprisingly, the introduction of a methyl group in the *para* position to the alkyne in **4k** resulted in a reaction with an excellent yield. Finally, a methyl group was introduced to the 2-diazo-2-phenylacetate moiety, but in the *meta* position. As anticipated, the reaction was efficient but yielded a mixture of regioisomers in a 25:75 relative ratio.

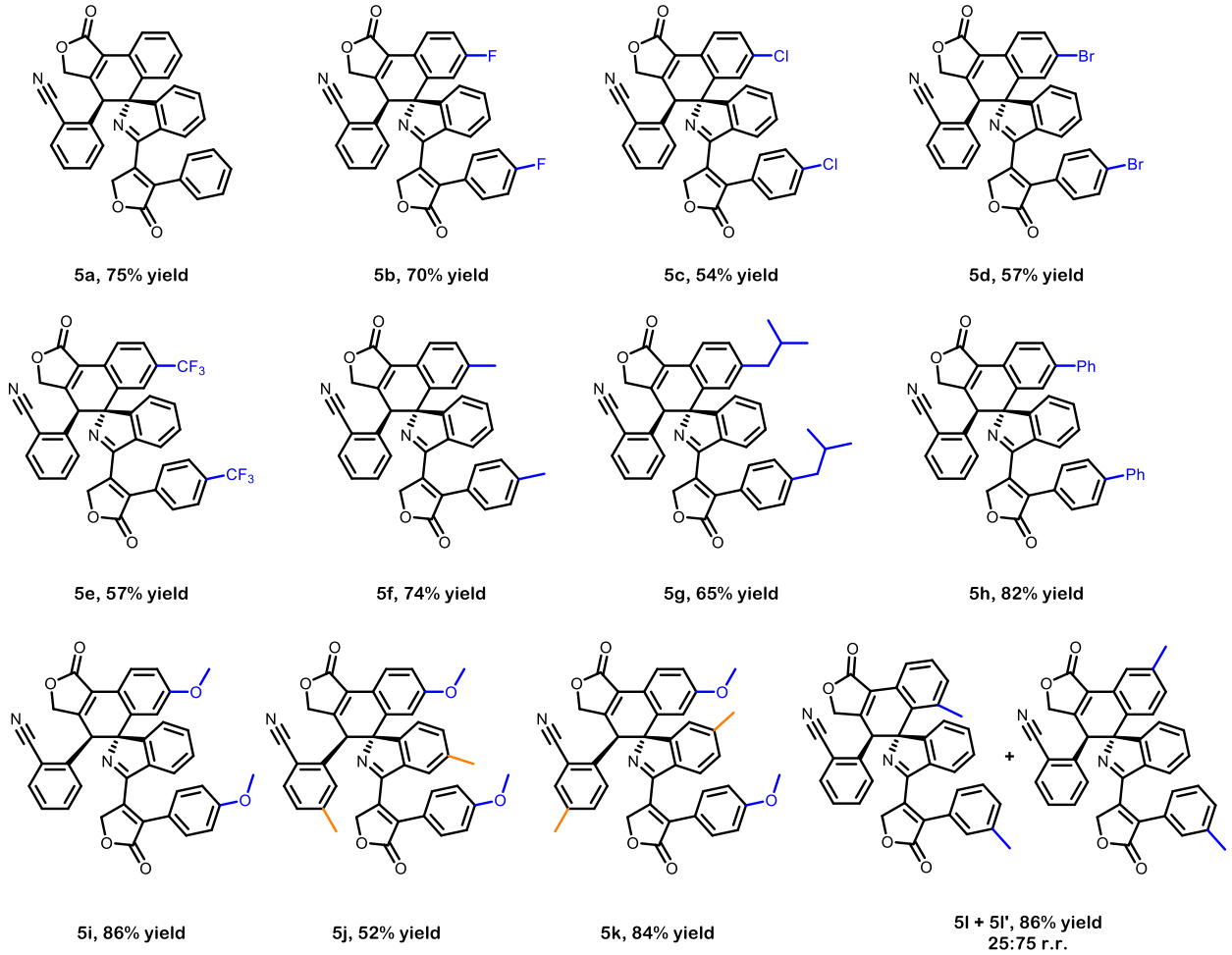

Figure 3.1. Scope of the reaction.

In an effort to comprehend the mechanism underlying the discovered transformation, a series of DFT calculations were performed alongside Roger Monreal-Corona (under the supervision of Prof. Miquel Solà and Dr. Albert Poater). The Gibbs energy profile was computed at the B3LYP-D3/6-311+G**~LANL2DZ-SMD(DCM)//B3LYP/6-31+G*~LANL2DZ level of theory, using the Gaussian16 software package.[199] Our exploration commenced by examining the pathway leading to the formation of the rhodium vinyl carbene species **D**. This transformation originates from the carbene-alkyne metathesis and subsequent intermolecular nitrile attack on the rhodium vinyl carbene, as illustrated in **Figure 3.2**. Given the size and complexity of the system involving two substrate molecules, coupled with the associated computational cost, we opted to employ [$Rh_2(OOCH)_4$] as a truncated model representing the catalytic system used in our experimental setup.[200, 201, 202] The reaction starts by coordination of the rhodium complex to the carbon linked to the diazo moiety in a mildly endergonic step (6.0 kcal/mol). Subsequently, the extrusion of nitrogen occurs through transition state **TS-AB**, presenting an overall energy barrier of 14.4 kcal/mol concerning reactants **A** and [$Rh_2(OAc)_4$], leading to the rhodium carbene **B** (-12.5 kcal/mol). After completing the initial step, the alkyne undergoes nucleophilic addition onto the carbenic carbon, leading to a 5-exo-*dig* cyclization. This process results in the formation of the zwitterionic vinyl cationic species **C** in an exergonic step with an energy release of 10.0 kcal/mol and a moderate energy barrier of 7.0 kcal/mol.

Subsequently, the reaction advances as the negatively charged rhodium atom engages in a nucleophilic attack on the carbocation, resulting in the direct formation of the rhodium η^1-vinylcarbene **D**. This step involves overcoming a reaction barrier of 8.9 kcal/mol. At this juncture, a second molecule of **A** becomes involved in the ongoing reaction. The addition of the nitrile moiety from the second unit of **A** to the newly formed vinylcarbene results in the formation of rhodium-bound ylide **F**, overcoming an energy barrier of 14.6 kcal/mol. Subsequently, one of the catalyst units is released, leading to the formation of the metal-unbound ylide **F-free.** Notably, the overall formation of the nitrile ylide **F-Free** is a highly exergonic process with an energy release of 46.6 kcal/mol. Depending on the substituents, nitrile ylides can be classified as either propargyl-type or allenyl-type. The notable bending observed in the N-C-C(Ph) unit, with an angle of 167.1º, indicates that **F-free** is best described as a 2-azonia-allenyl anion, a phenomenon previously identified in vinyl nitrile ylides by Fabian's group.[203] This specific bending facilitates the 1,7-electrocyclization through **TS-FG**, with an activation energy of 9.8 kcal/mol. Although this process is only mildly exergonic (3.4 kcal/mol), it is likely attributed to the loss of aromaticity in one of the six-membered rings in intermediate **G**.

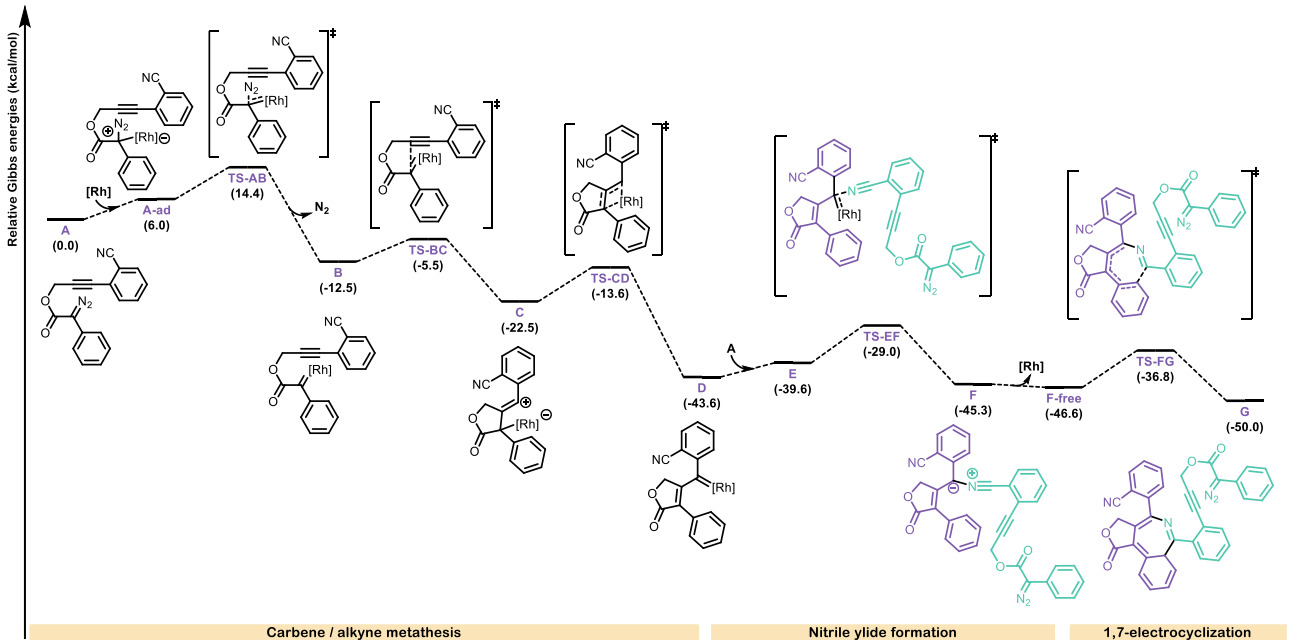

Figure 3.2. Gibbs energy for the first carbene formation and carbene-alkyne metathesis, nitrile ylide formation and 1,7-electrocyclization of **4a**. Gibbs energies (298 K) relative to **4a** and [$Rh_2(OOCH)_4$] are shown in kcal/mol ([Rh] = [$Rh_2(OOCH)_4$]).

Upon the formation of intermediate **G**, two distinct pathways were contemplated: the generation of a novel rhodium carbene through interaction of the catalyst with the diazo unit, or a 1,5-hydride shift leading to the formation of a benzoazepine core, akin to observations made with the addition external nitrile derivatives (**Scheme 3.2**). The energy barrier for the formation of the rhodium carbene is 8.8 kcal/mol lower, disregarding the possibility of a 1,5-hydride shift (**Figure 3.3**). Subsequently, the reaction proceeds via carbene formation through **TS-HI**, overcoming a barrier of 11.1 kcal/mol. Following this, a 5-exo-*dig* cyclization from the metal carbene species **I** occurs, overcoming a reaction barrier of 7.9 kcal/mol, yielding the zwitterionic vinyl cationic species **J**. Subsequent 1,3-rhodium migration gives rise to the η^1-vinylcarbene **K-[$Rh_2(OOCH)_4$]**, surpassing a reaction barrier of 13.2 kcal/mol, a process analogous to the one observed in the first CAM.

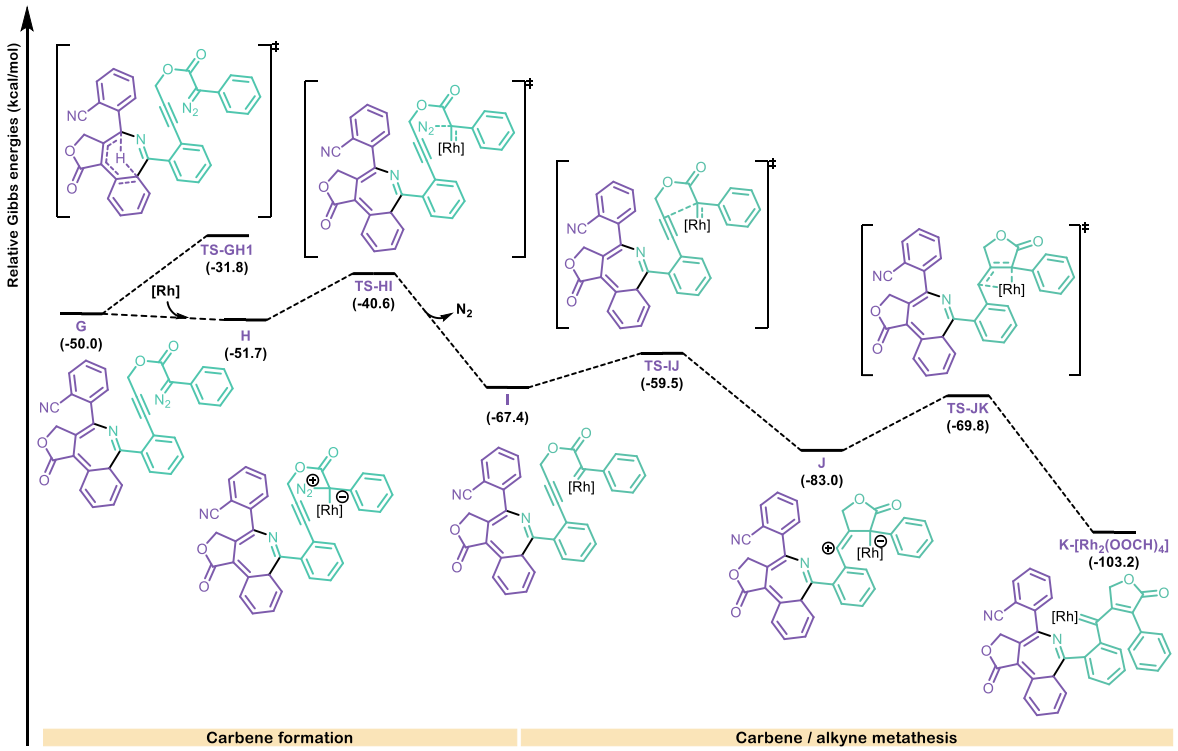

Figure 3.3. Gibbs energy for the second carbene formation and carbene-alkyne metathesis. Gibbs energies (298 K) relative to **4a** and $[Rh_2(OOCH)_4]$ are shown in kcal/mol ([Rh] = $[Rh_2(OOCH)_4]$).

From this intermediate, we opted to utilize the **[Rh₂(esp)₂]** catalyst (**Figure 3.4**) due to the considerable geometric differences that conditioned the outcome of the reaction. Substituting formates with esp ligands resulted in a 2.8 kcal/mol difference in the relative energies between **K-[Rh₂(OOCH)₄]** and **K-[Rh₂(esp)₂].** Proceeding from **K-[Rh₂(esp)₂]**, we explored two alternative reaction pathways. In the first scenario, **K-[Rh₂(esp)₂]** undergoes a 1,5-H shift, surmounting an energy barrier of 17.7 kcal/mol to form the benzoazepine core. In the second pathway, the azepine nitrogen undergoes nucleophilic addition to the carbenic carbon, resulting in the formation of the isoindole derivative **L** through a kinetically highly favorable reaction (reaction barrier of 1.3 kcal/mol). These energy barriers clearly highlight that the dominant pathway from intermediate **K-[Rh₂(esp)₂]** is the one involving azepine addition. Moving from intermediate **L**, a 1,5-H shift occurs through **TS-LM**. This step restores the aromaticity of the six-membered ring fused to the azepine, overcoming an energy barrier of 14.1 kcal/mol and releasing 25.9 kcal/mol, partly attributed to the rearomatization of the six-membered ring. Subsequently, at this stage, the rhodium dissociates from the system, concluding the metal-catalyzed cycle. However, a final ring contraction is mandatory to rationalize the formation of the final product. After exploring various possibilities, we identified that proton catalysis drives this concluding ring contraction. Protonation of the isoindole nitrogen induces a shift in the nitrogen's geometry, transforming it from approximately planar (C8-N64-C63-C44 dihedral angle of 170.8º, as indicated in **Figure 3.4** for atom labeling) to roughly tetrahedral (with a dihedral angle of 116.6º). This geometric alteration facilitates the ring contraction through **TS-NO**, involving an activation energy of 23.2 kcal/mol. This exergonic step yields **O**, which, upon subsequent deprotonation, gives rise to the formation of the isolated product **P**. Despite the reaction being conducted under anhydrous conditions, we hypothesize that this final stage of the transformation occurs either upon opening the reaction flask or as a result of treating the reaction crude with silica gel, as evidenced by a noticeable color change.

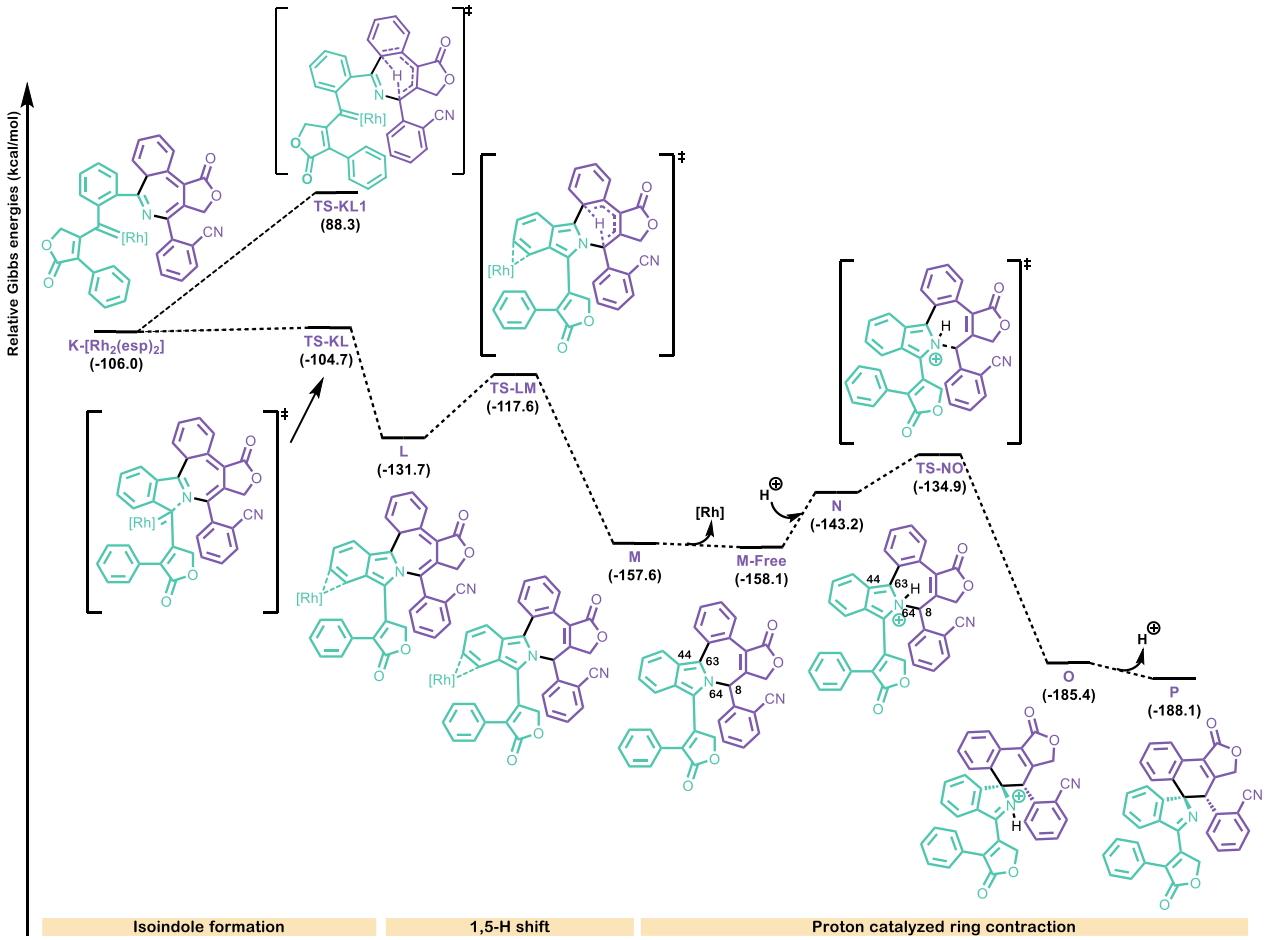

Figure 3.4. Gibbs energy for the electrocyclization, isoindole formation, 1,5-H shift and proton catalyzed ring contraction for the formation of **5a**. Gibbs energies (298 K) relative to **4a** and $[Rh_2(esp)_2]$ are shown in kcal/mol ([Rh] = $[Rh_2(esp)_2]$).

In this final step, we assumed that the proton is solvated in water, leading us to utilize the corresponding ΔG_{solv} (H^+) of 250.0 kcal/mol.[204] Regrettably, all attempts to experimentally detect the intermediate **M-free** have proven unsuccessful. Conversely, considering that the formation of compound **5** involves the migration of a hydrogen atom from the phenylacetic ring in **4**, we synthesized the corresponding C_6D_5 derivative **4a-D** to explore the fate of this H(D) (**Scheme 3.5**). The resulting product, **5a-D**, was obtained, with the deuterium originating exclusively from the C-D cleavage in the position anticipated for a 1,5-H shift, aligning with the proposed mechanism, and with no scrambling into other positions.

Altogether, the rhodium-catalyzed reaction (from **A** to **I**) exhibits an overall reaction energy of -157.6 kcal/mol through a highly extended cascade process. The energetic span between the turnover frequency (TOF)-determining intermediate (TDI, **D**) and the TOF determining transition state (TDTS, **TS-EF**) is 14.6 kcal/mol.[205] Notably, the energetic span in this carbene formation step is almost isoenergetic to that in the carbene formation step (span from TDI **A** to TDTS **TS-AB** is 14.4 kcal/mol) and 1,5-H shift (span from TDI **H** to TDTS **TS-HI** is 14.1 kcal/mol). The proton-catalyzed ring contraction is considered a distinct process, and we postulate that it occurs during the reaction work-up, releasing 2.7 kcal/mol.

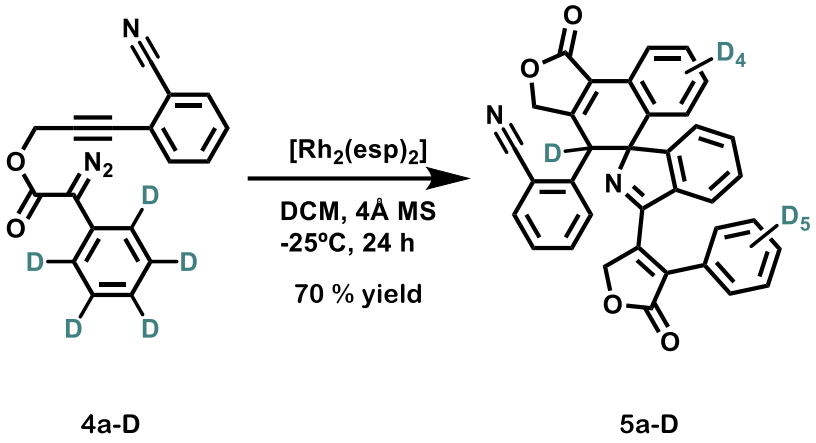

Scheme 3.5. Deuterium labelling experiment.

An alternative pathway, involving the reaction of two units of vinylcarbene intermediate **D**, has also been evaluated (**Figure 3.5**). This alternative pathway has an almost isoenergetic span between the turnover frequency (TOF) determining intermediate (TDI) and the TOF determining transition state (TDTS) and is not competitive with the limiting or selective steps. Although the two pathways can coexist, given the low probability of two carbenes lasting enough to react with one another, we believe that the pathway shown in **Figures 3.2, 3.3** and **3.4** is more favorable under the reaction conditions used.

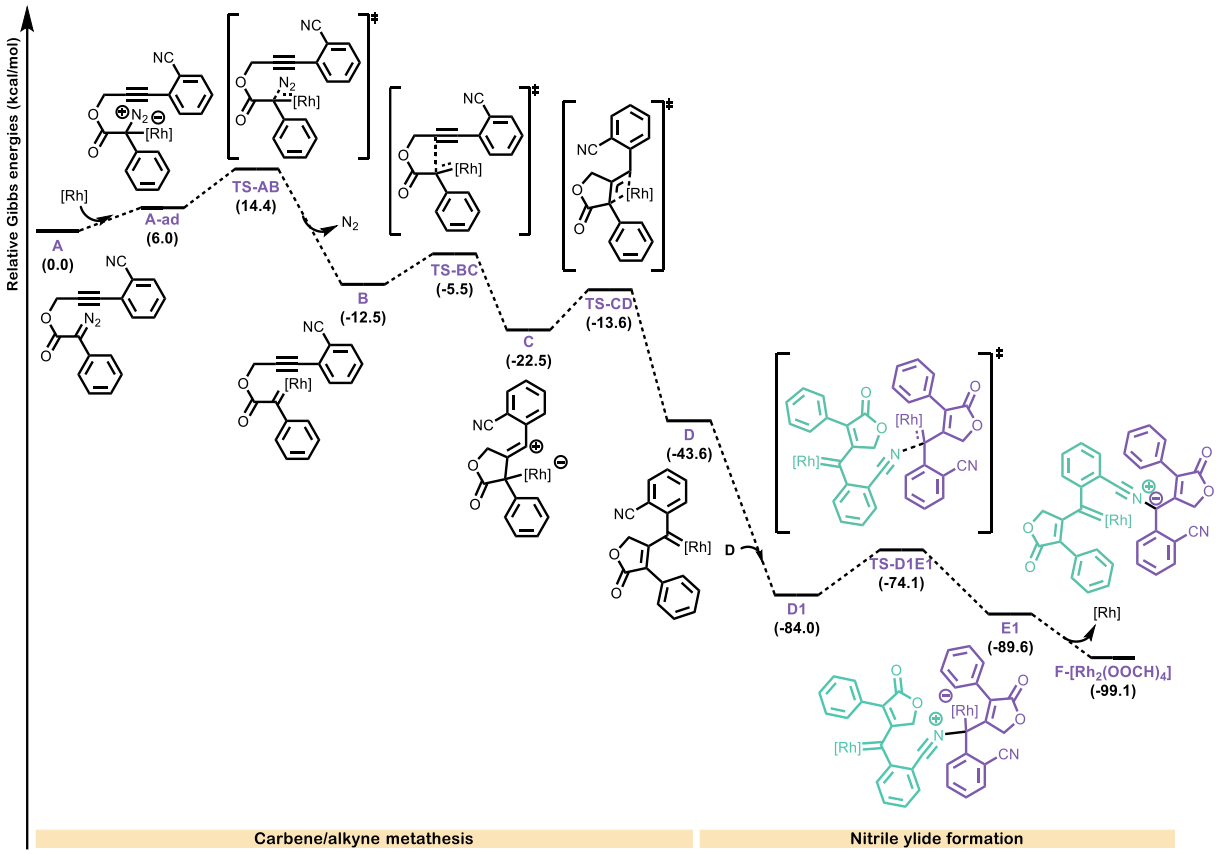

Figure 3.5. Gibbs energy for the mechanism involving two units of vinylcarbene **D.** Gibbs energies (298 K) relative to **4a** and $[Rh_2(OOCH)_4]$ are shown in kcal/mol ([Rh] = $[Rh_2(OOCH)_4]$).

In summary, we have presented a novel cascade process leading to a significant enhancement in molecular complexity for the diastereoselective synthesis of products cointaining the 1*H*-isoindole motif. The key feature of this transformation is the trapping of a vinylcarbene generated *in situ* by a nitrile group, eventually leading to the trifunctionalization of this nitrile moiety. This achievement marks the fulfillment of the first objective of this thesis, centered on the study of the intermolecular reactivity between CAM generated vinylcarbenes and nitriles.

All these results obtained in Chapter 3 are published in *ACS Catal.* **2024,** *14***,** 10, 7381–7388.

Chapter 4. Intramolecular Interception of the Remote Position of Vinylcarbene Silver Complex Intermediates by Csp^3−H Bond Insertion

Upon careful review of the literature precedents, we realized that no reports appeared utilizing silver as a catalyst for CAM-derived reactions. Nonetheless, the study of silver vinylcarbenes has been documented previously as exposed in the introduction (vide supra). In this regard, silver catalysts containing trispyrazolylborate ligands (Tp^x) have been described as highly active catalysts for the functionalization of CH bonds via carbene insertion. The versatility of Tp^x ligands has rendered them extremely valuable in both inorganic and organometallic chemistry, owing to their capacity for convenient tuning of electronic and steric properties via substituent modifications on the pyrazole ring (**Figure 4.1**).[206] In this context, the group of Prof. Pedro Pérez has reported several transformations capitalizing in this chemistry for the insertion of acceptor carbenes into gaseous alkanes,[207, 208] and more recently they also reported the use of donor-acceptor carbenes for the insertion into light alkanes.[209] The efficiency of these catalysts for the CH activation using vinylcarbenes has also been proved by the group of Rasika Dias[121] and more recently by Bi's group.[122]

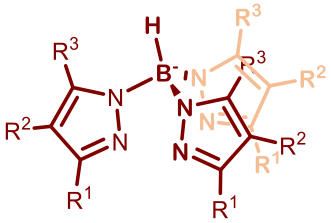

Tp^x ligands used in this study:

$Tp^{(CF3)2,Br}$ $R^1 = R^3 = CF_3$; $R^2 = Br$
Tp^{Br3} $R^1 = R^2 = R^3 = Br$
$Tp^{*,Br}$ $R^1 = R^3 = Me$; $R^2 = Br$

Figure 4.1. General structure of trispyrazolyl borate ligands and Tp^x ligands used in this study.

Furthermore, as previously mentioned, silver has proven to be more efficient than other metals for the functionalization at the vinylogous position. With all these precedents in hand, we wondered whether we could achieve the first example of silver catalyzed CAM reaction. Moreover, we decided to test the termination of the cascade reaction with a vinylogous Csp^3-H insertion, an elusive transformation not reported previously. To this end, we initiated a collaboration with Prof. Pedro Pérez and Dr. Ana Caballero from the CIQSO group at the University of Huelva. They provided us with an array of trispyrazolylborate silver complexes (**Figure 4.1.**), poised to function as catalysts for our envisioned reaction, opting for diazoalkynes with a tethered alkylated aniline as our model substrate, a system previously demonstrated to exclusively yield the carbenic Csp^3-H insertion adduct under rhodium catalysis, as previously mentioned in the introduction (**Scheme 4.1**).[173]

We performed a series of experiments to assess the catalytic capabilities of the three distinct silver Tp^x complexes (**Table 4.1**), employing the model substrate **6**.[173] Our results revealed the successful catalysis of the carbene/alkyne metathesis reaction by silver, leading to subsequent C-H insertion reactivity and yielding mixtures of up to four products. The use of $Tp^{(CF3)2,Br}$Ag(THF) (**entry 1**) produced a mixture of *anti* and *syn* diastereoisomers of the benzylic Csp^3-H insertion product **7**, accompanied by a minor subproduct whose identification was hindered by its low yield. Repeating the reaction at a lower concentration of **6** (3.8 mM) (**entry 2**) enhanced conversion, facilitating the characterization of the newly formed product. To our delight, isolation and NMR characterization confirmed the presence of benzoazepine **9**, resulting in the desired unprecedented primary Csp^3-H bond insertion to the vinylogous position of the silver vinylcarbene. The other two silver Tp^x complexes tested showed activity, albeit with reduced selectivity (**entries 3-4**). Furthermore, they induced the formation of a product resulting from carbene insertion into the primary Csp^3-H bond, **8**. Notably, employing simple silver salts as $AgBF_4$ and $AgSbF_6$ led to complete consumption of substrate **6** but

resulted in a non-selective reaction that did not provide any of the expected products, (**entries 5-6**), emphasizing the pivotal role of trispyrazolylborate ligands in this catalytic process.

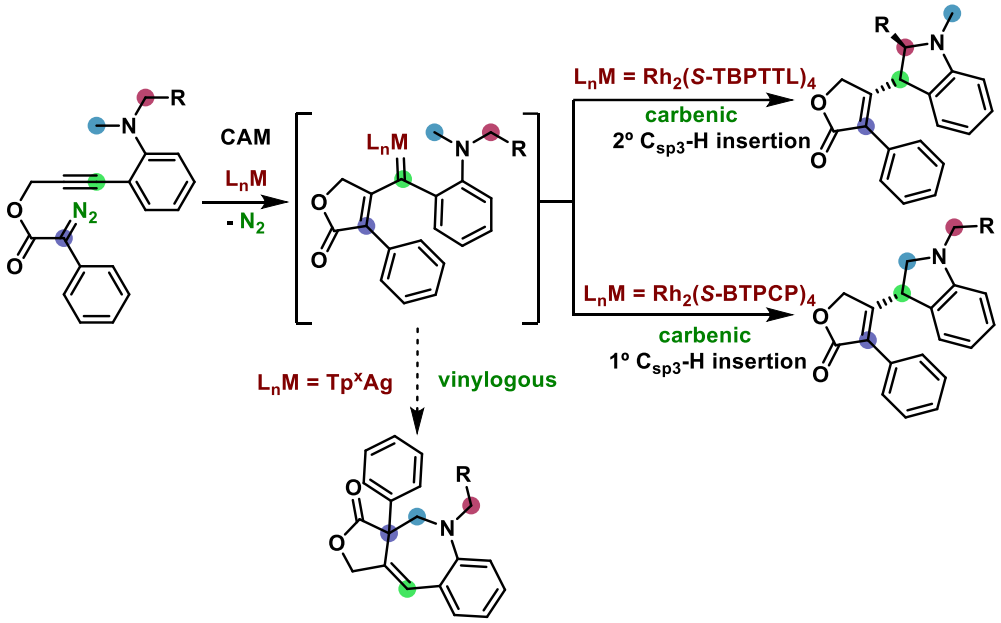

Scheme 4.1. CAM reaction terminated with C-H bond functionalization: carbenic vs vinylogous reactivity.

Table 4.1: Initial screening of silver-based catalysts for the CAM-cascade reaction. [a]

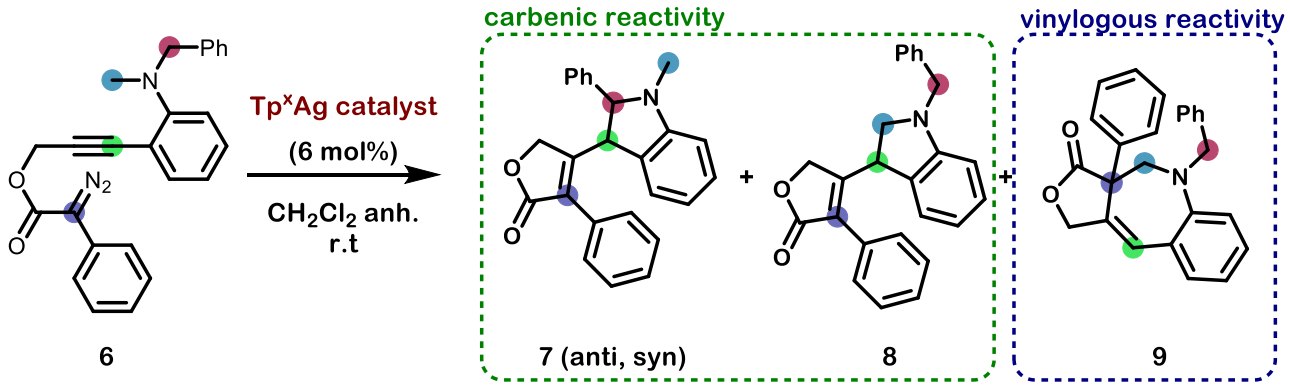

Entry	Catalyst	Yield (%) (7 *anti* / 7 *syn* / 8 / 9)
1[b]	$Tp^{(CF3)2,Br}Ag(THF)$	45[d] (23 / 17 / 0 / 5)
2	$Tp^{(CF3)2,Br}Ag(THF)$	82[d] (39 / 22 / 0 / 21)
3	$[Tp^{Br3}Ag]_2$	94 (35 / 21 / 18 / 21)
4[c]	$Tp^{*,Br}Ag(THF)$	39 (14 / 8 / 17 / 0)
5	$AgBF_4$	0
6	$AgSbF_6$	0

[a] Unless otherwise noted, reactions were carried out with 0.06 mmol of **6** ([**6**] = 3.8 mM), at room temperature in 16 mL of CH_2Cl_2 for 1.5h. The yield was determined by NMR using 4-chlorobenzaldehyde as internal standard. Product ratios were determined by NMR. [b] Reaction carried out at [**6**] = 20 mM for 1h. [c] Reaction run for 18h. [d] Isolated yield.

The uniqueness of this transformation lies not only in its vinylogous interception through an aliphatic bond but also in offering an alternative pathway to molecules incorporating the 1-benzoazepine scaffold. Therefore, we decided to optimize the synthesis of scaffolds analogous to **9** through the CAM cascade. Based on the previous findings, it became evident that the insertion of the benzylic Csp^3-H on the carbenic position directly competes with the desired methylic Csp^3-H insertion on the vinylogous position. For this reason, to attain the desired selective remote insertion, we opted to replace the benzyl moiety with another methyl unit. Consequently, we prepared dimethylated propargyl diazoacetate **10a** (see below for its synthesis), utilizing it as the starting point for refining the reaction conditions. (**Table 4.2**).

The optimization process started by using the same catalytic system employed for the benzyl-derived diazo compound **6**. In these conditions, the desired benzoazepine **12a** was favoured over the corresponding carbenic product **11a** (**entry 1**). The replacement of dichloromethane with dichloroethane, chlorobenzene, and dichlorobenzene as reaction solvents (**entries 2-5**) resulted in diminished yields and product ratios. Conversely, when the reaction was conducted in chloroform (**entry 6**), the yield of **12a** increased to 57%, while the yield of **11a** decreased to 10%. Adjusting the temperature to 45 ºC maintained similar yields (**entry 7**), but the most favorable outcome was achieved at 35 ºC, yielding **12a** in 71% with a 7.1:1 ratio with respect to the corresponding carbenic product (**entry 8**). The reaction, carried out at the same temperature using dichloromethane as the solvent, resulted in higher total yields but a lower product ratio (**entry 9**).

Exploration of alternative Tp^x silver catalysts revealed distinct outcomes. The use of $[Tp^{Br3}Ag]_2$ led to an almost equal 1:1 ratio of **11a** and **12a** (**entry 10**), while $Tp^{*,Br}Ag(THF)$ failed to initiate any reaction (**entry 11**). For comparison, we tested other metals as catalysts. Copper-derived Tp^x catalysts exhibited either no reactivity (**entry 12**) or favored the carbenic product as the major outcome (**entry 13**). Not unexpectedly, rhodium (II)-based catalysts resulted in the carbenic Csp^3-H insertion as the predominant product (**entries 14-15**), aligning with previous findings reported by Xu and Doyle.[173] Based on these results, we identified entry 8 as the optimized reaction conditions.

Upon optimizing the reaction conditions, a series of diverse aniline derived propargyl diazoacetates (**10a-10j**) were tested to evaluate the scope of the reaction. We selected 10 diazo compounds to analyze the electronic effects of various substituents within both the aniline and phenylacetic acid frameworks. These compounds were synthesized according to the conditions outlined in **Scheme 4.2** (for experimental details see **Supplementary Material**). Starting from *N,N*-dimethyl-2-ethynylaniline, the *in situ* generation of the corresponding alkynyllithium in the presence of n-butylithium, followed by its reaction with paraformaldehyde, yields the respective aryl-substituted propargyl alcohols. In cases where substrates harbor substituents in the aniline ring, the production of the desired arylated propargyl alcohols is performed by direct Sonogashira coupling between propargyl alcohol and the 2-iodo dimethylaniline derivatives. Subsequently, esterification employing *para*-substituted phenylacetic acids in the presence of DCC results in the formation of the corresponding esters. Finally, the synthesis of diazo compounds **10a-10j** is accomplished in the presence of *p*-ABSA and DBU.

Table 4.2: Optimization of the reaction conditions. [a]

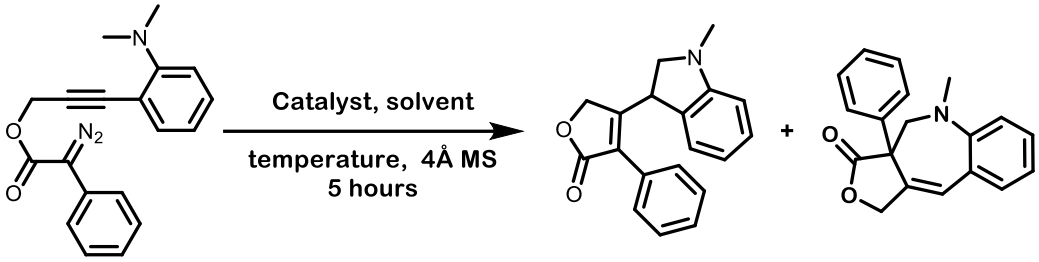

10a **11a** **12a**

Entry	Catalyst	Solvent	T (ºC)	Yield (%) (11a / 12a)
1	$Tp^{(CF3)2,Br}Ag(THF)$	CH_2Cl_2	r.t	57 (12 / 45)
2	$Tp^{(CF3)2,Br}Ag(THF)$	DCE	r.t	28 (5 /23)[b,d]
3	$Tp^{(CF3)2,Br}Ag(THF)$	Chlorobenzene	r.t	54 (13 / 41)[c,d]
4	$Tp^{(CF3)2,Br}Ag(THF)$	1,2-Dichlorobenzene	r.t	36 (10 / 26)[d]
5	$Tp^{(CF3)2,Br}Ag(THF)$	1,2-Dichloropropane	r.t	NR
6	$Tp^{(CF3)2,Br}Ag(THF)$	$CHCl_3$	r.t	67 (10 / 57)
7	$Tp^{(CF3)2,Br}Ag(THF)$	$CHCl_3$	45 ºC	72 (13 / 59)
8	$Tp^{(CF3)2,Br}Ag(THF)$	$CHCl_3$	35 ºC	81 (10 / 71)
9	$Tp^{(CF3)2,Br}Ag(THF)$	CH_2Cl_2	35 ºC	90 (19 / 71)
10	$[Tp^{Br3}Ag]_2$	CH_2Cl_2	35 ºC	69 (34 / 35)
11	$Tp^{*,Br}Ag(THF)$	CH_2Cl_2	35 ºC	N.R.
12	$Tp^{(CF3)2,Br}Cu(AcN)$	$CHCl_3$	35 ºC	N.R.
13	$Tp^{Br3}Cu(AcN)$	$CHCl_3$	35 ºC	100 (80 / 20)
14	$[Rh_2(OAc)_4]$	$CHCl_3$	35 ºC	73 (54 / 19)
15	$[Rh_2(esp)_2]$	$CHCl_3$	35 ºC	95 (88 / 7)

[a] Unless otherwise noted, reactions were carried out with 0.06 mmol of **10a** ([**10a**] = 3.8 mM), at room temperature in 16 mL of $CHCl_3$ for 5h. The yields given are isolated yields. [b] 26% starting material was recovered. [c] 14% starting material was recovered. [d] Yields and product ratios were determined by NMR using 1,3,5-trimethoxybenzene as internal standard. r.t, room temperature; N.R., no reaction.

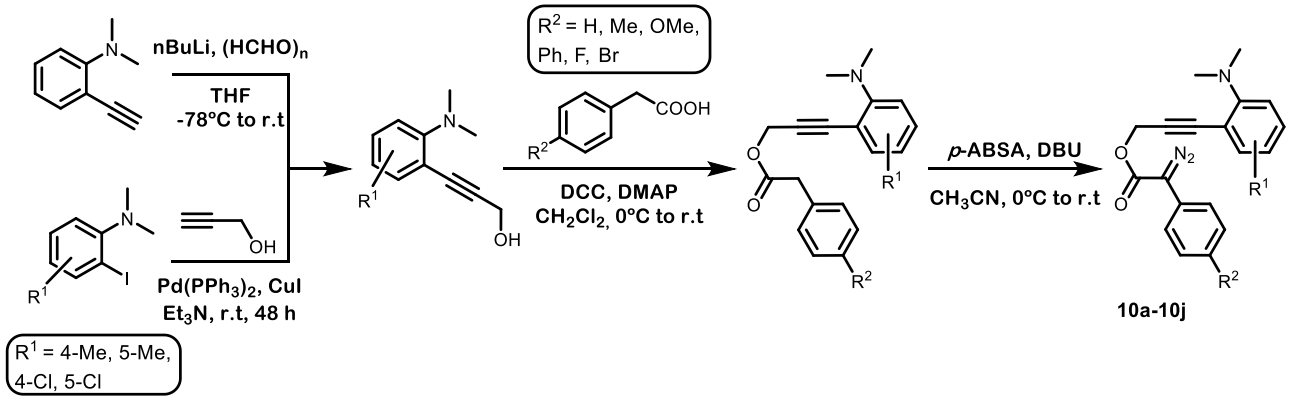

Scheme 4.2. Synthesis of dimethylaniline propargyl diazoacetates **10a**-**10j.**

We then proceed to evaluate the scope of the reaction (**Figure 4.2**). The introduction of electron-donating substituents (methyl, methoxy and phenyl) in the phenyldiazo moiety resulted in moderate yields of **12b-d**. The inclusion of electron-withdrawing halogen substituents in that ring not only reduced overall conversion but also shifted the selectivity towards the carbenic insertion product (vinylogous:carbenic ratio of 0.9:1 for **12e** and 0.6:1 for **12f**). On the contrary, excellent efficiency and selectivity were observed for substrates with substituents in the dimethylaminophenyl ring, maintaining yields in the 58-69% range. These substrates favored vinylogous reactivity, regardless of whether they bore electron-withdrawing or electron-donating substituents in the *meta*- (**12g, 12h**) or *para*- (**12i, 12j**) positions relative to the dimethylamino moiety. Additionally, the reaction demonstrated scalability to a 1 mmol scale, with only a slight decrease in yield (57% for **12a**).

Given that the formation of compounds **12** implies the migration of a hydrogen from one of the methyl groups of the dimethylamino fragment, we prepared the corresponding $N(CD_3)_2$ derivative **10a-d$_6$** to trace the fate of the initial H(D). As illustrated in **Scheme 4.3**, products **12a-d$_6$** and **11a-d$_6$** were obtained in a 6.7:1 ratio, mirroring the ratio observed for the protio derivatives (7.1:1). The deuterium originating from the C-D cleavage was exclusively localized in one position in both compounds, without scrambling into other positions.

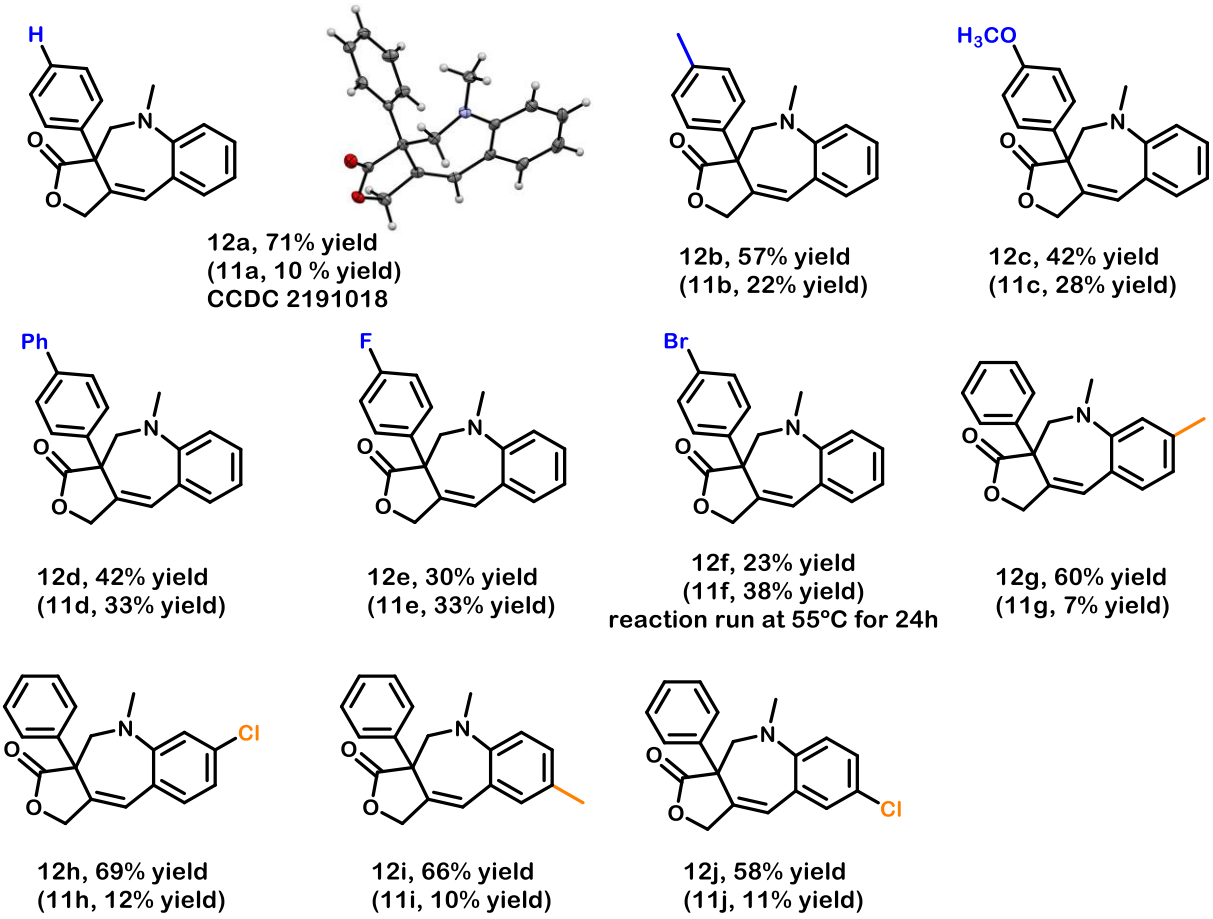

Figure 4.2. Scope of the reaction.

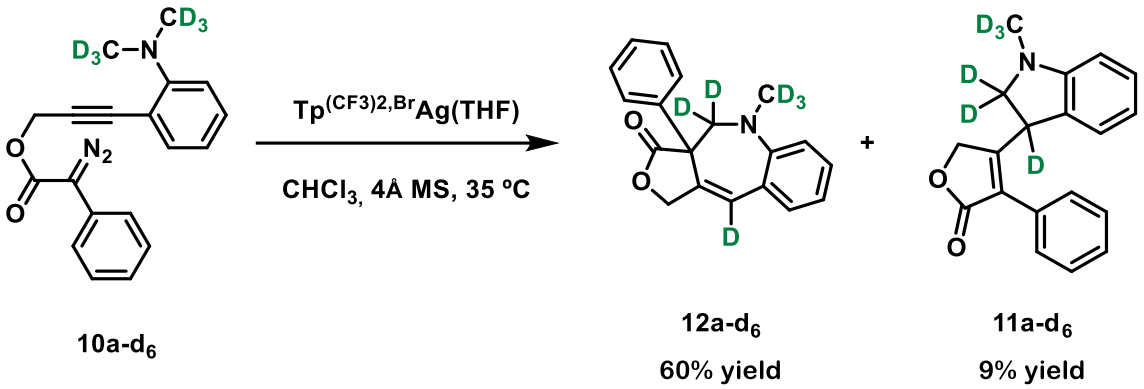

Scheme 4.3. Deuterium labelling experiment.

Concerning the mechanistic insights of this transformation, the literature presents several pathways for CAM processes (**Scheme 4.4**). The May group have reported the isolation and mechanistic relevance of ring-fused cyclopropenes with rhodium catalysts (**path I**).[171] Some of us postulated the formation of a rhodium(I) η^3-vinylcarbene intermediate through a [π2s+π2a] addition, subsequently evolving into the rhodium(I) η^1-vinylcarbene,[174] a proposal also shared by Saá in their intermolecular Ru-catalyzed CAM cascade processes (**path II**).[210] Yu and Xu proposed a 5-exo-*dig* cyclization leading to a highly reactive zwitterionic vinyl cationic species, which, upon a Rh-1,3-shift, transforms into the rhodium(II) η^1-vinylcarbene (**path III**).[200] An analogous mechanism was also postulated by Xue under $Rh(OAc)_2$ catalysis.[211] Alternatively, Xu and Hashmi [212] and Hu[213] reported gold-catalyzed cascade reactions generating vinylcarbenes through nucleophilic addition of the diazo compound onto the gold-activated alkyne (diazo-yne reaction), followed by the expulsion of dinitrogen (**path IV**).

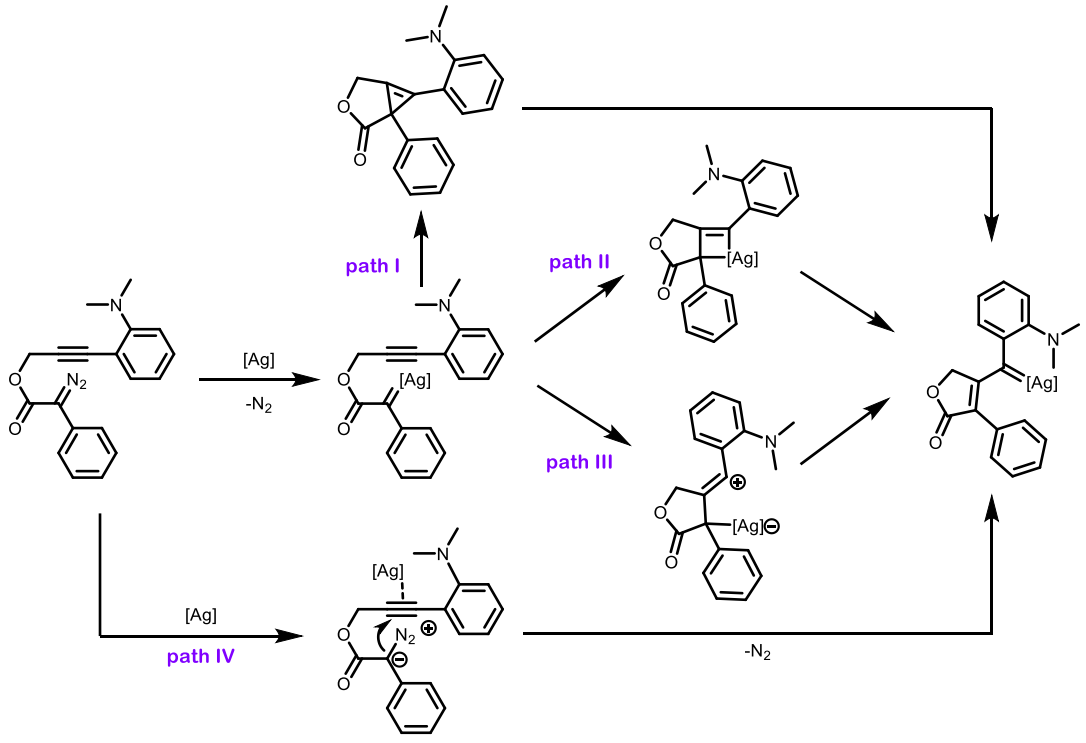

Scheme 4.4. Plausible mechanistic pathways for the silver-catalyzed CAM.

Based on the plausible operation of various pathways, a series of DFT calculations were carried out by Roger Monreal-Corona under de supervision of Dr. Albert Poater at the B3LYP-D3/Def2TZVP-SDD-SMD($CHCl_3$)//BP86-D3/Def2SVP-SDD level of theory using the Gaussian16 software package to elucidate the reaction mechanism of our silver-catalyzed CAM (**Figure 4.3**).

The coordination of the silver complex to the carbenic carbon of the diazo species represents a mildly endergonic step (3.7 kcal/mol). This is followed by the extrusion of nitrogen through transition state **TS-BC**, resulting in an overall energy barrier of 11.9 kcal/mol, leading to the formation of the silver carbene **C** (-16.2 kcal/mol). Notably, this silver carbene **C** serves as a common intermediate for the proposed paths I, II, and III (**Scheme 4.4**). A computed single-step path IV barrier was determined to be 15.9 kcal/mol, therefore it was discarded. From carbene species **C**, nucleophilic addition of the alkyne onto the carbenic carbon in a 5-exo-*dig* cyclization process leads to the formation of the zwitterionic vinyl cationic species **D** in a barrierless exergonic manner.[214] At this stage, the formation of the ring-fused cyclopropene (path I) required a kinetic effort of 31.5 kcal/mol. Additionally, we considered the possibility of a direct hydride transfer to the vinyl cation, revealing an energy barrier of 12.6 kcal/mol.[215]

However, both of these pathways were dismissed in favor of the barrierless nucleophilic attack of the negatively charged silver atom onto the carbocation. This leads to the formation of the silver η^3-vinylcarbene **E**, which undergoes rearrangement to the nearly isoenergetic silver η^1-vinylcarbene **F**. Overall, the formation of silver η^1-vinylcarbene F is highly exergonic (-65.7 kcal/mol) and occurs through a novel pathway that combines the previously postulated paths II and III. Next, the silver carbene insertion into the C-H bond was computed. The insertion typically manifests in a concerted manner, although occasionally it occurs asynchronously, with the formation of the new C−H taking place earlier than the formation of the C−C bond.[208, 216] In our system, all attempts to locate the concerted C-H insertion from intermediate **F** proved unsuccessful. Instead, an alternative stepwise C-H insertion mechanism involving a zwitterionic intermediate was identified, resembling the mechanism reported by Shaw and Tantillo for the C-H insertion of donor/donor dirhodium carbenes.[217] Specifically, from the silver vinyl carbene **F**, a hydride shift surpassing an energy barrier of 18.0 kcal/mol leads to the zwitterionic intermediate **G** in a slightly exergonic process (ΔG = -4.0 kcal/mol). This hydride shift represents the rate-determining step in the overall process.

Following this, an S_E2[218] C-C bond-closing step occurs from **G** through transition state **TS-GI** with an energy barrier of 10.9 kcal/mol. This step leads, upon silver decoordination, to **I**, the carbenic C-H insertion product **11**. Alternatively, intermediate **G** may undergo an electrophilic substitution reaction at the γ carbon atom (in an S_E2' reaction or bimolecular electrophilic substitution reaction with rearrangement). This reaction exhibits a lower energy barrier of 10.5 kcal/mol, leading to the less thermodynamically stable product **H**, corresponding to the vinylogous C-H insertion product **12**, which thus corresponds with the kinetic product of the reaction. Both pathways are consistent with the observations from the deuterium-labelling experiment.

To gain deeper insights into the experimental ratio of products involving the Csp^3-H insertion in the vinylogous and carbenic positions, we conducted additional DFT calculations. Specifically, we computed intermediate **G** and transition states **TS-GI** and **TS-GH** for compounds with *para*-substituted Me, OMe, Ph, F, and Br in the phenyldiazo ring, comparing them to the case of H. Computational results precisely aligned with experimental

data, predicting a preference for the vinylogous product formation for substrates bearing H, Me, OMe, and Ph ($\Delta\Delta G^{\ddagger}$ values of 0.4, 0.9, 1.4, and 1.3 kcal/mol, respectively). In the case of the F-containing substrate, which experimentally resulted in an almost equimolecular mixture of **12e** and **11e**, a computed value of 0.0 kcal/mol was obtained. Conversely, for Br, which experimentally favored the carbenic **11f** over the vinylogous **12f** insertion, a kinetic barrier difference of -1.2 kcal/mol was computed. The kinetic preference for vinylogous addition can be attributed to the fact that the vinylogous carbon is less sterically hindered than the carbenic one, both in intermediate **G** and in transition states **TS-GH** and **TS-GI**. This is evidenced by an 8.0% lower percentage buried volume (%VBur)[219] of the vinylogous carbon compared to the carbenic one in the case of intermediate **G**, with a further 3.9% reduction in the subsequent transition states.

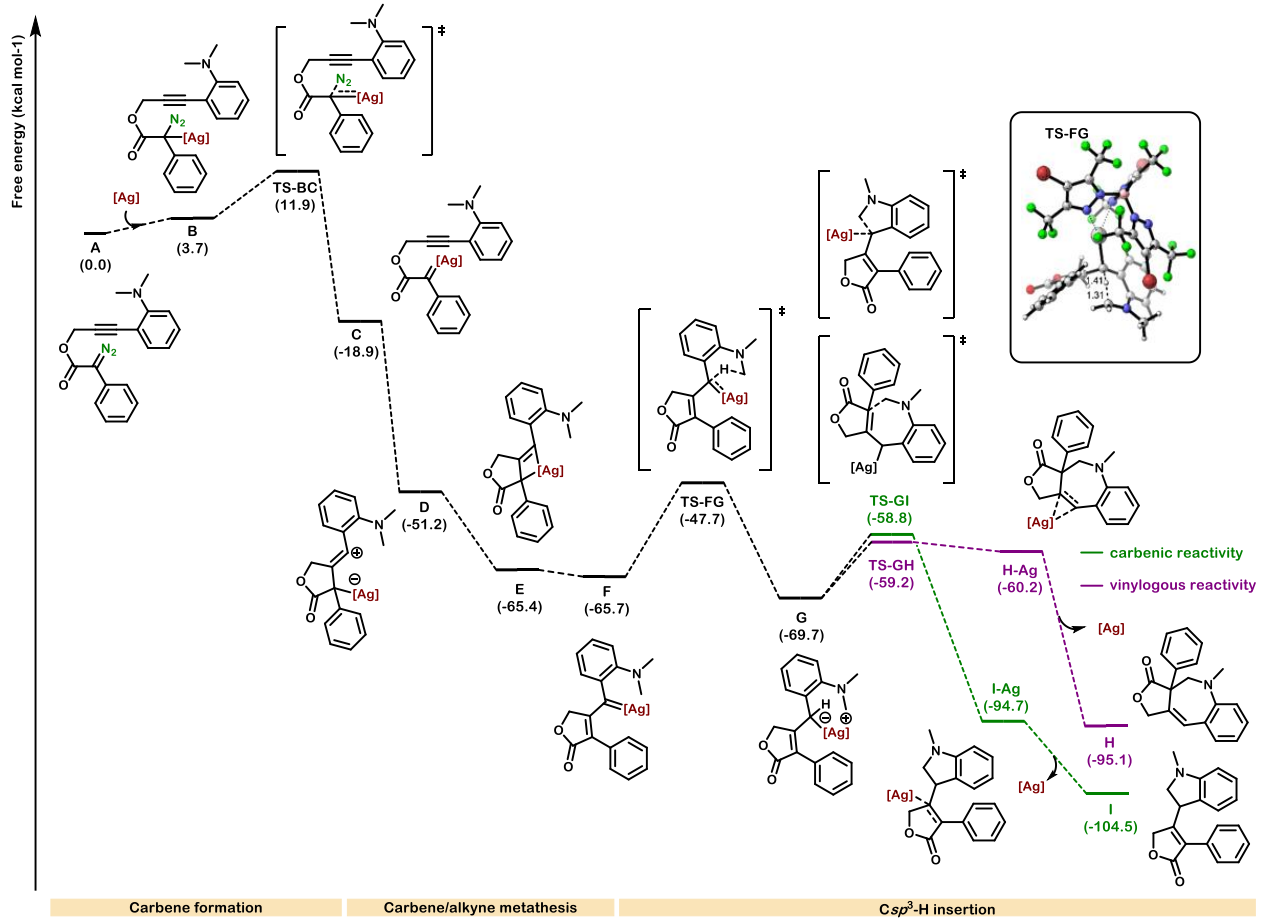

Figure 4.3. Gibbs energy profile (in kcal/mol) of the silver-catalyzed CAM reaction ([Ag] = $Tp^{(CF3)2,Br}Ag$).

In summary, we have achieved the second objective of this thesis by establishing a platform for generating silver vinylcarbenes via carbene-alkyne metathesis. Moreover, we have provided an unprecedented interception of the vinylogous position with a Csp^3-H bond. Furthermore, the combination of experimental and computational techniques was key to reveal the mechanism and especially that the Csp^3-H bond interception occurs through a stepwise, hydrogen shift pathway, at variance with previously described silver-catalyzed C-H functionalization by carbene insertion reactions.

All these results obtained in Chapter 4 are published in *Angew.Chem. Int. Ed*. **2023**, *62*, e202215163.

Chapter 5. Concerted or stepwise carbene transfer reactions to Csp^2-H bonds? A mechanistic insight

The insertion of carbenes into C*sp*^{3}-H bonds typically proceeds in a concerted manner, as discussed in the preceding chapter. Conversely, for C*sp*^{2}-H bonds, the mechanism is generally proposed to occur in a stepwise fashion. Initially, a C-C bond formation takes place, followed by hydrogen migration. In the first step, the transient metal carbene intermediate undergoes electrophilic addition to the aromatic ring, giving rise to a Wheland intermediate. The details of the subsequent step are less clear. A [1,2]-H migration step has been postulated for reactions involving donor-donor carbenes (**Scheme 5.1a**).[201, 220] Alternatively, when carbenes contain (at least) an acceptor substituent, a proton transfer to the adjacent carbonyl oxygen is proposed. This results in the formation of an enol intermediate, which eventually tautomerizes to the keto form, yielding the formal C-H insertion adduct (**Scheme 5.1b**).[221] Only in one example by Xu *et al*. involving a donor-donor carbene, a concerted mechanism is postulated upon DFT calculations, although the authors did not comment further on this unprecedented point.[200]

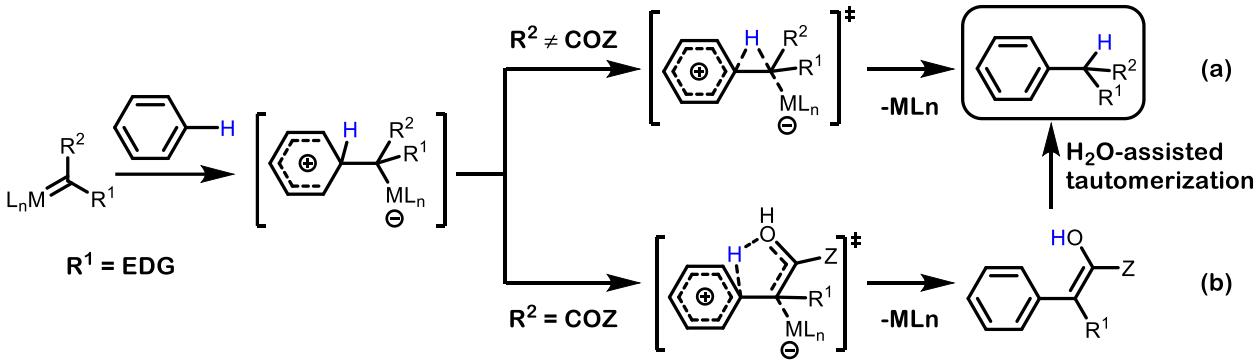

Scheme 5.1. Conventional proposed mechanism for metal carbene C*sp*^{2}-H bond insertion.

Building upon the findings of the previous chapter, where we elucidated the unique mechanism governing the C*sp*^{3}-H insertion of our *in situ* generated silver Tp^x vinylcarbenes, diverging from conventional knowledge in the literature, we posed the question of whether the insertion of this vinylcarbene into a C*sp*^{2}-H bond would also exhibit similar deviations from the norm. To explore this hypothesis, we capitalized on a similar platform that proved effective in Chapter 4 and removed the dimethylamino moiety from the starting material and used diazo compound **13a** as the model substrate. Ideally the vinylcarbene generated would insert into the C*sp*^{2}-H bond of the initial phenylacetic moiety leading to indene fused product **14a** (**Scheme 5.2**) a reactivity pattern that has been previously reported by Padwa[169] and Doyle[177] using rhodium and copper catalysts.

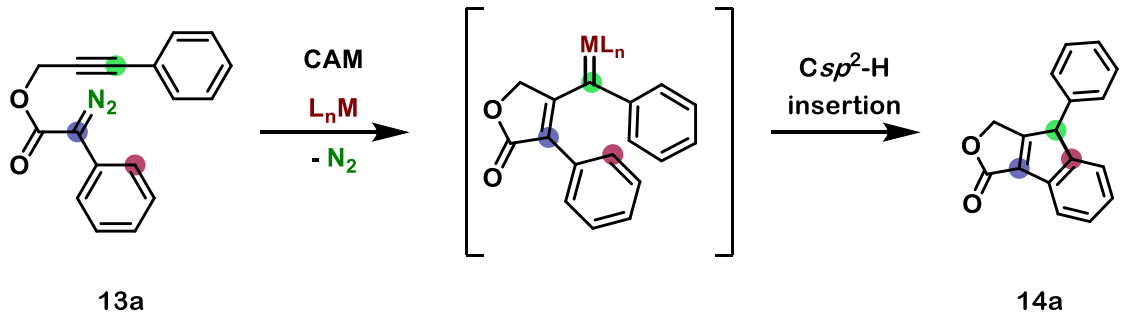

Scheme 5.2. General scheme for the CAM terminated in C*sp*^{2}-H bond insertion.

We commenced our investigation by employing similar conditions to the highest yielding ones identified in Chapter 4, utilizing Tp$^{(CF3)2,Br}$Ag(THF) as the catalyst (5 mol%) in dichloromethane, which afforded the desired

product in a quantitative yield. However, reducing the catalyst loading to 2.5 mol% proved to be detrimental to the transformation, resulting in a decreased yield of 78% for product **14a**. Based on these two experiments, we established the initially employed conditions as the optimized ones.

We chose 13 diazo compounds to analyze the chemoselectivity of the reaction and the electronic and steric effects of various substituents within both aromatic rings present in the starting material. These compounds were synthesized following the conditions outlined in **Scheme 5.3** (for experimental details see **Supplementary Material**). Starting from iodophenyl derivatives, Sonogashira coupling with propargyl alcohol, followed by esterification with *para*-substituted phenylacetic acids using DCC, yields the corresponding esters. Finally, the reaction of the prepared esters in the presence of *p*-ABSA and DBU affords the diazo compounds (**13a-13m**).

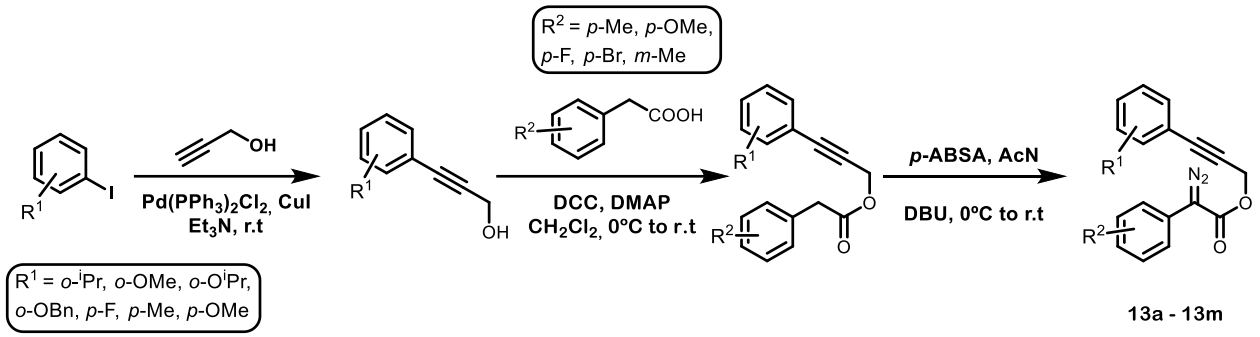

Scheme 5.3. Synthesis of phenyl propargyl diazoacetates **13a-13m.**

We then explored the scope of the transformation (**Scheme 5.4**). Initially, we examined the chemoselectivity of the reaction by introducing substituents at the *ortho*-position of the phenylpropynyl moiety (**Figure 5.1 and Scheme 5.4**). In the previous chapter, the presence of an *o*-dimethylamino group led exclusively to functionalization at the Csp^3-H bond, with no detection of the product corresponding to Csp^2-H bond insertion. Conversely, upon introduction of an *o*-methoxy group, a complete reversal of chemoselectivity was observed, resulting in the formation of indene **14b** with an 82% yield. To delve deeper into this chemoselectivity, secondary and tertiary CH bonds were introduced into the -OR moiety. It is widely known that the bond dissociation energy for secondary or tertiary Csp^3-H bonds is lower than for primary ones, thereby reducing the energy barrier for carbene insertion into these bonds. However, for substrates bearing O^{i}Pr and OBn groups, we exclusively isolated the corresponding Csp^2-H insertion products, **14c** and **14d**, in quantitative yields. Finally, to test the consistency of this trend, we used diazo compound **13e,** bearing an *o*-^{i}Pr group, yielding indene **14e** as the sole product, albeit with a slightly reduced yield of 81%.

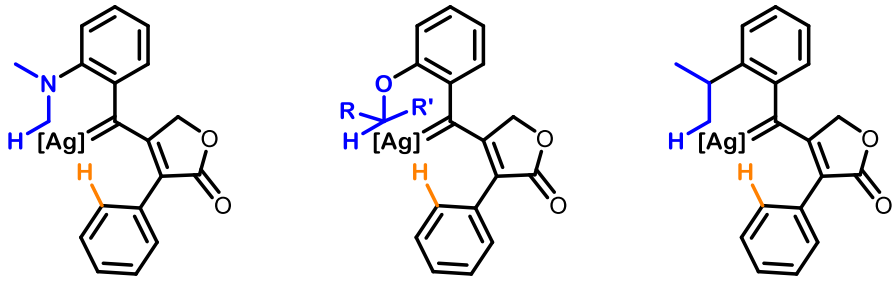

Figure 5.1. Selectivity observed for *o*-substituted substrates.

We then studied the effect of introducing substituents in the *para* position of the phenyl acetylene ring. The presence of a F, CH_3 or OCH_3 was compatible with the reaction, albeit resulting in slightly decreased yields for both electron-withdrawing F (81%, **14f**) and electron-donating OCH_3 (88%, **14h**) substituents. Subsequently, we assessed the impact of *para* substituents in the phenylacetic-derived ring. The incorporation of electron-donating groups (Me, OMe) provided the desired products in nearly quantitative yields. Conversely, the introduction of halogen groups led to a slight decrease in yield, with fluorine yielding 88% (**14k**) and bromine yielding 90% (**14l**). Finally, the introduction of a methyl in *meta* position in the bottom ring resulted in the formation of a mixture of regioisomers (**14m** and **14m'**) with yields of 50% and 34%, respectively. The regioisomers were successfully separated using flash chromatography and identified through selective NOESY experiments.

In pursuit of understanding the mechanism driving the transformation, a series of DFT calculations were carried out by Roger Monreal-Corona under the supervision of Dr. Albert Poater. The Gibbs energy profile was computed at the B3LYP-D3/Def2TZVP-SDD-SMD(CH_2Cl_2)//BP86-D3/Def2SVP-SDD level of theory, using the Gaussian16 software package (**Figure 5.2**) and employing **13a** as the model. The mechanism begins with the coordination of the silver catalyst to the carbon linked to the diazo moiety, followed by dinitrogen extrusion, resulting in silver carbene **C** with a transition state barrier of 12.2 kcal/mol. Subsequent CAM proceeds barrierlessly, leading to the formation of the desired vinylcarbene **F**. Despite our efforts to explore the conventional stepwise Csp^2-H insertion mechanism, the transition state leading to a Wheland intermediate could not be located. Conversely, a direct, concerted Csp^2-H insertion pathway was identified, via **TS-FG**, overcoming a barrier of 18.6 kcal/mol and yielding the final indene product in a highly exergonic process (-93.3 kcal/mol).

The obtained results support our hypothesis that the *in situ* generated donor-donor silver vinylcarbenes via CAM could pave the way for an unexplored mechanistic proposal in the Csp^2-H insertion of metal carbenes. To delve deeper into this feature, we conducted calculations for the Csp^2-H insertion step with various substituents decorating the aryl group close to the vinylcarbene (**Table 5.1**).

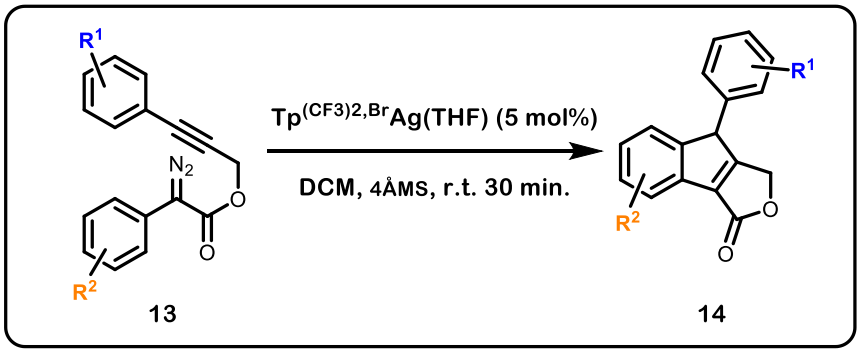

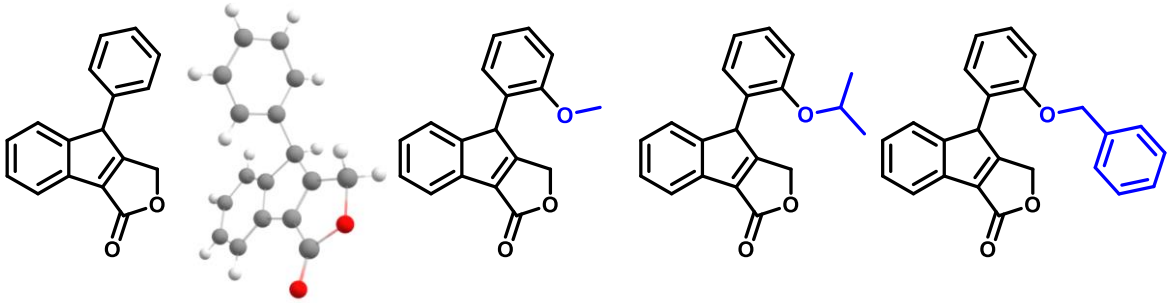

14a, 99% yield | 14b, 82% yield | 14c, 99% yield | 14d, 99% yield [b]

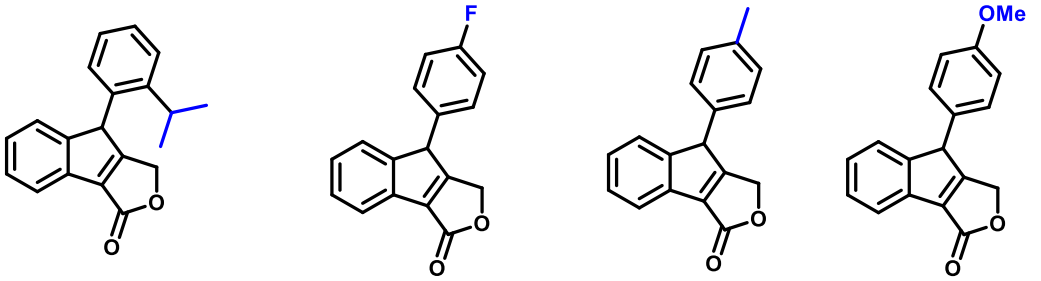

14e, 81% yield | 14f, 81% yield (99 % yield [c]) | 14g, 99% yield (92 % yield [c]) | 14h, 88% yield (79 % yield [c])

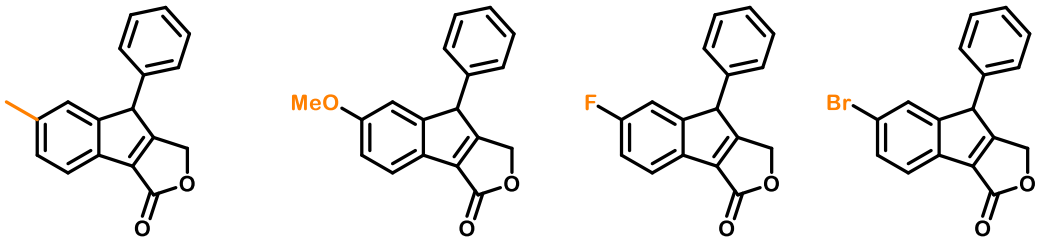

14i, 99% yield | 14j, 98% yield | 14k, 88% yield | 14l, 90% yield

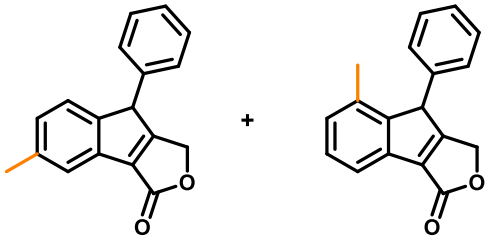

14m (50 % yield) + 14m' (34 % yield)

Scheme 5.4. Scope of the transformation. [a] Unless otherwise noted, reactions were carried out with 0.07 mmol of **13** ([**13**] = 4.7 mM), at room temperature for 30 mins. [b] Reaction run for 1.5h. [c] Using $Tp^{Br3}Ag(THF)$ as the catalyst.

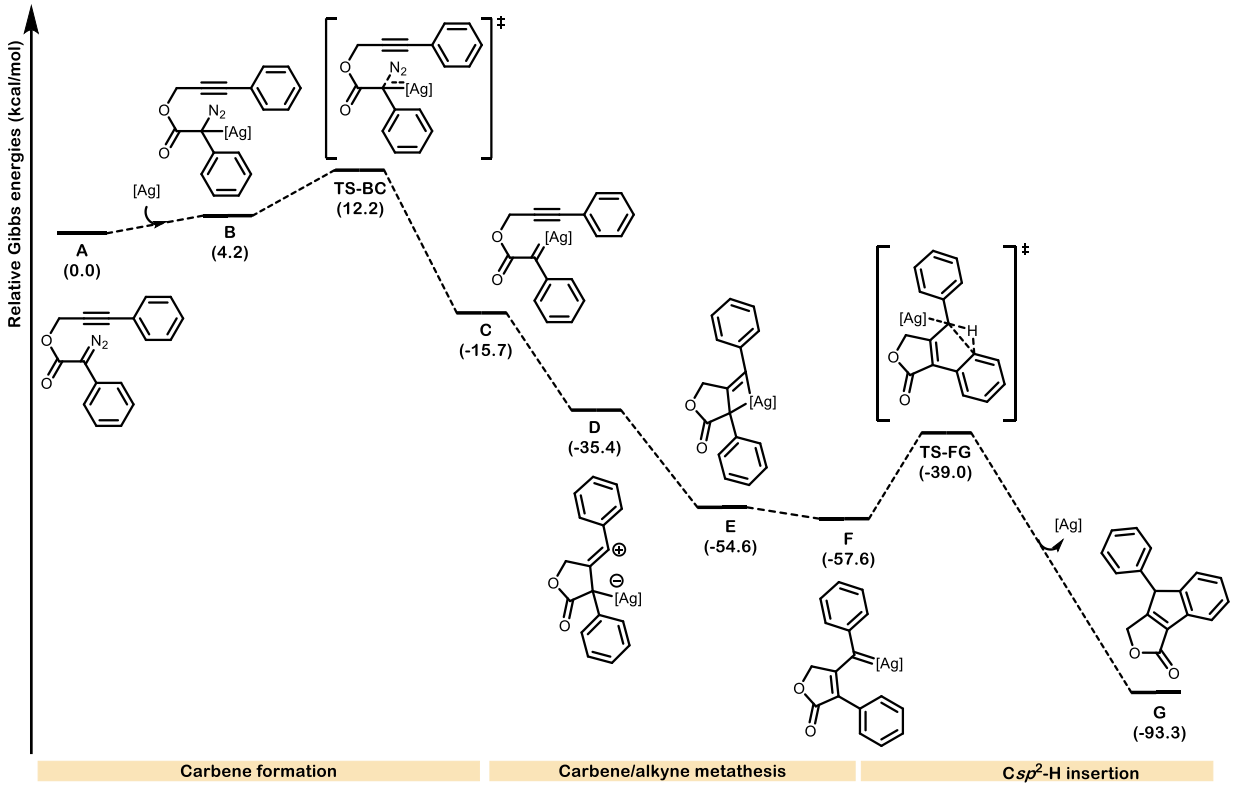

Figure 5.2. Gibbs energy profile (in kcal/mol) of the silver-catalyzed CAM reaction of **13a** ([Ag] = $Tp^{(CF3)2,Br}Ag$).

We initiated our analysis by studying substituents in the *ortho* position of the phenylpropynyl moiety, and in all three cases studied, the transition state for the concerted pathway could not be located (**entries 2-4**). Conversely, the reaction proceeds through electrophilic addition of the carbene to the arene, leading to intermediate **G**, which is analogous to a Wheland intermediate. Subsequently silver decoordinates to yield 3H-indene intermediate **G-free** in an exergonic process. From there, a 1,2-H shift that recovers the aromaticity of the arene ring occurs yielding the final product. Of note, in these cases where the reaction proceeds stepwise, the rate-determining step corresponds to the electrophilic addition of the carbene to the arene (**TS-FG**). Therefore, for the rest of the chapter, we will refer as the energy value of this transition state as the stepwise TS. The stepwise Csp^2-H insertion was found for the three cases, indicating it as the operative pathway for the *ortho* substitution pattern. Notably, in the instance of a substrate bearing the dimethylamino moiety (**entry 2**), Csp^2-H insertion would proceed in a stepwise manner. However, the barrier is notably high at 33.5 kcal/mol, nearly 14 kcal/mol higher than the pathway leading to the Csp^3-H insertion as reported in Chapter 4. These results unequivocally support the selectivity observed in the previous chapter regarding C-H insertion.

For substituents situated in the *para* position of the phenylacetylene ring, both concerted and stepwise transition states could be located (**entries 5-7**). In all cases, the pathway with the lowest energy was based on the unprecedented, concerted mechanism, irrespective of the electron-donating or electron-withdrawing nature of these substituents. These findings indicate a Csp^2-H insertion sensitive to steric factors. When substituents are in proximity to the carbenic carbon (*ortho*), the reaction proceeds in a stepwise fashion. Conversely, when substituents are distant from the carbene (*para*), the lowest energy path involves the concerted mechanism, regardless of electronic factors. The only difference we observed among the different structures obtained is that the presence of substituents in *ortho* position prevents the arene ring from adopting a coplanar orientation

with the (empty) 2p carbene orbital in the vinylcarbene, thus suggesting that sterics are responsible for the difference in behaviour.

Next, we examined substituents in the *para* position of the phenylacetic ring (**entries 8-11**). In all cases, the concerted mechanism was the only one observed, regardless of the electronic nature of the substituent. We then evaluated substituents located at the *meta* position, as these can stabilize the Wheland intermediate through mesomeric effects. Based on experimental results, two regioisomers are obtained upon Csp^2-H insertion. However, to benchmark the effects of *meta* substituents on the insertion, we only carried out calculations for the transition state (TS) leading to the major regioisomer obtained. For fluorine, methoxy or dimethylamino groups, exclusive stepwise insertion was observed (**entries 12-14**). Conversely, for a methyl or trifluoromethyl group, only the concerted insertion was operative (**entries 15-16**). This supports our hypothesis that the substituents bearing lone pairs that can be delocalized and contribute to an additional resonance form in the Wheland intermediate (**Scheme 5.5**), provide sufficient stabilization to favor the stepwise mechanism for the reaction pathway. On the contrary, substituents that do not have lone pairs or are located in *para* position are not able to stabilize a plausible Wheland intermediate and directly evolve through the concerted pathway.

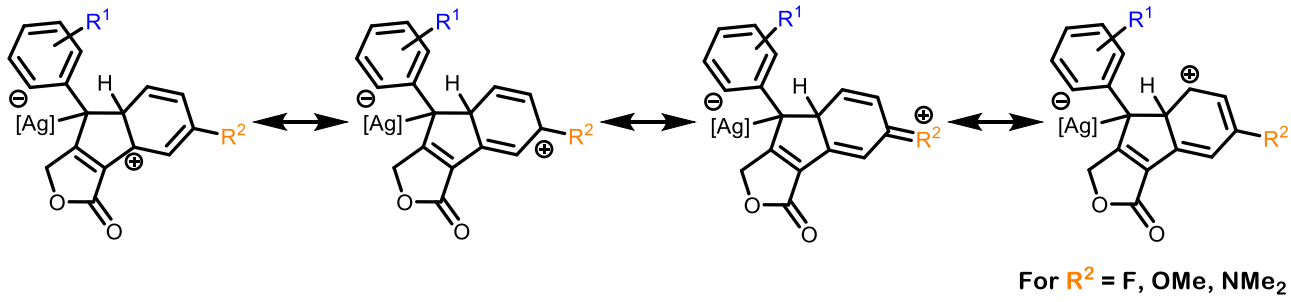

Scheme 5.5. Resonance structures for the Wheland intermediate.

Table 5.1. Obtained $\Delta G^{\#}$ values for the TS leading to concerted and stepwise Csp^2-H insertion.

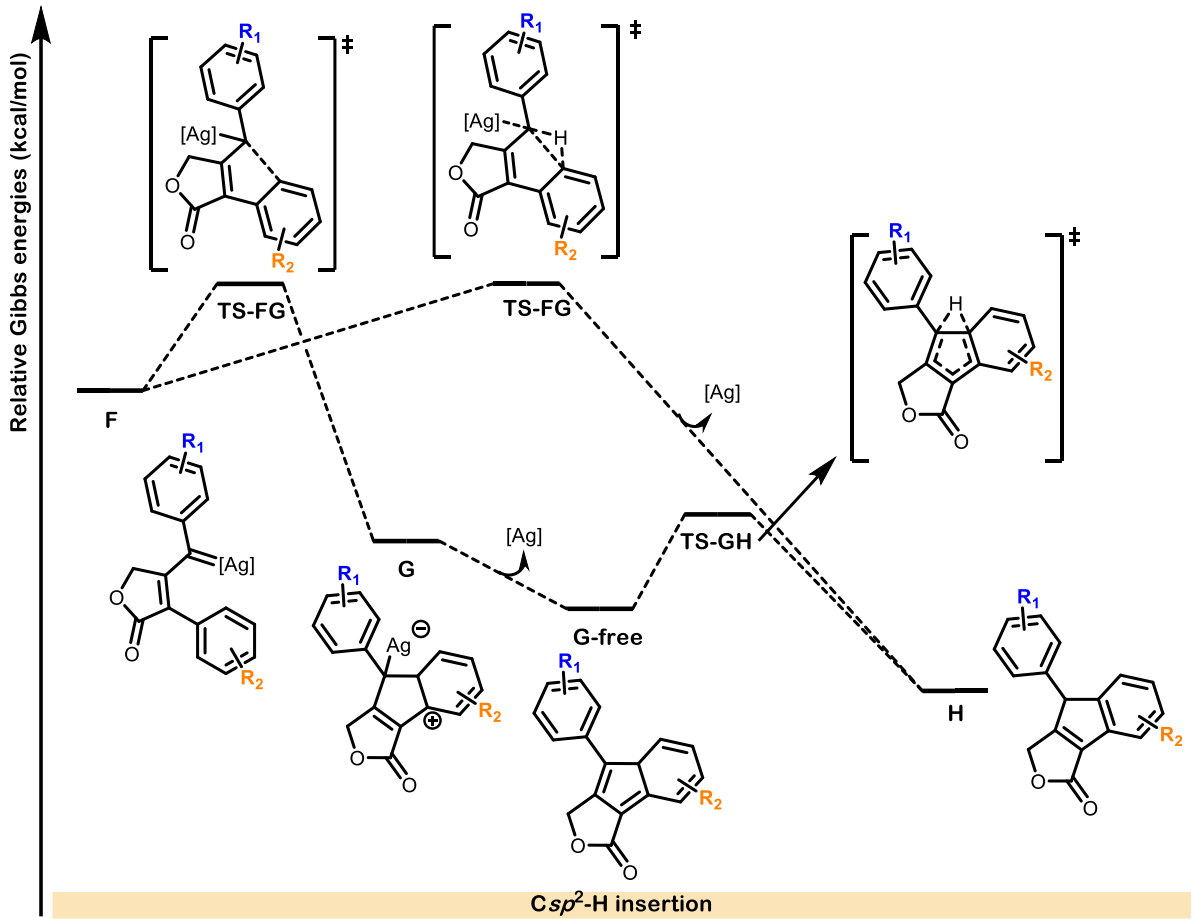

Entry	R^x	R	$\Delta G^{\#}$ Concerted (Kcal/mol)	$\Delta G^{\#}$ Stepwise (Kcal/mol)
1	No substituent		18.6	-
2	R^1	*o*-NMe_2	-	33.5
3	R^1	*o*-OMe	-	23.2
4	R^1	*o*-iPr	-	20.3
5	R^1	*p*-I	19.7	24.8
6	R^1	*p*-Me	20.1	24.7
7	R^1	*p*-OMe	24.4	29.7
8	R^2	*p*-Me	20.2	-
9	R^2	*p*-OMe	20.9	-
10	R^2	*p*-F	21.7	-
11	R^2	*p*-Br	21.8	-
12	R^2	*m*-F	-	23.0
13	R^2	*m*-OMe	-	18.8
14	R^2	*m*-NMe_2	-	12.5
15	R^2	*m*-Me	19.7	-
16	R^2	*m*-CF_3	21.6	-

To validate the generality of our results, we extended our analysis to include calculations using the $[Tp^{Br3}Ag]_2$ catalyst (**Table 5.2**), which has proven to be effective for this transformation (*vide supra*). We computed barriers for both mechanisms for substrates featuring a *para* substituent in R^1. Across all three cases examined, our results are consistent with the ones obtained for $Tp^{(CF3)2,Br}Ag$, reaffirming the predominance of the concerted mechanism.

Table 5.2. Obtained $\Delta G^{\#}$ values for the TS leading to concerted and stepwise Csp^2-H insertion using $[Tp^{Br3}Ag]_2$.

Entry	R^1	$\Delta G^{\#}$ Concerted (Kcal/mol)	$\Delta G^{\#}$ Stepwise (Kcal/mol)
1	***p*-F**	19.5	20.6
2	***p*-Me**	17.3	-
3	***p*-OMe**	22.2	25.7

While the formation of the vinylcarbene has been postulated in CAM reactions in literature, to our knowledge, direct detection of the vinylcarbene intermediate has not been reported. Furthermore, reports regarding the isolation and characterization of silver carbenes are scarce with only two examples reported.[222, 223] In the two cases, besides the characterization, limited reactivity of the silver carbene was studied. The detailed mechanistic insights gained through our DFT calculations prompted us to recognize that the energy difference required for vinylcarbene formation (**TS-BC** = 12.2 kcal/mol, **Figure 5.2**) compared to Csp^2-H insertion (**TS-FG** = 18.6 kcal/mol, **Figure 5.2**) could potentially enable the detection of the vinylcarbene using spectroscopic techniques. To pursue this, we initiated a collaboration with Andrea Álvarez and Dr. Anna Company (QBIS-Cat, Universitat de Girona). A series of ^{1}H-NMR experiments were conducted by mixing diazo compound **13a** in the presence of 1.1 equivalents of $Tp^{(CF3)2,Br}Ag$ in $CDCl_3$ at -40°C. Upon recording the ^{1}H-NMR experiments, a new singlet emerged at 5.51 ppm, persisting for approximately one hour before fading away (**Figure 5.3)**. This new signal appears at distinct chemical shifts compared to both the initial diazo compound and the final product. In the case of diazo **13a**, only a singlet integrating two protons can be observed in the aliphatic region of the spectra, corresponding to the protons at the propargylic site within the molecule. Conversely, in the product, three signals appear in the aliphatic region. A new singlet manifests at 4.91 ppm, aligning with the proton in the newly formed Csp^3-Csp^2 bond following the C-H insertion. The formation of this bond leads to a newly formed stereogenic center, thereby rendering the two protons at the propargylic site in the starting material diastereotopic. Consequently, these two protons appear as two sets of doublets at 5.13 and 4.96 ppm in indene **14a** (**Figure 5.4**). Therefore, we speculated that this singlet could correspond to aliphatic protons in the vinylcarbene lactone core ($\mathbf{H_a}$, **Figure 5.3**). To confirm this hypothesis, we conducted a two-dimensional HMBC experiment, which revealed that the singlet correlated to four different carbons as expected for the proton in the vinylcarbene lactone (**Figure 5.5**). Based on chemical shift analysis, we postulated that the carbenic carbon appeared at 227.7 ppm, consistent with previously reported isolated coinage metal carbenes.[223, 224] This spectroscopic evidence confirms, for the first time, the formation of a vinylcarbene in carbene/alkyne metathesis reactions.

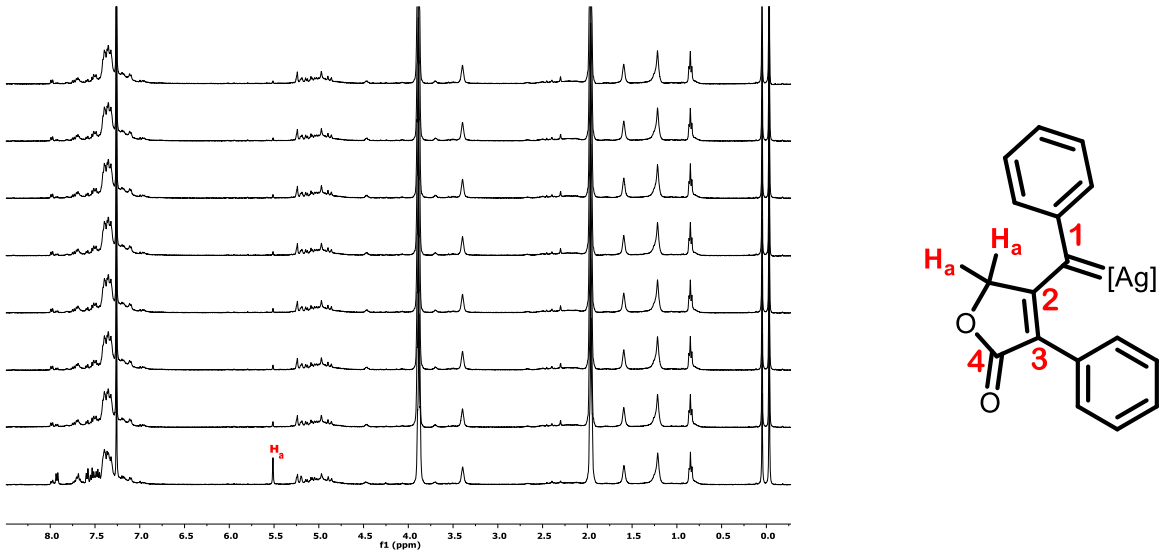

Figure 5.3. ^{1}H-NMR spectrum recorded every 10 minutes for the detection of the silver vinylcarbene.

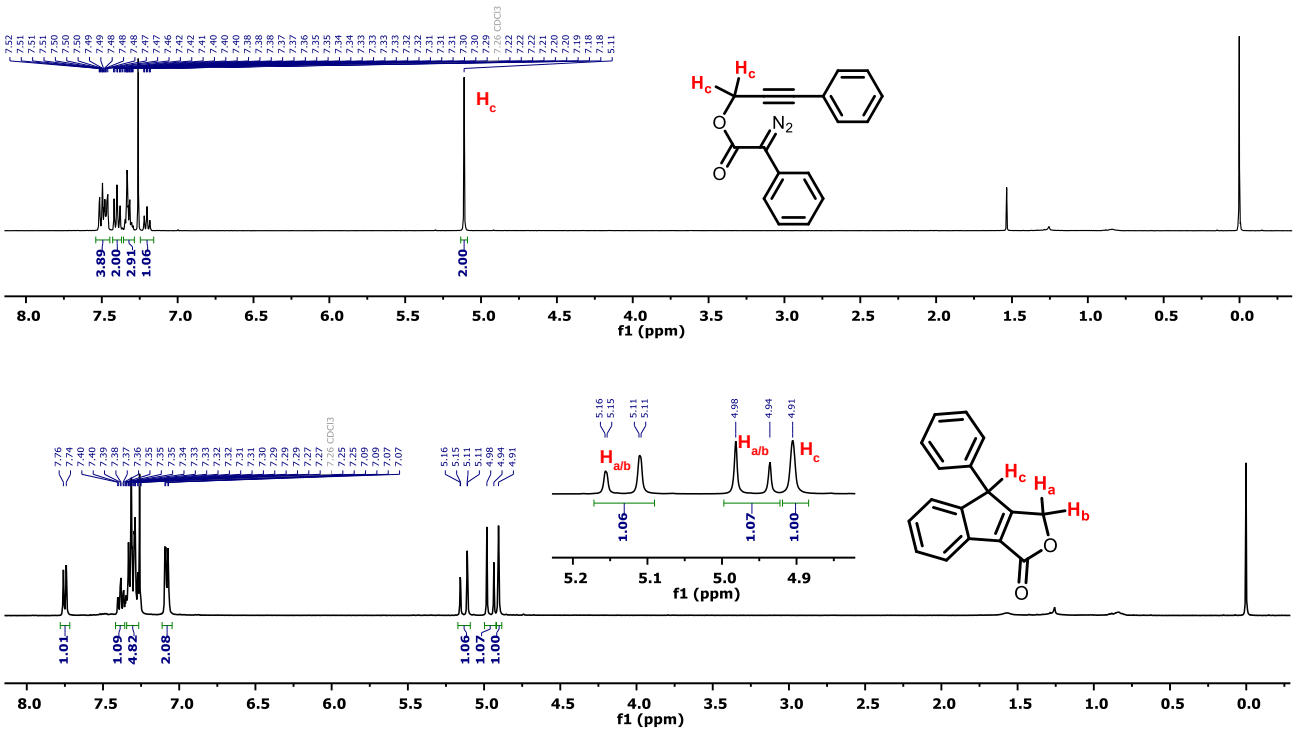

Figure 5.4. 1H-NMR spectra for the starting material **13a** and final product **14a**.

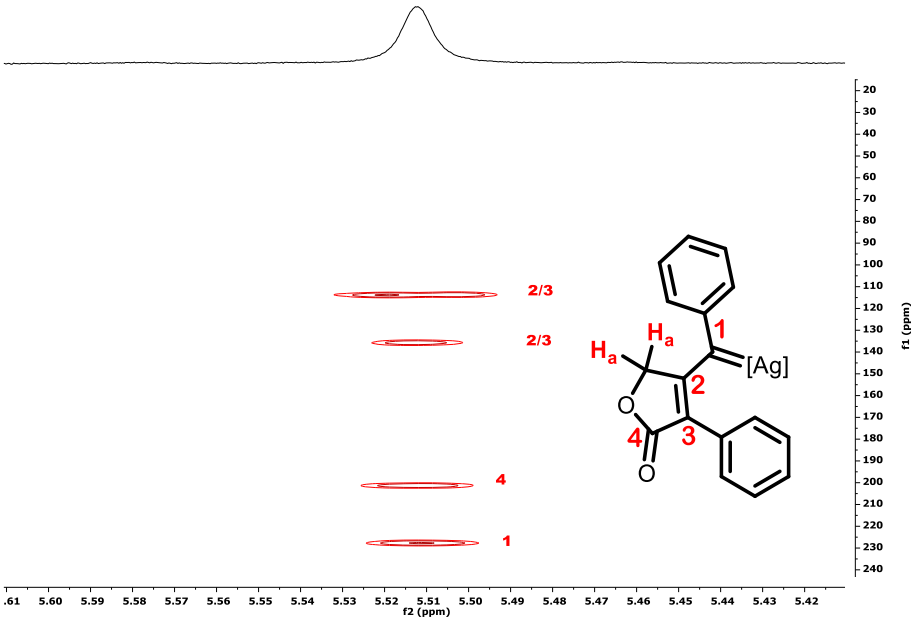

Figure 5.5. HMBC correlation experiment for the detection of the silver vinylcarbene.

In summary, we developed a silver catalyzed carbene-alkyne metathesis reaction finished in a Csp^2-H insertion process. Our comprehensive mechanistic study reveals that, depending on the substitution pattern, the transformation's mechanism proceeds though a concerted Csp^2-H bond insertion, at variance with previously described carbene Csp^2-H functionalization. Notably, we successfully spectroscopically identified the *in situ* generated vinylcarbene.

Chapter 6. Mechanistic insights into metal-dependent vinylcarbene generation via carbene/alkyne metathesis of terminal diazoalkynes

The methodologies outlined in both the introduction and preceding chapters are based on the generation of 5-exocyclic vinylcarbenes via carbene alkyne/metathesis. This outcome stands as the most extensively studied one for CAM transformations. However, it presents a clear limitation: the requirement of employing disubstituted alkynes for the reaction (**Scheme 6.1a**). Nonetheless, despite their potential to yield spiro- or polycyclic scaffolds, reports on the generation of endocyclic vinylcarbenes remain scarce thorough the literature.[52, 225]

In this context, early CAM examples by Hoye,[226] Padwa,[227] and Maas[228] reported how rhodium and copper catalysts could promote the selective formation of a 6-endocyclic vinylcarbene using terminal alkynes, albeit with moderate yields and limited substrate scopes (**Scheme 6.1b**). Based on their results, a consensus mechanism for the divergent reactivity was proposed, involving nucleophilic addition from the less sterically hindered carbon of the alkyne onto the electrophilic metal carbene. Inspired by these results, alongside our findings in Chapters 4 and 5, we envisaged that silver trispyrazolylborate complexes could be efficient catalysts for the generation of endocyclic carbenes from terminal alkynes via CAM. Moreover, recognizing the lack of insight into the mechanism of 6-endocyclic vinylcarbene formation in carbene/alkyne reactions, DFT calculations could reveal the mechanistic pathway in which the reaction operates.

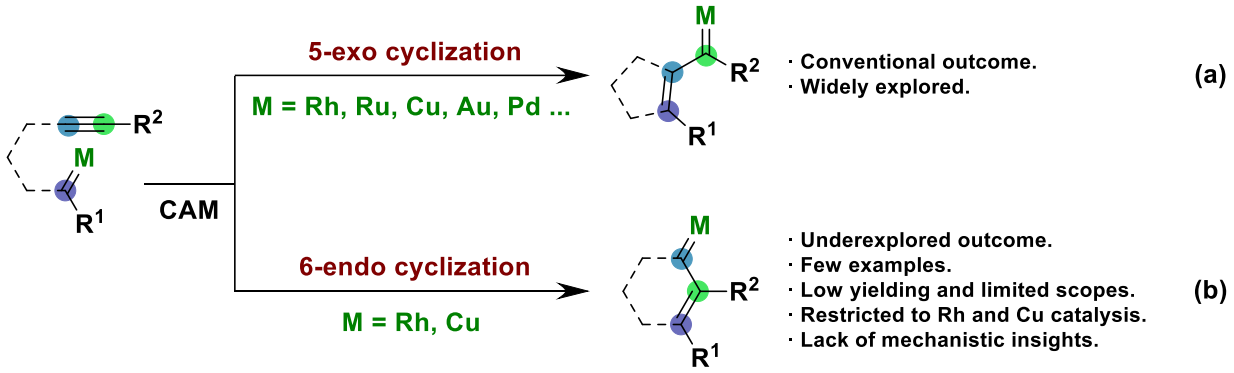

Scheme 6.1. Divergent vinylcarbene generation in CAM reactions.

We started our studies by testing the selectivity of the reaction employing commercially available rhodium (II) catalysts (**Table 6.1**). Racemic catalysts $[Rh_2(esp)_2]$ and $[Rh_2(OAc)_4]$ afforded exclusively the 5-exo adduct with low yields (**entries 1-2**). In order to improve the yield of the transformation, we decided to test phthalimide-based chiral complexes developed by Hashimoto and Davies, which afforded lactone **17a** in 33% and 37% yields, respectively (**entries 3-4**). Finally, by employing the sterically congested cyclopropane-based Davies catalyst $[Rh_2(S\text{-}BTPCP)_2]$, 5-exo adduct **17a** was obtained in a 73% yield (**entry 5**). In any of the reactions ran using the rhodium catalyst, the 6-endo adduct could be observed, serving as a benchmark for the generality of rhodium to only afford the 5-exo vinyl-carbene in our system. Given the fact that the core of lactone **17a** has been reported previously in CAM transformations, we decided not to study this reactivity further and to focus on the silver-based catalysts.

Table 6.1: Optimization of the reaction conditions.

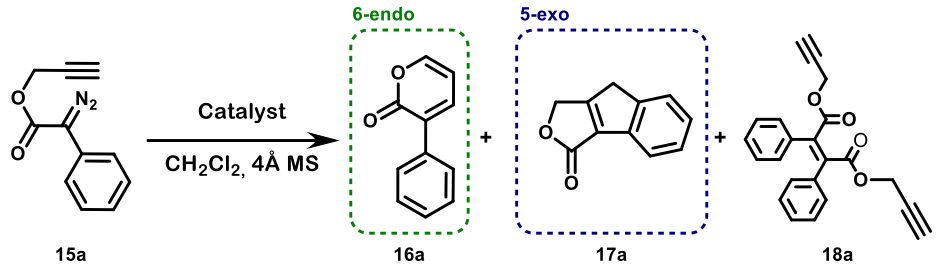

Entry	Catalyst	Yield (%) (16a /17a /18a)
1[a]	$[Rh_2(esp)_2]$	41 (0 / 41 / 0)
2[a]	$[Rh_2(OAc)_4]$	28 (0 / 28 / 0)
3[a]	$[Rh_2(S\text{-}PTTL)_4]$	33 (0 / 33 / 0)
4[a]	$[Rh_2(S\text{-}PTAD)_4]$	37 (0 / 37 / 0)
5[a]	$[Rh_2(S\text{-}BTPCP)_2]$	73 (0 / 73 / 0)
6[b]	$Tp^{(CF3)2,Br}Ag(THF)$	80 (36 / 0/ 44)
7[c], [d]	$Tp^{(CF3)2,Br}Ag(THF)$	99 (37 / 0 / 62)
8[c]	$Tp^{(CF3)2,Br}Ag(THF)$	61 (61 / 0 / 0)
9[c]	$[Tp^{Br3}Ag]_2$	68 (68 / 0 / 0)

[a] Reactions were carried out with 0.1 mmol of diazo **15a** and 1 mol% catalyst loading, at room temperature in 3 mL of CH_2Cl_2 for 1.5h. [b] Reactions were carried out with 0.1 mmol of diazo 1a and 5 mol % catalyst loading, at room temperature in 20 mL of CH_2Cl_2 for 1 h. [c] Diazo **15a** was added dropwise over 30 minutes. [d] Reaction carried out at 0ºC.

We began by employing $Tp^{(CF3)2,Br}Ag(THF)$ as the catalyst, and we were delighted to observe the exclusive formation of the 6-endo pyrone **16a** in a 36% yield, along with the dimerization of the starting material (**entry 6**). To reduce the dimerization process, we decided to add the diazo compound in a dropwise manner using a syringe pump and running the reaction at 0ºC. This increased the overall yield of the transformation, although a significant amount of dimer was still formed (**entry 7**). Finally, by employing the same conditions but running the reaction at room temperature, we were able to suppress dimerization and obtain only the desired product in a 61% yield (**entry 8**). When we modified the silver catalyst to $[Tp^{Br3}Ag]_2$, the yield of **16a** improved to 68% (**entry 9**). Given the novelty of this transformation in the presence of silver and the prevalence of the 2-pyrone moiety in several medicinal applications,[229] we decided to further study this transformation.

We chose 9 diazo compounds to analyze the electronic and steric effects of various substituents in the aryl ring and in the propargylic position of the alkyne. These compounds were synthesized following the conditions outlined in **Scheme 6.2** (for experimental details see **Supplementary Material**).

For the substrates bearing a substituent in the aryl ring, direct alkylation of the corresponding phenylacetic acid was performed using propargyl bromide in presence of K_2CO_3 in refluxed acetone. Conversely, for derivatives including substituents in the propargyl position, esterification of phenylacetic acid with the corresponding propargyl alcohol was carried out. From the synthetized esters, diazo compounds (**15a-15i**) were prepared using p-ABSA as the diazo transfer reagent in presence of DBU as the base.

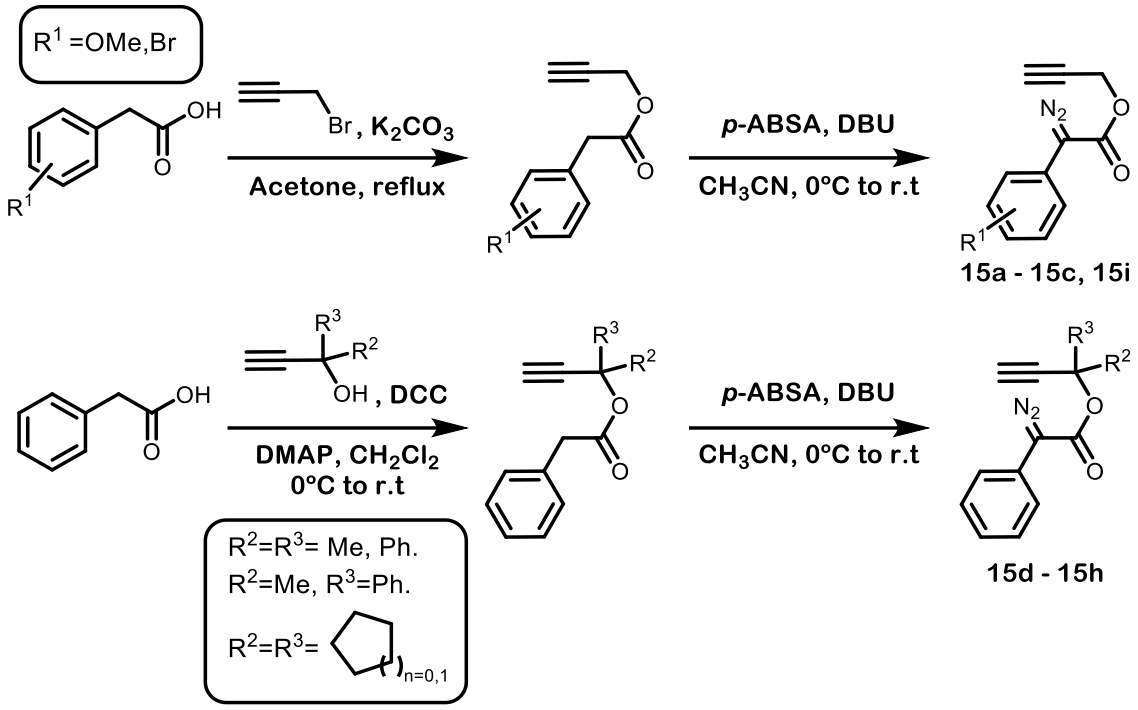

Scheme 6.2. Synthesis of propargyl diazoacetates **15a-15i.**

We then explored the scope of the transformation (**Scheme 6.**3). Introduction of substituents in the pending aryl group of the diazo compound resulted in a slight decrease in yield. An electron-donating methoxy group afforded **16b** in a 59% yield, whereas an electron-withdrawing bromine furnished **16c** in a 56% yield, indicating that electronic factors do not play a crucial role in modifying the reaction. Next, we decided to modify the propargylic position of the initial substrate. By adding two methyl units, **16d** could be isolated in an excellent 92% yield, upon 1,2-alkyl migration from the endocyclic vinylcarbene. This improved yield can be attributed to the Thorpe-Ingold effect. In cases where a cyclic alkyl chain was added next to the alkyne moiety, six and seven-membered ring-fused 2-pyrones, **16e** and **16f**, could be achieved in an excellent 98% and 82% yield, respectively. In addition to alkyl substituents, aryl groups proved to be compatible with the reaction. When employing diazo compound **15g**, featuring two phenyl units, pyrone **16g** was obtained in an excellent 89 % yield, through 1,2-aryl migration. To delve deeper into the mechanism of the 1,2-shift step, we investigated diazo compound **15h**, which contains a methyl and a phenyl group in the propargyl position, under the optimized reaction conditions. Remarkably, exclusive migration of the aryl group was observed, resulting in **16h** with a yield of 79%. This finding unequivocally proves the preferential migration of the aryl group over the 1,2-alkyl shift. Finally, to test the limits of the reaction, diazo compound **15i**, bearing a methyl group at the terminal position of the alkyne, was subjected to the reaction conditions, completely suppressing the 6-endo mechanism, and yielding exclusively the 5-exo lactone **17b** in a 90% yield.

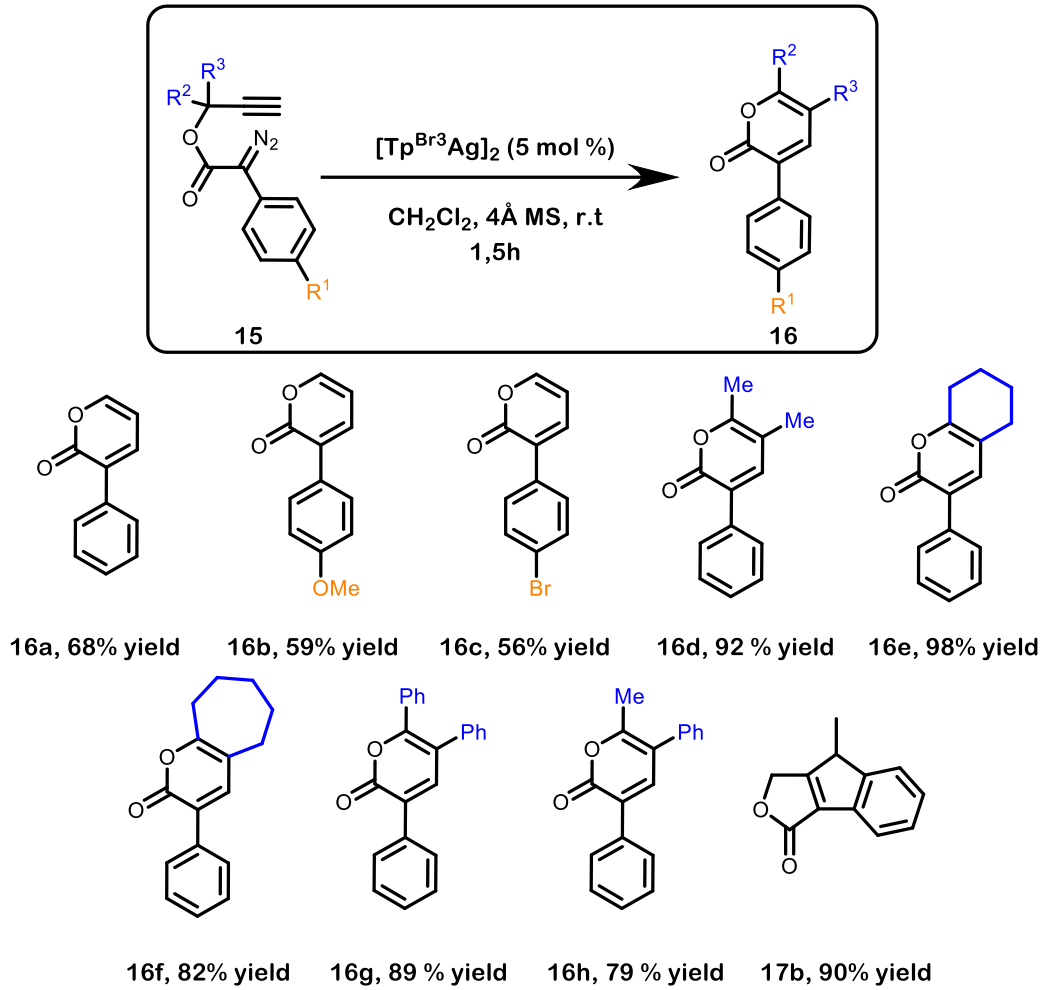

Scheme 6.3. Scope of the transformation

Intrigued by the divergent selectivity exhibited by rhodium and silver catalysts, as well as the lack of mechanistic insight into the 6-endo mode of cyclization in previous CAM reports, we decided to elucidate the reaction mechanism. DFT calculations were performed at the M06-2X-D3/6-31G**(for all atoms besides Rh and Ag) and LANL2DZ (for Rh and Ag)/SMD(dichloromethane)//B3LYP-D3/6-31G(d)** (for all atoms besides Rh and Ag) and LANL2DZ (for Rh and Ag) under the supervision of Dr. Albert Poater. We started by analysing the mechanistic profile for the silver-catalyzed reaction. Since similar yields were obtained using the two described catalyst we decided to use $Tp^{(CF3)2,Br}Ag(THF)$ to reduce the computational cost. The established mechanism for CAM transformations relies on dinitrogen extrusion, leading to the formation of an initial carbene. However, prior reports have demonstrated the formation of silver carbenes from alkynes through nucleophilic addition. In light of the recently reported gold-catalyzed diazo-yne reaction,[212, 213, 230] one could also envision the direct generation of a vinylcarbene from the initial diazo compound and the silver catalyst. To rule out this possibility, we examined both potential pathways as illustrated in **Figure 6.1**.

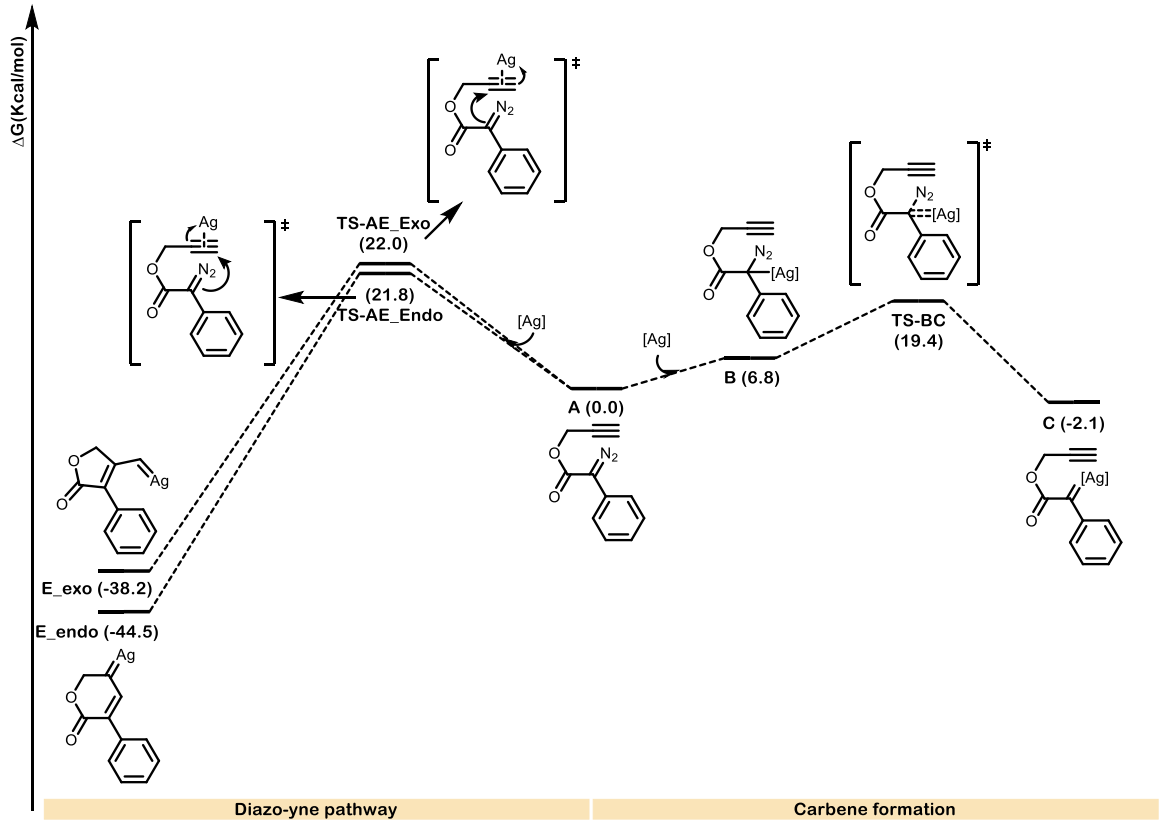

Figure 6.1. Gibbs energy comparison for diazo-yne reaction and carbene formation mechanism. (Ag=$Tp^{(CF3)2,Br}$Ag(THF)).

Starting from diazo compound **A**, the formation of the 5-exocyclic vinyl carbene **E_exo**, initiated by silver's activation of the distal carbon of the alkyne, requires a barrier of 22 kcal/mol via **TS-AE_exo**. Conversely, the formation of the 6-endocyclic vinylcarbene is slightly more favorable by 0.2 kcal/mol (**TS-AE_endo**). On the other hand, the coordination of silver to the carbenic carbon of **A** is a slightly endergonic process, requiring 6.8 kcal/mol, leading to the formation of intermediate **B**. This intermediate subsequently undergoes N_2 release through **TS-BC**, furnishing silver carbene **C** after overcoming a barrier of 19.4 kcal/mol. Overall, carbene formation is 2.4 kcal/mol more favourable, discarding the diazo-yne route as the one leading to the vinylcarbene.

From carbene **C,** the nucleophilic addition of the internal carbon of the pending alkyne is feasible, surpassing a barrier of 4.1 kcal/mol via **TS-CD'** (**Figure 6.2**). This process leads to the formation of the ylide intermediate **D'**, which can further evolve in a barrierless manner toward the 5-exocyclic vinylcarbene **E_Exo**. Alternatively, the concerted cyclopropenation of the alkyne through **TS-CD** was found to be 2.8 kcal/mol, leading to cyclopropene **D**. Due to the non-symmetric structure of this intermediate, it can give rise to both exocyclic and endocyclic vinylcarbenes, depending on the opening of the cyclopropene. When silver coordination and ring opening occur at the terminal position, the formation of **E_Exo** takes place with a barrier of 21.4 kcal/mol (**TS-DE_Exo**). On the other hand, the transition state for the formation of the endocyclic carbene **E_Endo** (**TS-DE_Endo**) requires 6.5 kcal/mol. These results clearly indicate that the formation of the endocyclic vinylcarbene from **D** is favored over the formation of **E_Exo**. Overall, considering the lower energy barrier and experimental results hinting at the intermediacy of **E_Endo**, we propose the cyclopropenation pathway as the one operating in our system. To complete the full mechanistic profile, intermediate **E_Endo** undergoes a 1,2-H shift, ultimately yielding 2-pyrone **F**. This transformation takes place through a transition state (**TS-EF**) with

an energy barrier of only 4.4 kcal/mol. Moreover, we have conducted energy barrier calculations for both the 1,2-alkyl and aryl shifts. Interestingly, for diazo **15d**, the 1,2-methyl shift exhibits a slightly higher energy barrier of 7.7 kcal/mol compared to the corresponding hydrogen shift. Conversely, for **15g**, the barrier for the 1,2-phenyl shift is notably lower at just 1.6 kcal/mol. To gain further insight into the selective migration observed in substrate **15h**, we calculated the barriers for both potential 1,2-shifts. The methyl group demonstrated a barrier of 8.2 kcal/mol, whereas the 1,2-phenyl migration exhibited a significantly lower barrier of just 0.8 kcal/mol. These results clearly support the exclusive formation of pyrone **16h**.

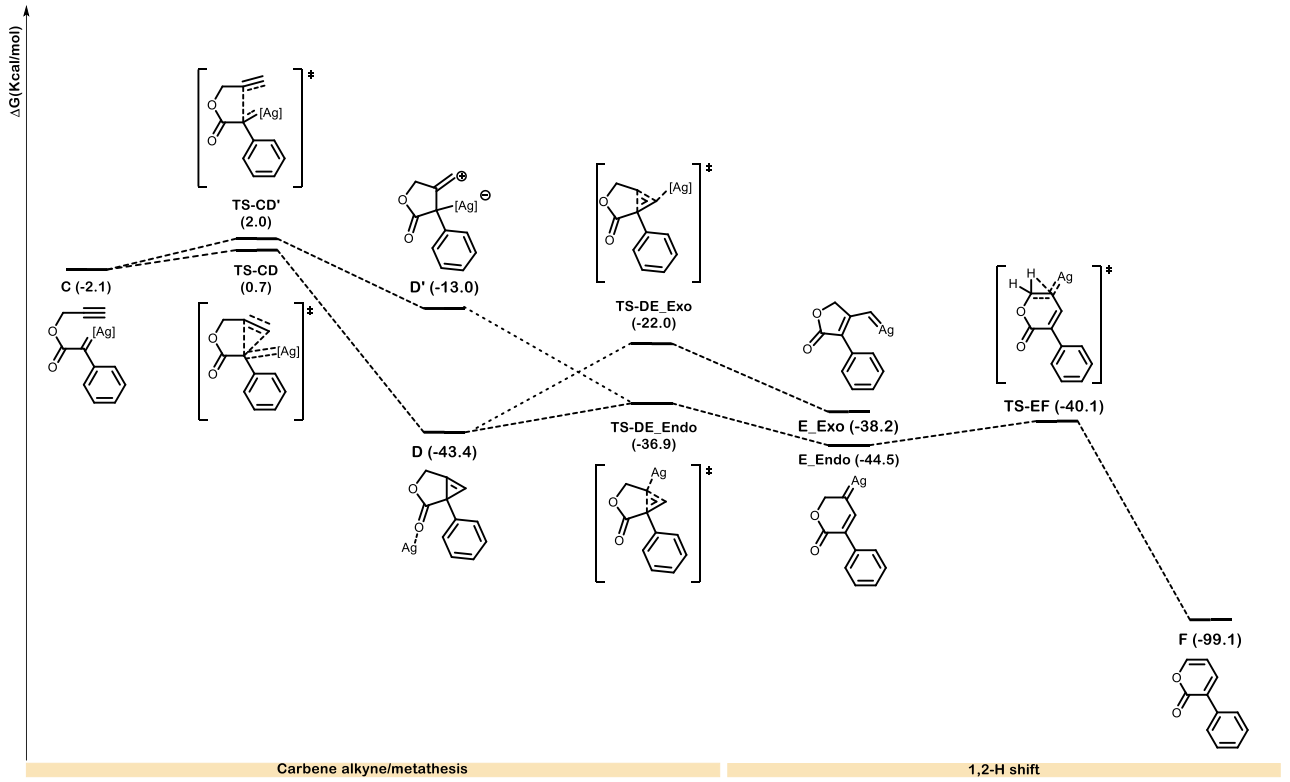

Figure 6.2. Gibbs energy profile for the silver catalyzed CAM leading to the 6-endo vinylcarbene and 2-pyrone formation. Energies are relative to A. (Ag=$Tp^{(CF3)2,Br}$Ag(THF)).

To gain a deeper understanding of the reaction's selectivity, we extended our investigation to diazo compound **15i** (**Figure 6.3**) which exclusively generated the 5-exo product **17b**, as illustrated in **Scheme 6.3**. Building on the insights gained from our analysis of **15a**, where the initial carbene formation emerged as the preferred route, we initiated our study from carbene **C_Me**. From that intermediate, the energy barrier for alkyne nucleophilic addition proved to be remarkably low at just 0.1 kcal/mol (**TS-CD_Me**), in contrast to the previously observed for the terminal alkyne. Presumably, the presence of an electron-donating group in the terminal position renders the alkyne more nucleophilic. This nucleophilicity enhancement facilitates the addition to the carbenic carbon, thereby lowering the barrier for **TS-CD_Me**. These findings are consistent with our prior studies, where alkynes featuring aryl groups were employed and the nucleophilic addition was computed to occur in a barrierless manner. Conversely, our attempts to locate the transition state for the cyclopropenation pathway were unsuccessful, likely due to the increased steric hindrance in the alkyne moiety. As our calculations state, the pathway leading to the 6-endo vinylcarbene is effectively blocked, leaving the 5-exo vinylcarbene as the sole viable option. This provides a complete explanation of the selectivity change observed in our experimental findings.

Following **TS-CD_Me**, the ylide intermediate **C_Me** can engage in a 1,3-Ag migration, in a step requiring 0.9 kcal/mol (**TS-DE_Me**). This transition leds to the generation of the highly reactive vinylcarbene, **E_Me**, in a highly exergonic process by 31.1 kcal/mol. Subsequently, this vinylcarbene can then insert into the pending aryl ring ultimately yielding the desired lactone product. Based on the results of the previous chapter, we decided to explore both concerted and stepwise Csp^2-H insertion mechanisms starting from carbene **E_Me**.

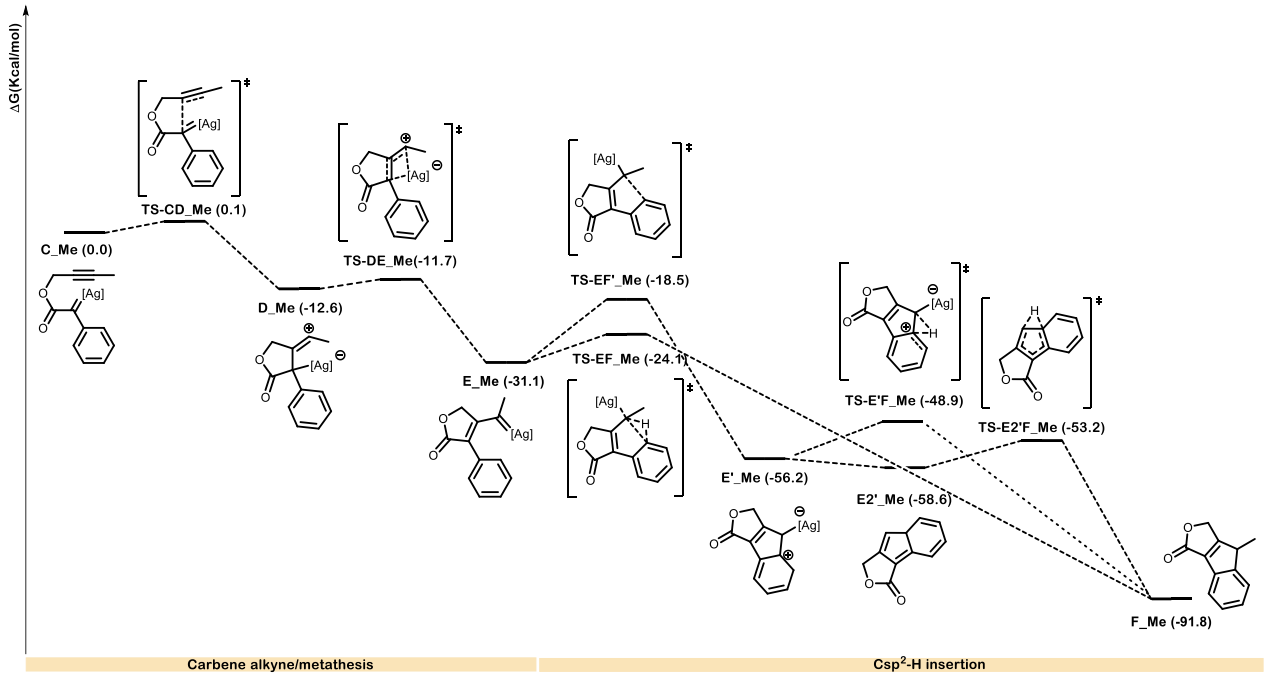

Figure 6.3. Gibbs energy profile for the silver catalyzed CAM leading to the 5-exo vinylcarbene. Energies are relative to **C_Me**. (Ag=$Tp^{(CF3)2,BrAg}$(THF)).

For the stepwise mechanism, the formation of intermediate **E'_Me** requires a barrier of 12.6 kcal/mol (**TS-EF'_Me**). Following this, the newly formed ylide undergoes a 1,2-H shift, ultimately yielding the final product **F_Me**, surpassing a barrier of 7.3 kcal/mol (**TS-E'F_Me**). However, we also considered the possibility of a metal-unbound pathway, involving the dissociation of silver from intermediate **E'_Me**. Upon silver release, the more thermodynamically stable **E2'_Me** is formed, and the subsequent 1,2-H shift from this intermediate requires only 5.4 kcal/mol (**TS-E2'F_Me**). Therefore, the metal-unbound shift proves to be the more energetically favorable route. Finally, our initial proposal for the concerted mechanism was studied. The transition state for this insertion is of just 7 kcal/mol (**TS-EF_Me**), 5.6 kcal/mol lower than the corresponding stepwise insertion. This obtained data unequivocally supports the conclusion that the concerted mechanism is the preferred and energetically favored route for the Csp^2-H insertion step.

To explain the distinct reactivity exhibited by silver and rhodium, our focus turned towards exploring the catalytic mechanism involving Rh(II) (**Figure 6.4**). To reduce the computational cost, rhodium formate was used as the model for the catalyst. Starting from diazo compound **A**, coordination of rhodium leads to intermediate **B**, an exergonic process by 4 kcal/mol. From **B**, dinitrogen extrusion requires a barrier of 10.5 kcal/mol (**TS-BC**), leading to the generation of carbene **C**. Notably, unlike the situation with silver, the transition state for the cyclopropenation of the alkyne (**TS-CD'**) in the rhodium-catalyzed reaction exhibits higher energy than the nucleophilic addition of the alkyne (**TS-CD**) by 2.5 kcal/mol. This energy differential accounts for the

preferred formation of the 5-exo vinylcarbene when utilizing rhodium as a catalyst, providing a comprehensive explanation for the disparities in selectivity between rhodium and silver as catalysts. Building on these results, it becomes evident that the choice of metal catalyst can dictate different mechanistic pathways in carbene/alkyne metathesis, resulting in the formation of distinct vinylcarbenes with inherently diverse reactivities, all generated from the same initial diazo compound. To complete the catalytic cycle, subsequent to **TS-CD**, zwitterionic intermediate **D** is formed. This intermediate can evolve, surpassing a 14.4 kcal/mol barrier, to yield the vinylcarbene **E** through the previously mentioned 1,3-metal shift. Once again, intermediate **E** can evolve further via a stepwise or concerted C*sp*^{2}-H insertion. In this case, the concerted mechanism was found to be slightly higher in energy by 0.6 kcal/mol when compared to the stepwise counterpart (**TS-EG vs. TS-EF**). Following the stepwise pathway, Wheeland intermediate **F** can undergo a metal-bound 1,2-H shift (**TS-FG**) with an energy barrier of 8.9 kcal/mol, or it can generate the more thermodynamically stable metal-unbound **F'**. In the latter case, the metal-free 1,2-H shift requires 4.4 kcal/mol to yield lactone **G**, once again being the metal unbound mechanism the more favourable one.

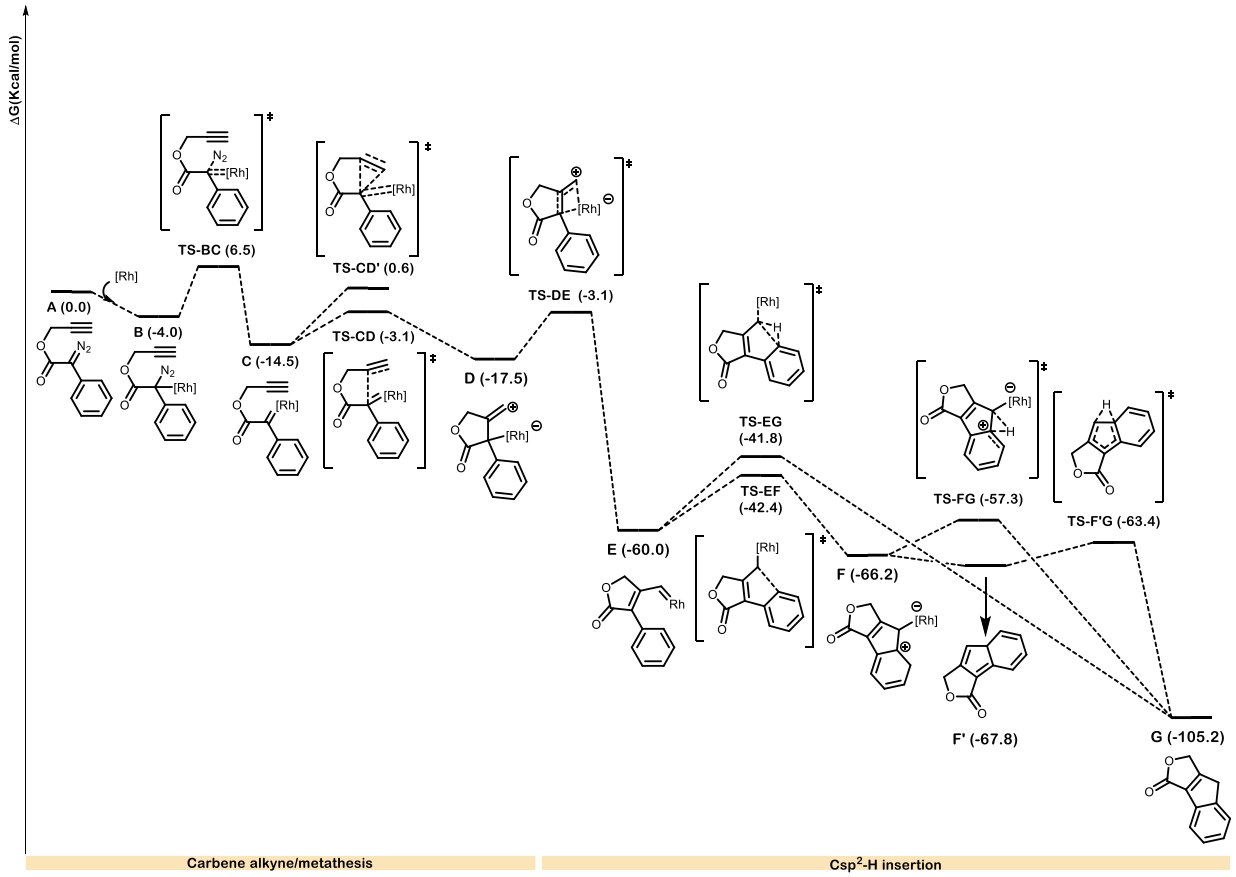

Figure 6.4. Gibbs energy profile for the rhodium catalyzed CAM leading to the 5-exo vinylcarbene. Energies are relative to **A**. ([Rh]=[$Rh_2(HCOOH)_4$]).

In summary, we have achieved the final objective of this thesis by developing a carbene alkyne-metathesis reaction capable of selectively generate a 6-endocyclic vinylcarbene. Notably, this selectivity can be finely tuned by transitioning from a silver catalyst to a rhodium one. Additionally, computational techniques have been employed to elucidate the underlying reasons for the selectivity variance when altering catalysts, as well as to analyze the diverse outcomes resulting from substituent modifications in the initial diazo compound

Chapter 7. General conclusions

The first objective of this thesis was to study the intermolecular reactivity between rhodium vinylcarbenes generated from CAM. We envisioned trapping the *in situ* generated vinylcarbene with an external nitrile to produce benzoazepine derivatives. Although we successfully obtained the desired product by introducing externally nitriles into the reaction, unfortunately, the predominant outcome was intramolecular Csp^2-H carbene insertion. To circumvent this limitation, we integrated the nitrile group into the initial diazo compound, resulting in a more prolonged cascade reaction that yielded 1*H*-isoindole derivatives (**Scheme 7.1a**). The experimental and computational work carried out allowed us to extract the following conclusions:

- A variety of spirocyclic 1*H*-isoindole derivatives were successfully synthesized via an extended CAM reaction, yielding good yields and complete diastereoselectivity. Furthermore, this process encompasses a formal nitrile trifunctionalization, representing an unprecedented transformation to the best of our knowledge.
- DFT calculations, along with deuterium labeling experiments, provide sufficient insight to propose a mechanism centered on nitrile formation, followed by 1,7-electrocyclization leading to azepine core formation. Subsequently, a second unit of vinylcarbene intercepts the azepine scaffold, ultimately triggering spirocyclization and yielding the final product.

The second objective of this thesis was to develop a platform for the efficient generation of silver vinylcarbenes via intramolecular CAM. Upon the formation of the vinylcarbene, the strategically positioned o-dimethylamino unit in the aryl group at the terminal position of the alkyne facilitated selective vinylogous Csp^3-H insertion (**Scheme 7.1b**). Through exhaustive experimental and computational studies, we arrived at the following conclusions:

- A diverse array of benzoazepine derivatives was synthesized via selective Csp^3-H vinylogous insertion reactions. These products were obtained in good yields, with excellent selectivity observed in most cases towards the desired vinylogous functionalization.
- DFT calculations, in conjunction with deuterium labeling experiments, allowed us to unravel the mechanism of the reaction, revealing a stepwise Csp^3-H insertion process. Following vinylcarbene formation, a hydride shift occurs, leading to a zwitterionic intermediate that favors the formation of the kinetically favorable vinylogous product.

The third objective aimed to capitalize on silver-catalyzed CAM reactions and study the reactivity of vinylcarbenes in Csp^2-H insertion (**Scheme 7.1c**). By eliminating the *o*-dimethylamino group from the previous chapter, we anticipated the reaction to proceed through C-H insertion with the pending aryl group. The experimental and computational studies conducted led us to the following conclusions:

- A variety of indene derivatives were easily synthesized in excellent yields via silver catalysis, with complete selectivity towards Csp^2-H bond insertion over potential Csp^3-H insertion.
- Through a comprehensive mechanistic study, we proposed that, depending on the substitution pattern, the mechanism of this transformation proceeds via a concerted Csp^2-H bond insertion, at variance from previously described carbene Csp^2-H functionalization pathways.
- The mechanistic insights gained during the chapter facilitated the spectroscopic identification of the *in situ* generated silver vinylcarbene.

The last objective of this thesis was to overcome the limitation of employing internal alkynes in intramolecular CAM reactions. In this regard, we proposed that by utilizing terminal diazo alkynes under silver catalysis, an efficient method for generating a 6-endocyclic vinylcarbene could be achieved. Following carbene/alkyne metathesis, the newly formed vinylcarbene underwent a 1,2-shift, ultimately leading to the formation of 2-pyrone derivatives (**Scheme 7.1d**). The experimental studies alongside with an exhaustive mechanistic study led us to the following conclusions:

- A myriad of 2-pyrone derivatives could be synthesized with good to excellent yields through the selective generation of 6-endocyclic vinylcarbenes using silver catalysts. Conversely, when the reaction was conducted in the presence of a rhodium(II) catalyst, exclusive formation of the 5-exo adduct was observed.
- An in-depth DFT mechanistic study enabled us to fully rationalize the observed selectivity in CAM reactions. When terminal alkynes were employed in the presence of silver, the CAM proceeded via cyclopropenation of the alkyne, followed by ring opening, leading to the formation of the endocyclic carbene. In contrast, when using rhodium, the CAM proceeded via nucleophilic addition from the alkyne, yielding exclusively the exocyclic vinylcarbene.

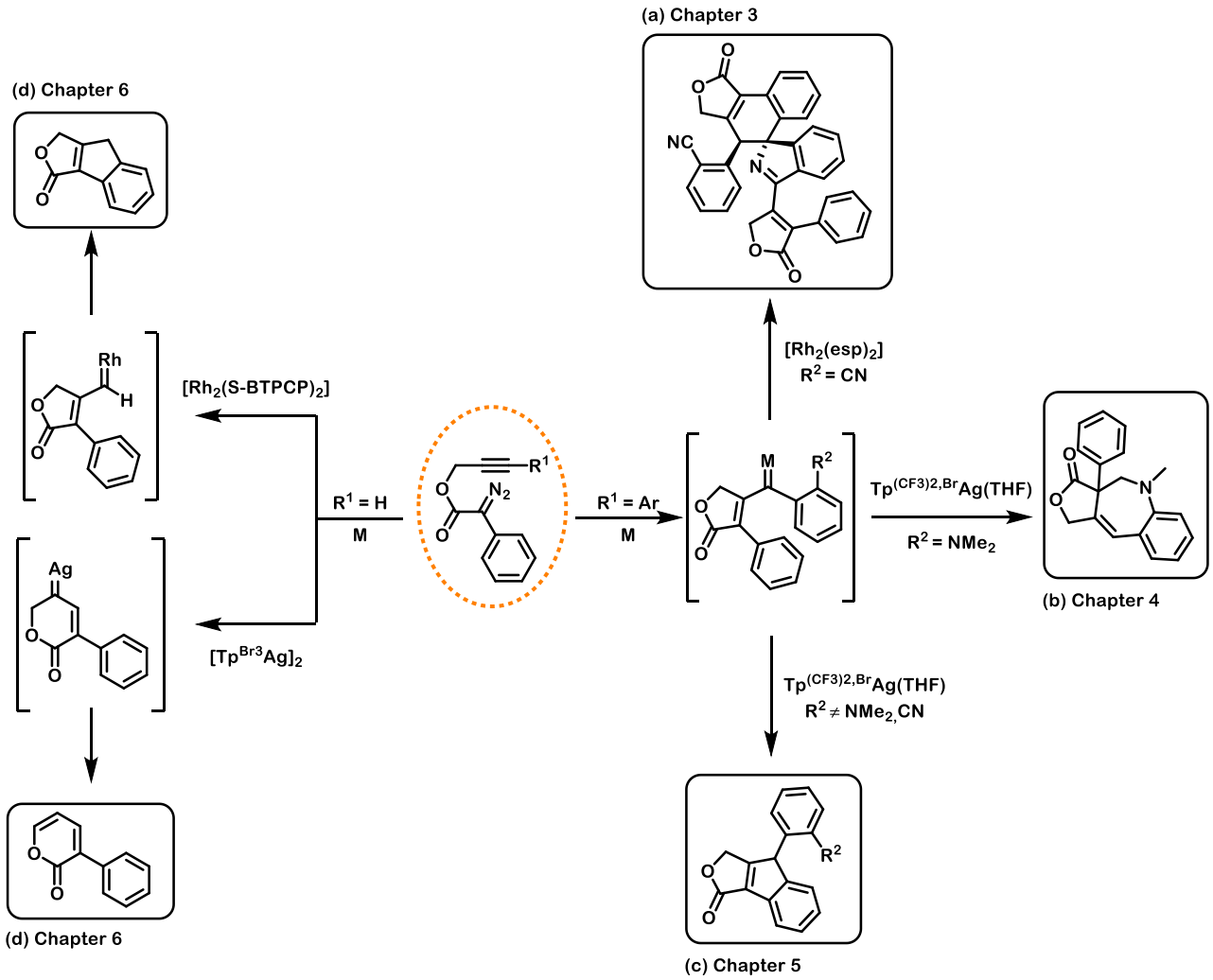

Scheme 7.1. Summary of all carbene/alkyne metathesis reactions developed in this thesi

Chapter 8. Methods

General methods

Unless otherwise specified, materials were obtained from commercial suppliers and used without further purification. All reactions requiring anhydrous and oxygen-free conditions were carried out in oven-dried glassware under a dry nitrogen atmosphere. Dichloromethane was dried and degassed under nitrogen by passing it through solvent purification columns (MBraun, SPS-800). Activated molecular sieves (4Å) were introduced to commercially available anhydrous chloroform, and nitrogen gas was bubbled through it for 30 minutes to ensure anhydrous and degassed conditions. The progress of reactions in the synthesis of all compounds was monitored using thin-layer chromatography on Macherey-Nagel Xtra SIL G/UV254 silica gel plates. Solvents were evaporated under reduced pressure using a rotary evaporator. Reaction mixtures were purified through silica gel chromatography using an automated purification instrument, the Interchim PuriFlash XS 520 Plus, equipped with a quaternary gradient pump (up to 300 ml/min, 20 bar) and a UV-Vis 200-800 nm diode array detector.

Spectroscopy

NMR Spectroscopy: All ^{1}H and ^{13}C NMR spectra were acquired using a Bruker ASCEND 400 spectrometer equipped with a 5 mm BBFO probe using $CDCl_3$ as a deuterated solvent. Chemical shifts for ^{1}H and ^{13}C NMR are reported in ppm (δ) relative to residual solvent signals ($CDCl_3$**:** 7.26 ppm for ^{1}H and 77,16 ppm for ^{13}C). Coupling constants are provided in Hertz (Hz). Signal assignments for ^{1}H and ^{13}C NMR were established through 2D-NMR experiments including HSQC, HMBC, COSY, and TOCSY.

Infrared Spectroscopy (IR): IR spectra were recorded using a benchtop Agilent Cary 630 FT-IR spectrometer equipped with a single reflection ATR (attenuated total reflectance) sampling accessory.

Spectrometry

High resolution mass spectrometry (ESI-HRMS): Electrospray ionisation high-resolution mass spectra were recorded using a Bruker microTOF-Q II instrument with a quadrupole-Time-Of-Flight hybrid analyzer operated in the positive ESI(+) ion mode.

Single crystal X-ray diffraction

X-ray intensity data were collected on a Bruker D8 QUEST ECO three-circle diffractometer system, featuring a Ceramic X-ray tube (Mo Kα, λ = 0.71076 Å) and a doubly curved silicon crystal Bruker Triumph monochromator.

Melting points

Melting points were determined using an SMP10 apparatus from Stuart without any correction applied.

Supplementary material for Chapter 3

Experimental procedure for the synthesis of propargyl alcohol S1a

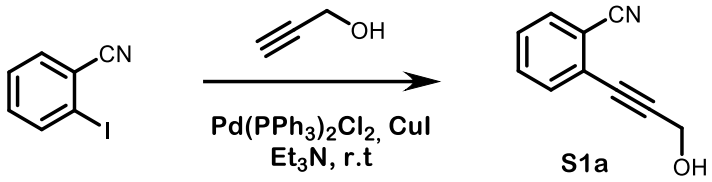

Scheme 8.1. Synthesis of propagyl alcohol **S1a**.

To a 100 mL round-bottom flask containing a mixture of **2-iodobenzonitrile** (1.5 g, 6.55 mmol), CuI (24.9 mg, 0.13 mmol), $Pd(PPh_3)_2Cl_2$ (45.9 mg, 0.65 mmol) in triethylamine (26 mL), propargyl alcohol (0.42 ml, 7.20 mmol) was added dropwise under nitrogen atmosphere. After the addition, the solution was then stirred overnight at room temperature. Upon completion of the reaction (TLC monitoring), the crude was filtered through a Celite pad, rinsed with EtOAc and concentrated under reduced pressure. The crude product was purified by column chromatography on silica gel (hexanes:EtOAc = 80:20 to 70:30) to afford **S1a** as a colorless solid (0.99 g, 96% yield).

MW ($C_{10}H_7NO$): 157.50 g/mol; **Rf:** 0.48 (hexanes/EtOAc 6:4); **1H NMR ($CDCl_3$, 400 MHz):** δ_H 7.64 (dt, 1H, J = 7.8, 1.0 Hz), 7.59 – 7.48 (m, 2H), 7.43 – 7.39 (m, 1H), 4.57 (d, 2H, J = 5.3 Hz), 2.19 (bs, 1H); **$^{13}C^{231}$ NMR ($CDCl_3$, 101 MHz):** δ_C 132.7, 132.6, 132.5, 128.7, 126.7, 117.7, 115.4, 94.2, 81.8, 51.6.

The spectroscopic data agrees with those previously reported in the literature.[232]

Experimental procedure for the synthesis of propargyl alcohols S2a and S3a

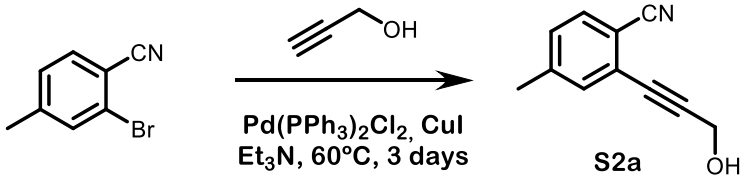

Scheme 8.2. General procedure for the preparation of propargyl alcohols **S2a** and **S3a**.

To a 100 mL round-bottom flask containing a mixture of **2-bromo-4-methylbenzonitrile** (1.59 g, 8.11 mmol), CuI (61.8 mg, 0.32 mmol), and $Pd(PPh_3)_2Cl_2$ (116.7 mg, 0.16 mmol) in triethylamine (34 mL), propargyl alcohol (0.257 mL, 49.80 mmol) was added dropwise under a nitrogen atmosphere. After the addition, the solution was then heated at 60ºC and stirred for 3 days. Upon completion of the reaction (TLC monitoring), the crude was filtered through a Celite pad, rinsed with EtOAc and concentrated under reduced pressure. The crude product was purified by column chromatography on silica gel (hexanes:EtOAc = 80:20 to 70:30) to afford **S2a** as a colorless solid (0.89 g, 64% yield).

MW ($C_{11}H_9NO$): 171.20 g/mol; **Rf:** 0.40 (hexanes/EtOAc 7:3); **MP (ºC):** 68-70. **IR (ATR) ν (cm^{-1}):** 3379, 2917, 2229, 1597, 1415, 1030, 813. **^{1}H NMR ($CDCl_3$, 400 MHz):** δ_H 7.51 (d, 1H, J = 7.9 Hz), 7.35 (s, 1H), 7.20 (d,

1H, J = 7.9 Hz), 4.55 (d, 2H, J = 5.7 Hz), 2.38 (s, 3H), 2.29 (t, 1H, J = 5.7 Hz). **^{13}C{H} NMR ($CDCl_3$, 101 MHz):** δ_C 143.6, 133.2, 132.5, 129.6, 126.5, 117.9, 112.3, 93.6, 81.9, 51.5, 21.7. **HRMS (ESI) m/z:** $[M+Na]^+$ calcd. for $C_{11}H_9NONa$ 194.0576; Found 194.0579.

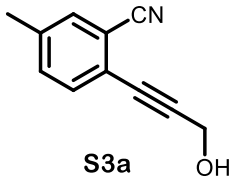

S3a

Propargyl alcohol **S3** was obtained from **2-Bromo-5-methylbenzonitrile** (1.52 g, 7.75 mmol) as colorless solid (0.57 g, 43% yield) following the same procedure as for **S3a**.

MW ($C_{11}H_9NO$): 171.20 g/mol; **Rf:** 0.30 (hexanes/EtOAc 7:3); **MP (ºC):** 89-91. **IR (ATR) ν (cm^{-1}):** 3215, 2923, 2226, 1492, 1031, 827. **^{1}H NMR ($CDCl_3$, 400 MHz):** δ_H 7.48 – 7.41 (m, 2H), 7.35 (dd, 1H, J = 8.0, 1.0 Hz).), 4.56 (d, 2H, J = 6.2 Hz), 2.39 (s, 3H), 1.78 (t, 1H, J = 6.2 Hz).**^{13}C{H} NMR ($CDCl_3$, 101 MHz):** δ_C 139.4, 133.5, 133.1, 132.5, 123.7, 117.8, 115.3, 93.2, 82.0, 51.7, 21.3. **HRMS (ESI) m/z:** $[M+Na]^+$ calcd. for $C_{11}H_9NONa$ 194.0576; Found 194.0578.

Experimental procedure for the synthesis of propargyl esters S4a-S4l

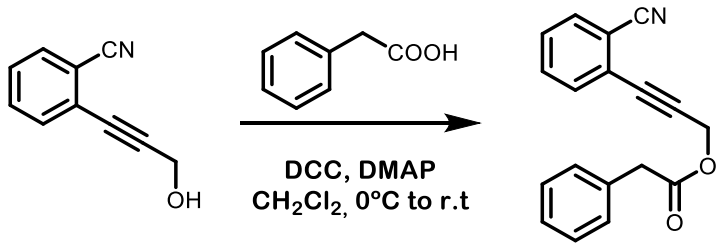

S1a **S4a**

Scheme 8.3. General procedure for the preparation of propargyl esters **S4a**-**S4l**.

To a 25 mL round-bottom flask containing a mixture of **S1a** (0.42 g, 2.68 mmol), phenylacetic acid (0.39 g, 2.87 mmol), and 4-dimethylaminopyridine (DMAP) (31.8 mg, 0.26 mmol) in dichloromethane (13 mL), N,N'-dicyclohexylcarbodiimide (DCC) (0.65 g, 3.15 mmol) was added in batches at 0 ºC. After the addition, the reaction mixture was slowly warmed to room temperature and stirred overnight. Upon completion of the reaction (TLC monitoring), the crude was filtrated through a Celite pad, rinsed with EtOAc and concentrated under reduced pressure. The crude product was then purified by column chromatography on silica gel (Hexanes/EtOAc = 9:1) to afford ester **S4a** as a yellow oil (0.69 g, 94% yield).

MW ($C_{18}H_{13}NO_2$): 275.31 g/mol; **Rf:** 0.75 (hexanes/EtOAc 6:4); **IR (ATR) ν (cm^{-1}):** 3028, 2931, 1737, 1134, 761. **^{1}H NMR ($CDCl_3$, 400 MHz):** δ_H 7.66 (dt, 1H, J = 7.7, 1.0 Hz), 7.58 – 7.52 (m, 2H), 7.47 – 7.39 (m, 1H), 7.38 – 7.27 (m, 5H), 4.99 (s, 2H), 3.72 (s, 2H). **^{13}C{H} NMR ($CDCl_3$, 101 MHz):** δ_C 170.7, 133.4, 132.6, 132.6, 132.4, 129.3, 128.9, 128.6, 127.2, 125.9, 117.2, 115.4, 89.5, 82.6, 52.7, 40.9. **HRMS (ESI) m/z:** $[M+Na]^+$ calcd. for $C_{18}H_{13}NO_2Na$ 298.0838; Found 298.0841.

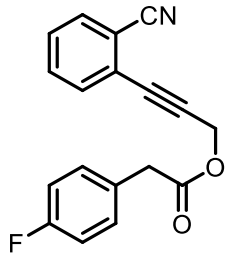

Ester **S4b** was obtained from **S1a** (0.50 g, 3.18 mmol) and *p*-fluorophenylacetic acid as a colorless solid (0.92 g, 99% yield) following the same procedure as for **S4a**.

MW ($C_{18}H_{12}FNO_2$): 293.30 g/mol; **Rf:** 0.61 (hexanes/EtOAc 6:4); **MP (ºC):** 74-76. **IR (ATR) ν (cm^{-1}):** 3038, 2938, 1735, 1217, 1148, 775. **^{1}H NMR ($CDCl_3$, 400 MHz):** δ_H 7.66 (dt, 1H, J = 7.7, 1.1 Hz), 7.59 – 7.52 (m, 2H), 7.44 (ddd, 1H, J = 7.7, 5.8, 3.1 Hz), 7.32 – 7.26 (m, 2H), 7.06 – 6.97 (m, 2H), 4.99 (s, 2H), 3.69 (s, 2H)**. ^{13}C{H} NMR ($CDCl_3$, 101 MHz):** δ_C 170.7 (d, J = 1.4 Hz), 162.2 (d, J = 245.5 Hz), 132.8, 132.7, 132.5, 131.1 (d, J = 8.1 Hz), 129.2 (d, J = 3.3 Hz), 129.0, 126.0, 117.3, 115.6, 115.6 (d, J = 21.5 Hz), 89.5, 82.8, 52.9, 40.1. **^{19}F NMR ($CDCl_3$, 376 MHz):** δ_F -115.47 (ddd, *J* = 14.1, 8.9, 5.3 Hz). **HRMS (ESI) m/z:** $[M+Na]^+$ calcd. for $C_{18}H_{12}FNO_2Na$ 316.0744; Found 316.0749.

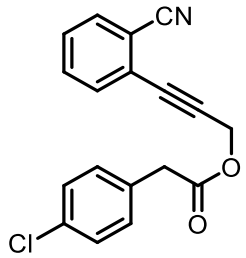

Ester **S4c** was obtained from **S1a** (0.50 g, 3.18 mmol) and *p*-chlorophenylacetic acid as a colorless solid (0.89 g, 91% yield) following the same procedure as for **S4a**.

MW ($C_{18}H_{12}ClNO_2$): 309.75 g/mol; **Rf:** 0.60; **MP (ºC):** 76-78. **IR (ATR) ν (cm^{-1}):** 3035, 2932, 1735, 1213, 1153, 776. **^{1}H NMR ($CDCl_3$, 400 MHz):** δ_H 7.66 (dt, 1H, J = 7.7, 1.0 Hz), 7.61 – 7.50 (m, 2H), 7.44 (ddd, 1H, J = 7.7, 6.3, 2.5 Hz), 7.35 – 7.30 (m, 2H), 7.27 – 7.25 (m, 2H (overlapped with chloroform)), 4.99 (s, 2H), 3.69 (s, 2H). **^{13}C{H} NMR ($CDCl_3$, 101 MHz):** δ_C 170.5, 133.4, 132.8, 132.7, 132.5, 132.0, 130.9, 129.1, 128.9, 126.0, 117.3, 115.6, 89.4, 82.8, 53.0, 40.3. **HRMS (ESI) m/z:** $[M+Na]^+$ calcd. for $C_{18}H_{12}ClNO_2Na$ 332.0449; Found 332.0452.

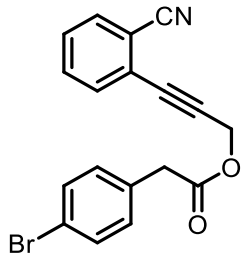

Ester **S4d** was obtained from **S1a** (0.50 g, 3.18 mmol) and *p*-bromophenylacetic acid as a colorless solid (1.07 g, 95% yield) following the same procedure as for **S4a**.

MW ($C_{18}H_{12}BrNO_2$): 354.20 g/mol; **Rf:** 0.73 (hexanes/EtOAc 6:4); **MP (ºC):** 83-85. **IR (ATR) ν (cm^{-1}):** 3035, 2932, 1734, 1211, 1154, 774. **^{1}H NMR ($CDCl_3$, 400 MHz):** δ_H 7.65 (dt, 1H, J = 7.7, 1.0 Hz), 7.58 – 7.50 (m, 2H), 7.49 – 7.44 (m, 2H), 7.44 – 7.40 (m, 1H), 7.22 – 7.17 (m, 2H), 4.98 (s, 2H), 3.67 (s, 2H). **^{13}C{H} NMR ($CDCl_3$, 101 MHz):** δ_C 170.4, 132.8, 132.7, 132.6, 132.5, 131.8, 131.2, 129.0, 126.0, 121.4, 117.3, 115.6, 89.4, 82.8, 53.0, 40.4. **HRMS (ESI) m/z:** $[M+Na]^+$ calcd. for $C_{18}H_{12}BrNO_2Na$ 375.9944-377.9924; Found 375.9951-377.9928.

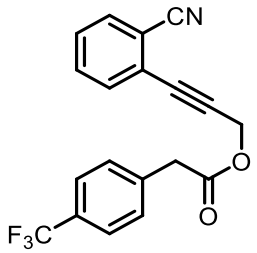

Ester **S4e** was obtained from **S1a** (0.61 g, 3.89 mmol) and *p*-trifluoromethylphenylacetic acid as a colorless solid (1.22 g, 92% yield) following the same procedure as for **S4a**.

MW ($C_{19}H_{12}F_3NO_2$): 343.41 g/mol; **Rf:** 0.73 (hexanes/EtOAc 6:4); **MP (ºC):** 73-75. **IR (ATR) ν (cm^{-1}):** 3033, 2934, 1735, 1321, 1154, 1102, 774. **^{1}H NMR ($CDCl_3$, 400 MHz):** δ_H 7.66 (dt, 1H, J = 8.0, 1.0 Hz), 7.60 (d, 2H, J = 8.0 Hz), 7.58 – 7.50 (m, 2H), 7.48 – 7.39 (m, 3H), 5.00 (s, 2H), 3.78 (s, 2H). **^{13}C{H} NMR ($CDCl_3$, 101 MHz):** δ_C 170.1, 137.5, 132.8, 132.7, 132.5, 129.9, 129.1, 126.0, 125.7 (q, J = 3.8 Hz), 117.3, 115.7, 89.3, 82.9, 53.1, 40.8. **^{19}F NMR ($CDCl_3$, 376 MHz):** δ_F -63.5 (s, 3F). **HRMS (ESI) m/z:** $[M+Na]^+$ calcd. for $C_{19}H_{12}F_3NO_2Na$ 366.0712; Found 366.0710.

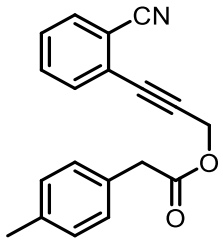

Ester **S4f** was obtained from **S1a** (0.50 g, 3.18 mmol) and *p*-tolylacetic acid as a yellow oil (0.90 g, 98% yield) following the same procedure as for **S4a**.

MW ($C_{19}H_{15}NO_2$): 289.33 g/mol; **Rf:** 0.75 (hexanes/EtOAc 6:4); **IR (ATR) ν (cm^{-1}):** 3261, 2918, 1732, 1147, 966, 767. **^{1}H NMR ($CDCl_3$, 400 MHz)):** δ_H 7.66 (dt, 1H, J = 7.7, 1.0 Hz), 7.60 – 7.50 (m, 2H), 7.49 – 7.38 (m, 1H), 7.21 (d, 2H, *J* = 8.1 Hz), 7.15 (d, 2H, *J* = 8.1 Hz), 4.98 (s, 2H), 3.68 (s, 2H), 2.33 (s, 3H). **^{13}C{H} NMR ($CDCl_3$, 101 MHz):** δ_C 171.0, 136.9, 132.7, 132.4, 130.4, 129.4, 129.2, 128.9, 126.0, 117.2, 115.5, 89.6, 82.6, 52.7, 40.6, 21.1. **HRMS (ESI) m/z:** $[M+Na]^+$ calcd. for $C_{19}H_{15}NO_2Na$ 312.0995; Found 312.0998.

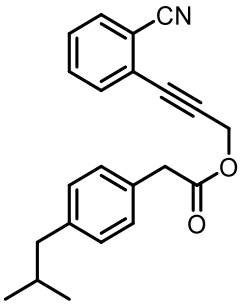

Ester **S4g** was obtained from **S1a** (0.65 g, 4.13 mmol) and *p*-isobutylphenylacetic acid as a yellow oil (0.62 g, 45% yield) following the same procedure as for **S4a**.

MW ($C_{22}H_{21}NO_2$): 331.42 g/mol; **Rf:** 0.86 (hexanes/EtOAc 6:4); **IR (ATR) ν (cm^{-1}):** 2950, 1739, 1236, 1133, 998, 763. **^{1}H NMR ($CDCl_3$, 400 MHz):** δ_H 7.64 (dd, 1H, J = 8.0, 1.1 Hz), 7.54 (d, 2H, J = 5.0 Hz), 7.45 – 7.40m, 1H), 7.23 (d, 2H, J = 8.0 Hz), 7.11 (d, 2H, J = 8.0 Hz), 4.98 (s, 2H), 3.69 (s, 2H), 2.45 (d, 2H, J = 7.0 Hz), 1.85 (hept, 1H, J = 7.0 Hz), 0.90 (d, 6H, J = 7.0 Hz). **^{13}C{H} NMR ($CDCl_3$, 101 MHz):** δ_C 171.0, 140.7, 132.8, 132.7, 132.4, 130.7, 129.4, 129.1, 128.9, 126.0, 117.3, 115.6, 89.7, 82.6, 52.8, 45.1, 40.6, 30.2, 22.4. **HRMS (ESI) m/z:** $[M+Na]^+$ calcd. for $C_{22}H_{21}NO_2Na$, 354.1465; Found 354.1465.

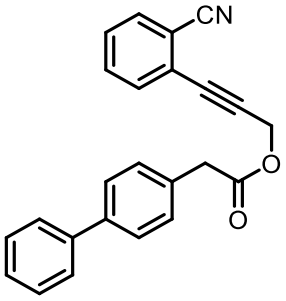

Ester **S4h** was obtained from **S1a** (0.61 g, 3.89 mmol) and *p*-biphenylacetic acid as a colorless solid (1.35 g, 99% yield) following the same procedure as for **S4a**.

MW ($C_{24}H_{17}NO_2$): 351.41 g/mol; **Rf:** 0.70 (hexanes/EtOAc 6:4); **MP (ºC):** 69-71. **IR (ATR) ν (cm^{-1}):** 3028, 2926, 2226, 1740, 1227, 1128, 750. **^{1}H NMR ($CDCl_3$, 400 MHz):** δ_H 7.66 (dt, 1H, J = 7.6, 1.1 Hz), 7.62 – 7.50 (m, 6H), 7.47 – 7.39 (m, 5H), 7.39 – 7.30 (m, 1H), 5.02 (s, 2H), 3.77 (s, 2H). **^{13}C{H} NMR ($CDCl_3$, 101 MHz):** δ_C 170.9, 140.9, 140.4, 132.8, 132.6, 132.5, 129.9, 129.0, 128.9, 127.5, 127.4, 127.2, 126.1, 117.4, 115.7, 89.6, 82.8, 53.0, 40.7. **HRMS (ESI) m/z:** $[M+Na]^+$ calcd. for $C_{24}H_{17}NO_2Na$ 374.1151; Found 374.1153.

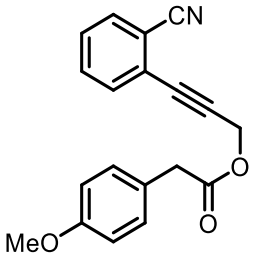

Ester **S4i** was obtained from **S1a** (0.50 g, 3.18 mmol) and *p*-methoxyphenylacetic acid as an orange oil (0.91 g, 94% yield) following the same procedure as for **S4a**.

MW ($C_{19}H_{15}NO_3$): 305.33 g/mol; **Rf:** 0.48 (hexanes/EtOAc 6:4); **IR (ATR) ν (cm^{-1}):** 2914, 1737, 1510, 1244, 1133, 763. **^{1}H NMR ($CDCl_3$, 400 MHz):** δ_H 7.64 (dt, 1H, J = 7.7, 1.1 Hz), 7.58 – 7.49 (m, 2H), 7.44 – 7.40 (m, 1H), 7.25 – 7.21 (m, 2H), 6.91 – 6.83 (m, 2H), 4.97 (s, 2H), 3.78 (s, 3H), 3.65 (s, 2H). **^{13}C{H} NMR ($CDCl_3$, 101 MHz):** δ_C 171.1, 158.9, 132.7, 132.5, 130.5, 129.0, 126.0, 125.5, 117.3, 115.5, 114.1, 89.6, 82.6, 55.3, 52.8, 40.1. **HRMS (ESI) m/z:** $[M+Na]^+$ calcd. for $C_{19}H_{15}NO_3Na$ 328.0944; Found 328.0950.

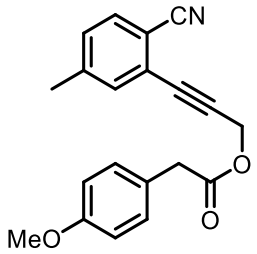

Ester **S4j** was obtained from **S2a** (0.41 g, 2.39 mmol) and p-methoxyphenylacetic acid as an orange oil (0.740 g, 97% yield) following the same procedure as for **S4a**.

MW ($C_{20}H_{17}NO_3$): 319.36 g/mol; **Rf:** 0.79 (hexanes/EtOAc 6:4); **IR (ATR) ν (cm^{-1}):** 2914, 1737, 1510, 1244, 1133, 763. **^{1}H NMR ($CDCl_3$, 400 MHz):** δ_H 7.50 (d, 1H, J = 8.0 Hz), 7.33 (s, 1H), 7.25 – 7.18 (m, 3H), 6.90 – 6.82 (m, 2H), 4.95 (s, 2H), 3.77 (s, 3H), 3.64 (s, 2H), 2.37 (s, 3H). **^{13}C{H} NMR ($CDCl_3$, 101 MHz):** δ_C 171.1, 158.8, 143.5, 133.3, 132.5, 130.4, 129.8, 125.7, 125.5, 117.5, 114.1, 112.4, 89.0, 82.7, 55.2, 52.7, 40.0, 21.5. **HRMS (ESI) m/z:** $[M+Na]^+$ calcd. for $C_{20}H_{17}NO_3Na$ 342.1101; Found 342.1100.

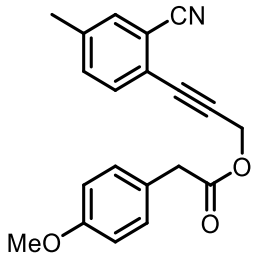

Ester **S4k** was obtained from **S3a** (0.31 g, 1.81 mmol) and *p*-methoxyphenylacetic acid as an orange oil (0.53 g, 91% yield) following the same procedure as for **S4a**.

MW ($C_{20}H_{17}NO_3$): 319.36 g/mol; **Rf:** 0.63 (hexanes/EtOAc 6:4); **IR (ATR) ν (cm^{-1}):** 2929, 1737, 1510, 1244, 1133, 822. **^{1}H NMR ($CDCl_3$, 400 MHz):** δ_H 7.43 – 7.37 (m, 2H), 7.32 (d, 1H, J = 7.0 Hz), 7.26 – 7.19 (m, 2H), 6.90 – 6.81 (m, 2H), 4.95 (s, 2H), 3.77 (s, 3H), 3.64 (s, 2H), 2.36 (s, 3H). **^{13}C{H} NMR ($CDCl_3$, 101 MHz):** δ_C 171.0, 158.8, 139.6, 133.3, 133.0, 132.5, 130.3, 125.5, 122.9, 117.3, 115.2, 114.0, 88.6, 82.6, 55.2, 52.7, 40.0, 21.1. **HRMS (ESI) m/z:** $[M+Na]^+$ calcd. for $C_{20}H_{17}NO_3Na$ 342.1101; Found 342.1102.

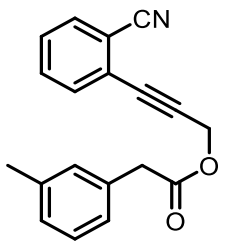

Ester **S4l** was obtained from **S1a** (0.44 g, 2.80 mmol) and 3-methylphenylacetic acid as an orange oil (0.79 g, 98% yield) following the same procedure as for **S4a**.

MW ($C_{19}H_{15}NO_2$): 289.33 g/mol; **Rf:** 0.65 (hexanes/EtOAc 6:4); **IR (ATR) ν (cm^{-1}):** 3020, 2916, 1737, 1249, 1133, 762. **^{1}H NMR ($CDCl_3$, 400 MHz):** δ_H 7.66 (dt, 1H, J = 7.8, 1.0 Hz), 7.58 – 7.52 (m, 2H), 7.43 (dt, 1H, J = 7.8, 4.4 Hz), 7.23 (t, 1H, J = 7.5 Hz), 7.16 – 7.06 (m, 3H), 4.99 (s, 2H), 3.68 (s, 2H), 2.34 (s, 3H). **^{13}C{H} NMR ($CDCl_3$, 101 MHz):** δ_C 170.8, 138.2, 133.3, 132.6, 132.4, 130.1, 128.9, 128.5, 128.0, 126.3, 125.9, 117.2, 115.4, 89.5, 82.6, 52.7, 40.9, 21.3. **HRMS (ESI) m/z:** $[M+Na]^+$ calcd. for $C_{19}H_{15}NO_2Na$ 312.0995; Found 312.0997.

Experimental procedure for the synthesis of diazo compounds 1 and 4a-4l

Diazo compound **1** was prepared as previously reported in the literature.[233]

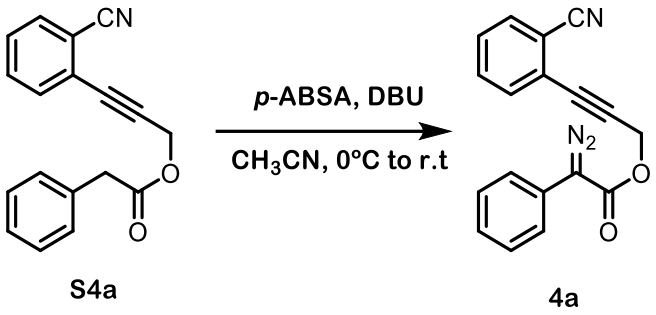

Scheme 8.4. General procedure for the preparation of diazo compounds **4a-4l**.

To a 50 mL oven-dried flask containing a mixture of **S4a** (0.40 g, 1.45 mmol) and *p*-acetamidobenzenesulfonyl azide (*p*-ABSA) (0.45 g, 1.88 mmol) in anhydrous CH_3CN (9.6 mL), a solution of 1,8-diazabicyclo[5.4.0]undec-7-ene (DBU) (0.32 mL, 2.14 mmol) in anhydrous CH_3CN (1.9 mL) was added dropwise at 0 ºC. After the addition, the reaction mixture was slowly warmed to room temperature and stirred overnight. Upon completion of the reaction (TLC monitoring), the crude was diluted with dichloromethane, and washed with saturated aqueous NH_4Cl, saturated aqueous $NaHCO_3$ and brine. The combined organic extracts were dried over anhydrous Na_2SO_4 and concentrated under reduced pressure. The crude product was purified by column chromatography on silica gel (hexanes: Et_3N= 99:1) to afford diazo compound **4a** as an orange solid (0.26 g, 59% yield).

MW ($C_{18}H_{11}N_3O_2$): 301.31; **Rf:** 0.48 (hexanes/EtOAc 8:2); **IR (ATR) ν (cm^{-1}):** 3036, 2919, 2087, 1478, 1236, 1139, 1041, 753. **^{1}H NMR ($CDCl_3$, 400 MHz):** δ_H 7.66 (ddd, 1H, J = 7.6, 1.3, 0.7 Hz), 7.62 – 7.53 (m, 2H), 7.53 – 7.48 (m, 2H), 7.45 (dd, 1H, J = 7.6, 1.7 Hz), 7.43 – 7.38 (m, 2H), 7.20 (ddt, 1H, J = 7.6, 7.0, 1.3 Hz), 5.17 (s, 2H). **^{13}C{H} NMR ($CDCl_3$, 101 MHz):** δ_C 164.4, 132.9, 132.8, 132.5, 129.2, 129.1, 126.2, 126.1, 125.2, 124.3, 117.4, 115.8, 89.7, 82.9, 52.8. **HRMS (ESI) m/z:** $[M+Na]^+$ calcd. for $C_{18}H_{11}N_3O_2Na$ 324.0743; Found 324.0748.

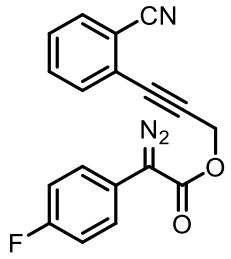

Diazo **4b** was obtained from **S4b** (0.39 g, 1.33 mmol) as a yellow solid (0.29 g, 69% yield) following the same procedure as for **4a**.

MW ($C_{18}H_{10}FN_3O_2$): 319.30 g/mol; **Rf:** 0.48 (hexanes/EtOAc 8:2). **IR (ATR) ν (cm^{-1}):** 2989, 2089, 1692, 1507, 1231, 1136, 1023, 831, 767. **^{1}H NMR ($CDCl_3$, 400 MHz):** δ_H 7.66 (dt, 1H, J = 7.9, 0.8 Hz), 7.61 – 7.53 (m, 2H), 7.50 – 7.41 (m, 3H), 7.16 – 7.06 (m, 2H), 5.16 (s, 2H). **^{13}C{H} NMR ($CDCl_3$, 101 MHz):** δ_C 164.4, 161.3 (d, J = 246.7 Hz), 132.9, 132.8, 132.5, 129.1, 126.2 (d, J = 8.0 Hz), 126.0, 120.9 (d, J = 3.3 Hz), 117.3, 116.2 (d, J = 22.0 Hz), 115.7, 89.5, 82.9, 52.9. **^{19}F NMR ($CDCl_3$, 376 MHz):** δ_F -115.84 (br.abs., 1F). **HRMS (ESI) m/z:** $[M+Na]^+$ calcd. for $C_{18}H_{10}FN_3O_2Na$ 342.0649; Found 342.0652.

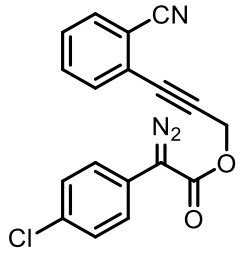

Diazo **4c** was obtained from **S4c** (0.45 g, 1.45 mmol) as a yellow solid (0.28 g, 57% yield) following the same procedure as for **4a**.

MW ($C_{18}H_{10}ClN_3O_2$): 335.75 g/mol; **Rf:** 0.45 (hexanes/EtOAc 8:2); **IR (ATR) ν (cm^{-1}):** 3032,2990, 2087, 1694, 1235, 1143, 1022, 769. **^{1}H NMR ($CDCl_3$, 400 MHz):** δ_H 7.66 (d, 1H, *J* = 7.3 Hz), 7.62 – 7.51 (m, 2H), 7.47 – 7.41 (m, 3H), 7.39 – 7.34 (m, 2H), 5.16 (s, 2H). **^{13}C{H} NMR ($CDCl_3$, 101 MHz):** δ_C 164.1, 132.8, 132.7, 132.5, 131.8, 129.3, 129.1, 125.9, 125.3, 123.8, 117.3, 115.7, 89.4, 83.0, 52.9. **HRMS (ESI) m/z:** $[M+Na]^+$ calcd. for $C_{18}H_{10}ClN_3O_2Na$ 358.0354; Found 358.0353.

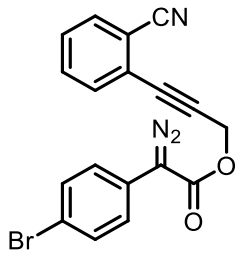

Diazo **4d** was obtained from **S4d** (0.42 g, 1.19 mmol) as an orange oil (0.24 g, 53% yield) following the same procedure as for **4a**.

MW ($C_{18}H_{10}BrN_3O_2$): 380.20 g/mol; **Rf:** 0.30 (hexanes/EtOAc 8:2); **IR (ATR) ν (cm^{-1}):** 3035. 2988, 2061, 1691, 1235, 1142, 755. **^{1}H NMR ($CDCl_3$, 400 MHz):** δ_H 7.64 (d, 1H, J = 7.5 Hz), 7.61 – 7.50 (m, 2H), 7.49 (d, 2H, J = 8.6 Hz), 7.43 (td, 1H, J = 7.5, 2.0 Hz), 7.36 (d, 2H, J = 8.6 Hz), 5.15 (s, 2H). **^{13}C{H} NMR ($CDCl_3$, 101 MHz):** δ_C 164.0, 132.8, 132.7, 132.5, 132.2, 129.1, 125.9, 125.5, 124.4, 119.7, 117.3, 115.7, 89.4, 83.0, 52.9. **HRMS (ESI) m/z:** $[M+Na]^+$ calcd. for $C_{18}H_{10}BrN_3O_2Na$ 401.9849-403.9829; Found 401.9845-403.9826.

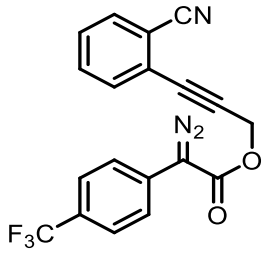

Diazo **4e** was obtained from **S4e** (0.51 g, 1.48 mmol) as a yellow solid (0.28 g, 51% yield) following the same procedure as for **4a**.

MW ($C_{19}H_{10}F_3N_3O_2$): 369.30 g/mol; **Rf:** 0.40 (hexanes/EtOAc 8:2). **IR (ATR) ν (cm^{-1}):** 3067, 2927, 2095, 1691, 1322, 1234, 1097, 759. **^{1}H NMR ($CDCl_3$, 400 MHz):** δ_H 7.67 (d, 1H, *J* = 7.5 Hz), 7.63 (br. abs., 4H), 7.61 – 7.53 (m, 2H), 7.49 – 7.40 (m, 1H), 5.19 (s, 2H). **^{13}C{H} NMR ($CDCl_3$, 101 MHz):** δ_C 163.7, 132.8, 132.7, 132.5, 129.8, 129.1, 127.8, 126.0 (q, *J* = 3.9 Hz), 125.9, 123.7, 117.3, 115.8, 89.3, 83.1, 53.1. **^{19}F NMR ($CDCl_3$, 376 MHz):** δ_F -63.48 (s, 3F). **HRMS (ESI) m/z:** $[M+Na]^+$ calcd. for $C_{19}H_{10}F_3N_3O_2Na$ 392.0629; Found 392.0617.

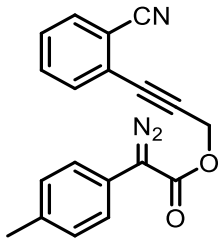

Diazo **4f** was obtained from **S4f** (0.42 g, 1.45 mmol) as an orange solid (0.12 g, 26% yield) following the same procedure as for **4a**.

MW ($C_{19}H_{13}N_3O_2$): 315.33; **Rf:** 0.43 (hexanes/EtOAc 8:2); **IR (ATR) ν (cm^{-1}):** 3014, 2969, 2079, 1738, 1373, 1229, 771. **^{1}H NMR ($CDCl_3$, 400 MHz):** δ_H 7.66 (d, 1H, J = 7.7 Hz), 7.59 (dd, 1H, J = 7.7, 1.7 Hz), 7.55 (td, 1H, J = 7.5, 1.3 Hz), 7.43 (td, 1H, J = 7.5, 1.7 Hz), 7.38 (d, 2H, J = 8.2 Hz), 7.21 (d, 2H, J = 8.2 Hz), 5.16 (s, 2H), 2.35 (s, 3H). **^{13}C{H} NMR ($CDCl_3$, 101 MHz):** δ_C 164.7, 136.2, 132.9, 132.8, 132.5, 129.9, 129.0, 126.1, 124.4, 121.8, 117.4, 115.7, 89.7, 82.8, 52.8, 21.1. **HRMS (ESI) m/z:** $[M+Na]^+$ calcd. for $C_{19}H_{13}N_3O_2Na$ 338.0904; Found 338.0900.

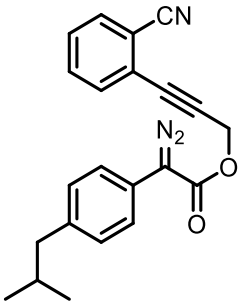

Diazo **4g** was obtained from **S4g** (0.37 g, 1.12 mmol) as an orange solid (0.16 g, 40% yield) following the same procedure as for **4a**.

MW ($C_{22}H_{19}N_3O_2$): 357.41; **Rf:** 0.53 (hexanes/EtOAc 8:2); **IR (ATR) ν (cm^{-1}):** 3033, 2953, 2084, 1688, 1151, 1044, 755. **^{1}H NMR ($CDCl_3$, 400 MHz):** δ_H 7.66 (dd, 1H, J = 7.7, 0.9 Hz), 7.59 (dd, 1H, J = 7.5, 1.5 Hz), 7.55 (td, 1H, J = 7.7, 1.3 Hz), 7.43 (td, 1H, J = 7.5, 1.7 Hz), 7.40 (d, 2H, J = 8.4 Hz), 7.18 (d, 2H, J = 8.4 Hz), 5.16 (s, 2H), 2.47 (d, 2H, J = 6.8 Hz), 1.85 (hept, 1H, J = 6.8 Hz), 0.90 (d, 6H, J = 6.8 Hz). **^{13}C{H} NMR ($CDCl_3$, 101 MHz):** δ_C 164.7, 140.0, 132.9, 132.8, 132.5, 130.0, 129.0, 126.1, 124.2, 122.1, 117.4, 115.7, 89.8, 82.8, 52.8, 45.1, 30.4, 22.5. **HRMS (ESI) m/z:** $[M+Na]^+$ calcd. for $C_{22}H_{19}N_3O_2Na$ 380.1383; Found 380.1369.

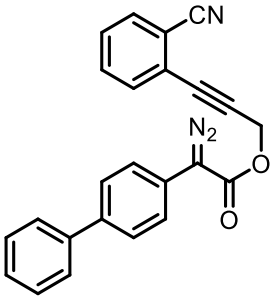

Diazo **4h** was obtained from **S4h** (0.51 g, 1.45 mmol) as an orange solid (0.17 g, 31% yield) following the same procedure as for **4a**.

MW ($C_{24}H_{15}N_3O_2$): 377.40; **Rf:** 0.48 (hexanes/EtOAc 8:2); **IR (ATR) ν (cm^{-1}):** 3030, 2925, 2082, 1695, 1232, 1147, 757. **^{1}H NMR ($CDCl_3$, 400 MHz):** δ_H 7.70 – 7.62 (m, 3H), 7.62 – 7.51 (m, 6H), 7.47 – 7.41 (m, 3H), 7.39 – 7.31 (m, 1H), 5.19 (s, 2H). **^{13}C{H} NMR ($CDCl_3$, 101 MHz):** δ_C 164.4, 140.4, 139.0, 132.9, 132.8, 132.5, 129.1, 129.0, 127.8, 127.5, 127.0, 126.1, 124.6, 124.1, 117.4, 115.8, 89.6, 82.9, 52.9. **HRMS (ESI) m/z:** $[M+Na]^+$ calcd. for $C_{24}H_{15}N_3O_2Na$ 400.1064; Found 400.1056.

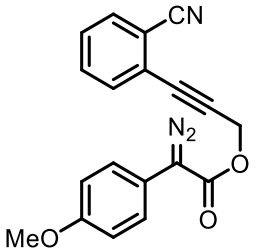

Diazo **4i** was obtained from **S4i** (0.45 g, 1.47 mmol) as an orange solid (0.11 g, 23% yield) following the same procedure as for **4a**.

MW ($C_{19}H_{13}N_3O_3$): 331.33; **Rf:** 0.38 (hexanes/EtOAc 8:2); **IR (ATR) ν (cm^{-1}):** 3010, 2933, 2084, 1692, 1506,1236, 1148, 1020, 757. **^{1}H NMR ($CDCl_3$, 400 MHz):** δ_H 7.65 (dt, 1H, *J* = 7.6, 1.0 Hz,), 7.61 – 7.51 (m, 2H), 7.44 (dd, 1H, J = 7.6, 1.7 Hz), 7.42 – 7.37 (m, 2H), 7.00 – 6.93 (m, 2H), 5.15 (s, 2H), 3.81 (s, 3H). **^{13}C{H} NMR ($CDCl_3$, 101 MHz):** δ_C 165.0, 158.4, 132.9, 132.8, 132.5, 129.0, 128.7, 126.3, 126.1, 117.4, 116.6, 115.7, 114.8, 89.8, 82.8, 55.5, 52.8. **HRMS (ESI) m/z:** $[M+Na]^+$ calcd. for $C_{19}H_{13}N_3O_3Na$ 354.0852; Found 354.0849.

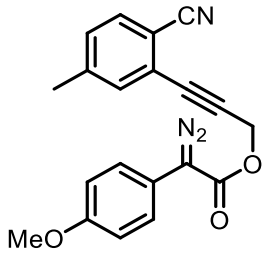

Diazo **4j** was obtained from **S4j** (0.46 g, 1.44 mmol) as an orange solid (0.18 g, 36% yield) following the same procedure as for **4a**.

MW ($C_{20}H_{15}N_3O_3$): 345.36 g/mol; **Rf:** 0.40 (hexanes/EtOAc 8:2); **IR (ATR) ν (cm^{-1}):** 2934, 2089, 1679, 1511, 1239, 1150, 1027, 819. **^{1}H NMR ($CDCl_3$, 400 MHz):** δ_H 7.53 (d, 1H, J = 8.0 Hz), 7.45 – 7.35 (m, 3H), 7.23 (dd, 1H, J = 8.0, 1.0 Hz), 7.00 – 6.91 (m, 2H), 5.14 (s, 2H), 3.81 (s, 3H), 2.39 (s, 3H). **^{13}C{H} NMR ($CDCl_3$, 101 MHz):** δ_C 165.0, 158.4, 143.6, 133.5, 132.7, 130.0, 126.3, 125.9, 117.7, 116.6, 114.8, 112.7, 89.2, 82.9, 55.5, 52.8, 21.7. **HRMS (ESI) m/z:** $[M+Na]^+$ calcd. for $C_{20}H_{15}N_3O_3Na$ 368.1014; Found 368.1006.

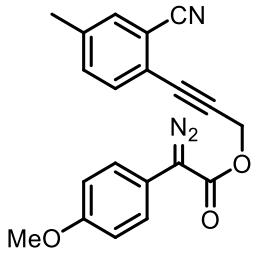

Diazo **4k** was obtained from **S4k** (0.31 g, 0.97 mmol) as an orange solid (0.19 g, 57% yield) following the same procedure as for **4a**.

MW ($C_{20}H_{15}N_3O_3$): 345.36 g/mol; **Rf:** 0.38 (hexanes/EtOAc 8:2); **IR (ATR) ν (cm^{-1}):** 2997, 2092, 1694, 1509, 1252, 1150, 1024, 828. **^{1}H NMR ($CDCl_3$, 400 MHz):** δ_H 7.47 (d, 2H, J = 8.2 Hz), 7.43 – 7.38 (m, 2H), 7.35 (dd, 1H, J = 8.2, 1.5 Hz), 6.98 – 6.92 (m, 2H), 5.14 (s, 2H), 3.81 (s, 3H), 2.39 (s, 3H). **^{13}C{H} NMR ($CDCl_3$, 101 MHz):** δ_C 158.4, 139.7, 133.4, 133.2, 132.8, 126.3, 123.2, 117.5, 116.7, 115.6, 114.8, 88.9, 82.9, 55.5, 52.9, 21.3. **HRMS (ESI) m/z:** $[M+Na]^+$ calcd. for $C_{20}H_{15}N_3O_3Na$ 368.1013; Found 368.1006.

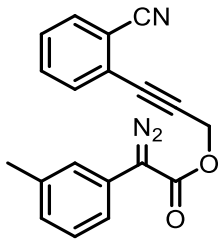

Diazo **4l** was obtained from **S4l** (0.49 g, 1.69 mmol) as an orange solid (0.24 g, 45% yield) following the same procedure as for **4a**.

MW ($C_{19}H_{13}N_3O_2$): 315.33 g/mol; **Rf:** 0.48 (hexanes/EtOAc 8:2); **IR (ATR) ν (cm^{-1}):** 3036, 2919, 2087, 1697, 1236, 1139, 753. **^{1}H NMR ($CDCl_3$, 400 MHz):** δ_H 7.66 (dt, 1H, J = 8.2, 1.0 Hz), 7.59 (dd, 1H, J = 8.2, 1.7 Hz), 7.55 (td, 1H, J = 7.6, 1.3 Hz), 7.44 (td, 1H, J = 7.6, 1.7 Hz), 7.34 – 7.28 (m, 3H), 7.06 – 6.98 (m, 1H), 5.16 (s, 2H), 2.37 (s, 3H). **^{13}C{H} NMR ($CDCl_3$, 101 MHz):** δ_C 165.3, 138.0, 132.9, 132.8, 132.5, 131.1, 131.0, 129.2, 129.0, 126.6, 126.1, 123.9, 117.3, 115.7, 89.8, 82.7, 52.9, 20.1. **HRMS (ESI) m/z:** $[M+Na]^+$ calcd. for $C_{19}H_{13}N_3O_2Na$ 338.0900; Found 338.0916.

Preparation of 4a-d_5

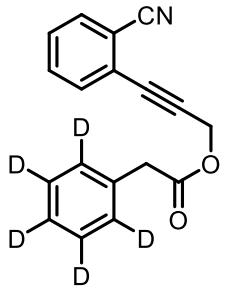

Ester **S4-$_{d5}$** was obtained from **S1a** (0.30 g, 1.91 mmol) and phenylacetic acid d_5 [234] (0.30 g, 2.10 mmol) as a colorless oil (0.45 g, 84% yield) following the same procedure as for **S4a**.

MW ($C_{18}H_8D_5NO_2$): 280.13 g/mol; **Rf:** 0.63 (hexanes/EtOAc 6:4); **IR (ATR) ν (cm^{-1}):** 2918, 2227, 1742, 1133, 761. **^{1}H NMR ($CDCl_3$, 400 MHz):** δ_H 7.66 (dt, 1H, J = 7.7, 1.0 Hz), 7.59 – 7.50 (m, 2H), 7.48 – 7.38 (m, 1H), 4.99 (s, 2H), 3.73 (s, 2H). **^{13}C{H} NMR ($CDCl_3$, 101 MHz):** δ_C 170.8, 133.3, 132.7, 132.6, 132.4, 129.1 – 128.7 (m), 128.9, 128.5 – 127.7 (m), 127.0 – 126.5 (m), 125.9, 117.2, 115.5, 89.5, 82.6, 52.8, 40.9. **HRMS (ESI) m/z:** $[M+Na]^+$ calcd. for $C_{18}H_8D_5NO_2Na$ 303.1152; Found 303.1158.

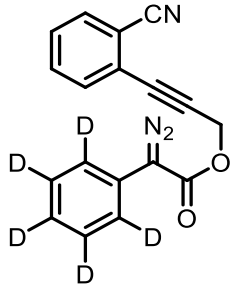

Diazo **4a-$_{d5}$** was obtained from **S4-$_{d5}$** (0.32 g, 1.14 mmol) as an orange solid (0.13 g, 38% yield) following the same procedure as for **4a**.

MW ($C_{18}H_6D_5N_3O_2$): 306.12 g/mol; **Rf:** 0.5 (hexanes/EtOAc 8:2); **IR (ATR) ν (cm^{-1}):** 2936, 2084, 1736, 1700, 1230, 1121, 726. **^{1}H NMR ($CDCl_3$, 400 MHz):** δ_H 7.66 (dd, 1H, J = 8.0, 1.2 Hz), 7.59 (dd, 1H, J = 8.0, 1.7 Hz), 7.55 (td, 1H, J = 7.5, 1.2 Hz), 7.44 (td, 1H, J = 7.5, 1.7 Hz), 5.17 (s, 2H). **^{13}C{H} NMR ($CDCl_3$, 101 MHz):** δ_C 164.4, 132.9, 132.8, 132.5, 129.1, 129.0 – 128.9 (m), 128.6 – 128.4 (m), 126.1, 125.0, 124.3 – 123.4 (m),

117.4, 115.7, 89.7, 82.8, 52.8. **HRMS (ESI) m/z:** $[M+Na]^+$ calcd. for $C_{18}H_6D_5N_3O_2Na$ 329.1057; Found 329.1060.

General procedure for the rhodium-catalyzed carbene/alkyne metathesis adding external nitriles

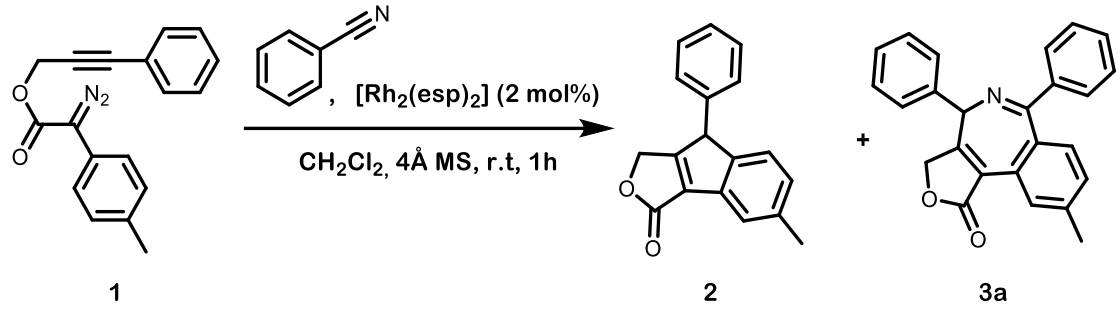

Scheme 8.5. General procedure for the rhodium-catalyzed intermolecular carbene/alkyne metathesis adding external nitriles.

To an oven-dried Schlenk flask containing diazo compound **1** (43.5 mg, 0.15 mmol), benzonitrile (154 µL, 1.5 mmol), and 4Å MS (100 mg) in anhydrous dichloromethane (3.2 mL), a solution of $[Rh_2(esp)_2]$ (2.3 mg, 0.003 mmol) in dichloromethane (0.8 mL) was added dropwise under a nitrogen atmosphere at room temperature and the mixture was then stirred for 1h. The solvent was then removed under reduced pressure and the crude reaction mixture was purified by column chromatography on silica gel using hexanes/EtOAc mixtures as the eluent (95:5 to 85:15). The first eluted fraction afforded compound **3a** (18.0 mg, 33% yield) as a colorless solid. Further elution provided compound **2** (25.9 mg, 66% yield) as a colorless solid.

3a: MW ($C_{25}H_{19}NO_2$): 365.43 g/mol; **Rf:** 0.54 (Hexanes/EtOAc 8:2). **MP (ºC):** 250 (dec.). **IR (ATR) ν (cm^{-1}):** 3025, 2918, 1750, 1592, 1023, 694. **^{1}H NMR ($CDCl_3$, 400 MHz):** δ_H 8.14 (d, 1H, J = 8.1 Hz), 7.71 (d, 2H, J = 7.2 Hz), 7.53 – 7.34 (m, 9H), 7.33 (s, 1H), 4.86 (br s, 1H), 4.64 (dd, 1H, J = 18.7, 1.6 Hz), 4.44 (d, 1H, J = 18.7 Hz), 2.41 (s, 3H). **^{13}C{H} NMR ($CDCl_3$, 101 MHz):** δ_C 171.5, 169.0, 165.1, 141.1, 138.5, 137.3, 136.2, 131.9, 131.5, 130.3, 130.2, 129.0, 128.5, 128.4, 128.2, 127.8, 127.1, 124.7, 69.6, 61.7, 21.6**. HRMS (ESI) m/z:** $[M+H]^+$ calcd. for **$C_{26}H_{20}NO_2$** 366.1489; Found 366.1481.

2: MW ($C_{18}H_{14}O_2$): 262.31 g/mol; **Rf:** 0.45 (Hexanes/EtOAc 8:2). **MP (ºC):** 175. **IR (ATR) ν (cm^{-1}):** 3028, 2914,1742, 1013, 824, 695. **^{1}H NMR ($CDCl_3$, 400 MHz):** δ_H 7.62 (d, 1H, J = 7.7 Hz), 7.37 – 7.27 (m, 3H), 7.18 (d, 1H, J = 8.5 Hz), 7.13 – 7.05 (m, 3H), 5.11 (dd, 1H, J = 18.1, 1.1 Hz), 4.94 (d, 1H, J = 18.1 Hz), 4.85 (s, 1H), 2.35 (s, 3H). **^{13}C{H} NMR ($CDCl_3$, 101 MHz):** δ_C 174.9, 167.8, 152.0, 137.3, 136.9, 136.6, 131.4, 129.5, 128.6, 128.0, 127.9, 126.0, 120.9, 69.2, 53.0, 21.7. **HRMS (ESI) m/z:** $[M+Na]^+$ calcd. for $C_{18}H_{14}O_2Na$ 285.0886; Found 285.0892.

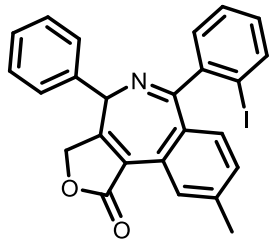

Starting from diazo compound **1** (35 mg, 0.12 mmol) and 2-iodobenzonitrile (275 mg, 1.2 mmol) compound **3b** (22.5 mg, 38% yield) was obtained as a colorless solid, alongside **2** (19.1 mg, 60 % yield).

3b: MW ($C_{25}H_{18}INO_2$): 491.33 g/mol; **Rf:** 0.58 (Hexanes/EtOAc 8:2). **IR (ATR) ν (cm^{-1}):** 3036, 1761, 1603, 1106, 1036, 714. **^{1}H NMR ($CDCl_3$, 400 MHz):** δ_H 8.15 (d, 1H, J = 8.1 Hz), 7.83 (d, 1H, J = 7.9 Hz), 7.65 (d, 2H, J = 7.1 Hz), 7.50 – 7.34 (m, 6H), 7.09 (ddd, 1H, J = 7.9, 7.1, 2.0 Hz), 7.04 (s, 1H), 4.94 (br s, 1H), 4.69 (dd, 1H, J = 18.7, 1.8 Hz), 4.47 (d, 1H, J = 18.7 Hz), 2.35 (s, 3H). **^{13}C{H} NMR ($CDCl_3$, 101 MHz):** δ_C 171.3, 171.0, 163.7, 145.7, 139.9, 138.1, 138.0, 136.1, 131.7, 131.1, 130.9, 130.4, 129.2, 129.0, 128.4, 128.1, 127.9, 127.5, 125.0, 97.0, 69.5, 61.7, 21.7. **HRMS (ESI) m/z:** $[M+H]^+$ calcd. for **$C_{25}H_{19}INO_2$** 492.0455; Found 492.0461.

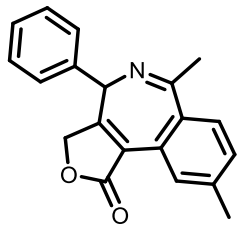

Starting from diazo compound **1** (43.5 mg, 0.15 mmol), and acetonitrile (157 µL, 3.0 mmol), compound **3c** (17.4 mg, 38% yield) was obtained as a pale pink solid. alongside **2** (22.7 mg, 58 % yield).

3c: MW ($C_{20}H_{17}NO_2$): 303.36 g/mol; **Rf:** 0.56 (Hexanes/EtOAc 8:2). **IR (ATR) ν (cm^{-1}):** 3038, 2919, 1747, 1604,1117, 1027, 829, 700. **^{1}H NMR ($CDCl_3$, 400 MHz):** δ_H 8.08 (d, 1H, J = 8.1 Hz), 7.57 (s, 3H), 7.49 – 7.31 (m, 4H), 4.79 – 4.57 (m, 2H), 4.36 (d, 1H, J = 18.8 Hz). (Wide signals are observed due potential imine-enamine tautomerism), 2.49 (s, 6H). **^{13}C{H} NMR ($CDCl_3$, 101 MHz):** δ_C 171.6, 164.3, 138.4, 138.2, 137.8, 131.1, 129.1, 128.4, 127.7, 127.6, 126.4, 124.4, 69.5, 61.4, 27.7, 21.8. **HRMS (ESI) m/z:** $[M+H]^+$ calcd. for **$C_{20}H_{18}NO_2$** 304.1332; Found 304.1329.

General procedure for the rhodium-catalyzed carbene/alkyne metathesis tandem reaction

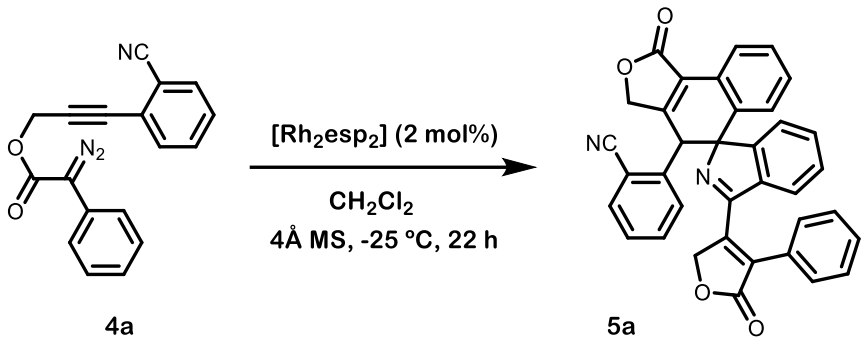

Scheme 8.6. General procedure for the rhodium-catalyzed carbene/alkyne metathesis tandem reaction.

To an oven-dried Schlenk flask containing diazo compound **4a** (33.3 mg, 0.11 mmol) and 4Å MS (100 mg) in anhydrous dichloromethane (2.7 mL), a solution of [Rh_2esp_2] (1.7 mg, 0.0022 mmol) in dichloromethane (0.4 mL) was added dropwise under a nitrogen atmosphere at -25 ºC. The mixture was then placed in a freezer at -25 ºC and the reaction was stirred for 22h. The solvent was then removed under reduced pressure and the crude reaction mixture was purified by column chromatography on silica gel using hexanes/EtOAc mixtures as the eluent (95:5 to 80:20). Concentration under reduced pressure afforded compound **5a** (22.5 mg, 75% yield) as a colorless solid.

MW ($C_{36}H_{22}N_2O_4$): 546.58 g/mol; **Rf:** 0.25 (hexanes/EtOAc 6:4); **MP (ºC):** 200 (dec.). **IR (ATR) ν (cm^{-1}):** 3064, 2928, 1749, 1443, 1028, 958, 760. **^{1}H NMR ($CDCl_3$, 400 MHz):** δ_H 8.51 (dd, 1H, J = 7.7, 1.4 Hz), 7.58 (dt, 1H, J = 7.7, 3.7 Hz), 7.48 (td, 1H, J = 7.7, 1.4 Hz), 7.44 (dd, 2H, J = 5.8, 3.4 Hz), 7.41 – 7.32 (m, 3H), 7.32 – 7.26 (m, 2H), 7.17 (td, 1H, J = 7.6, 1.4 Hz), 7.09 – 7.00 (m, 3H), 6.65 – 6.57 (m, 1H), 6.41 (dd, 1H, J = 7.8, 1.2 Hz), 6.24 – 6.18 (m, 1H), 5.29 (d, 1H, J = 18.0 Hz), 5.09 (d, 1H, J = 18.0 Hz), 4.95 (dd, 1H, J = 18.3, 1.4 Hz), 4.71 (d, 1H, J = 18.3 Hz), 4.36 (s, 1H). **^{13}C{H} NMR ($CDCl_3$, 101 MHz):** δ_C 172.3, 170.8, 165.2, 159.5, 151.3, 149.6, 138.4, 137.5, 133.2, 133.1, 132.4, 132.1, 130.2, 130.0, 129.9, 129.8, 129.4, 129.3, 129.2, 128.9, 128.8, 128.7, 127.8, 125.8, 125.4, 125.1, 124.5, 124.3, 116.5, 115.0, 85.0, 71.0, 69.9, 46.9. **HRMS (ESI) m/z:** $[M+Na]^+$ calcd. for $C_{36}H_{22}N_2O_4Na$ 569.1472; Found 569.1481.

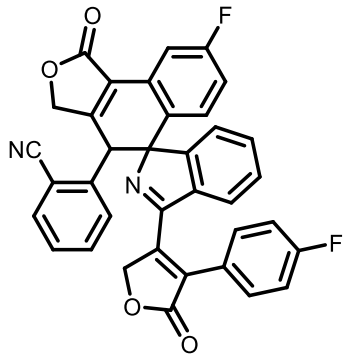

Starting from diazo compound **4b (**44.4 mg, 0.14 mmol), compound **5b** was obtained as a colorless solid (28.3 mg, 70% yield).

MW ($C_{36}H_{20}FN_2O_4$): 582.56 g/mol; **Rf:** 0.35 (hexanes/EtOAc 6:4)**; IR (ATR) ν (cm^{-1}):** 3066, 2928, 1749, 1498, 1225, 836. **^{1}H NMR ($CDCl_3$, 400 MHz):** δ_H 8.53 (dd, 1H, J = 8.5, 5.8 Hz), 7.64 – 7.56 (m, 1H), 7.51 – 7.46 (m, 2H), 7.46 – 7.41 (m, 2H), 7.22 – 6.97 (m, 6H), 6.68 (dd, 1H, J = 6.6, 1.2 Hz), 6.13 (dd, 1H, J = 6.6, 1.2 Hz), 6.07 (dd, 1H, J = 9.5, 2.6 Hz), 5.31 (d, 1H, J = 18.1 Hz), 5.08 – 4.91 (m, 2H), 4.71 (d, 1H, J = 18.1 Hz), 4.27 (s, 1H). **^{13}C{H} NMR ($CDCl_3$, 101 MHz):** δ_C (due to the complexity of the coupled C-F spectrum, the C-F doublets are not described, and all the peaks visible in the spectrum are listed) 172.2, 170.7, 165.3, 150.6, 149.1, 138.2, 137.5, 135.0, 133.3 (d, J = 5.3 Hz), 132.1 (d, J = 8.5 Hz), 131.2, 129.6, 129.3, 128.6, 127.0, 124.7 (d, J = 8.4 Hz), 124.4, 116.6, 116.4, 116.3, 116.3, 116.1, 115.0, 113.9, 84.9, 70.9, 69.9, 46.6. **^{19}F NMR ($CDCl_3$, 376 MHz):** δ_F -109.45 (s, 1F), -110.49 (s, 1F). **HRMS (ESI) m/z:** $[M+Na]^+$ calcd. for $C_{36}H_{20}FN_2O_4Na$ 605.1283; Found 605.1300.

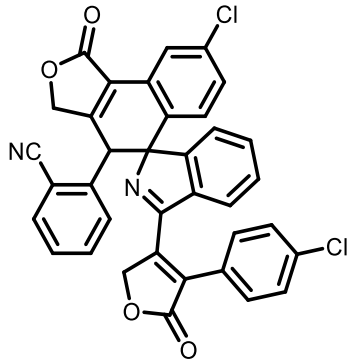

Starting from diazo compound **4c (**59.8 mg, 0.18 mmol), compound **5c** was obtained as a colorless solid (29.4 mg, 54% yield).

MW ($C_{36}H_{20}Cl_2N_2O_4$): 615.47 g/mol; **Rf:** 0.48 (hexanes/EtOAc 6:4); **IR (ATR) ν (cm^{-1}):** 3076, 2932, 1752, 1487, 1089, 957, 834. **^{1}H NMR ($CDCl_3$, 400 MHz):** δ_H 8.48 (d, 1H, J = 8.3 Hz), 7.60 (dd, 1H, J = 7.2, 2.0 Hz), 7.54 – 7.44 (m, 3H), 7.41 – 7.36 (m, 2H), 7.34 – 7.28 (m, 2H), 7.23 – 7.16 (m, 1H), 7.12 (td, 1H, J = 7.5, 1.4 Hz), 7.08 – 7.03 (m, 1H), 6.72 (d, 1H, J = 7.5 Hz), 6.32 (d, 1H, J = 2.1 Hz), 6.12 (d, 1H, J = 7.5 Hz), 5.30 (d, 1H, J = 18.1 Hz), 5.05 (d, 1H, J = 18.1 Hz), 4.99 (dd, 1H, J = 18.3, 1.3 Hz), 4.71 (d, 1H, J = 18.3 Hz), 4.24 (s, 1H). **^{13}C{H} NMR ($CDCl_3$, 101 MHz):** δ_C 171.9, 170.5, 165.2, 159.6, 150.5, 149.6, 138.0, 137.5, 136.4, 136.0, 134.2, 133.4, 133.3, 131.3, 131.1, 130.0, 129.7, 129.6, 129.4, 129.2, 128.5, 127.7, 126.5, 126.4, 126.3, 124.7, 124.4, 116.4, 115.0, 84.8, 71.0, 70.0, 46.7. **HRMS (ESI) m/z:** $[M+Na]^+$ calcd. for $C_{36}H_{20}Cl_2N_2O_4Na$ 726.9665 - 728.9643; Found 726.9667- 728.9653.

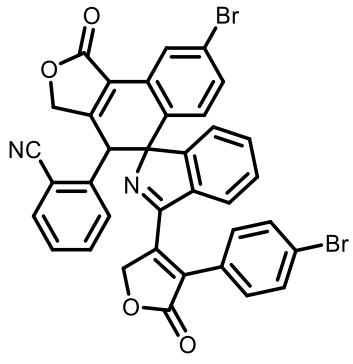

Starting from diazo compound **4d (**51.9 mg, 0.14 mmol), compound **5d** was obtained as a colorless solid (27.7 mg, 57% yield).

MW ($C_{36}H_{20}Br_2N_2O_4$): 704.37 g/mol; **Rf:** 0.38 (hexanes/EtOAc 6:4); **IR (ATR) ν (cm^{-1}):** 3075, 2931, 1750, 1486, 1089, 955, 831. **^{1}H NMR ($CDCl_3$, 400 MHz):** δ_H 8.41 (d, 1H, J = 8.3 Hz), 7.66 – 7.56 (m, 2H), 7.53 – 7.47 (m, 3H), 7.36 – 7.28 (m, 2H), 7.22 – 7.09 (m, 3H), 7.08 – 7.02 (m, 1H), 6.73 (d, 1H, J = 8.5 Hz), 6.46 (d, 1H, J = 2.0 Hz), 6.13 (d, 1H, J = 7.3 Hz), 5.29 (d, 1H, J = 18.2 Hz), 5.06 (d, 1H, J = 18.2 Hz), 4.97 (dd, 1H, J = 18.4, 1.3 Hz), 4.70 (d,1H, J = 18.4 Hz), 4.23 (s, 1H). **^{13}C{H} NMR ($CDCl_3$, 101 MHz):** δ_C 171.9, 170.4, 165.3, 159.8, 150.4, 149.7, 137.9, 137.4, 134.9, 134.3, 133.4, 133.3, 133.0, , 132.2, 131.8, 131.4, 131.0, 129.8, 129.6, 129.4, 129.0, 128.5, 128.1, 126.9, 126.6, 124.8, 124.7, 124.6, 124.4, 124.3, 116.4, 115.0, 84.7, 71.0, 70.0, 46.8. **HRMS (ESI) m/z:** $[M+Na]^+$ calcd. for $C_{36}H_{20}Br_2N_2O_4Na$ 726.9665 - 728.9643; Found 726.9667- 728.9653.

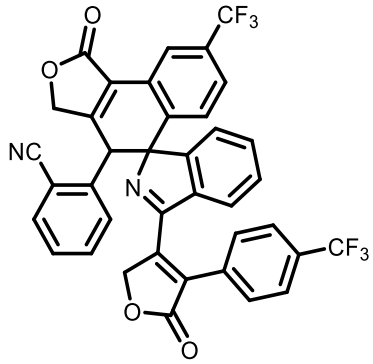

Starting from diazo compound **4e (**86.8 mg, 0.24 mmol)**,** compound **5e** was obtained as a colorless solid (45.4 mg, 57% yield).

MW ($C_{38}H_{20}F_6N_2O_4$): 682.58 g/mol; **Rf:** 0.45 (hexanes/EtOAc 6:4); **IR (ATR) ν (cm^{-1}):** 2925, 1751, 1321, 1119, 1065, 842, 685. **^{1}H NMR ($CDCl_3$, 400 MHz):** δ_H 8.67 (d, 1H, J = 8.1 Hz), 7.80 – 7.73 (m, 1H), 7.65 – 7.58 (m, 1H), 7.58 (s, 4H), 7.50 (ddd, 2H, J = 6.9, 4.6, 1.8 Hz), 7.17 – 7.13 (m, 2H), 7.06 – 7.00 (m, 1H), 6.73 – 6.65 (m, 1H), 6.57 (s, 1H), 6.15 – 6.07 (m, 1H), 5.33 (d, 1H, J = 18.2 Hz), 5.10 (d, 1H, J = 18.2 Hz), 5.02 (d, 1H, J = 18.6 Hz), 4.74 (d, 1H, J = 18.5 Hz), 4.27 (s, 1H).**^{13}C{H} NMR ($CDCl_3$, 101 MHz):** δ_C (due to the complexity of the coupled C-F spectrum, the C-F doublets are not described, and all the peaks visible in the spectrum are listed) 171.6, 170.2, 165.1, 161.7, 151.0, 150.3, 137.6, 137.4, 133.5, 133.4, 133.2, 132.8 – 132.7 (m), 132.1 (d, J = 3.7 Hz), 131.8 (d, J = 4.0 Hz), 131.2, 131.1, 130.3, 129.9, 129.8, 129.5, 128.4, 127.1 (d, J = 3.6 Hz), 125.8 (d, J = 3.9 Hz), 125.5, 124.7, 124.6, 124.3, 122.5, 116.3, 115.0, 84.8, 71.0, 70.0, 46.7. **^{19}F NMR ($CDCl_3$, 376 MHz):** δ_F -63.90 (s, 3F), -63.91 (s, 3F).**HRMS (ESI) m/z:** $[M+Na]^+$ calcd. for $C_{38}H_{20}F_6N_2O_4Na$ 705.1219; Found 705.1219.

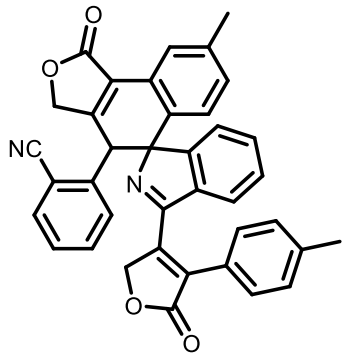

Starting from diazo compound **4f (**39.6 mg, 0.13 mmol)**,** compound **5f** was obtained as a colorless solid (26.7 mg, 74% yield).

MW ($C_{38}H_{26}N_2O_4$): 574.68 g/mol; **Rf:** 0.35 (hexanes/EtOAc 6:4); **IR (ATR) ν (cm^{-1}):** 3032, 2914, 1753, 1446, 1125, 954, 828. **^{1}H NMR ($CDCl_3$, 400 MHz):** δ_H 8.38 (d, 1H, J = 7.8 Hz), 7.58 (dt, 1H, J = 6.3, 3.5 Hz), 7.46 – 7.39 (m, 2H), 7.30 – 7.26 (m, 3H), 7.12 – 7.04 (m, 4H), 7.05 – 6.96 (m, 1H), 6.67 – 6.62 (m, 1H), 6.31 – 6.24 (m, 1H), 6.22 (d, 1H, J = 1.7 Hz), 5.26 (d, 1H, J = 17.9 Hz), 5.09 (d, 1H, J = 17.9 Hz), 4.92 (dd, 1H, J = 18.2, 1.7 Hz), 4.70 (d, 1H, J = 18.2 Hz), 4.41 (s, 1H), 2.33 (s, 3H), 2.17 (s, 3H). **^{13}C{H} NMR ($CDCl_3$, 101 MHz):** δ_C 172.5, 170.9, 165.4, 158.4, 151.5, 148.7, 140.4, 140.2, 138.6, 137.5, 133.1, 133.0, 132.6, 131.9, 130.3, 129.8, 129.5, 129.2, 129.1, 128.9, 128.7, 126.6, 126.4, 125.5, 125.0, 124.9, 124.4, 124.3, 116.6, 115.1, 85.0, 70.9, 69.9, 47.1, 21.8, 21.6. **HRMS (ESI) m/z:** $[M+Na]^+$ calcd. for $C_{38}H_{26}N_2O_4Na$ 597.1785; Found 597.1785.

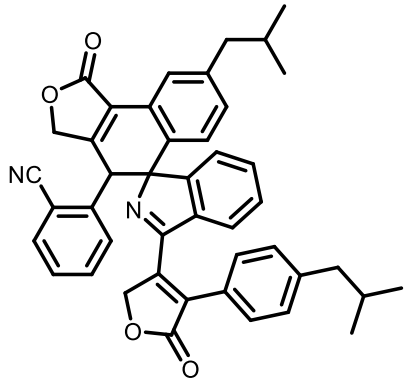

Starting from diazo compound **4g (**87.1 mg, 0.24 mmol)**,** compound **5g** was obtained as a colorless solid (52.5 mg, 65% yield).

MW ($C_{44}H_{38}N_2O_4$): 658.80 g/mol; **Rf:** 0.49 (hexanes/EtOAc 6:4)**; IR (ATR) ν (cm^{-1}):** 3025, 2950, 1743, 1365, 1215, 955, 845. **^{1}H NMR ($CDCl_3$, 400 MHz):** δ_H 8.39 (d, 1H, J = 7.8 Hz), 7.62 – 7.55 (m, 1H), 7.45 – 7.34 (m, 2H), 7.26 – 7.23 (m, 3H, overlapped with chloroform), 7.07 – 7.02 (m, 3H), 7.01 – 6.96 (m, 2H), 6.54 (d, 1H, J = 7.6 Hz), 6.27 (d, 1H, J = 7.6 Hz), 6.19 (d, 1H, *J* = 1.7 Hz), 5.24 (d, 1H, J = 17.9 Hz), 5.11 (d, 1H, J = 17.9 Hz), 4.92 (dd, 1H, J = 18.2, 1.5 Hz), 4.71 (d, 1H, J = 18.2 Hz), 4.44 (s, 1H), 2.45 (d, 2H, J = 7.2 Hz), 2.28 (d, 2H, J = 7.2 Hz), 1.82 (hept, 1H, J = 6.8 Hz), 1.65 (hept, 1H, J = 7.0 Hz), 0.86 (d, 6H, J = 7.0 Hz), 0.75 (t, 6H, J = 6.8 Hz). **^{13}C{H} NMR ($CDCl_3$, 101 MHz):** δ_C 172.6, 170.9, 165.4, 158.5, 151.6, 148.9, 144.2, 144.1, 138.6, 137.4, 133.1, 132.9, 132.4, 132.0, 130.3, 129.7, 129.5, 129.2, 129.1, 128.8, 128.5, 126.9, 126.4, 125.5, 125.2,

124.9, 124.5, 124.3, 116.6, 115.1, 85.0, 70.9, 69.9, 47.1, 45.4, 45.3, 30.3, 30.1, 22.4, 22.3, 22.2. **HRMS (ESI) m/z:** $[M+Na]^+$ calcd. for $C_{44}H_{38}N_2O_4Na$ 681.2724; Found 681.2719.

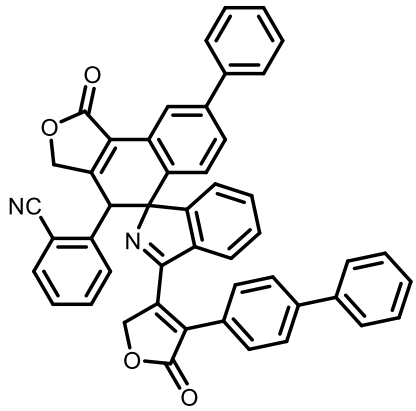

Starting from diazo compound **4h (**107.9 mg, 0.29 mmol), compound **5h** was obtained as a colorless solid (81.4 mg, 82% yield).

MW ($C_{48}H_{30}N_2O_4$): 698.78 g/mol; **Rf:** 0.35 (hexanes/EtOAc 6:4); **IR (ATR) ν (cm^{-1}):** 3014, 2968, 1738, 1366, 1214, 757. **^{1}H NMR ($CDCl_3$, 400 MHz):** δ_H 8.58 (d, 1H, J = 8.0 Hz), 7.72 (dd, 1H, J = 8.0, 1.9 Hz), 7.65 – 7.55 (m, 2H), 7.52 – 7.39 (m, 11H), 7.40 – 7.33 (m, 3H), 7.35 – 7.30 (m, 5H), 7.15 – 7.05 (m, 3H), 6.81 – 6.71 (m, 1H), 6.65 (d, 1H, J = 1.9 Hz), 6.30 – 6.21 (m, 1H), 5.31 (d, 1H, J = 17.9 Hz), 5.14 (d, 1H, J = 17.9 Hz), 4.99 (dd, 1H, J = 18.3, 1.3 Hz), 4.74 (d, 1H, J = 18.3 Hz), 4.40 (s, 1H). **^{13}C{H} NMR ($CDCl_3$, 101 MHz):** δ_C 172.3, 170.8, 165.4, 159.3, 151.3, 149.4, 143.0, 142.6, 140.1, 139.9, 138.5, 137.7, 133.2, 133.0, 131.7, 130.3, 129.4, 129.3, 129.1, 129.0, 128.9, 128.8, 128.3, 128.2, 128.1, 127.9, 127.3, 127.2, 127.1, 126.9, 126.7, 125.5, 125.2, 124.6, 124.5, 124.4, 116.5, 115.0, 85.2, 71.0, 70.0, 46.9. **HRMS (ESI) m/z:** $[M+Na]^+$ calcd. for $C_{48}H_{30}N_2O_4Na$ 721.2098; Found 721.2085.

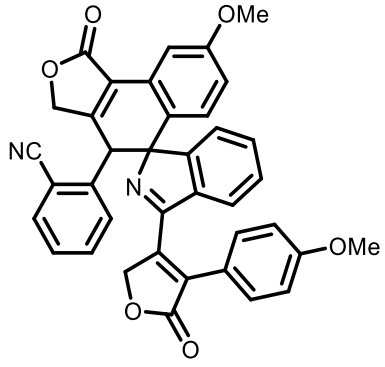

Starting from diazo compound **4i (**39.9 mg, 0.12 mmol)**,** compound **5i** was obtained as a colorless solid (31.3 mg, 86% yield).

MW ($C_{38}H_{26}N_2O_6$): 606.63 g/mol; **Rf:** 0.23 (hexanes/EtOAc 6:4)**; IR (ATR) ν (cm^{-1}):** 2923, 1746, 1603, 1505, 1248, 1024, 831. **^{1}H NMR ($CDCl_3$, 400 MHz):** δ_H 8.44 (d, 1H, J = 8.6 Hz), 7.60 – 7.55 (m, 1H), 7.43 (dd, 2H, J = 5.8, 3.4 Hz), 7.38 – 7.29 (m, 2H), 7.10 – 7.05 (m, 2H), 7.05 – 7.01 (m, 1H), 6.96 (dd, 1H, J = 8.6, 2.6 Hz), 6.85 – 6.77 (m, 2H), 6.70 – 6.66 (m, 1H), 6.29 – 6.19 (m, 1H), 5.99 (d, 1H, J = 2.6 Hz), 5.25 (d, 1H, J = 17.8 Hz), 5.06 (d, 1H, J = 17.8 Hz), 4.93 (dd, 1H, J = 18.1, 1.4 Hz), 4.70 (d, 1H, J = 18.1 Hz), 4.36 (s, 1H), 3.79 (s,

3H), 3.69 (s, 3H). **^{13}C{H} NMR ($CDCl_3$, 101 MHz):** δ_C 172.7, 171.1, 165.5, 161.0, 160.9, 156.8, 151.2, 147.5, 138.7, 137.6, 134.6, 133.1, 133.0, 131.4, 129.3, 129.2, 128.9, 128.8, 126.5, 125.2, 124.5, 124.4, 121.8, 120.6, 116.6, 115.0, 114.3, 113.7, 112.6, 85.0, 70.9, 69.9, 55.5, 55.4, 47.0. **HRMS (ESI) m/z:** $[M+Na]^+$ calcd. for $C_{38}H_{26}N_2O_6Na$ 629.1683; Found 629.1684.

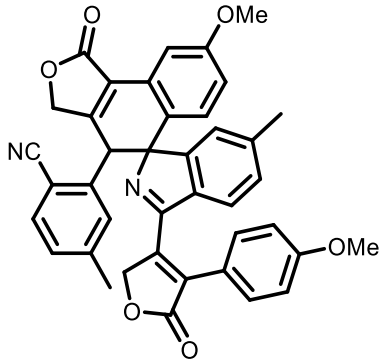

Starting from diazo compound **4j (**74.6 mg, 0.22 mmol)**,** compound **5j** was obtained as a colorless solid (35.5 mg, 52% yield).

MW ($C_{40}H_{30}N_2O_6$): 634.69 g/mol; **Rf:** 0.25 (hexanes/EtOAc 6:4); **IR (ATR) ν (cm^{-1}):** 2920, 1743, 1602, 1230, 1024, 825. **^{1}H NMR ($CDCl_3$, 400 MHz):** δ_H 8.43 (d, 1H, J = 8.5 Hz), 7.44 (d, 1H, J = 8.0 Hz), 7.37 – 7.31 (m, 2H), 7.20 (d, 1H, J = 8.5 Hz), 6.94 (dd, 1H, J = 8.5, 2.6 Hz), 6.87 (d, 1H, J = 7.4 Hz), 6.85 – 6.80 (m, 2H), 6.77 (s, 1H), 6.42 (s, 1H), 6.11 (d, 1H, J = 7.8 Hz), 6.00 (d, 1H, J = 2.6 Hz), 5.22 (d, 1H, J = 17.8 Hz), 5.07 (d, 1H, J = 17.8 Hz), 4.91 (dd, 1H, J = 18.1, 1.4 Hz), 4.68 (d, 1H, J = 18.1 Hz), 4.29 (s, 1H), 3.79 (s, 3H), 3.69 (s, 3H), 2.23 (s, 3H), 2.06 (s, 3H). **^{13}C{H} NMR ($CDCl_3$, 101 MHz):** δ_C 172.7, 171.3, 165.4, 161.0, 160.9, 157.1, 148.4, 148.1, 144.1, 138.9, 138.7, 138.0, 134.9, 132.9, 131.5, 130.1, 130.0, 129.3, 126.4, 125.0, 124.9, 124.1, 122.0, 120.6, 116.9, 114.2, 113.6, 112.5, 112.0, 84.6, 70.9, 70.0, 55.5, 55.4, 46.7, 22.1, 21.2. **HRMS (ESI) m/z:** $[M+Na]^+$ calcd. for $C_{40}H_{30}N_2O_6Na$ 657.1996, found 657.1989.

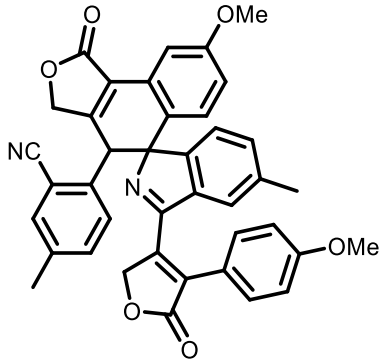

Starting from diazo compound **4k (**72.1 mg, 0.23 mmol)**,** compound **5k** was obtained as a colorless solid (55.6 mg, 84% yield).

MW ($C_{40}H_{30}N_2O_6$): 634.69 g/mol; **Rf:** 0.25 (hexanes/EtOAc 6:4); **IR (ATR) ν (cm^{-1}):** 2920, 1749, 1603, 1249, 1025, 830. **^{1}H NMR ($CDCl_3$, 400 MHz):** δ_H 8.42 (d, 1H, J = 8.5 Hz), 7.38 (s, 1H), , 7.28 – 7.25 (m, 2H, overlapped with chloroform), 7.24 – 7.20 (m, 1H), 6.94 (dd, 1H, J = 8.5, 2.7 Hz), 6.85 (dd, 2H, J = 8.0, 5.3 Hz), 6.81 – 6.76 (m, 2H), 6.50 (d, 1H, J = 8.0 Hz), 6.09 (s, 1H), 6.05 (d, 1H, J = 2.6 Hz), 5.24 (d, 1H, J = 17.8 Hz), 5.08 (d, 1H,

J = 17.8 Hz), 4.88 (dd, 1H, J = 18.1, 1.5 Hz), 4.70 (d, 1H, J = 18.1 Hz), 4.42 (s, 1H), 3.80 (s, 3H), 3.70 (s, 3H), 2.36 (s, 3H), 2.13 (s, 3H). **^{13}C{H} NMR ($CDCl_3$, 101 MHz):** δ_C 172.8, 171.2, 165.5, 160.9, 160.8, 157.1, 151.9, 147.8, 139.8, 139.6, 135.5, 135.1, 135.0, 133.8, 133.1, 131.4, 131.2, 129.7, 128.8, 126.5, 125.2, 125.1, 123.9, 121.9, 120.4, 116.8, 115.0, 114.2, 113.6, 112.4, 84.6, 70.9, 70.0, 55.5, 55.4, 46.8, 21.8, 21.0. **HRMS (ESI) m/z:** $[M+Na]^+$ calcd. for $C_{40}H_{30}N_2O_6Na$ 657.1996; Found 657.1990.

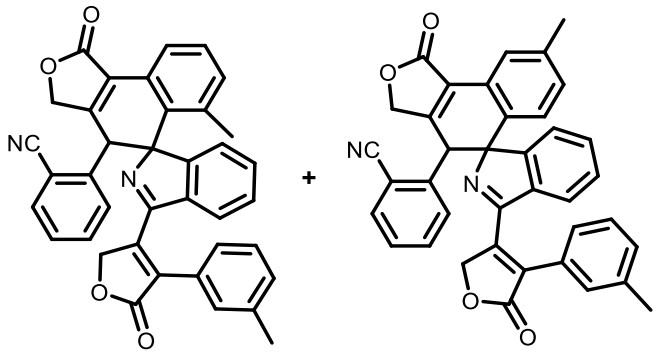

Starting from diazo compound **4l (**49.6 mg, 0.16 mmol), an inseparable mixture of regioisomers **5l** and **5l'** were obtained as a colorless solid (39.4 mg, 86 % yield, r.r = 25:75).

MW ($C_{38}H_{26}N_2O_4$): 574.64 g/mol; **Rf:** 0.38 (hexanes/EtOAc 6:4); **IR (ATR) ν (cm^{-1}):** 3051, 2918, 1749, 1441, 1209, 1038, 765. **^{1}H NMR ($CDCl_3$, 400 MHz):** δ_H 8.33 (d, *J* = 1.9 Hz), 8.20 (d, *J* = 7.7 Hz), 8.05 (d, *J* = 7.8 Hz), 7.75 (dd, *J* = 7.6, 1.4 Hz), 7.63 (q, *J* = 7.4 Hz), 7.60 – 7.47 (m), 7.47 – 7.39 (m), 7.39 – 7.33 (m), 7.29 (d, *J* = 2.2 Hz), 7.23 – 6.82 (m), 6.69 – 6.51 (m), 6.30 (d, *J* = 7.9 Hz), 6.20 – 6.07 (m), 5.23 (d, *J* = 17.9 Hz), 5.12 (d, *J* = 17.9 Hz), 4.95 (dd, *J* = 18.1, 1.5 Hz), 4.68 (dd, *J* = 18.2, 15.1 Hz), 4.63 – 4.54 (m), 4.31 (s), 4.27 (s), 2.42 (s), 2.29 (s), 2.17 (s), 1.91 (s). The regioisomeric ratio was determined by integrating one of the tolyl groups. The remaining signals were incorporated into the peak profile without integration due to the intricate nature of the NMR spectra. **^{13}C{H} NMR ($CDCl_3$, 101 MHz):** δ_C 173.2, 172.4, 170.9, 170.7, 168.1, 165.0, 163.0, 159.7, 151.3, 150.7, 149.6, 141.2, 140.6, 140.0, 139.2, 138.5, 138.4, 137.6, 137.5, 135.5, 134.8, 133.7, 133.4, 133.1, 132.1, 131.7, 131.0, 130.8, 130.6, 130.2, 130.1, 129.9, 129.5, 129.4, 129.3, 129.3, 129.1, 129.1, 128.7, 128.7, 128.2, 128.0, 127.7, 127.4, 126.7, 126.0, 125.8, 125.7, 125.3, 124.9, 124.4, 124.3, 116.6, 116.5, 114.9, 111.9, 84.9, 70.9, 70.1, 69.9, 68.7, 60.5, 60.2, 46.8, 31.1, 29.8, 22.8, 22.2, 21.5, 20.8. **HRMS (ESI) m/z:** $[M+Na]^+$ calcd. for $C_{38}H_{26}N_2O_4Na$ 597.1785; Found 597.1780.

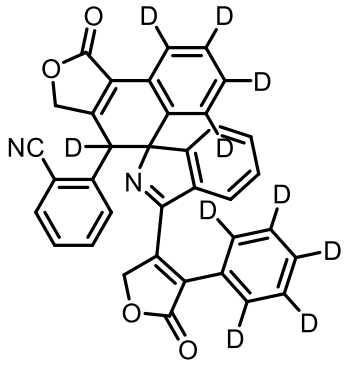

Starting from diazo compound **4a-d_5 (**74.5 mg, 0.24 mmol)**,** compound **5a-d_5** was obtained as a colorless solid (47.1 mg, 70% yield).

MW ($C_{36}H_{12}D_{10}N_2O_4$): 556.64 g/mol; **Rf:** 0.25 (hexanes/EtOAc 6:4); **IR (ATR) ν (cm^{-1}):** 3011, 2947, 1747, 1440, 1362. 1120, 1043, 769. **^{1}H NMR ($CDCl_3$, 400 MHz):** δ_H 7.61 – 7.54 (m, 1H), 7.47 – 7.41 (m, 2H), 7.10 – 7.00 (m, 3H), 6.66 – 6.57 (m, 1H), 6.23 – 6.15 (m, 1H), 5.29 (d, 1H, *J* = 18.0 Hz), 5.08 (d, 1H, *J* = 18.0 Hz), 4.96 (d, 1H, *J* = 18.2 Hz), 4.71 (d, 1H, *J* = 18.2 Hz). **^{13}C{H NMR ($CDCl_3$, 101 MHz):** δ_C 172.4, 170.8, 165.1, 159.5, 151.3, 149.6, 138.4, 137.6, 133.2, 133.1, 132.3, 132.1, 129.8 – 129.7 (m), 129.7 – 129.3 (m), 129.4, 129.2, 129.1, 128.8, 128.7, 127.7, 125.4, 124.5, 124.3, 116.5, 115.0, 85.0, 71.0, 69.9. **HRMS (ESI) m/z:** $[M+Na]^+$ calcd. for $C_{36}H_{12}D_{10}N_2O_4Na$ 579.2099, found 579.2110.

Supplementary material for Chapter 4

Experimental procedure for the synthesis of propargyl alcohol S5a

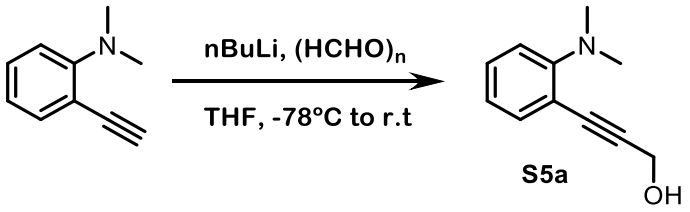

Scheme 8.7. Experimental procedure for the synthesis of propargyl alcohol **S5a**.

To a stirred solution of ***N,N*-dimethyl-2-ethynylaniline**[235] (0.89 g, 6.16 mmol) in THF (30 mL) under a nitrogen atmosphere, a 1.6 M solution of nBuLi in hexane (5.0 mL, 8.0 mmol) was added dropwise. The resulting mixture was stirred at -78ºC for 1h and paraformaldehyde (0.55 g, 18.32 mmol) was then added in one portion. After the addition, the reaction mixture was slowly warmed to room temperature and stirred overnight. Upon completion of the reaction (TLC monitoring), the crude was partitioned into water and diethyl ether. The separated aqueous layer was then extracted with diethyl ether (twice) and the combined organic extracts were dried over anhydrous Na_2SO_4 and concentrated under reduced pressure. The crude product was purified by column chromatography on silica gel (Hexanes:EtOAc = 9:1 to 7:3) to afford **S5a** as a brown oil (0.85 g, 79 % yield).

MW ($C_{11}H_{13}NO$): 175.23 g/mol; **Rf:** 0.20 (Hexanes/EtOAc 7:3); **^{1}H NMR ($CDCl_3$, 400 MHz):** δ_H 7.38 (dd, *J* = 7.5, 1.7 Hz, 1H), 7.26 (ddd, *J* = 8.5, 7.5, 1.7 Hz, 1H), 6.95 (d, *J* = 8.5 Hz, 1H), 6.91 (td, *J* = 7.5, 1.1 Hz, 1H), 4.55 (s, 2H), 3.36 (broad s, 1H), 2.91 (s, 6H).

^{13}C{H} NMR ($CDCl_3$, 101 MHz):δ_C 154.9, 134.3, 129.4, 121.3, 117.3, 115.5, 93.0, 84.5, 51.6, 43.8. **IR (ATR) ν (cm^{-1}):** 3301, 2919, 1488, 1018, 742; **HRMS (ESI) m/z:** calcd. for $C_{11}H_{13}NONa$ $[M+Na]^+$ 198.0889; Found 198.0893.

General procedure for the synthesis of propargyl alcohols S6a-S6d

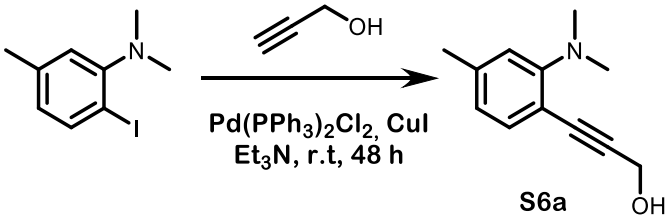

Scheme 8.8. General procedure for the synthesis of propargyl alcohols **S6a-6ad**.

Toa 100 mL round-bottom flask containing a mixture of ***N,N*-Dimethyl-2-iodo-5-methylaniline** [236] (1.51 g, 5.78 mmol), CuI (0.04 g, 0.23 mmol), and $Pd(PPh_3)_2Cl_2$ (0.10 g, 0.14 mmol) in triethylamine (40 mL), propargyl alcohol (0.40 mL, 6.87 mmol) was added dropwise under a nitrogen atmosphere. After the addition, the solution was stirred at room temperature for 48h. Upon completion of the reaction (TLC monitoring), the crude

was filtered through a Celite pad, rinsed with EtOAc and concentrated under reduced pressure. The crude product was then purified by column chromatography on silica gel (CH_2Cl_2/AcOEt = 98:2) to afford **S6a** as a brown oil (0.52 g, 47 % yield).

MW ($C_{12}H_{15}NO$): 189.26 g/mol; **Rf:** 0.38 (CH_2Cl_2/EtOAc 8:2); **^{1}H NMR ($CDCl_3$, 400 MHz):** δ_H 7.26 (d, *J* = 7.7 Hz, 1H,), 6.73 (s, 1H), 6.70 (d, *J* = 7.7 Hz, 1H), 4.52 (s, 2H), 2.89 (s, 6H), 2.72 (broad s, 1H), 2.32 (s, 3H). **^{13}C{H} NMR ($CDCl_3$, 101 MHz):** δ_C 154.9, 139.7, 134.2, 122.1, 118.1, 112.4, 92.2, 84.8, 51.9, 43.8, 21.9. **IR (ATR) ν (cm^{-1}):** 3297, 2915, 1599, 1498, 1019, 807. **HRMS (ESI) m/z:** calcd. for $C_{12}H_{15}NONa$ $[M+Na]^+$ 212.1046; Found 212.1052.

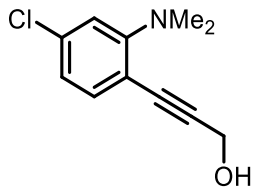

Propargyl alcohol **S6b** was obtained from ***N,N*-Dimethyl-2-iodo-5-chloroaniline**[237] (1.18 g, 4.19 mmol) as a brown oil (0.29 g, 33 %) following the same procedure as for **S6a**.

MW ($C_{11}H_{12}ClNO$): 209.67 g/mol; **Rf:** 0.28 (CH_2Cl_2/EtOAc 8:2); **^{1}H NMR ($CDCl_3$, 400 MHz):** δ_H 7.28 (dd, *J* = 8.2, 1.4 Hz, 1H), 6.86 (d, *J* = 2.0 Hz, 1H), 6.83 (dd, *J* = 8.2, 2.0 Hz, 1H), 4.53 (d, *J* = 5.7 Hz, 2H), 2.92 (s, 6H), 2.04 (broad s, 1H). **^{13}C{H} NMR ($CDCl_3$, 101 MHz):** δ_C 155.9, 135.4, 135.3, 120.8, 117.6, 113.0, 93.4, 84.1, 52.0, 43.5. **IR (ATR) ν (cm^{-1}):** 3290, 2839, 1581, 1452, 1019, 818. **HRMS (ESI) m/z:** calcd. for $C_{11}H_{13}ClNO$ $[M+H]^+$ 210.0680; Found 210.0689.

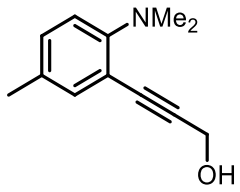

Propargyl alcohol **S6c** was obtained from ***N,N*-Dimethyl-2-iodo-4-methylaniline**[238] (2.53 g, 9.69 mmol) as a brown oil (0.85 g, 46%) following the same procedure as for **S6a**.

MW ($C_{12}H_{15}NO$): 189.26 g/mol; **Rf:** 0.25 (CH_2Cl_2/EtOAc 8:2); **^{1}H NMR ($CDCl_3$, 400 MHz):** δ_H 7.21 (d, *J* = 2.2 Hz, 1H), 7.06 (dd, *J* = 8.3, 2.2 Hz, 1H), 6.84 (d, *J* = 8.3 Hz, 1H), 4.53 (s, 2H), 2.87 (s, 6H), 2.24 (s, 3H). **^{13}C{H} NMR ($CDCl_3$, 101 MHz):** δ_C 152.8, 134.8, 130.7, 130.3, 117.3, 115.4, 92.5, 84.8, 51.9, 44.1, 20.4. **IR (ATR) ν (cm^{-1}):** 3309, 2919, 1737, 1497, 1029, 814. **HRMS (ESI) m/z:** calcd. for $C_{12}H_{15}NONa$ $[M+Na]^+$ 212.1046; Found 212.1049.

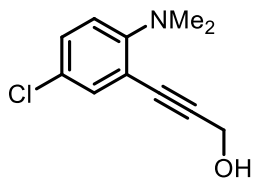

Propargyl alcohol **S6d** was obtained from ***N,N*-Dimethyl-2-iodo-4-chloroaniline**[238] (2.53 g, 8.99 mmol) as a brown oil (1.09 g, 58%) following the same procedure as for **S6a**.

MW ($C_{11}H_{12}ClNO$): 209.67 g/mol; **Rf:** 0.28 (CH_2Cl_2/EtOAc 8:2); **^{1}H NMR ($CDCl_3$, 400 MHz):** δ_H 7.34 (d, *J* = 2.6 Hz, 1H), 7.18 (dd, *J* = 8.8, 2.6 Hz, 1H), 6.83 (d, *J* = 8.8 Hz, 1H), 4.54 (s, 2H), 2.89 (s, 6H). **^{13}C{H} NMR ($CDCl_3$, 101 Mz):** δ_C 153.7, 133.873, 129.5, 125.6, 118.5, 116.4, 93.7, 83.7, 51.9, 43.7. **IR (ATR) ν (cm^{-1}):** 3294, 2917, 1487, 1022, 812. **HRMS (ESI) m/z:** calcd. for $C_{11}H_{12}ClNONa$ $[M+Na]^+$ 232.0500; Found 232.0507.

General procedure for the synthesis of propargyl esters S7a-S7j

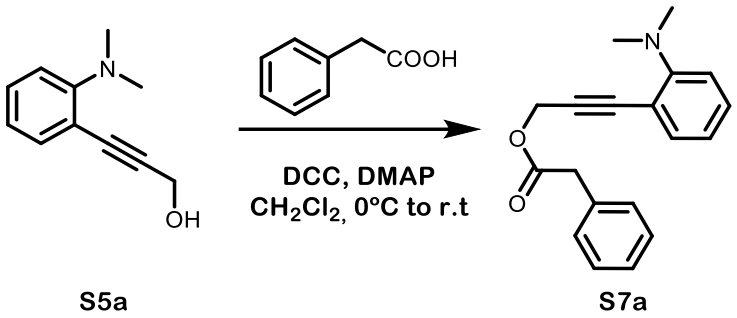

S5a **S7a**

Scheme 8.9. General procedure for the synthesis of propargyl esters **S7a-S7j**.

To a 25 mL round-bottom flask containing a mixture of **S5a** (0.22 g, 1.26 mmol), phenylacetic acid (0.17 g, 1.25 mmol), and 4-dimethylaminopyridine (DMAP) (13.9 mg, 0.11 mmol) in dichloromethane (6mL), N,N'-dicyclohexylcarbodiimide (DCC) (0.28 g, 1.36 mmol) was added in batches at 0 ºC. After the addition, the reaction mixture was slowly warmed to room temperature and stirred overnight. Upon completion of the reaction (TLC monitoring), the crude was filtrated through a Celite pad, rinsed with EtOAc and concentrated under reduced pressure. The crude product was then purified by column chromatography on silica gel (Hexanes/EtOAc = 95:05) to afford ester **S7a** as a yellow oil (0.31 g, 86 % yield).

MW ($C_{19}H_{19}NO_2$): 293.37 g/mol; **Rf:** 0.50 (Hexanes/EtOAc 8:2); **^{1}H NMR ($CDCl_3$, 400 MHz):** δ_H 7.40 (dd, J = 7.6, 1.4 Hz, 1H), 7.37 – 7.26 (m, 5H), 7.26 – 7.23 (m, 1H), 6.90 (d, *J* = 8.3 Hz, 1H), 6.86 (td, *J* = 7.6, 1.1 Hz, 1H), 5.00 (s, 2H), 3.70 (s, 2H), 2.90 (s, 6H) **^{13}C{H} NMR ($CDCl_3$, 101 MHz:** δ_C 171.0, 155.3, 134.8, 133.7, 129.8, 129.4, 128.7, 127.3, 120.6, 117.0, 114.2, 88.1, 86.1, 53.7, 43.6, 41.3. **IR (ATR) ν (cm^{-1}):** 2918, 1736, 1491, 1135, 754. **HRMS (ESI) m/z:** calcd. for $C_{19}H_{19}NO_2Na$ $[M+Na]^+$ 316.1308; Found 316.1312.

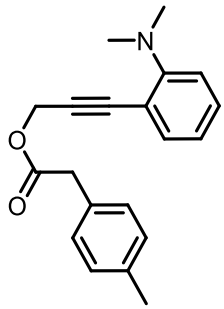

Ester **S7b** was obtained from **S5a** (0.35 g, 1.98 mmol) as yellow oil (0.25 g, 41%) following the same procedure as for **S7a**.

MW ($C_{20}H_{21}NO_2$): 307.39 g/mol; **Rf:** 0.53 (Hexanes/EtOAc 8:2); **^{1}H NMR ($CDCl_3$, 400 MHz):** δ_H 7.38 (dd, *J* = 7.8, 1.7 Hz, 1H), 7.26 – 7.22 (m, 1H (overlapped with chloroform)), 7.19 (d, *J* = 8.2 Hz, 2H), 7.13 (d, *J* = 7.8 Hz, 2H), 6.89 (dd, *J* = 8.2, 1.1 Hz, 1H), 6.85 (dt, *J* = 7.4, 1.1 Hz, 1H), 4.98 (s, 2H), 3.65 (s, 2H), 2.89 (s, 6H), 2.33 (s, 3H). **^{13}C{H} NMR ($CDCl_3$, 101 MHz):** δ_C 171.2, 155.3, 136.9, 134.8, 130.7, 129.8, 129.4, 129.3, 120.5, 117.0, 114.2, 88.2, 86.0, 53.7, 43.6, 40.8, 21.2. **IR (ATR) ν (cm^{-1}):** 2938, 1736, 1490, 1133, 755. **HRMS (ESI) m/z:** calcd. for $C_{20}H_{21}NO_2Na$ $[M+Na]^+$ 330.1465; Found 330.1462.

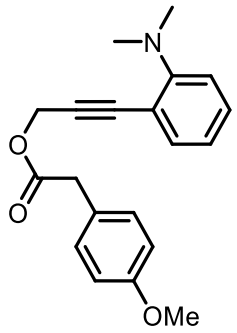

Ester **S7c** was obtained from **S5a** (0.19 g, 1.09 mmol) as a yellow oil (0.32 g, 92%) following the same procedure as for **S7a**.

MW ($C_{20}H_{21}NO_3$): 323.39 g/mol; **Rf:** 0.33 (Hexanes/EtOAc 8:2); **^{1}H NMR ($CDCl_3$, 400 MHz):** δ_H 7.38 (dd, *J* = 7.6, 1.7 Hz, 1H), 7.26 – 7.19 (m, 3H), 6.88 (d, *J* = 8.2 Hz, 1H), 6.87 – 6.81 (m, 3H), 4.97 (s, 2H), 3.77 (s, 3H), 3.62 (s, 2H), 2.88 (s, 6H). **^{13}C{H} NMR ($CDCl_3$, 101 MHz):** δ_C 171.3, 158.8, 155.2, 134.7, 130.4, 129.8, 125.8, 120.5, 117.0, 114.1, 88.2, 86.0, 55.3, 53.6, 43.6, 40.3. **IR (ATR) ν (cm^{-1}):** 2936, 1735, 1510, 1243, 1133, 755. **HRMS (ESI) m/z:** calcd. for $C_{20}H_{21}NO_3Na$ $[M+Na]^+$ 346.1414; Found 346.1405.

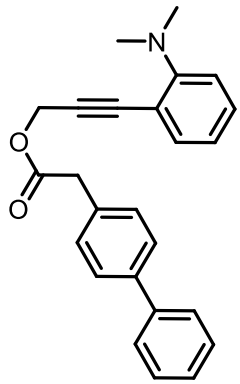

Ester **S7d** was obtained from **S5a** (0.26 g, 1.46 mmol) as a yellow oil (0.28 g, 52%) following the same procedure as for **S7a**.

MW ($C_{25}H_{23}NO_2$): 369.46 g/mol; **Rf:** 0.43 (Hexanes/EtOAc 8:2); **^{1}H NMR ($CDCl_3$, 400 MHz):** δ_H 7.59 – 7.54 (m, 4H), 7.47 – 7.41 (m, 2H), 7.41 – 7.37 (m, 3H), 7.37 – 7.32 (m, 1H), 7.26 – 7.22 (m, 1H), 6.89 (dd, *J* = 8.3, 1.1 Hz, 1H), 6.85 (dt, *J* = 7.4, 1.1 Hz, 1H), 5.01 (s, 2H), 3.74 (s, 2H), 2.89 (s, 6H). **^{13}C{H} NMR ($CDCl_3$, 101 MHz):** δ_C 171.0, 155.3, 140.9, 140.3, 134.8, 132.8, 129.8, 128.9, 127.5, 127.4, 127.2, 120.6, 117.1, 114,1, 88.1, 86.1, 53.8, 43.6, 40.9); **IR (ATR) ν (cm^{-1}):** 2937, 1735, 1487, 1135, 752. **HRMS (ESI) m/z:** calcd. for $C_{25}H_{24}NO_2$ $[M+H]^+$ 370.1802; Found 370.1813

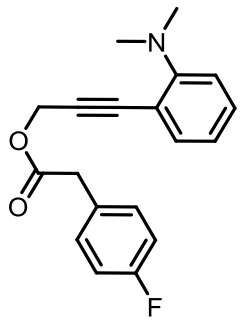

Ester **S7e** was obtained from **S5a** (0.19 g, 1.09 mmol) as a brown oil (0.30 g, 89%) following the same procedure as for **S7a**.

MW ($C_{19}H_{18}FNO_2$): 311.36 g/mol; **Rf:** 0.3 (Hexanes/EtOAc 8:2); **^{1}H NMR ($CDCl_3$, 400 MHz):** δ_H 7.38 (dd, *J* = 7.6, 1.7 Hz, 1H), 7.30 – 7.22 (m, 3H (overlapped with chloroform)), 7.05 – 6.97 (m, 2H), 6.90 (dd, *J* = 8.3, 1.1 Hz, 1H), 6.86 (td, *J* = 7.4, 1.1 Hz, 1H), 4.99 (s, 2H), 3.66 (s, 2H), 2.89 (s, 6H). **^{13}C{H} NMR ($CDCl_3$, 101 MHz):** δ_C 170.9, 162.2 (d, $^1J_{C-F}$ = 246.4 Hz), 155.3, 134.8, 131.0 (d, $^3J_{C-F}$ = 8.1 Hz), 129.9, 129.4 (d, $^4J_{C-F}$ = 3.3 Hz), 120.6, 117.1, 115.6 (d, $^2J_{C-F}$ = 21.5 Hz), 114.1, 88.0, 86.2, 53.8, 43.6, 40.3. **^{19}F NMR ($CDCl_3$, 376 MHz):** δ_F -116.51 (s, 1F). **IR (ATR) ν (cm^{-1}):** 2926, 1736, 1134, 1219, 753. **HRMS (ESI) m/z:** calcd. for $C_{19}H_{18}FNO_2Na$ $[M+Na]^+$ 334.1214; Found 334.1222.

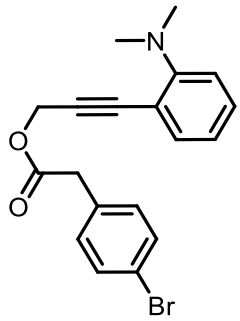

Ester **S7f** was obtained from **S5a** (0.19 g, 1.09 mmol) as a yellow oil (0.36 g, 88%) following the same procedure as for **S7a**.

MW ($C_{19}H_{18}BrNO_2$): 372.26 g/mol; **Rf:** 0.33 (Hexanes/EtOAc 8:2); **^{1}H NMR ($CDCl_3$, 400 MHz):** δ_H 7.49 – 7.42 (m, 2H), 7.39 (dd, *J* = 7.6, 1.7 Hz, 1H), 7.30 – 7.22 (m, 1H (overlapped with chloroform)), 7.22 – 7.16 (m, 2H), 6.90 (dd, *J* = 8.3, 1.1 Hz, 1H), 6.86 (td, *J* = 7.4, 1.1 Hz, 1H), 4.99 (s, 2H), 3.64 (s, 2H), 2.89 (s, 6H). **^{13}C{H} NMR ($CDCl_3$, 101 MHz):** δ_H 170.4, 155.2, 134.7, 132.7, 131.8, 131.1, 129.9, 121.4, 120.5, 117.0, 114.0, 87.9, 86.2, 53.8, 43.6, 40.6. **IR (ATR) ν (cm^{-1}):** 2936, 1736, 1487, 1137, 753. **HRMS (ESI) m/z:** calcd. for $C_{19}H_{19}BrNO_2$ $[M+H]^+$ 372.0594-374.0574; Found 372.0597-374.0577.

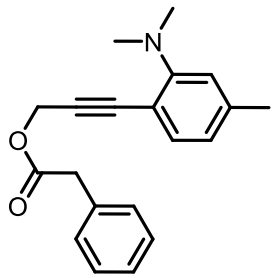

Ester **S7g** was obtained from **S6a** (0.21 g, 1.11 mmol) as a yellow oil (0.32 g, 94%) following the same procedure as for **S7a**.

MW ($C_{20}H_{21}NO_2$): 307.39 g/mol; **Rf:** 0.38 (Hexanes/EtOAc 8:2); **^{1}H NMR ($CDCl_3$, 400 MHz):** δ_H 7.36 – 7.25 (m, 6H), 6.70 (s, 1H), 6.69 – 6.66 (m, 1H), 4.98 (s, 2H), 3.69 (s, 2H), 2.88 (s, 6H), 2.32 (s, 3H). **^{13}C{H} NMR ($CDCl_3$, 101 MHz):** δ_C 171.0, 153.1, 135.1, 133.8, 130.6, 130.2, 129.4, 128.7, 127.3, 117.2, 114.5, 87.8, 86.1, 53.8, 43.9, 41.3, 20.3. **IR (ATR) ν (cm^{-1}):** 2969, 1757, 1341, 770. **HRMS (ESI) m/z:** calcd. for $C_{20}H_{21}NO_2Na$ $[M+Na]^+$ 330.1465; Found 330.1467.

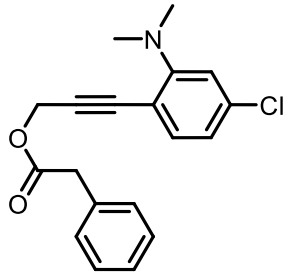

Ester **S7h** was obtained from **S6b** (0.30 g, 1.44 mmol) as a yellow oil (0.36 g, 76%) following the same procedure as for **S7a**.

MW ($C_{19}H_{18}ClNO_2$): 327.81 g/mol; **Rf:** 0.60 (Hexanes/EtOAc 8:2); **^{1}H NMR ($CDCl_3$, 400 MHz):** δ_H 7.36 – 7.26 (m, 6H), 6.83 (d, *J* = 2.0 Hz, 1H), 6.80 (dd, *J* = 8.1, 2.0 Hz, 1H), 4.96 (s, 2H), 3.69 (s, 2H), 2.89 (s, 6H). **^{13}C{H} NMR ($CDCl_3$, 101 MHz):** δ_C 171.0, 156.0, 135.7, 135.6, 133.7, 129.4, 128.8, 127.4, 120.3, 117.3, 112.0, 88.9, 85.3, 53.6, 43.3, 41.3. **IR (ATR) ν (cm^{-1}):** 2941, 1736, 1491, 1134. **HRMS (ESI) m/z:** calcd. for $C_{19}H_{18}ClNO_2Na$ $[M+Na]^+$ 350.0918; Found 350.0920.

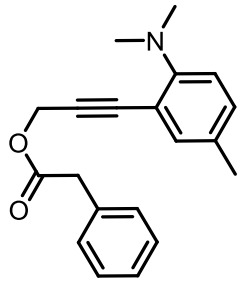

Ester **S7i** was obtained from **S6c** (0.31 g, 1.62 mmol) as a brown oil (0.32 g, 64%) following the same procedure as for **S7a**.

MW ($C_{20}H_{21}NO_2$): 307.39 g/mol; **Rf:** 0.42 (Hexanes/EtOAc 8:2); **^{1}H NMR ($CDCl_3$, 400 MHz):** δ_H 7.37 – 7.26 (m, 5H), 7.22 (d, *J* = 2.2 Hz, 1H), 7.06 (dd, *J* = 8.3, 2.2 Hz, 1H), 6.81 (d, *J* = 8.3 Hz, 1H), 4.98 (s, 2H), 3.69 (s, 2H), 2.84 (s, 6H), 2.24 (s, 3H). **^{13}C{H} NMR ($CDCl_3$, 101 MHz):** δ_C 171.0, 153.1, 135.1, 133.8, 130.6, 130.2, 129.4, 128.7, 127.3, 117.2, 114.4, 87.8, 86.1, 53.8, 43.9, 41.3, 20.3. **IR (ATR) ν (cm^{-1}):** 2917, 1736, 1499, 1125. **HRMS (ESI) m/z:** calcd. for $C_{20}H_{21}NO_2Na$ $[M+Na]^+$ 330.1465; Found 330.1466.

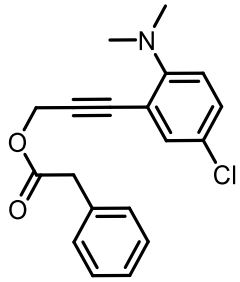

Ester **S7j** was obtained from **S6d** (0.30 g, 1.44 mmol) as a brown oil (0.27 g, 58%) following the same procedure as for **S7a**.

MW ($C_{19}H_{18}ClNO_2$): 327.81 g/mol; **Rf:** 0.40 (Hexanes/EtOAc 8:2); **^{1}H NMR ($CDCl_3$, 400 MHz):** δ_H 7.36 – 7.26 (m, 6H), 7.18 (dd, *J* = 8.8, 2.6 Hz, 1H), 6.80 (d, *J* = 8.8 Hz, 1H), 4.97 (s, 2H), 3.69 (s, 2H), 2.86 (s, 6H). **^{13}C{H} NMR ($CDCl_3$, 101 MHz):** δ_C 170.9, 153.8, 134.0, 133.7, 129.7, 129.4, 128.8, 127.4, 125.2, 118.2, 115.4, 89.2, 84.8, 53.5, 43.6, 41.3. **IR (ATR) ν (cm^{-1}):** 2940, 1736, 1490, 1127. **HRMS (ESI) m/z:** calcd. for $C_{19}H_{18}ClNO_2Na$ $[M+Na]^+$ 350.0918; Found 350.0930.

General procedure for the synthesis of diazo compounds 10a-10j

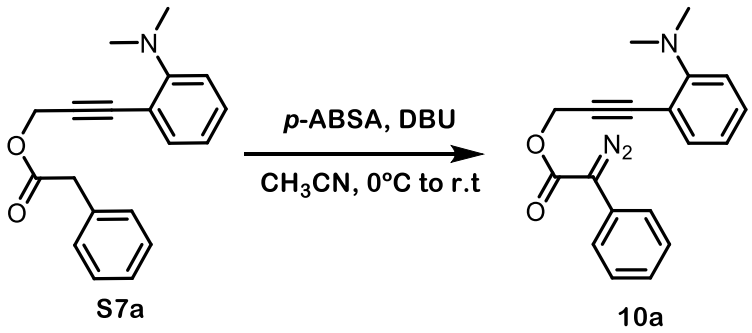

Scheme 8.10. General procedure for the synthesis of diazo compounds **10a-10j**.

To a 25 mL oven-dried flask containing a mixture of **S7a** (0.21 g, 0.72 mmol) and *p*-acetamidobenzenesulfonyl azide (*p*-ABSA) (0.21 g, 0.87 mmol) in anhydrous CH_3CN (4.5 mL), a solution of 1,8-diazabicyclo[5.4.0]undec-7-ene (DBU) (0.15 mL, 1.00 mmol) in anhydrous CH_3CN (0.9 mL) was added dropwise at 0 ºC. After the addition, the reaction mixture was slowly warmed to room temperature and stirred overnight. Upon completion of the reaction (TLC monitoring), the crude was diluted with Et_2O, and washed with saturated aqueous NH_4Cl, saturated aqueous $NaHCO_3$ and brine. The combined organic extracts were dried over anhydrous Na_2SO_4 and concentrated under reduced pressure. The crude product was purified by column chromatography on silica gel (Hexanes: EtOAc: Et_3N= 96:3:1) to afford diazo compound **10a** as an orange oil (0.20 g, 94% yield).

MW ($C_{19}H_{17}N_3O_2$): 319.36 g/mol; **Rf:** 0.63 (Hexanes/EtOAc 8:2); **^{1}H NMR ($CDCl_3$, 400 MHz):** δ_H 7.53 – 7.48 (m, 2H), 7.44 – 7.36 (m, 3H), 7.29 – 7.23 (m, 1H (overlapped with chloroform)), 7.23 – 7.17 (m, 1H), 6.91 (dd, *J* = 8.4, 1.1 Hz, 1H), 6.87 (td, *J* = 7.4, 1.1 Hz, 1H), 5.17 (s, 2H), 2.93 (s, 6H). **^{13}C{H} NMR ($CDCl_3$, 101 MHz):** δ_C 164.6, 155.3, 134.8, 129.9, 129.1, 126.1, 125.4, 124.2, 120.6, 117.1, 114.1 88.2, 86.3, 53.7, 43.7. **IR (ATR) ν (cm^{-1}):** 2925, 2082, 1699, 1238, 1140, 751. **HRMS (ESI) m/z:** calcd. for $C_{19}H_{17}N_3O_2Na$ $[M+Na]^+$ 342.1213; Found 342.1213.

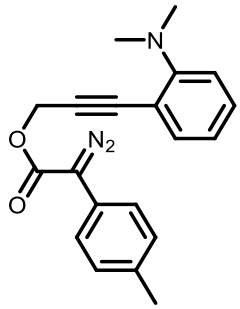

Diazo compound **10b** was obtained from **S7b** (0.18 g, 0.59 mmol) as an orange oil (0.17 g, 86%) following the same procedure as for **10a**.

MW ($C_{20}H_{19}N_3O_2$): 333.39 g/mol; **Rf:** 0.64 (Hexanes/EtOAc 8:2); **^{1}H NMR ($CDCl_3$, 400 MHz):** δ_H 7.42 (dd, *J* = 7.6, 1.7 Hz, 1H), 7.38 (d, *J* = 8.2 Hz, 2H), 7.28 – 7.23 (m, 1H (overlapped with chloroform)), 7.21 (d, *J* = 8.2 Hz, 2H), 6.90 (dd, *J* = 8.3, 1.1 Hz, 1H), 6.86 (td, *J* = 7.5, 1.1 Hz, 1H), 5.16 (s, 2H), 2.93 (s, 6H), 2.35 (s, 3H). **^{13}C{H} NMR ($CDCl_3$, 101 MHz):** δ_C 164.9, 155.3, 136.0 134.8, 129.9, 129.8, 124.3, 122.0, 120.6, 117.1, 114.2, 88.3, 86.3, 53.7, 43.7, 21.2. **IR (ATR) ν (cm^{-1}):** 2919, 2082, 1703, 1241, 1139, 756. **HRMS (ESI) m/z:** calcd. for $C_{20}H_{19}N_3O_2Na$ $[M+Na]^+$ 356.1369; Found 356.1367.

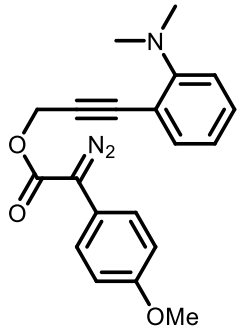

Diazo compound **10c** was obtained from **S7c** (0.18 g, 0.56 mmol) as an orange oil (0.17 g, 88%) following the same procedure as for **10a**.

MW ($C_{20}H_{19}N_3O_3$): 349.39 g/mol; **Rf:** 0.45 (Hexanes/EtOAc 8:2; **^{1}H NMR ($CDCl_3$, 400 MHz):** δ_H 7.43 – 7.38 (m, 3H), 7.28 – 7.23 (m, 1H (overlapped with chloroform)), 6.97 – 6.93 (m, 2H), 6.90 (d, *J* = 7.4 Hz, 1H), 6.86 (td, *J* = 7.4, 1.1 Hz, 1H), 5.15 (s, 2H), 3.81 (s, 3H), 2.93 (s, 6H). **^{13}C{H} NMR ($CDCl_3$, 101 MHz):** δ_C 165.0, 158.2, 155.2, 134.7, 129.8, 126.1, 120.5, 117.0, 116.7, 114.7, 114.0, 88.2, 86.1, 55.4, 53.5, 43.6. **IR (ATR) ν (cm^{-1}):** 2920, 2079, 1696, 1239, 1141, 754. **HRMS (ESI) m/z:** calcd. for $C_{20}H_{20}NO_3$ $[M+H-N_2]^+$ 322.1438; Found 322.1449.

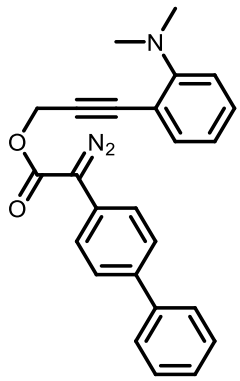

Diazo compound **10d** was obtained from **S7d** (0.15 g, 0.41 mol) as an orange solid (0.15 g, 93%) following the same procedure as for **10a**.

MW ($C_{25}H_{21}N_3O_2$): 395.46 g/mol; **Rf:** 0.53 (Hexanes/EtOAc 8:2); **^{1}H NMR ($CDCl_3$, 400 MHz):** δ_H 7.67 – 7.55 (m, 6H), 7.48 – 7.41 (m, 3H), 7.38 – 7.32 (m, 1H), 7.29 – 7.23 (m,12H, (overlapped with chloroform)), 6.91 (dd, *J* = 8.3, 1.1 Hz, 1H), 6.87 (td, *J* = 7.5, 1.1 Hz, 1H), 5.19 (s, 2H), 2.94 (s, 6H). **^{13}C{H} NMR ($CDCl_3$, 101 MHz):** δ_C 164.6, 155.3, 140.4, 138.9, 134.8, 129.9, 129.0, 127.8, 127.5, 127.0, 124.5, 124.3, 120.6, 117.1, 88.2, 86.4, 53.8, 43.7. **IR (ATR) ν (cm^{-1}):** 2935, 2086, 1704, 1234, 1141, 752. **HRMS (ESI)m/z:** calcd. for $C_{25}H_{21}N_3O_2Na$ $[M+Na]^+$ 418.1526; Found 418.1536.

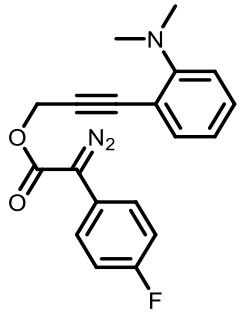

Diazo compound **10e** was obtained from **S7e** (0.19 g, 0.61 mmol) as an orange solid (0.19 g, 92%) following the same procedure as for **10a**.

MW ($C_{19}H_{16}FN_3O_2$): 337.35 g/mol; **Rf:** 0.55 (Hexanes/EtOAc 8:2); **^{1}H NMR ($CDCl_3$, 400 MHz):** δ_H 7.49 – 7.43 (m, 2H), 7.41 (dd, *J* = 7.6, 1.7 Hz, 1H), 7.29 – 7.22 (m, 1H (overlapped with chloroform)), 7.14 – 7.06 (m, 2H), 6.91 (dd, *J* = 8.4, 1.1 Hz, 1H), 6.87 (td, *J* = 7.6, 1.1 Hz, 1H), 5.16 (s, 2H), 2.93 (s, 6H). **^{13}C{H} NMR ($CDCl_3$, 101 MHz):** δ_C 164.6, 161.2 (d, $^1J_{C\text{-}F}$ = 247.4 Hz), 155.3, 134.8, 129.9, 126.1 (d, $^3J_{C\text{-}F}$ = 7.9 Hz), 121.1 (d, $^4J_{C\text{-}F}$ = 3.2 Hz), 120.6, 117.1, 116.1 (d, $^2J_{C\text{-}F}$ = 22.2 Hz), 114.1, 88.1, 86.4, 53.8, 43.7. **^{19}F NMR (376 MHz, $CDCl_3$):** δ_F -116.96. (s, 1F). **IR (ATR) ν (cm^{-1}):** 2938, 2083, 1742, 1230, 1145, 752. **HRMS (ESI) m/z:** calcd. for $C_{19}H_{16}FN_3O_2Na$ $[M+Na]^+$ 360.1119; Found 360.1119.

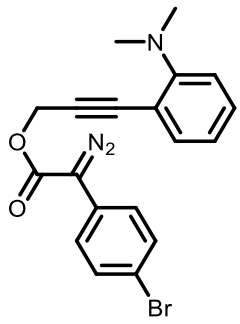

Diazo compound **10f** was obtained from **S7f** (0.21 g, 0.56 mmol) as an orange solid (0.22 g, 99%) following the same procedure as for **10a.**

MW ($C_{19}H_{16}BrN_3O_2$): 398.26 g/mol; **Rf:** 0.60 (Hexanes/EtOAc 8:2 **^{1}H NMR ($CDCl_3$, 400 MHz):** δ_H 7.53 – 7.48 (m, 2H), 7.41 (dd, *J* = 7.5, 1.7 Hz, 1H), 7.40 – 7.35 (m,1H) 7.29 – 7.23 (m, 1H, overlapped with chloroform), 6.91 (dd, *J* = 8.3, 1.1 Hz, 1H), 6.86 (td, *J* = 7.5, 1.1 Hz, 1H), 5.16 (s, 2H), 2.93 (s, 6H). **^{13}C{H} NMR ($CDCl_3$, 101 MHz):** δ_C 164.2, 155.3, 134.8, 132.2, 130.0, 125.5, 124.6, 120.6, 119.7, 117.1, 114.0, 88.0, 86.5, 53.9, 43.7. **IR (ATR) ν (cm^{-1}):** 2941, 2086, 1703, 1237, 1147, 754. **HRMS (ESI) m/z:** calcd. for $C_{19}H_{16}BrN_3O_2Na$ $[M+Na]^+$ 420.0318-422.0298; Found 420.0321-422.0303.

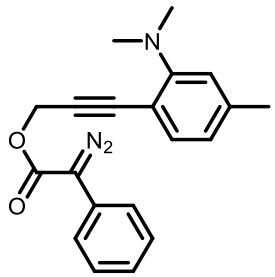

Diazo compound **10g** was obtained from **S7g** (0.16 g, 0.52 mmol) as an orange solid (0.15 g, 87%) following the same procedure as for **10a**.

MW ($C_{20}H_{19}N_3O_2$): 333.39 g/mol; **Rf:** 0.63 (Hexanes/EtOAc 8:2); **^{1}H NMR ($CDCl_3$, 400 MHz):** δ_H 7.52 – 7.47 (m, 2H), 7.42 – 7.36 (m, 2H), 7.31 (d, *J* = 7.6 Hz, 1H), 7.20 (td, *J* = 7.2, 1.2 Hz, 1H), 6.71 (s, 1H), 6.69 (d, *J* = 7.6 Hz, 1H), 5.16 (s, 2H), 2.92 (s, 6H), 2.32 (s, 3H). **^{13}C{H} NMR ($CDCl_3$, 101 MHz):** δ_C 164.6, 155.2, 140.2, 134.6, 129.1 126.1, 125.4, 124.2, 121.6, 117.9, 111.2, 87.5, 86.5, 53.8, 43.7, 22.0. **IR (ATR) ν (cm^{-1}):** 2940, 2087, 1699, 1241, 1142, 753. **HRMS (ESI) m/z:** calcd. for $C_{20}H_{19}N_3O_2Na$ $[M+Na]^+$ 356.1369; Found 356.1372.

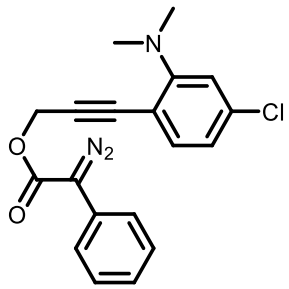

Diazo compound **10h** was obtained from **S7h** (0.18 g, 0.55 mmol) as an orange solid (0.16 g, 82%) following the same procedure as for **10a**.

MW ($C_{19}H_{16}ClN_3O_2$): 353.81 g/mol; **Rf:** 0.65 (Hexanes/EtOAc 8:2); **^{1}H NMR ($CDCl_3$, 400 MHz):** δ_H 7.52 – 7.47 (m, 2H), 7.43 – 7.36 (m, 2H), 7.31 (d, *J* = 8.1 Hz, 1H), 7.23 – 7.16 (m, 1H), 6.84 (d, *J* = 2.0 Hz, 1H), 6.82 (dd, *J* = 8.1, 2.0 Hz, 1H), 5.14 (s, 2H), 2.94 (s, 6H). **^{13}C{H} NMR ($CDCl_3$, 101 MHz):** δ_C 164.5, 156.1, 135.7, 129.1, 126.2, 125.3, 124.2, 120.4, 117.4, 111.9, 88.9, 85.5, 53.6, 43.4. **IR (ATR) ν (cm^{-1}):** 2946, 2082, 1737, 1231, 1138, 756. **HRMS (ESI) m/z:** calcd. for $C_{19}H_{16}ClN_3O_2Na$ $[M+Na]^+$ 376.0823; Found 376.0826.

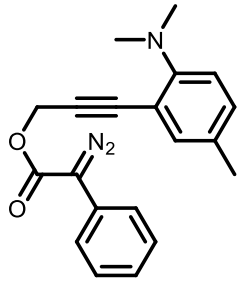

Diazo compound **10i** was obtained from **S7i** (0.21 g, 0.68 mmol) as an orange oil (0.20 g, 88%) following the same procedure as for **10a**.

MW ($C_{20}H_{19}N_3O_2$): 333.39 g/mol; **Rf:** 0.73 (Hexanes/EtOAc 8:2); **^{1}H NMR ($CDCl_3$, 400 MHz):** δ_H 7.53 – 7.47 (m, 2H), 7.43 – 7.35 (m, 2H), 7.25 (d, *J* = 2.3 Hz, 1H), 7.23 – 7.17 (m, 1H), 7.07 (dd, *J* = 8.3, 1.8 Hz, 1H), 6.83 (d, *J* = 8.3 Hz, 1H), 5.16 (s, 2H), 2.88 (s, 6H), 2.25 (s, 3H). **^{13}C{H} NMR ($CDCl_3$, 101 MHz):** δ_C 164.6,153.2, 135.0, 130.7, 130.3, 129.1, 126.1, 125.4, 124.2, 117.2, 114.4, 87.9, 86.3, 53.8, 44.0, 20.3. **IR (ATR) ν (cm^{-1}):** 2938, 2081, 1699, 1238, 1141, 753. **HRMS (ESI) m/z:** calcd.for $C_{20}H_{19}N_3O_2Na$ $[M+Na]^+$ 356.1369; Found 356.1373.

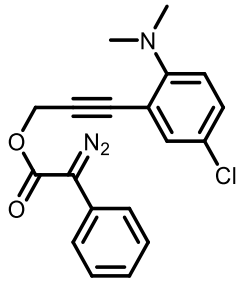

Diazo compound **10j** was obtained from **S7j** (0.17 g, 0.52 mmol) as an orange oil (0.16 g, 87%) following the same procedure as for **10a**.

MW ($C_{19}H_{16}ClN_3O_2$): 353.81 g/mol; **Rf:** 0.70 (Hexanes/EtOAc 8:2); **^{1}H NMR ($CDCl_3$, 400 MHz):** δ_H 7.54 – 7.46 (m, 2H), 7.44 – 7.36 (m, 3H), 7.24 – 7.15 (m, 2H), 6.81 (d, *J* = 8.8 Hz, 1H), 5.15 (s, 2H), 2.91 (s, 6H). **^{13}C{H} NMR ($CDCl_3$, 101 MHz):** δ_C 164.5, 153.9, 134.0, 129.8, 129.1, 126.2, 125.3,125.2, 124.2, 118.3, 115.4, 89.2, 85.0, 53.5, 43.6. **IR (ATR) ν (cm^{-1}):** 2940, 2081, 1698, 1236, 1139, 751. **HRMS (ESI) m/z:** calcd. for $C_{19}H_{16}ClN_3O_2Na$ $[M+Na]^+$ 376.0823; Found 376.0830.

Preparation of 10a-d$_6$

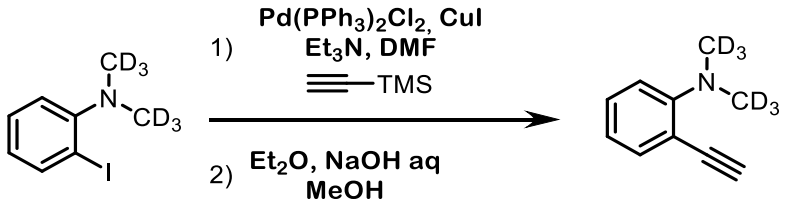

Scheme 8.11. Experimental procedure for the deuterated alkyne.

In a 50 mL round-bottom flask containing a mixture of ***N,N*-Dimethyl-*d*$_3$-2-iodoaniline**[239] (1.23 g, 4.86 mmol), CuI (37.1 mg, 0.20 mmol), $Pd(PPh_3)_2Cl_2$ (68.2 mg, 0.10 mmol.), and triethylamine (0.68 mL, 4.88 mmol.) in DMF (12 mL), trimethylsilylacetylene (0.81 mL, 5.86 mmol) was added dropwise under a nitrogen atmosphere. After the addition, the solution was stirred at room temperature overnight. Upon completion of the reaction (TLC monitoring), the crude was diluted with Et_2O, and washed with saturated aqueous NH_4Cl and brine. The organic layer was dried over anhydrous Na_2SO_4 and concentrated under reduced pressure. The crude was then dissolved with methanol (19 mL) and Et_2O (19 mL) and a 10% aqueous NaOH solution (11 mL) was added and the mixture was stirred at room temperature overnight. Upon completion of the reaction (TLC monitoring), the organic layer was separated, and the aqueous layer was back-extracted with Et_2O twice. The combined organic extracts were washed with brine, dried over anhydrous Na_2SO_4 and concentrated under reduced pressure. The crude product was purified by column chromatography on silica gel (Hexanes 100%) to afford the corresponding deuterated alkyne as a yellow oil (0.52 g, 71 % yield).

MW ($C_{10}H_5D_6N$): 151.24 g/mol; **Rf:** 0.50 (Hexanes/EtOAc 8:2); **^{1}H NMR ($CDCl_3$, 400 MHz):** δ_H 7.46 (dd, *J* = 7.6, 1.7 Hz, 1H), 7.27 (ddd, *J* = 8.3, 7.3, 1.7 Hz (overlapped with chloroform), 1H), 6.92 (dd, *J* = 8.3, 1.1 Hz, 1H), 6.88 (td, *J* = 7.6, 1.1 Hz, 1H), 3.41 (s, 1H). **^{13}C{H} NMR ($CDCl_3$, 101 MHz):** δ_C 135.0, 129.7, 120.7, 117.1, 114.4, 83.0, 82.3 (carbons bonded to deuterium are not observed in the spectrum with the standard acquisition parameters). **IR (ATR) ν (cm^{-1}):** 3280, 2046, 1482, 749. **HRMS (ESI) m/z:** calcd. for $C_{10}H_6D_6N$ $[M+H]^+$ 152.1341; Found 152.1348.

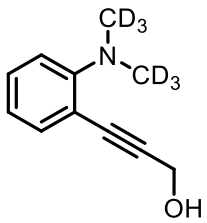

Propargyl alcohol **S5a-d$_6$** was obtained from the deuterated alkyne (0.52 g, 3.44 mmol) as a brown oil (0.51 g, 82%) following the same procedure as for **S5a**.

MW ($C_{11}H_7D_6NO$): 181.27 g/mol; **Rf:** 0.25 (Hexanes/EtOAc 7:3); **^{1}H NMR ($CDCl_3$, 400 MHz):** δ_H 7.38 (dd, *J* = 7.6, 1.7 Hz, 1H), 7.27 – 7.22 (m, 1H, (overlapped with chloroform)), 6.93 (d, *J* = 1.1 Hz, 1H), 6.92 (dd, *J* = 8.2, 1.1 Hz, 1H), 4.55 (s, 2H), 2.21 (broad s, 1H). **^{13}C{H} NMR ($CDCl_3$, 101 MHz):** δ_C 155.1, 134.5, 129.6, 121.0, 117.2, 115.1, 92.7, 84.9, 52.0 (carbons bonded to deuterium are not observed in the spectrum with the standard acquisition parameters). **IR (ATR) ν (cm^{-1}):** 3290, 2918, 1590, 1483, 1021, 752. **HRMS (ESI)m/z:** calcd. for $C_{11}H_8D_6NO$ $[M+H]^+$ 182.1447; Found 182.1456.

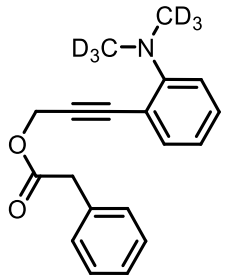

Ester **S7a-d_6** was obtained from **S5a-d_6** (0.39 g, 2.15 mmol) as an orange oil (0.57 g, 88%) following the same procedure as for **S6a.**

MW ($C_{19}H_{13}D_6NO_2$): 299.40 g/mol; **Rf:** 0.55 (Hexanes/EtOAc 8:2); **^{1}H NMR ($CDCl_3$, 400 MHz):** δ_H 7.39 (dd, *J* = 7.6, 1.7 Hz, 1H), 7.34 – 7.26 (m, 6H), 7.25 – 7.23 (m, 1H), 6.91 – 6.82 (m, 2H), 4.99 (s, 2H), 3.70 (s, 2H). **^{13}C{H} NMR ($CDCl_3$, 101 MHz):** δ_C 171.0, 155.3, 134.8, 133.8, 129.8, 129.4, 128.7, 127.3, 120.5, 117.0, 114.1, 88.1, 86.1, 53.8, 41.3 (carbons bonded to deuterium are not observed in the spectrum with the standard acquisition parameters). **IR (ATR) ν (cm^{-1}):** 2918, 1736, 1485, 1131, 751. **HRMS (ESI)m/z:** calcd. for $C_{19}H_{13}D_6NO_2Na$ $[M+Na]^+$ 322.1685; Found 322.1691.

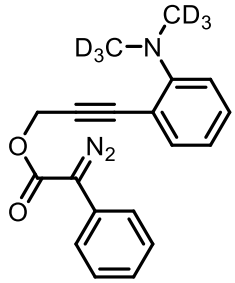

Diazo **10a-d_6** was obtained from **S5a-d_6** (0.32 g, 1.07 mmol) as an orange solid (0.26 g, 75%) following the same procedure as for **10a.**

MW ($C_{19}H_{11}D_6N_3O_2$): 325.40 g/mol; **Rf:** 0.58 (Hexanes/EtOAc 8:2); **^{1}H NMR ($CDCl_3$, 400 MHz):** δ_H 7.54 – 7.45 (m, 2H), 7.45 – 7.34 (m, 3H), 7.31 – 7.23 (m, 2H, (overlapped with chloroform)), 7.23 – 7.17 (m, 1H), 6.89 (dd, *J* = 8.0, 1.1 Hz, 1H), 6.86 (td, *J* = 8.0, 1.1 Hz, 1H), 5.17 (s, 2H). **^{13}C{H} NMR ($CDCl_3$, 101 MHz):** δ_C 164.6, 155.3, 134.8, 129.9, 129.1, 126.1, 125.4, 124.2, 120.5, 117.0, 114.0, 88.1, 86.4, 53.7 (carbons bonded to deuterium are not observed in the spectrum with the standard acquisition parameters). **IR (ATR) ν (cm^{-1}):** 2927, 2085, 1700, 1242, 1143, 748. **HRMS (ESI) m/z:** calcd. for $C_{19}H_{11}D_6N_3O_2Na$ $[M+Na]^+$ 348.1590; Found 348.1589.

NMR characterization of compound 9

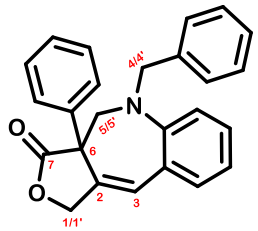

MW ($C_{25}H_{21}NO_2$): 367.15 g/mol; **Rf:** 0.53 (Hexanes/EtOAc 8:2)**; ^{1}H NMR ($CDCl_3$, 400 MHz):** δ_H 7.50 – 7.43 (m, 2H, H_{Ph}), 7.38 – 7.19 (m, 7H, H_{Ph} (overlapped with chloroform), 7.10 – 7.04 (m, 1H, H_{Ph}), 6.97 (d, J = 7.0 Hz, 2H, H_{Ph}), 6.86 (s, 1H, H_3), 6.83 (d, *J* = 7.0 Hz, 1H, H_{Ph}), 6.66 (d, *J* = 8.3 Hz, 1H, H_{Ph}), 4.93 (dd, *J* = 11.8, 1.8 Hz, 1H, $H_{1/1'}$), 4.84 (d, *J* = 11.8 Hz, 1H, $H_{1/1'}$), 4.25 (d, *J* = 18.1 Hz, 1H, $H_{4/4'}$,), 4.16 (d, *J* = 13.8 Hz, 1H, $H_{5/5'}$), 3.40 (d, *J* = 18.1 Hz, 1H, $H_{4/4'}$), 3.34 (dd, *J* = 13.8, 1.6 Hz, 1H, $H_{5/5'}$).**^{13}C{H} NMR ($CDCl_3$, 101 MHz):** δ_C 175.6 (C_7), 148.9 (C_{Ph}), 138.3 (C_{Ph}), 136.0 (C_{Ph}), 134.9 (C_{Ph}), 133.7 (C_2), 129.5 (C_3), 129.2 (C_{Ph}), 128.8 (C_{Ph}), 128.4 (C_{Ph}), 127.7 (C_{Ph}), 127.1 (C_{Ph}), 126.2 (C_{Ph}), 120.9 (C_{Ph}), 118.7 (C_{Ph}), 116.7 (C_{Ph}), 71.0 (C_1), 58.6 (C_4), 58.4 (C_6), 57.0 (C_5).

General procedure for the silver carbene/alkyne metathesis tandem reaction terminated in vinylogous C*sp*^{3}-H insertion.

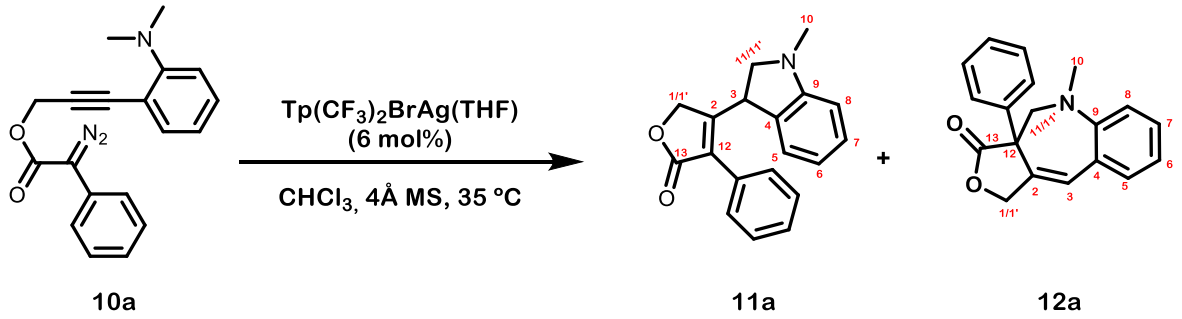

Scheme 8.12. General procedure for the silver carbene/alkyne metathesis tandem reaction terminated in vinylogous C*sp*^{3}-H insertion.

To an oven-dried Schlenk flask containing diazo compound **10a** (18.5 mg, 0.0580 mmol) and 4Å MS (100 mg) in anhydrous chloroform (14.4 mL), a solution of $Tp(CF_3)_2BrAg(THF)$ (3.6 mg, 0.0035 mmol) in chloroform (0.6 mL) was added dropwise under a nitrogen atmosphere. The mixture was then heated to 35ºC and stirred in the dark for 5h. The solvent was then removed under reduced pressure and the crude reaction mixture was purified by column chromatography on silica gel using hexane/EtOAc mixtures as the eluent (96:4 to 75:25). Concentration under reduced pressure afforded compound **12a** (12.0 mg, 71% yield) as a colorless solid, and **11a** (1.7 mg, 10% yield) as a colorless solid.

A mmol scale reaction was carried using the following amounts of materials: diazo compound **10a** (320.5 mg, 1.00 mmol), 4Å MS (1000 mg), anhydrous chloroform (251 mL + 3 mL (for the catalyst addition)) and $Tp(CF_3)_2BrAg(THF)$ (62.2 mg, 0.06 mmol) affording compound **12a** (166.7 mg, 57% yield), and **11a** (28.4 mg, 10 % yield).

12a: MW ($C_{19}H_{17}NO_2$): 291.35 g/mol; **Rf:** 0.53 (Hexanes/EtOAc 8:2). **MP (ºC):** 165. **^{1}H NMR ($CDCl_3$, 400 MHz):** δ_H 7.47 – 7.40 (m, 2H, **H_{Ph}**), 7.34 – 7.27 (m, 3H, **H_{Ph}**), 7.26 (m, 1H, **H5** (overlapped with chloroform)), 7.20 (ddd, *J* = 8.6, 7.4, 1.7 Hz, 1H, **H7**), 6.84 (td, *J* = 7.4, 1.1 Hz, 1H, **H6**), 6.80 (broad s, 1H, **H3**), 6.73 (d, *J* = 7.5 Hz, 1H, **H8**), 4.91 (dd, *J* = 11.3, 1.9 Hz, 1H, **H1/1'**), 4.80 (dd, *J* = 11.3, 1.0 Hz, 1H, **H1/1'**), 3.98 (d, *J* = 13.5 Hz, 1H, **H11/11'**), 3.17 (d, *J* = 13.5 Hz, 1H, **H11/11'**), 2.52 (s, 3H, **H10**). **^{13}C{H} NMR ($CDCl_3$, 101 MHz):** δ_C 175.7 (**C13)**, 149.1(**C9**), 136.7 (**C_{Ph}**), 134.8 (**C5**), 133.5 (**C2**), 129.5 (**C3**), 129.0 (**C7**), 128.6 (**C_{Ph}**), 128.1 (**C_{Ph}**), 127.5 (**C_{Ph}**), 121.1 (**C4**), 118.3 (**C6**), 115.2 (**C8)**, 71.1 (**C1**), 59.1 (**C11**), 58.3 (**C12**), 42.3 (**C10**). **IR (ATR) ν (cm^{-1}):** 3016, 2858, 1753, 1491, 756. **HRMS (ESI) m/z:** calcd. for $C_{19}H_{17}NO_2Na$ $[M+Na]^+$ 314.1151; Found 314.1149.

11a: MW ($C_{19}H_{17}NO_2$): 291.35 g/mol; **Rf:** 0.27 (Hexanes/EtOAc 8:2). **MP (ºC):** 139. **^{1}H NMR ($CDCl_3$, 400 MHz):** δ_H 7.56 – 7.39 (m, 5H, **H_{Ph}**), 7.18 (t, *J* = 7.9 Hz, 1H, **H7**), 7.00 (d, *J* = 7.5 Hz, 1H,**H5**), 6.73 (td, *J* = 7.5, 1.0 Hz, 1H, **H6**), 6.57 (d, *J* = 7.9 Hz, 1H, **H8**), 4.88 (d, *J* = 17.8, 1H, **H1/1'**), 4.70 (dd, *J* = 8.8, 6.2 Hz, 1H, **H3**), 4.63 (d, J = 17.9 Hz, 1H, **H1/1'**), 3.58 (t, *J* = 8.8 Hz, 1H, **H11/11'**), 3.30 (dd, *J* = 8.8, 6.2 Hz, 1H, **H11/11'**), 2.79 (s, 3H, **H10**). **^{13}C{H} NMR ($CDCl_3$, 101 MHz):** δ_C 173.3 (**C13**), 161.7 (**C2**), 153.1 (**C9**), 129.8 (**C4**), 129.3 (**C7**), 129.2 (**C_{Ph}**), 129.1 (**C_{Ph}**), 129.0 (**C_{Ph}**), 128.9 (**C_{Ph}**), 127.7 (**C12**), 124.4 (**C5**), 118.9 (**C6**), 108.3 (**C8**), 69.5 (**C1**), 61.4 (**C11)**, 39.9 (**C3**), 36.0 (**C10**). **IR (ATR) ν (cm^{-1}):** 2918, 2853, 1742, 1127, 736. **HRMS (ESI) m/z:** calcd. for $C_{19}H_{17}NO_2Na$ $[M+Na]^+$ 314.1151; Found 314.1157.

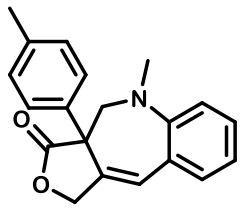

Starting from diazo compound **10b (**33.7 mg, 0.10 mmol)**,** compound **12b** was obtained as a yellow oil (17.7 mg, 57 % yield), alongside **11b** (6.7 mg, 22% yield).

MW ($C_{20}H_{19}NO_2$): 305.38 g/mol; **Rf:** 0.48 (Hexanes/EtOAc 8:2); **^{1}H NMR ($CDCl_3$, 400 MHz):** δ_H 7.31 (*d*, J = 8.4 Hz, 2H), 7.26-7.24 (m, 1H (overlapped with chloroform)), 7.19 (ddd, *J* = 8.8, 7.3, 1.7 Hz, 1H), 7.11 (d, *J* = 8.4 Hz, 2H), 6.83 (td, *J* = 7.3, 1.1 Hz, 1H), 6.77 (broad s, 1H), 6.73 (d, *J* = 8.8 Hz, 1H), 4.90 (dd, *J* = 11.3, 1.9 Hz, 1H), 4.78 (dd, *J* = 11.3, 1.1 Hz, 1H), 3.96 (d, *J* = 13.5 Hz, 1H), 3.15 (d, *J* = 13.5 Hz, 1H), 2.55 (s, 3H), 2.32 (s, 3H). **^{13}C{H} NMR ($CDCl_3$, 101 MHz):** δ_C 175.8, 149.2, 137.9, 134.7, 133.8, 133.7, 129.3, 129.2, 129.0, 127.4, 121.2, 118.2, 115.1, 71.1, 59.0, 58.0, 42.4, 21.2. **IR (ATR) ν (cm^{-1}):** 3018, 2876, 1758, 1494, 745. **HRMS (ESI) m/z:** calcd. for $C_{20}H_{19}NO_2Na$ $[M+Na]^+$ 328.1308; Found 328.1313.

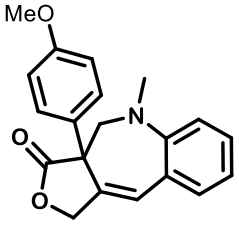

Starting from diazo compound **10c** (35.1 mg, 0.10 mmol), compound **12c** was obtained as a yellow oil (13.5 mg, 42 % yield), alongside **11c** (8.9 mg, 28% yield).

MW ($C_{20}H_{19}NO_3$): 321.38 g/mol; **Rf:** 0.38 (Hexanes/EtOAc 8:2); **^{1}H NMR (400 MHz, $CDCl_3$) δ (ppm):** 7.37 – 7.31 (m, 2H), 7.28 – 7.24 (m, 1H (overlapped with chloroform)), 7.20 (ddd, *J* = 8.6, 7.2, 1.7 Hz, 1H), 6.86 – 6.80 (m, 3H), 6.76 (broad s, 1H), 6.74 (d, *J* = 8.6 Hz, 1H), 4.90 (dd, *J* = 11.3, 1.9 Hz, 1H), 4.78 (d, *J* = 11.3 Hz, 1H), 3.92 (d, *J* = 13.5 Hz, 1H), 3.78 (s, 3H), 3.14 (d, *J* = 13.5 Hz, 1H), 2.56 (s, 3H). **^{13}C{H} NMR ($CDCl_3$, 101 MHz):** δ_C 175.9, 159.5, 149.2, 134.7, 133.9, 129.1, 129.0, 128.8, 128.7, 121.2, 118.2, 115.2, 113.9, 71.1, 59.0, 57.6, 55.4, 42.4. **IR (ATR) ν (cm^{-1}):** 3060, 2849, 1756, 1494, 746. **HRMS (ESI) m/z:** calcd. for $C_{20}H_{19}NO_3Na$ $[M+Na]^+$ 344.1257; Found 344.1260.

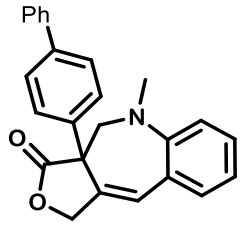

Starting from diazo compound **10d** (23.8 mg, 0.060 mmol)**,** compound **12d** was obtained as a colorless solid (9.3 mg, 42 % yield), alongside **11d** (7.4 mg, 33% yield).

MW ($C_{25}H_{21}NO_2$): 367.45 g/mol; **Rf:** 0.53 (Hexanes/EtOAc 8:2); **MP (ºC):** 99; **^{1}H NMR ($CDCl_3$, 400 MHz):** δ_H 7.60 – 7.48 (m, 6H), 7.47 – 7.40 (m, 2H), 7.38 – 7.32 (m, 1H), 7.29 (dd, *J* = 7.6, 1.7 Hz, 1H), 7.21 (ddd, *J* = 8.4, 7.6, 1.7 Hz, 1H), 6.85 (td, *J* = 7.6, 1.1 Hz, 1H), 6.82 (broad s, 1H), 6.75 (d, *J* = 8.4 Hz, 1H), 4.95 (dd, J = 11.4, 1.9 Hz, 1H), 4.83 (d, J = 11.4 Hz, 1H), 4.03 (d, *J* = 13.6 Hz, 1H), 3.20 (d, *J* = 13.6 Hz, 1H), 2.59 (s, 3H). **^{13}C{H} NMR ($CDCl_3$, 101 MHz):** δ_C 175.7, 149.1, 140.9, 140.4, 135.8, 134.8, 133.5, 129.5, 129.1, 129.0, 128.0, 127.7, 127.2, 127.1, 121.2, 118.3, 115.2, 71.2, 59.0, 58.1, 42.5. **IR (ATR) ν (cm^{-1}):** 3027, 2875, 1721, 1493, 746. **HRMS (ESI) m/z:** calcd. for $C_{25}H_{21}NO_2Na$ $[M+Na]^+$ 390.1465; Found 390.1477.

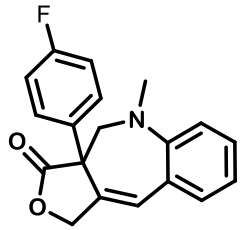

Starting from diazo compound **10e** (38.0 mg, 0.11 mmol)**,** compound **12e** was obtained as a colorless solid (10.5 mg, 31 % yield), alongside **11e** (11.5 mg, 34 % yield).

MW ($C_{19}H_{16}FNO_2$): 309.34 g/mol; **Rf:** 0.58 (Hexanes/EtOAc 8:2); **MP (ºC):** 126; **^{1}H NMR ($CDCl_3$, 400 MHz):** δ_H 7.46 – 7.37 (m, 2H), 7.29 – 7.25 (m, 1H, (overlapped with chloroform)), 7.21 (ddd, *J* = 8.4, 7.3, 1.7 Hz, 1H), 7.05 – 6.95 (m, 2H), 6.85 (td, *J* = 7.3, 1.2 Hz, 1H), 6.79 (broad s, 1H), 6.74 (d, *J* = 8.4 Hz, 1H), 4.89 (dd, *J* = 11.4, 1.9 Hz, 1H), 4.81 (d, *J* = 11.4 Hz, 1H), 3.93 (d, *J* = 13.6 Hz, 1H), 3.16 (d, *J* = 13.6 Hz, 1H), 2.55 (s, 3H). **^{13}C{H} NMR ($CDCl_3$, 101 MHz):** δ_C 175.6, 162.7 (d, $^1J_{C\text{-}F}$ = 248.4 Hz), 149.0, 134.9, 133.3, 132.5 (d, $^4J_{C\text{-}F}$ = 3.2 Hz), 129.6, 129.3, 129.2 (d, $^3J_{C\text{-}F}$ = 6.2 Hz), 121.0, 118.5, 115.6, 115.3 (d, $^2J_{C\text{-}F}$ = 23.4 Hz), 71.1, 59.0, 57.8, 42.4. **^{19}F NMR ($CDCl_3$, 376 MHz):** δ_F -115.16. (s, 1F). **IR (ATR) ν (cm^{-1}):** 3014, 2851, 1749, 1491, 759. **HRMS (ESI) m/z:** calcd. for $C_{19}H_{16}FNO_2Na$ $[M+Na]^+$ 332.1057; Found 332.1069.

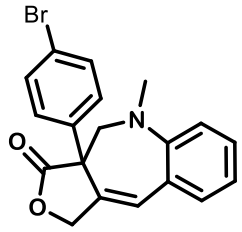

The reaction was run at 55ºC for 24h instead of 35ºC for 5h. Starting from diazo compound **10f** (23.2 mg, 0.058 mmol)**,** compound **12f** was obtained as a colorless solid (5.0 mg, 24 % yield), alongside **11f** (8.1 mg, 38 % yield).

MW ($C_{19}H_{16}BrNO_2$): 370.25 g/mol; **Rf:** 0.61 (Hexanes/EtOAc 8:2); **MP (ºC):** 77; **^{1}H NMR ($CDCl_3$, 400 MHz):** δ_H 7.48 – 7.40 (m, 2H), 7.35 – 7.29 (m, 2H), 7.28 – 7.25 (m, 1H , (overlapped with chloroform)), 7.21 (ddd, *J* = 8.5, 7.3, 1.7 Hz, 1H), 6.85 (td, *J* = 7.3, 1.2 Hz, 1H), 6.80 (s, 1H), 6.75 (d, *J* = 8.5 Hz, 1H), 4.88 (dd, *J* = 11.4, 1.9 Hz, 1H), 4.80 (d, *J* = 11.4 Hz, 1H), 3.94 (d, *J* = 13.6 Hz, 1H), 3.16 (d, *J* = 13.6 Hz, 1H), 2.57 (s, 3H). **^{13}C{H} NMR ($CDCl_3$, 101 MHz):** δ_C 175.3, 149.0, 135.9, 134.9, 132.8, 131.8, 129.9, 129.3, 129.3, 122.5, 121.0, 118.5, 115.2, 71.1, 59.0, 58.0, 42.6. **IR (ATR) ν (cm^{-1}):** 3066, 2880, 1764, 1481, 1003, 753. **HRMS (ESI) m/z:** calcd. for $C_{19}H_{16}BrNO_2Na$ $[M+Na]^+$ 392.0257-394.0237; Found 392.0244-394.0233.

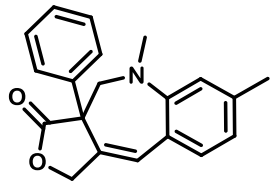

Starting from diazo compound **10g** (19.2 mg, 0.058 mmol), compound **12g** was obtained as a colorless solid (10.6, 60% yield)), alongside **11g** (1.2 mg, 7 % yield).

MW ($C_{20}H_{19}NO_2$): 305.38 g/mol; **Rf:** 0.55 (Hexanes/EtOAc 8:2); **MP (ºC):** 110; **^{1}H NMR ($CDCl_3$,400 MHz):** δ_H 7.46 – 7.41 (m, 2H), 7.34 – 7.27 (m, 3H), 7.16 (d, *J* = 7.8 Hz, 1H), 6.77 (s, 1H), 6.66 (dd, *J* = 7.8, 1.6 Hz, 1H), 6.53 (s, 1H), 4.89 (dd, *J* = 11.2, 1.9 Hz, 1H), 4.78 (d, *J* = 11.2 Hz, 1H), 3.96 (d, *J* = 13.5 Hz, 1H), 3.17 (d, *J* = 13.5 Hz, 1H), 2.51 (s, 3H), 2.32 (s, 3H). **^{13}C{H} NMR ($CDCl_3$, 101 MHz):** δ_C 175.8, 149.0, 139.2, 136.8, 134.8, 132.3, 129.2,128.1, 127.6, 119.4, 118.7, 115.7, 71.2, 59.1, 58.3, 42.3, 21.7. **IR (ATR) ν (cm^{-1}):** 3024, 2848, 1757, 1341, 770. **HRMS (ESI) m/z:** calcd. for $C_{20}H_{19}NO_2Na$ $[M+Na]^+$ 328.1308; Found 328.1312.

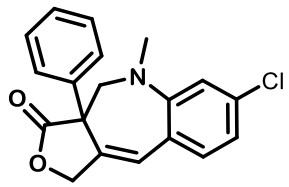

Starting from diazo compound **10h** (21.0 mg, 0.59 mmol)**,** compound **12h** was obtained as a colorless solid (13.4 mg, 69 % yield), alongside **11h** (2.3 mg, 12 % yield).

MW ($C_{19}H_{16}ClNO_2$): 325.79 g/mol; **Rf:** 0.55 (Hexanes/EtOAc 8:2); **MP (ºC):** 154; **^{1}H NMR ($CDCl_3$, 400 MHz):** δ_H 7.44 – 7.36 (m, 2H), 7.35 – 7.28 (m, 3H), 7.17 (d, *J* = 8.3 Hz, 1H), 6.80 (dd, *J* = 8.3, 2.1 Hz, 1H), 6.75 (broad

s, 1H), 6.68 (d, *J* = 2.1 Hz, 1H), 4.89 (dd, *J* = 11.4, 1.9 Hz, 1H), 4.79 (d, *J* = 11.4 Hz, 1H), 3.98 (d, *J* = 13.6 Hz, 1H), 3.17 (d, *J* = 13.6 Hz, 1H), 2.51 (s, 3H). **^{13}C{H} NMR ($CDCl_3$, 101 MHz): δ_C** 175.4, 149.8, 136.3, 134.9, 133.9, 128.8, 128.4, 128.3, 127.4, 119.7, 118.4, 115.1, 71.0, 59.1, 58.2, 42.5. **IR (ATR) ν (cm^{-1}):** 3030, 2849, 1760, 1491, 702. **HRMS (ESI) m/z:** calcd. for $C_{19}H_{16}ClNO_2Na$ $[M+Na]^+$ 348.0762; Found 348.0769.

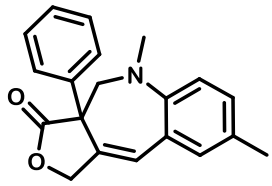

Starting from diazo compound **10i** (19.5 mg, 0.059 mmol)**,** compound **12i** was obtained as a colorless solid (11.8 mg, 66 % yield), alongside **11i** (1.7 mg, 10 % yield).

MW ($C_{20}H_{19}NO_2$): 305.38 g/mol; **Rf:** 0.60 (Hexanes/EtOAc 8:2); **MP (ºC):** 158; **^{1}H NMR ($CDCl_3$, 400 MHz): δ_H** 7.47 – 7.40 (m, 2H), 7.34 – 7.27 (m, 3H), 7.07 (d, *J* = 2.2 Hz, 1H), 7.02 (dd, *J* = 8.5, 2.2 Hz, 1H), 6.75 (broad s, 1H), 6.65 (d, *J* = 8.5 Hz, 1H), 4.90 (dd, *J* = 11.4, 1.9 Hz, 1H), 4.78 (d, *J* = 11.4 Hz, 1H), 3.95 (d, *J* = 13.5 Hz, 1H), 3.14 (d, *J* = 13.5 Hz, 1H), 2.50 (s, 3H), 2.30 (s, 3H). **^{13}C{H} NMR ($CDCl_3$,101 MHz): δ_C** 175.7, 147.0, 136.8, 135.0, 133.5, 129.9, 129.4, 128.6, 128.1, 127.5, 127.3, 121.0, 115.2, 71.2, 59.0, 58.4, 42.3, 20.2. **IR (ATR) ν (cm^{-1}):** 3002, 2945, 1738, 1365, 1214. **HRMS (ESI) m/z:** calcd. for $C_{20}H_{19}NO_2Na$ $[M+Na]^+$ 328.1308; Found 328.1315.

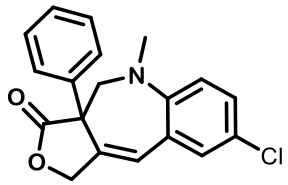

Starting from diazo compound **10j** (20.3 mg, 0.057 mmol) compound **12j** was obtained as a colorless solid (10.9 mg, 60 % yield), alongside **11j** (2.0 mg, 11 % yield).

MW ($C_{19}H_{16}ClNO_2$): 325.79 g/mol; **Rf:** 0.54 (Hexanes/EtOAc 8:2); **MP (ºC):** 193**^{1}H NMR ($CDCl_3$, 400 MHz): δ_H** 7.44 – 7.35 (m, 2H), 7.35 – 7.28 (m, 3H), 7.23 (d, *J* = 2.5 Hz, 1H), 7.13 (dd, *J* = 8.9, 2.5 Hz, 1H), 6.70 (broad s, 1H), 6.64 (d, *J* = 8.9 Hz, 1H), 4.91 (dd, *J* = 11.5, 1.9 Hz, 1H), 4.80 (d, *J* = 11.5 Hz, 1H), 3.99 (d, *J* = 13.6 Hz, 1H), 3.13 (d, *J* = 13.6 Hz, 1H), 2.50 (s, 3H). **^{13}C{H} NMR ($CDCl_3$, 101 MHz): δ_C** 175.3, 147.6, 136.3, 135.2, 133.6, 128.7, 128.7, 128.3, 128.2, 127.4, 122.8, 122.3, 116.5, 70.9, 59.0, 58.3, 42.6. **IR (ATR) ν (cm^{-1}):** 3031, 2851, 1742, 1491, 695. **HRMS (ESI) m/z:** calcd. for $C_{19}H_{16}ClNO_2Na$ $[M+Na]^+$ 348.0762; Found 348.0765.

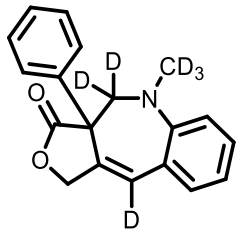

Starting from diazo compound **10a-d6** (19.2 mg, 0.059 mmol) compound **12a-d6** was obtained as a colorless solid (10.6 mg, 60 % yield), alongside **11a-d6** (1.5 mg, 9 % yield).

MW ($C_{19}H_{11}D_6NO_2$): 297.39 g/mol; **Rf:** 0.48 (Hexanes/EtOAc 8:2); **MP (ºC):** 162; **^{1}H NMR ($CDCl_3$, 400 MHz):** δ_H 7.47 – 7.38 (m, 2H), 7.35 – 7.27 (m, 3H), 7.26 (m, 1H (overlapped with chloroform)), 7.20 (ddd, *J* = 8.6, 7.3, 1.7 Hz, 1H), 6.83 (td, *J* = 7.3, 1.2 Hz, 1H), 6.72 (dd, *J* = 8.4, 1.2 Hz, 1H), 4.91 (d, *J* = 11.3 Hz, 1H), 4.80 (d, *J* = 11.3 Hz, 1H).**^{13}C{H} NMR ($CDCl_3$, 101 MHz):** δ_C 175.7, 149.1, 136.7, 134.7, 133.3, 129.0, 128.6, 128.1, 127.5, 121.0, 118.2, 115.1, 71.1, 58.2 (carbons bonded to deuterium are not observed in the spectrum with the standard acquisition parameters). **IR (ATR) ν (cm^{-1}):** 2919, 1752, 1484, 697. **HRMS (ESI) m/z:** calcd. for $C_{19}H_{12}D_6NO_2$ $[M+H]^+$ 298.1709; Found 298.1719.

Supplementary material for Chapter 5

Experimental procedure for the synthesis of propargyl alcohol S8a

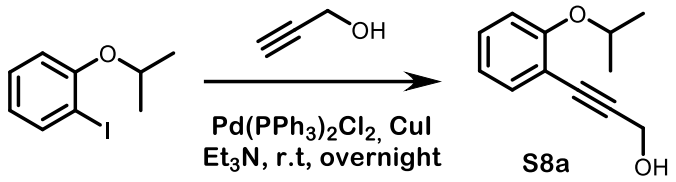

Scheme 8.13. Experimental procedure for the synthesis of propargyl alcohol **S8a**.

To a 50 mL round-bottom flask containing a mixture of **1-iodo-2-isopropoxybenzene**[240] (0.98 g, 3.74 mmol), CuI (28.5 mg, 0.15 mmol), and $Pd(PPh_3)_2Cl_2$ (65.6 mg, 0.09 mmol) in triethylamine (25 mL), propargyl alcohol (0.26 mL, 4.47 mmol) was added dropwise under a nitrogen atmosphere. After the addition, the solution was stirred at room temperature overnight. Upon completion of the reaction (TLC monitoring), the crude was filtered through a Celite pad, rinsed with EtOAc and concentrated under reduced pressure. The crude product was purified by column chromatography on silica gel (Hexanes:EtOAc = 7.5:2.5) to afford **S8a** as a yellow oil (0.42 g, 59 % yield).

MW ($C_{12}H_{14}O_2$): 190.24 g/mol; **Rf:** 0.35 (Hexanes/EtOAc 6:4); **IR (ATR) ν (cm^{-1}):** 3326, 2917, 1485, 1257, 749; **^{1}H NMR ($CDCl_3$, 400 MHz):** δ_H 7.39 (dd, 1H, J = 7.7, 1.8 Hz), 7.25 (ddd, 1H, J = 8.4, 7.7, 1.8 Hz), 6.92 – 6.85 (m, 2H), 4.62 – 4.55 (m, 1H), 4.53 (d, 2H, J = 6.0 Hz), 1.75 (t, 1H, J = 6.0 Hz), 1.37 (d, 6H, J = 6.1 Hz). **^{13}C{H} NMR ($CDCl_3$, 101 MHz):** δ_C 159.0, 134.0, 129.9, 120.8, 115.0, 113.7, 91.1, 82.6, 72.0, 52.1, 22.3. **HRMS (ESI) m/z:** $[M+Na]^+$ calcd. for $C_{12}H_{14}O_2Na$ 213.0886; Found 213.0886.

Experimental procedure for the synthesis of propargyl esters S9a-S9d.

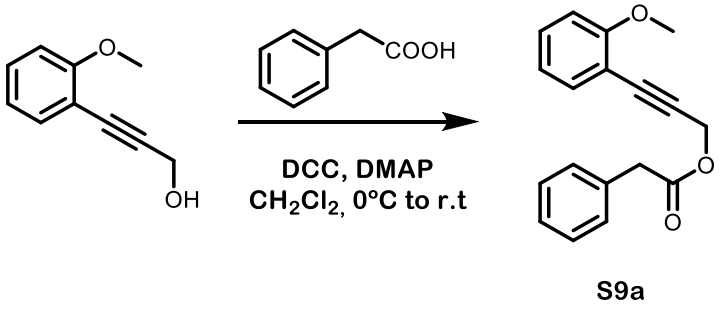

Scheme 8.14. General procedure for the preparation of propargyl esters **S9a-S9d**.

To a 25 mL round-bottom flask containing a mixture of **3-(2-methoxy-phenyl)-prop-2-yn-1-ol**[241] (0.42 g, 2.59 mmol), phenylacetic acid (0.39 g, 2.86 mmol), and 4-dimethylaminopyridine (DMAP) (31.8 mg, 0.26 mmol) in dichloromethane (13 mL), N,N'-dicyclohexylcarbodiimide (DCC) (0.65 g, 3.15 mmol) was added in batches at 0 ºC. After the addition, the reaction mixture was slowly warmed to room temperature and stirred overnight. Upon completion of the reaction (TLC monitoring), the crude was filtrated through a Celite pad, rinsed with

EtOAc and concentrated under reduced pressure. The crude product was then purified by column chromatography on silica gel (Hexanes/EtOAc = 9:1) to afford ester **S9a** as a yellow oil (0.69 g, 95 % yield).

MW ($C_{18}H_{16}O_3$): 280.32 g/mol; **Rf:** 0.68 (Hexanes/EtOAc 7:3); **IR (ATR) ν (cm^{-1}):** 2932, 1735, 1491, 1262, 1136, 752. **^{1}H NMR ($CDCl_3$, 400 MHz):** δ_H 7.42 (dd, 1H, J = 7.6, 1.7 Hz), 7.37 – 7.26 (m, 6H), 6.95 – 6.84 (m, 2H), 4.99 (s, 2H), 3.88 (s, 3H), 3.71 (s, 2H). **^{13}C{H} NMR ($CDCl_3$, 101 MHz:** δ_C 171.1, 160.4, 134.2, 133.8, 130.4, 129.5, 128.7, 127.3, 120.6, 111.4, 110.8, 86.9, 83.2, 55.9, 53.7, 41.2. **HRMS (ESI) m/z:** $[M+Na]^+$ calcd. for $C_{18}H_{16}O_3Na$ 303.0992; Found 303.0987.

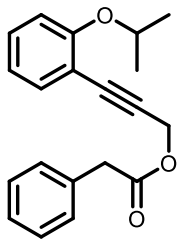

Ester **S9b** was obtained from **S8a** (0.21 g, 1.10 mmol) as yellow oil (0.29 g, 85%) following the same procedure as for **S9a**.

MW ($C_{20}H_{20}O_3$): 308.38 g/mol; **Rf:** 0.33 (Hexanes/EtOAc 7:3); **IR (ATR) ν (cm^{-1}):** 2974, 1736, 1486, 1261, 1121, 751. **^{1}H NMR ($CDCl_3$, 400 MHz):** δ_H 7.40 (dd, 1H, J = 7.8, 1.8 Hz), 7.38 – 7.23 (m, 6H), 6.93 – 6.85 (m, 2H), 4.97 (s, 2H), 4.55 (hept, 1H, J = 6.1 Hz), 3.70 (s, 2H), 1.36 (d, 6H, J = 6.1 Hz). **^{13}C{H} NMR ($CDCl_3$, 101 MHz):** δ_C 171.0, 159.2, 134.1, 133.8, 130.1, 129.5, 128.7, 127.3, 120.8, 115.2, 113.4, 86.5, 83.6, 72.1, 53.7, 41.2, 22.3. **HRMS (ESI) m/z:** $[M+Na]^+$ calcd. for $C_{20}H_{20}O_3Na$ 331.1305; Found 331.1310.

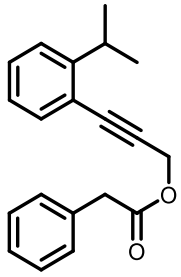

Ester **S9c** was obtained from **3-(2-Isopropylphenyl)prop-2-yn-1-ol**[242] (0.41 g, 2.35 mmol) as yellow oil (0.68 g, 99 %) following the same procedure as for **S9a**.

MW ($C_{20}H_{20}O_2$): 292.38 g/mol; **Rf:** 0.63 (Hexanes/EtOAc 8:2); **IR (ATR) ν (cm^{-1}):** 2958, 1737, 1235, 1133, 756. **^{1}H NMR ($CDCl_3$, 400 MHz):** δ_H 7.42 (dd, 1H, J = 7.6, 1.4 Hz), 7.38 – 7.27 (m, 7H), 7.13 (td, 1H, J = 7.3, 1.7 Hz), 4.97 (s, 2H), 3.71 (s, 2H), 3.40 (hept, 1H, J = 6.8 Hz), 1.24 (d, 6H, J = 6.8 Hz). **^{13}C{H} NMR ($CDCl_3$, 101 MHz):** δ_C 171.0, 151.0, 133.7, 132.8, 129.4, 129.2, 128.7, 127.3, 127.1, 125.6, 125.1, 121.0, 86.5, 85.5, 53.5, 41.2, 31.6, 23.2. **HRMS (ESI) m/z:** $[M+Na]^+$ calcd. $C_{20}H_{20}O_2Na$ 315.1356; Found 315.1362.

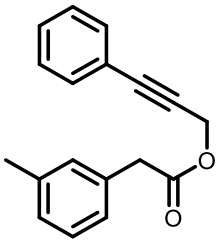

Ester **S9d** was obtained from **3-Phenylprop-2-yn-1-ol** (0.50 g, 3.78 mmol) as yellow oil (0.95 g, 95 %) following the same procedure as for **S9a**.

MW ($C_{18}H_{16}O_2$): 264.32 g/mol; **Rf:** 0.69 (Hexanes/EtOAc 9:1); **^{1}H NMR ($CDCl_3$, 400 MHz):** δ_H 7.49 – 7.40 (m, 2H), 7.35 – 7.29 (m, 3H), 7.25 – 7.18 (m, 1H), 7.16 – 7.05 (m, 3H), 4.94 (s, 2H), 3.67 (s, 2H), 2.35 (s, 3H). **^{13}C{H} NMR ($CDCl_3$, 101 MHz):** δ_C 171.2, 138.4, 133.6, 132.0, 130.2, 128.9, 128.7, 128.4, 128.1, 126.4, 122.3, 86.7, 83.0, 53.3, 41.1, 21.5. **HRMS (ESI) m/z:** $[M+Na]^+$ calcd. $C_{18}H_{16}O_2Na$ 287.1047; Found 287.1035.

Experimental procedure for the synthesis of diazo compounds

Diazo compounds **13a,13d,13f-i,13k-l**[233] and **13j**[243] were prepared in accordance with the experimental procedure previously described in the literature.

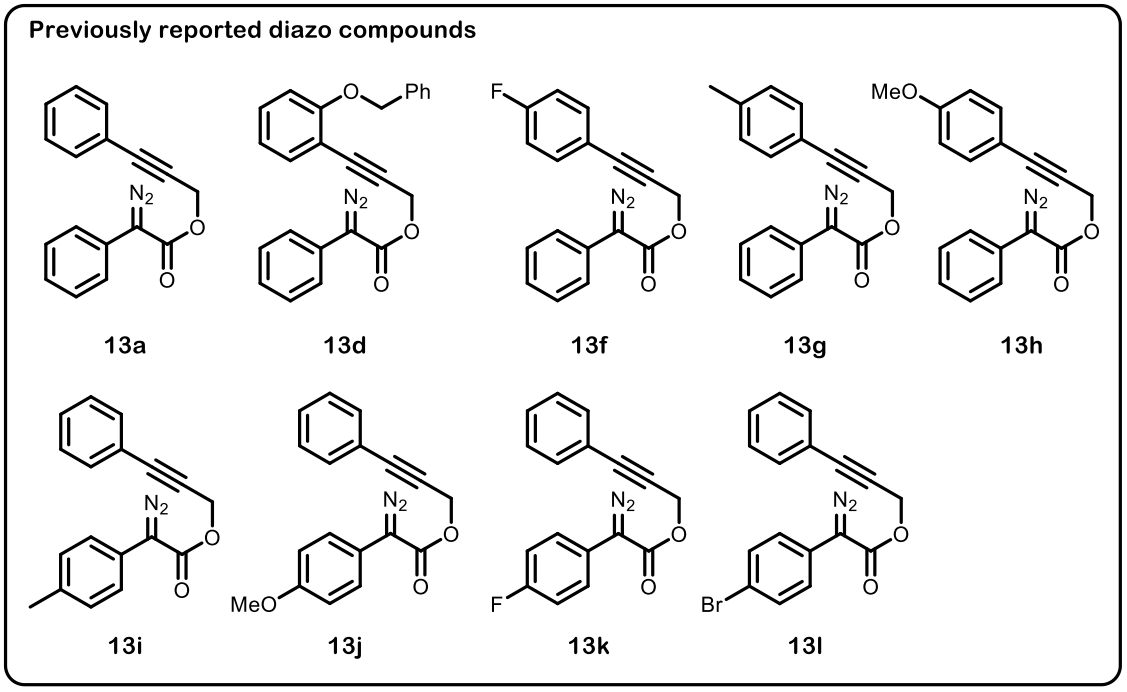

Figure 8.1. Previously reported diazo compounds **13a, 13d, 13f-13l.**

Experimental procedure for the synthesis of diazo compounds 13b, 13c, 13e and 13m

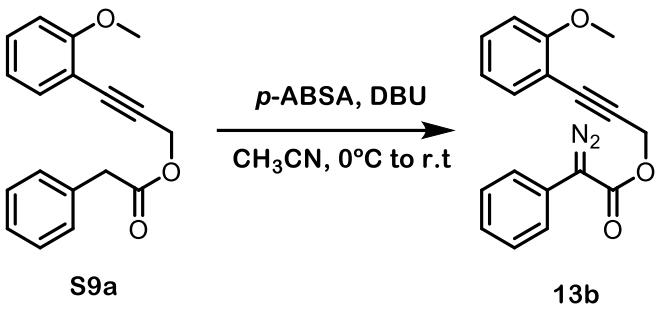

S9a **13b**

Scheme 8.15. General procedure for the preparation of diazo compounds **13b, 13c**, **13e and 13m**.

To a 50 mL oven-dried flask containing a mixture of **S9a** (0.40 g, 1.43 mmol) and *p*-acetamidobenzenesulfonyl azide (*p*-ABSA) (0.44 g, 1.83 mmol) in anhydrous CH_3CN (9.3 mL), a solution of 1,8-diazabicyclo[5.4.0]undec-7-ene (DBU) (0.32 mL, 2.14 mmol) in anhydrous CH_3CN (1.9 mL) was added dropwise at 0 ºC. After the addition, the reaction mixture was slowly warmed to room temperature and stirred overnight. Upon completion of the reaction (TLC monitoring), the crude was diluted with dichloromethane, and washed with saturated aqueous NH_4Cl, saturated aqueous $NaHCO_3$ and brine. The combined organic extracts were dried over anhydrous Na_2SO_4 and concentrated under reduced pressure. The crude product was purified by column chromatography on silica gel (Hexanes: Et_3N= 99:1) to afford diazo compound **13b** as a yellow solid (0.29 g, 66% yield).

MW ($C_{18}H_{14}N_2O_3$): 306.32 g/mol; **Rf:** 0.7 (Hexanes/EtOAc 8:2); **IR (ATR) ν (cm^{-1}):** 2935, 2092, 1698, 1235, 1139, 752. **^{1}H NMR ($CDCl_3$, 400 MHz):** δ_H 7.54 – 7.47 (m, 2H), 7.44 (dd, 1H, J = 7.6, 1.7 Hz), 7.44 – 7.35 (m, 2H), 7.32 (ddd, 1H, J = 8.3, 7.5, 1.7 Hz), 7.24 – 7.15 (m, 1H), 6.92 (dd, 1H, J = 7.6, 1.0 Hz), 6.88 (d, 1H, J = 9.2 Hz), 5.17 (s, 2H), 3.89 (s, 3H). **^{13}C{H} NMR ($CDCl_3$, 101 MHz):** δ_C 164.6, 160.4, 134.2, 130.5, 129.1, 126.1, 125.4, 124.2, 120.6, 111.4, 110.8, 87.0, 83.3, 55.9, 53.5. **HRMS (ESI) m/z:** $[M+Na]^+$ calcd. for $C_{18}H_{14}N_2O_3Na$ 329.0897; Found 329.0895.

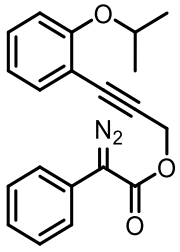

Diazo compound **13c** was obtained from **S9b** (0.29 g, 0.94 mmol) as an orange oil (0.25 g, 80%) following the same procedure as for **13b**.

MW ($C_{20}H_{18}N_2O_3$): 334.38 g/mol; **Rf:** 0.73 (Hexanes/EtOAc 8:2); **IR (ATR) ν (cm^{-1}):** 2974, 2082, 1699, 1486, 1238, 1141, 750. **^{1}H NMR ($CDCl_3$, 400 MHz):** δ_H 7.54 – 7.48 (m, 2H), 7.44 – 7.36 (m, 3H), 7.30 – 7.23 (m, 1H (overlapped with chloroform)), 7.23 – 7.16 (m, 1H), 6.93 – 6.86 (m, 2H), 5.15 (s, 2H), 4.56 (hept, 1H, J = 6.1 Hz), 1.37 (d, J = 6.1 Hz, 6H). **^{13}C{H} NMR ($CDCl_3$, 101 MHz):** δ_C 164.5, 159.3, 134.0, 130.1, 129.1, 126.0,

125.4, 124.1, 120.8, 115.2, 113.4, 86.6, 83.8, 72.1, 53.6, 22.2. **HRMS (ESI) m/z:** $[M+Na]^+$ calcd. for $C_{20}H_{18}N_2O_3Na$ 357.1210; Found 357.1220.

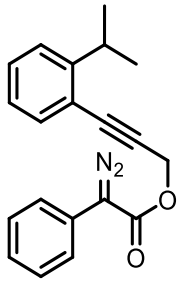

Diazo compound **13e** was obtained from **S9c** (0.18 g, 0.62 mmol) as an orange solid (0.17 g, 86%) following the same procedure as for **13b**.

MW ($C_{20}H_{18}N_2O_2$): 318.38 g/mol; **Rf:** 0.8 (Hexanes/EtOAc 9:1); **IR (ATR) ν (cm^{-1}):** 2960, 2094, 1703, 1237, 1138, 749. **^{1}H NMR ($CDCl_3$, 400 MHz):** δ_H 7.52 – 7.47 (m, 2H), 7.45 – 7.38 (m, 3H), 7.33 – 7.28 (m, 2H), 7.20 (ddt, 1H, J = 7.7, 7.0, 1.2 Hz), 7.14 (ddd, 1H, J = 7.7, 7.0, 1.7 Hz), 5.14 (s, 2H), 3.44 (hept, 1H, J = 6.9 Hz), 1.26 (d, 6H, J = 6.9 Hz). **^{13}C{H} NMR ($CDCl_3$, 101 MHz):** δ_C 164.6, 151.1, 132.8, 129.3, 129.1, 126.1, 125.6, 125.4, 125.1, 124.2, 121.0, 86.6, 85.8, 53.5, 31.7, 23.2. **HRMS (ESI) m/z:** $[M+H]^+$ calcd. for $C_{20}H_{18}N_2O_2Na$ 341.1260; Found 341.1267.

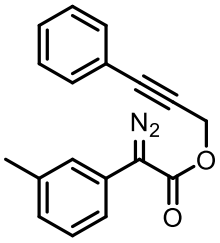

Diazo compound **13m** was obtained from **S9d** (0.55 g, 2.08 mmol) as an orange oil (0.40 g, 66%) following the same procedure as for **13b**.

MW ($C_{18}H_{14}N_2O_2$): 290.32 g/mol; **Rf:** 0.75 (Hexanes/EtOAc 9:1); **^{1}H NMR ($CDCl_3$, 400 MHz):** δ_H 7.50 – 7.45 (m, 2H), 7.37 – 7.27 (m, 6H), 7.06 – 6.98 (m, 1H), 5.10 (s, 2H), 2.37 (s, 3H).**^{13}C{H} NMR ($CDCl_3$, 101 MHz):** δ_C 164.7, 138.9, 132.1, 129.0, 128.9, 128.5, 127.0, 125.1, 124.8, 122.3, 121.4, 86.8, 83.1, 53.2, 21.7. **HRMS (ESI) m/z:** $[M+Na^+$ calcd. for $C_{18}H_{14}N_2O_2Na$ 313.0947; Found 313.0947.

General procedure for the silver catalyzed carbene/alkyne metathesis tandem reaction terminated in Csp^2-H insertion.

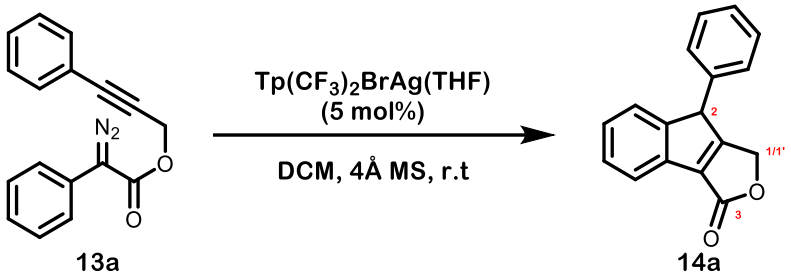

Scheme 8.16. General procedure for the silver catalyzed carbene/alkyne metathesis tandem reaction terminated in Csp^2-H insertion.

To an oven-dried Schlenk flask containing diazo compound **13a** (19.3 mg, 0.070 mmol) and 4Å MS (100 mg) in anhydrous dichloromethane (14.4 mL), a solution of $Tp(CF_3)_2BrAg(THF)$ (3.6 mg, 0.0035 mmol) in dichloromethane (0.6 mL) was added dropwise under a nitrogen atmosphere. The mixture was stirred in the dark at room temperature for 30 minutes. The solvent was then removed under reduced pressure and the crude reaction mixture was purified by column chromatography on silica gel using hexane/EtOAc mixtures as the eluent (94:6 to 86:14). Concentration under reduced pressure afforded compound **14a** (17.1 mg, 99% yield) as a colorless solid.

MW ($C_{17}H_{12}O_2$): 248.28 g/mol; **Rf:** 0.48 (Hexanes/EtOAc 8:2). **MP (ºC):** 160. **IR (ATR) ν (cm^{-1}):** 3028, 2927,1740, 1012, 748, 695. **^{1}H NMR ($CDCl_3$, 400 MHz):** δ_H 7.75 (d, 1H, J = 7.5 Hz), 7.38 (td, 1H, J = 7.2, 1.9 Hz), 7.34 – 7.27 (m, 5H), 7.08 (dd, 2H, J = 7.7, 1.8 Hz), 5.13 (dd, 1H, J = 18.2, 1.1 Hz, **H1/1'**) 4.96 (d, 1H, J = 18.2 Hz, **H1/1'**), 4.91 (s, 1H, **H2**). **^{13}C{H} NMR ($CDCl_3$, 101 MHz):** δ_C 175.8(**C3**), 167.7, 151.7, 137.0, 136.2, 134.1, 129.5, 128.1, 128.0, 127.8, 127.3, 125.2, 121.3, 69.2 (**C1**), 53.1(**C2**). **HRMS (ESI) m/z:** $[M+Na]^+$ calcd. for $C_{17}H_{12}O_2Na$ 271.0730; Found 271.0722.

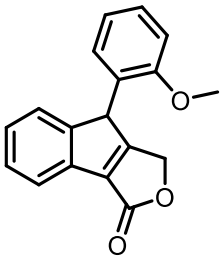

Starting from diazo compound **13b** (30.8 mg, 0.10 mmol), compound **14b** was obtained as a colorless solid (23.0 mg, 82% yield).

MW ($C_{18}H_{14}O_3$): 278.31 g/mol; **Rf:** 0.60 (Hexanes/EtOAc 8:2). **MP (ºC):** 131. **IR (ATR) ν (cm^{-1}):** 3009, 2936,1759, 1486, 1241, 1001, 758. **^{1}H NMR ($CDCl_3$, 400 MHz):** δ_H 7.76 (d, 1H, J = 7.4 Hz), 7.45 – 7.36 (m, 2H), 7.36 – 7.27 (m, 2H), 6.98 (d, 1H, J = 8.2 Hz), 6.89 – 6.78 (m, 2H), 5.34 (s, 1H), 5.16 (dd, 1H, J = 18.3, 1.2 Hz), 4.89 (d, 1H, J = 18.3 Hz), 3.94 (s, 3H).**^{13}C{H} NMR ($CDCl_3$, 101 MHz):** δ_C 176.5, 168.0, 157.5, 149.8, 135.8, 135.0, 129.1, 127.8, 127.7, 126.8, 125.7, 124.3, 121.4, 121.3, 110.7, 69.9, 55.7, 47.4.**HRMS (ESI) m/z:** $[M+Na]^+$ calcd. for $C_{18}H_{14}O_3Na$ 301.0835; Found 301.0831.

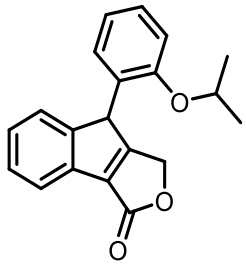

Starting from diazo compound **13c** (23.2 mg, 0.069 mmol), compound **14c** was obtained as a colorless solid (21.0 mg, 99% yield).

MW ($C_{20}H_{18}O_3$): 306.36 g/mol; **Rf:** 0.48 (Hexanes/EtOAc 8:2). **MP (ºC):** 165. **IR (ATR) ν (cm^{-1}):** 2983, 1757, 1449, 1240, 1110, 753. **^{1}H NMR ($DMSO_{d6}$, 400 MHz, 65ºC):** δ_H 7.58 (d, 1H, J = 7.3 Hz), 7.38 (td, 1H, J = 7.3, 1.5 Hz), 7.35 – 7.22 (m, 3H), 7.04 (d, 2H, J = 8.2 Hz), 6.85 (td, 1H, J = 7.4, 1.1 Hz), 5.30 (s, 1H), 5.28 (d, 2H, J = 17.5 Hz), 4.98 (d, 1H, J = 17.5 Hz), 4.63 (hept, 1H, J = 6.0 Hz), 1.24 (d, 3H, J = 6.0 Hz), 1.05 (d, 3H, J = 6.0 Hz).**^{13}C{H} NMR ($DMSO_{d6}$, 101 MHz, 65ºC):** δ_C 177.9, 166.9, 155.0, 150.7, 134.0, 133.9, 128.5, 126.9, 126.1, 124.7, 124.6, 120.1, 119.5, 112.9, 69.5, 69.2, 21.4, 21.0. **HRMS (ESI) m/z:** $[M+Na]^+$ calcd. for $C_{20}H_{18}O_3Na$ 329.1148; Found 329.1152.

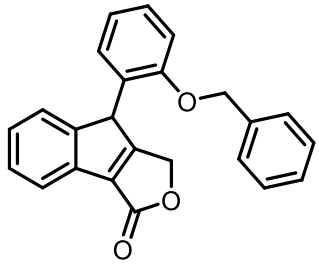

Starting from diazo compound **13d** (27.1 mg, 0.071 mmol), compound **14d** was obtained as a colorless solid (24.4 mg, 97% yield).

MW ($C_{24}H_{18}O_3$): 354.41 g/mol; **Rf:** 0.40 (Hexanes/EtOAc 8:2). **MP (ºC):** 139. **IR (ATR) ν (cm^{-1}):** 3033, 2915, 1756, 1449, 1241, 1008, 750. **^{1}H NMR ($CDCl_3$, 400 MHz):** δ_H 7.73 (dd, 1H, J = 7.5, 1.3 Hz), 7.45 – 7.35 (m, 7H), 7.34 – 7.27 (m, 2H), 7.07 (d, 1H, J = 8.2 Hz), 6.91 – 6.86 (m, 2H), 5.35 (s, 1H), 5.16 (d, 1H, J = 11.2 Hz), 5.12 (d, 1H, J = 11.2 Hz), 4.96 (dd, 1H, J = 18.4, 1.1 Hz), 4.85 (d, 1H, J = 18.4 Hz).**^{13}C{H} NMR ($CDCl_3$, 101 MHz):** δ_C 176.3, 167.8, 156.7, 149.8, 136.3, 135.8, 135.0, 129.2, 129.0, 128.6, 127.8, 126.8, 125.6, 124.6, 121.6, 121.3, 111.9, 70.6, 69.9, 47.8. **HRMS (ESI) m/z:** $[M+Na]^+$ calcd. for $C_{24}H_{18}O_3Na$ 377.1148; Found 377.1143.

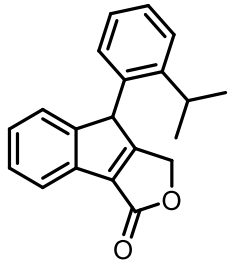

Starting from diazo compound **13e** (23.5 mg, 0.074 mmol), compound **14e** was obtained as a colorless solid (17.3 mg, 81% yield).

MW ($C_{20}H_{18}O_2$): 290.36 g/mol; **Rf:** 0.53 (Hexanes/EtOAc 8:2). **MP (ºC):** 145. **IR (ATR) ν (cm^{-1}):** 2960, 1753, 1361, 1215, 764. **^{1}H NMR ($CDCl_3$, 400 MHz):** δ_H 7.77 (d, 1H, J = 7.6 Hz), 7.42 – 7.36 (m, 2H), 7.28 – 7.23 (m, 3H, (overlapped with chloroform)), 7.00 (td, 1H, J = 7.6, 1.4 Hz), 6.47 (dd, 1H, J = 7.8, 1.4 Hz), 5.31 (s, 1H), 5.10 (d, 1H, J = 18.1 Hz), 4.92 (d, 1H, J = 18.1 Hz), 3.50 (hept, 1H, J = 6.8 Hz), 1.48 (d, 3H, J = 6.8 Hz), 1.37 (d, 3H, J = 6.8 Hz). Some small signals appear and some multiplets are wider due to restricted rotation alongside de C^{sp3}-C^{sp2} axis. **^{13}C{H} NMR ($CDCl_3$, 101 MHz):** δ_C 176.7, 167.7, 152.4, 146.8, 136.9, 134.4, 133.0, 128.3, 127.8, 127.2, 127.0, 126.8, 126.2, 125.1, 121.4, 69.1, 48.5, 29.8, 24.4, 24.2. **HRMS (ESI) m/z:** $[M+Na]^+$ calcd. for **$C_{20}H_{18}O_2$**Na 313.1199; Found 313.1202.

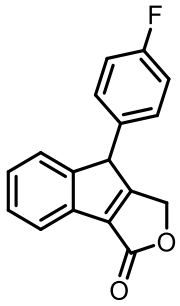

Starting from diazo compound **13f** (30.0 mg, 0.10 mmol), compound **14f** was obtained as a colorless solid (22.0 mg, 81% yield).

MW ($C_{17}H_{11}FO_2$): 266.27 g/mol; **Rf:** 0.48 (Hexanes/EtOAc 8:2). **MP (ºC):** 161. **IR (ATR) ν (cm^{-1}):** 3036, 2903,1741, 1501, 1217, 1010, 776. **^{1}H NMR ($CDCl_3$, 400 MHz):** δ_H 7.75 (d, 1H, J = 7.5 Hz), 7.39 (tt, 1H, J = 7.5, 4.9 Hz), 7.31 – 7.27 (m, 2H), 7.10 – 6.97 (m, 4H), 5.13 (dd, 1H, J = 18.3, 1.1 Hz), 4.94 (d, 1H, J = 18.3 Hz), 4.88 (s, 1H).**^{13}C{H} NMR ($CDCl_3$, 101 MHz):** δ_C 175.5, 167.5, 162.5 (d, J = 247.2 Hz), 151.6, 137.1, 134.0, 131.9 (d, J = 3.4 Hz), 129.5 (d, J = 8.2 Hz), 128.1, 127.4, 125.2, 121.3, 116.5 (d, J = 21.7 Hz), 69.1, 52.3. **^{19}F NMR ($CDCl_3$, 376 MHz):** δ_F -114.96. (s, 1F). **HRMS (ESI) m/z:** $[M+Na]^+$ calcd. for $C_{17}H_{11}FO_2Na$ 289.0635; Found 289.0634.

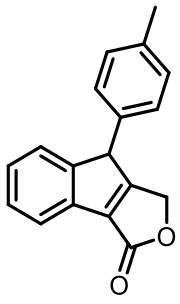

Starting from diazo compound **13g** (22.2 mg, 0.076 mmol), compound **14g** was obtained as a colorless solid (20.0 mg, 99% yield).

MW ($C_{18}H_{14}O_2$): 262.31 g/mol; **Rf:** 0.45 (Hexanes/EtOAc 8:2). **MP (ºC):** 175. **IR (ATR) ν (cm^{-1}):** 3014, 2922,1744, 1005, 774, 723. **^{1}H NMR ($CDCl_3$, 400 MHz):** δ_H 7.74 (d, 1H, J = 7.6 Hz), 7.37 (td, 1H, J = 7.2, 1.9

Hz), 7.31 – 7.26 (m, 2H), 7.13 (d, 2H, J = 7.8 Hz), 6.96 (d, 2H, J = 8.1 Hz), 5.12 (dd, 1H, J = 18.3, 1.1 Hz), 4.95 (d, 1H, J = 18.3 Hz), 4.87 (s, 1H), 2.33 (s, 3H).**^{13}C{H} NMR ($CDCl_3$, 101 MHz):** δ_C 176.1, 167.7, 151.9, 137.9, 136.8, 134.1, 133.1, 130.2, 127.9, 127.7, 127.2, 125.2, 121.2, 69.2, 52.8, 21.2. **HRMS (ESI) m/z:** $[M+Na]^+$ calcd. for $C_{18}H_{14}O_2Na$ 284.0803; Found 284.0808.

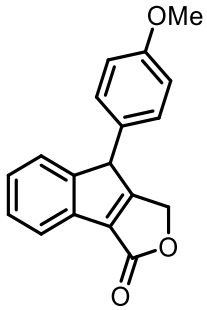

Starting from diazo compound **13h** (20.1 mg, 0.066 mmol), compound **14h** was obtained as a colorless solid (16.0 mg, 88% yield).

MW ($C_{18}H_{14}O_3$): 278.31 g/mol; **Rf:** 0.23 (Hexanes/EtOAc 8:2). **MP (ºC):** 178. **IR (ATR) ν (cm^{-1}):** 3009, 2918,1742, 1506, 1252, 1006, 774. **^{1}H NMR ($CDCl_3$, 400 MHz):** δ_H 7.74 (d, 1H, J = 7.5 Hz), 7.37 (ddd, 1H, J = 7.5, 6.1, 2.1 Hz), 7.30 – 7.26 (m, 2H), 7.02 – 6.95 (m, 2H), 6.89 – 6.81 (m, 2H), 5.12 (dd, 1H, J = 18.3, 1.1 Hz), 4.95 (d, 1H, J = 18.3 Hz), 4.86 (s, 1H), 3.79 (s, 3H).**^{13}C{H} NMR ($CDCl_3$, 101 MHz):** δ_C 176.2, 167.7, 159.4, 152.0, 136.7, 134.0, 128.9, 127.9, 127.8, 127.2, 125.2, 121.2, 114.9, 69.2, 55.5, 52.4. **HRMS (ESI) m/z:** $[M+Na]^+$ calcd. for $C_{18}H_{14}O_3Na$ 301.0835; Found 301.0835.

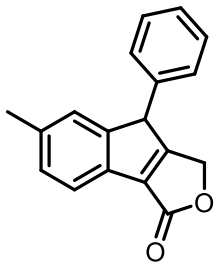

Starting from diazo compound **13i** (21.0 mg, 0.072 mmol), compound **14i** was obtained as a colorless solid (18.6 mg, 98% yield).

MW ($C_{18}H_{14}O_2$): 262.31 g/mol; **Rf:** 0.45 (Hexanes/EtOAc 8:2). **MP (ºC):** 175. **IR (ATR) ν (cm^{-1}):** 3028, 2914,1742, 1013, 824, 695. **^{1}H NMR ($CDCl_3$, 400 MHz):** δ_H 7.62 (d, 1H, J = 7.7 Hz), 7.37 – 7.27 (m, 3H), 7.18 (d, 1H, J = 8.5 Hz), 7.13 – 7.05 (m, 3H), 5.11 (dd, 1H, J = 18.1, 1.1 Hz), 4.94 (d, 1H, J = 18.1 Hz), 4.85 (s, 1H), 2.35 (s, 3H). **^{13}C{H} NMR ($CDCl_3$, 101 MHz):** δ_C 174.9, 167.8, 152.0, 137.3, 136.9, 136.6, 131.4, 129.5, 128.6, 128.0, 127.9, 126.0, 120.9, 69.2, 53.0, 21.7. **HRMS (ESI) m/z:** $[M+Na]^+$ calcd. for $C_{18}H_{14}O_2Na$ 285.0886; Found 285.0892.

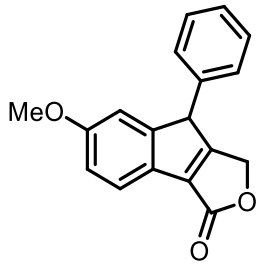

Starting from diazo compound **13j** (21.5 mg, 0.070 mmol), compound **14j** was obtained as a colorless solid (19.2 mg, 98% yield).

MW ($C_{18}H_{14}O_3$): 278.31 g/mol; **Rf:** 0.30 (Hexanes/EtOAc 8:2). **MP (ºC):** 163. **IR (ATR) ν (cm^{-1}):** 2931, 1735, 1478, 1269, 1013, 769. **^{1}H NMR ($CDCl_3$, 400 MHz):** δ_H 7.64 (d, 1H, J = 8.3 Hz), 7.38 – 7.28 (m, 3H), 7.12 – 7.05 (m, 2H), 6.90 (dd, 1H, J = 8.3, 2.4 Hz), 6.86 (d, 1H, J = 2.4 Hz), 5.09 (dd, 1H, J = 18.2, 1.2 Hz), 4.92 (d, 1H, J = 18.2 Hz), 4.85 (s, 1H), 3.78 (s, 3H).**^{13}C{H} NMR ($CDCl_3$, 101 MHz):** δ_C 173.6, 167.8, 159.6, 153.7, 136.6, 136.5, 129.5, 128.1, 127.9, 126.9, 121.7, 112.8, 112.3, 69.2, 55.7, 53.1. **HRMS (ESI) m/z:** $[M+Na]^+$ calcd. for $C_{18}H_{14}O_3Na$ 301.0835; Found 301.0833.

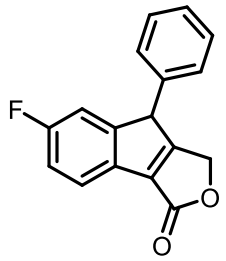

Starting from diazo compound **13k** (20.5 mg, 0.070 mmol), compound **14k** was obtained as a colorless solid (16.4 mg, 88% yield).

MW ($C_{17}H_{11}FO_2$): 266.27 g/mol; **Rf:** 0.40 (Hexanes/EtOAc 8:2). **MP (ºC):** 178. **IR (ATR) ν (cm^{-1}):** 2918, 1740, 1471, 1013, 834, 697. **^{1}H NMR ($CDCl_3$, 400 MHz):** δ_H 7.68 (dd, 1H, J = 8.6, 5.1 Hz), 7.40 – 7.28 (m, 3H), 7.13 – 7.04 (m, 3H), 7.01 (dd, 1H, J = 8.6, 2.3 Hz), 5.12 (d, 1H, J = 18.3 Hz), 4.95 (d, 1H, J = 18.3 Hz), 4.89 (s, 1H).**^{13}C{H} NMR ($CDCl_3$, 101 MHz):** δ_C 175.2 (d, J = 3.5 Hz), 167.4, 162.5 (d, J = 247.1 Hz), 154.0 (d, J = 8.3 Hz), 136.3, 135.6, 130.1 (d, J = 2.6 Hz), 129.7, 128.4, 127.8, 122.1 (d, J = 8.9 Hz), 115.0 (d, J = 23.1 Hz), 113.3 (d, J = 23.9 Hz), 69.1, 53.2, 53.1. **^{19}F NMR ($CDCl_3$, 376 MHz):** δ_F -114.68. (s, 1F). **HRMS (ESI) m/z:** $[M+Na]^+$ calcd. for $C_{17}H_{11}FO_2Na$ 289.0635; Found 289.0643.

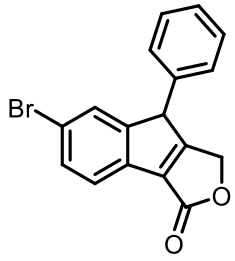

Starting from diazo compound **13l** (24.6 mg, 0.070 mmol), compound **14l** was obtained as a colorless solid (20.3 mg, 89% yield).

MW ($C_{17}H_{11}BrO_2$): 327.18 g/mol; **Rf:** 0.30 (Hexanes/EtOAc 8:2). **MP (ºC):** 163. **IR (ATR) ν (cm^{-1}):** 2918, 1745, 1451, 1012, 948, 827, 698. **^{1}H NMR ($CDCl_3$, 400 MHz):** δ_H 7.61 (d, 1H, J = 8.0 Hz), 7.53 (dd, 1H, J = 8.0, 1.8 Hz), 7.42 (broad signal, 1H), 7.40 – 7.28 (m, 3H), 7.07 (dd, 2H, J = 7.5, 2.1 Hz), 5.11 (dd, 1H, J = 18.4, 1.1 Hz), 4.95 (d, 1H, J = 18.4 Hz), 4.89 (s, 1H). **^{13}C{H} NMR ($CDCl_3$, 101 MHz):** δ_C 175.8, 167.2, 153.6, 136.5, 135.3, 133.0, 131.2, 129.7, 128.7, 128.4, 127.8, 122.4, 121.5, 69.1, 53.1. **HRMS (ESI) m/z:** $[M+Na]^+$ calcd. for $C_{17}H_{11}BrO_2Na$ 348.9835-350.9815; Found 348.9834-350.9816.

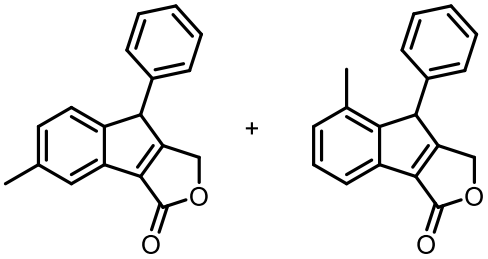

Starting from diazo compound **13m** (31.0 mg, 0.11 mmol), compound 1**4m** (13.9 mg, 50% yield) and compound **14m'** (9.6 mg, 34% yield) were obtained as colorless solids.

14m: MW ($C_{18}H_{14}O_2$): 262.31 g/mol; **Rf:** 0.33 (Hexanes/EtOAc 8:2). **MP (ºC):** 148. **^{1}H NMR ($CDCl_3$, 400 MHz):** δ_H 7.58 (s, 1H), 7.36 – 7.27 (m, 3H), 7.17 (d, *J* = 7.8 Hz, 1H), 7.10 – 7.04 (m, 3H), 5.12 (d, *J* = 18.4 Hz, 1H), 4.94 (d, *J* = 18.4 Hz, 1H), 4.87 (s, 1H), 2.41 (s, 3H). **^{13}C{H} NMR ($CDCl_3$, 101 MHz):** δ_C 176.1, 167.8, 148.8, 137.9, 136.8, 136.6, 134.2, 129.5, 128.0, 127.9, 127.8, 124.9, 122.0, 69.3, 52.8, 21.5. **HRMS (ESI) m/z:** $[M+H]^+$ calcd. for $C_{18}H_{15}O_2$ 263.1067; Found 263.1060.

14m': MW ($C_{18}H_{14}O_2$): 262.31 g/mol; **Rf:** 0.31 (Hexanes/EtOAc 8:2). **MP (ºC):** 185. **^{1}H NMR ($CDCl_3$, 400 MHz):** δ_H 7.61 (d, *J* = 7.6 Hz, 1H), 7.37 – 7.27 (m, 4H), 7.07 (d, *J* = 7.6 Hz, 1H), 7.04 – 6.99 (m, 2H), 5.10 (dd, *J* = 18.2, 1.1 Hz, 1H), 4.88 (s, 1H), 4.78 (d, *J* = 18.2 Hz, 1H), 2.05 (s, 3H). **^{13}C{H} NMR ($CDCl_3$, 101 MHz):** δ_C 176.4, 167.9, 149.3, 136.0, 135.3, 134.6, 129.5, 129.0, 128.4, 128.0, 127.8, 118.9, 69.0, 52.7, 18.8. **HRMS (ESI) m/z:** $[M+H]^+$ calcd. for $C_{18}H_{15}O_2$ 263.1067; Found 263.1064.

Supplementary material for Chapter 6

Experimental procedure for the synthesis of diazo compounds

Diazo compounds **15a-c**[244] **15d-e**[245] and **15i**[233] were prepared as previously described, and their spectroscopic data agrees with those reported in the literature

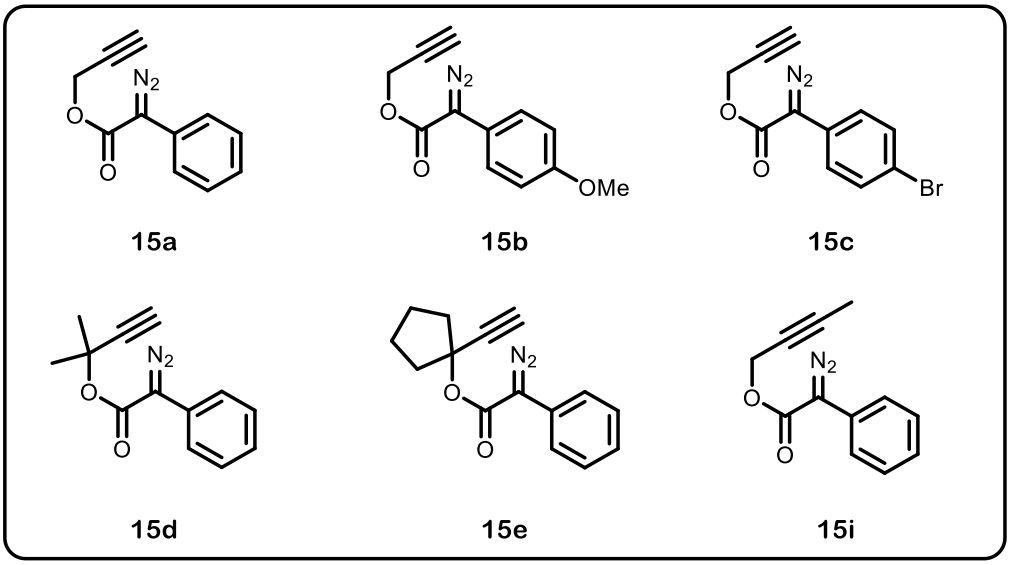

Figure 8.2. Previously reported diazo compounds **15a-15e** and **15i.**

Experimental procedure for the synthesis of diazo compounds 15f-15h

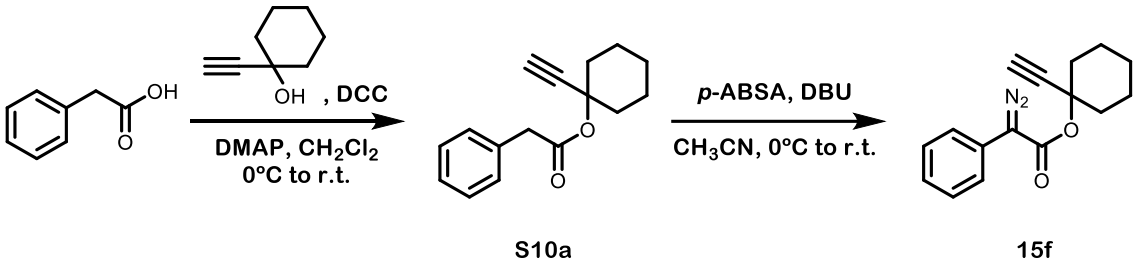

Scheme 8.17. General procedure for the preparation of diazo compounds **15f-15h**.

To a 25 mL round-bottom flask containing a mixture of 1-ethynyl-1-cyclohexanol (0.3 mL, 2.33 mmol), phenylacetic acid (0.32 g, 2.35 mmol), and 4-dimethylaminopyridine (DMAP) (28.5 mg, 0.23 mmol) in dichloromethane (12 mL), N,N'-dicyclohexylcarbodiimide (DCC) (0.51 g, 2.47 mmol) was added in batches at 0 ºC. After the addition, the reaction mixture was slowly warmed to room temperature and stirred overnight. Upon completion of the reaction (TLC monitoring), the crude was filtrated through a Celite pad, rinsed with EtOAc and concentrated under reduced pressure. The crude product was then purified by column chromatography on silica gel (hexanes 100 %) to afford ester **S10a** (0.42 g, 74% yield) as a yellow oil.

To a 50 mL oven-dried flask containing a mixture of **S10a** (0.35 g, 1.44 mmol) and *p*-acetamidobenzenesulfonyl azide (*p*-ABSA) (0.45 g, 1.87 mmol) in anhydrous CH_3CN (5.9 mL), a solution of 1,8-diazabicyclo[5.4.0]undec-

7-ene (DBU) (0.31 mL, 2.1 mmol) in anhydrous CH_3CN (1.3 mL) was added dropwise at 0 ºC. After the addition, the reaction mixture was slowly warmed to room temperature and stirred overnight. Upon completion of the reaction (TLC monitoring), the crude was diluted with dichloromethane, and washed with saturated aqueous NH_4Cl, saturated aqueous $NaHCO_3$ and brine. The combined organic extracts were dried over anhydrous Na_2SO_4 and concentrated under reduced pressure. The crude product was purified by column chromatography on silica gel (hexanes/Et_3N= 99:1) to afford diazo compound **15f** (0.21 g, 54% yield) as an orange solid.

MW ($C_{16}H_{16}N_2O_2$): 268.32; **Rf:** 0.70 (hexanes/EtOAc 9:1). **IR (ATR) ν (cm^{-1}):** 3247, 2930, 2847, 2081, 1697, 1240, 1148, 1017, 748. **^{1}H NMR ($CDCl_3$, 400 MHz):** δ_H 7.53 – 7.48 (m, 2H), 7.40 – 7.34 (m, 2H), 7.22 – 7.13 (m, 1H), 2.67 (s, 1H), 2.24 – 2.11 (m, 2H), 2.07 – 1.95 (m, 2H), 1.71 – 1.61 (m, 4H), 1.59 – 1.48 (m, 1H), 1.47 – 1.36 (m, 1H)**.^{13}C{H} NMR ($CDCl_3$, 101 MHz):** δ_C 163.4, 129.0, 125.9, 125.7, 124.1, 83.8, 76.4, 74.7, 37.4, 25.2, 22.5. **HRMS (ESI) m/z:** $[M+Na]^+$ calcd. for $C_{16}H_{16}N_2O_2Na$ 291.11095; Found 291.1099.

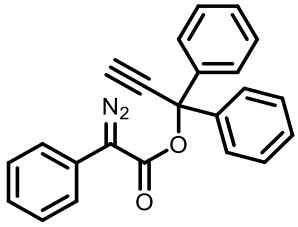

Starting from **1,1-diphenyl-2-propyn-1-ol** (0.46 g, 2.21 mmol)**,** compound **15g** was obtained as an orange solid (0.35 g, 45 % yield).

MW ($C_{23}H_{16}N_2O_2$): 352.39 g/mol; **Rf:** 0.32 (hexanes/EtOAc 9:1). **IR (ATR) ν (cm^{-1}):** 3275, 3055, 2078, 1706, 1136, 1001, 749. **^{1}H NMR ($CDCl_3$, 400 MHz):** δ_H 7.56 – 7.53 (m, 4H), 7.50 – 7.47 (m, 2H), 7.40 – 7.31 (m, 8H), 7.20 – 7.14 (m, 1H), 3.07 (s, 1H). **^{13}C{H} NMR ($CDCl_3$, 101 MHz):** δ_C 162.5, 142.2, 131.5, 131.4, 129.0, 128.9, 128.7, 128.6, 128.4, 128.3, 127.3, 126.2, 125.1, 124.2, 82.4, 80.0, 78.9. **HRMS (ESI) m/z:** $[M+Na]^+$ calcd. for **$C_{23}H_{16}N_2O_2$**Na 375.1104; Found 375.1093.

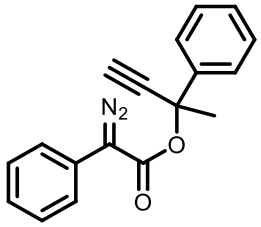

Starting from **2-phenyl-3-butyn-2-ol** (0.29 g, 1.99 mmol)**,** compound **15h** was obtained as an orange oil (0.28 g, 48 % yield).

MW ($C_{18}H_{14}N_2O_2$): 290.32 g/mol; **Rf:** 0.69 (hexanes/EtOAc 9:1). **IR (ATR) ν (cm^{-1}):** 3279, 3024 2081, 1706, 1241, 1143, 1052, 752. **^{1}H NMR ($CDCl_3$, 400 MHz):** δ_H 7.66 – 7.59 (m, 2H), 7.51 – 7.43 (m, 2H), 7.43 – 7.29 (m, 5H), 7.20 – 7.12 (m, 1H), 2.89 (s, 1H), 1.98 (s, 3H). **^{13}C{H} NMR ($CDCl_3$, 101 MHz):** δ_C 162.8, 142.0, 128.9, 128.5, 128.1, 125.9, 125.2, 124.8, 124.0, 82.8, 76.5, 76.2, 32.3. **HRMS (ESI) m/z:** $[M+Na]^+$ calcd. for **$C_{18}H_{14}N_2O_2$**Na 313.0947; Found 313.0951.

General procedure for the silver-catalyzed 6-endo carbene/alkyne metathesis tandem reaction

Scheme 8.18. General procedure for the silver-catalyzed 6-endo carbene/alkyne metathesis tandem reaction.

To an oven-dried Schlenk flask containing $[TpBr_3Ag]_2$ (11.3 mg, 0.0055 mmol) and 4Å MS (100 mg) in anhydrous dichloromethane (18 mL), a solution of diazo compound **15a** (22 mg, 0.11 mmol) in anhydrous dichloromethane (2 mL) was added dropwise over 30 minutes with a syringe pump under a nitrogen atmosphere. After the addition the reaction was stirred for 30 minutes (TLC monitoring). The solvent was then removed under reduced pressure and the crude reaction mixture was purified by column chromatography on silica gel (hexanes/EtOAc from 95:5 to 85:15) to afford compound **16a** (12.9 mg, 68% yield) as a colorless solid.

MW ($C_{11}H_8O_2$): 172.18 g/mol; **Rf:** 0.30 (hexanes/EtOAc 7:3). **^{1}H NMR ($CDCl_3$, 400 MHz):** δ_H 7.68 – 7.62 (m, 2H), 7.51 (dd, 1H, J = 5.1, 2.1 Hz), 7.47 – 7.34 (m, 4H), 6.34 (dd, 1H, J = 6.7, 5.1 Hz). **^{13}C{H} NMR ($CDCl_3$, 101 MHz):** δ_C 161.6, 150.9, 139.3, 134.8, 128.9, 128.8, 128.6, 128.3, 106.9.

The spectroscopic data of **16a** agrees with those previously reported in the literature.[246]

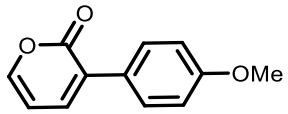

Starting from diazo compound **15b** (27.2 mg, 0.12 mmol)**,** compound **16b** was obtained as a colorless solid (14.1 mg, 58 % yield).

MW ($C_{12}H_{10}O_2$): 202.21 g/mol; **Rf:** 0.48 (hexanes/EtOAc 7:3). **^{1}H NMR ($CDCl_3$, 400 MHz):** δ_H 7.66 – 7.58 (m, 2H), 7.47 (dd, 1H, J = 5.1, 2.1 Hz), 7.39 (dd, 1H, J = 6.7, 2.1 Hz), 6.98 – 6.91 (m, 2H), 6.32 (dd, 1H, J = 6.7, 5.1 Hz), 3.84 (s, 3H). **^{13}C{H} NMR ($CDCl_3$, 101 MHz):** δ_C 161.9, 160.2, 150.2, 138.0, 129.6, 128.4, 127.2, 114.0, 106.9, 55.5.

The spectroscopic data of **16b** agrees with those previously reported in the literature.[246]

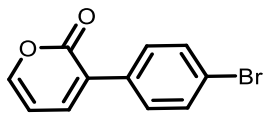

Starting from diazo compound **15c** (28.0 mg, 0.100 mmol)**,** compound **16c** was obtained as a colorless solid (14.2 mg, 56 % yield).

MW ($C_{11}H_7BrO_2$): 251.08 g/mol; **Rf:** 0.22 (hexanes/EtOAc 7:3). **^{1}H NMR ($CDCl_3$, 400 MHz):** δ_H 7.55 (s, 4H), 7.53 (dd, 1H, J = 5.1, 2.1 Hz), 7.45 (dd, 1H, J = 6.7, 2.1 Hz), 6.35 (dd, 1H, J = 6.7, 5.1 Hz). **^{13}C{H} NMR ($CDCl_3$, 101 MHz):** δ_C 161.3, 151.3, 139.4, 133.6, 131.8, 129.9, 127.7, 123.2, 106.8.

The spectroscopic data of **16c** agrees with those previously reported in the literature.[246]

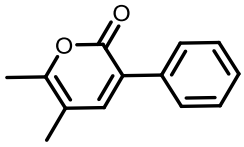

Starting from diazo compound **15d** (22.3 mg, 0.098 mmol)**,** compound **16d** was obtained as a colorless solid (18 mg, 92 % yield).

MW ($C_{13}H_{12}O_2$): 200.24 g/mol; **Rf:** 0.51 (hexanes/EtOAc 7:3). **MP (ºC):** 117-119. **IR (ATR) ν (cm^{-1}):** 3045, 2916, 1698, 1635, 925, 779, 694. **^{1}H NMR ($CDCl_3$, 400 MHz):** δ_H 7.67 – 7.62 (m, 2H), 7.44 – 7.37 (m, 2H), 7.37 – 7.31 (m, 1H), 7.30 (s, 1H), 2.27 (d, J = 1.1 Hz, 3H), 2.05 (d, J = 1.0 Hz, 3H). **^{13}C{H} NMR ($CDCl_3$, 101 MHz):** δ_C 162.4, 157.5, 144.8, 135.0, 128.5, 128.4, 128.2, 124.9, 111.3, 17.5, 15.5. **HRMS (ESI) m/z:** $[M+Na]^+$ calcd. for $C_{13}H_{12}O_2Na$ 223.0730; Found 223.0735.

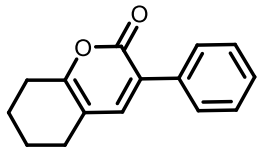

Starting from diazo compound **15e** (29.2 mg, 0.115 mmol)**,** compound **16e** was obtained as a colorless solid (25.4 mg, 98 % yield).

MW ($C_{15}H_{14}O_2$): 226.28 g/mol; **Rf:** 0.6 (hexanes/EtOAc 7:3). **MP (ºC):** 75- 77. **IR (ATR) ν (cm^{-1}):** 3054, 2936, 1795, 1556, 783, 692. **^{1}H NMR ($CDCl_3$, 400 MHz):** δ_H 7.69 – 7.63 (m, 2H), 7.46 – 7.28 (m, 4H), 2.65 – 2.54 (m, 2H), 2.53 – 2.44 (m, 2H), 2.16 – 2.03 (m, 1H), 1.91 – 1.74 (m, 4H). **^{13}C{H} NMR ($CDCl_3$, 101 MHz):** δ_C 162.4, 159.1, 143.2, 135.2, 128.5, 128.3, 128.2, 125.1, 113.2, 27.4, 25.7, 22.2, 21.8. **HRMS (ESI) m/z:** $[M+Na]^+$ calcd. for $C_{15}H_{14}O_2Na$ 249.0888; Found 249.0890.

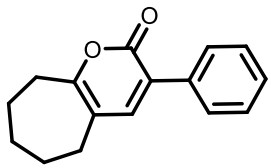

Starting from diazo compound **15f** (26.1 mg, 0.097 mmol)**,** compound **16f** was obtained as a colorless solid (19.2 mg, 82 % yield).

MW ($C_{16}H_{16}O_2$): 240.30 g/mol; **Rf:** 0.68 (hexanes/EtOAc 7:3). **MP (ºC):** 115 – 117. **IR (ATR) ν (cm^{-1}):** 3052, 2911, 1695, 1545, 934, 783, 695. **^{1}H NMR ($CDCl_3$, 400 MHz):** δ_H 7.69 – 7.63 (m, 2H), 7.44 – 7.37 (m, 2H), 7.36 – 7.32 (m, 1H), 7.31 (s, 1H), 2.81 – 2.72 (m, 2H), 2.58 – 2.50 (m, 2H), 1.89 – 1.78 (m, 2H), 1.76 – 1.62 (m,

4H). **^{13}C{H} NMR ($CDCl_3$, 101 MHz):** δ_C 164.5, 162.4, 145.2, 135.1, 128.5, 128.3, 128.2, 123.9, 118.5, 34.3, 31.7, 31.6, 27.1, 24.9. **HRMS (ESI) m/z:** $[M+Na]^+$ calcd. for $C_{16}H_{16}O_2Na$ 263.1043; Found 263.1043.

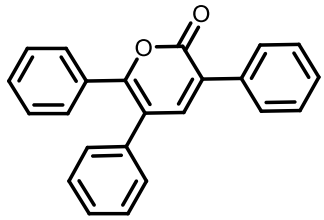

Starting from diazo compound **15g (**51.5 mg, 0.146 mmol)**,** compound **16g** was obtained as a yellow solid (42.4 mg, 89% yield).

MW ($C_{23}H_{16}O_2$): 324.38 g/mol; **Rf:** 0.62 (hexanes/EtOAc 8:2). **^{1}H NMR ($CDCl_3$, 400 MHz):** δ_H 7.79 – 7.73 (m, 2H), 7.62 (s, 1H), 7.47 – 7.37 (m, 5H), 7.37 – 7.30 (m, 4H), 7.30 – 7.24 (m, 1H), 7.26 – 7.22 (m, 3H). **^{13}C{H} NMR ($CDCl_3$, 101 MHz):** δ_C 161.4, 156.9, 144.5, 136.6, 134.6, 132.1, 130.1, 129.4, 129.3, 129.2, 128.8, 128.7, 128.4, 128.3, 128.1, 125.8, 118.8.

The spectroscopic data of **2h** agrees with those previously reported in the literature.[247]

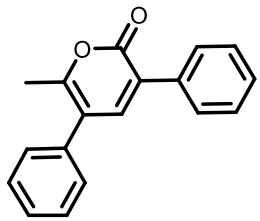

Starting from diazo compound **15h (**47.6 mg, 0.164 mmol)**,** compound **16h** was obtained as colorless oil (34.1 mg, 79 % yield).

MW ($C_{18}H_{14}O_2$): 262.31 g/mol; **Rf:** 0.61 (hexanes/EtOAc 8:2). **^{1}H NMR ($CDCl_3$, 400 MHz):** δ_H 7.72 – 7.67 (m, 2H), 7.50 (s, 1H), 7.48 – 7.35 (m, 6H), 7.35 – 7.28 (m, 2H), 2.33 (s, 3H). **^{13}C{H} NMR ($CDCl_3$, 101 MHz):** δ_C 162.0, 158.5, 143.6, 136.1, 134.7, 129.04, 128.99, 128.60, 128.59, 128.3, 128.1, 125.0, 118.9, 18.5.

The spectroscopic data of **16h** agrees with those previously reported in the literature.[247]

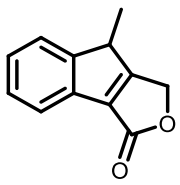

Starting from diazo compound **15i** (44.3 mg, 0.207 mmol)**,** compound **17b** was obtained as a colorless solid (34.7 mg, 90 % yield).

MW ($C_{12}H_{10}O_2$): 186.21 g/mol; **Rf:** 0.40 (hexanes/EtOAc 7:3). **^{1}H NMR ($CDCl_3$, 400 MHz):** δ_H 7.70 (d, 1H, J = 7.0 Hz), 7.46 (d, 1H, J = 7.0 Hz), 7.36 (td, 1H, J = 7.5, 1.5 Hz), 7.32 (td, 1H, J = 7.5, 1.5 Hz), 5.14 (s, 2H), 3.83

(q, 1H, J = 7.7), 1.48 (d, 3H, J = 7.7 Hz). **^{13}C{H} NMR ($CDCl_3$, 101 MHz):** δ_C 177.3, 167.9, 152.4, 135.8, 133.9, 127.6, 126.8, 123.9, 121.1, 69.1, 41.9, 15.7.

The spectroscopic data of **17b** agrees with those previously reported in the literature.[248]

General procedure for the rhodium-catalyzed 5-exo carbene/alkyne metathesis tandem reaction

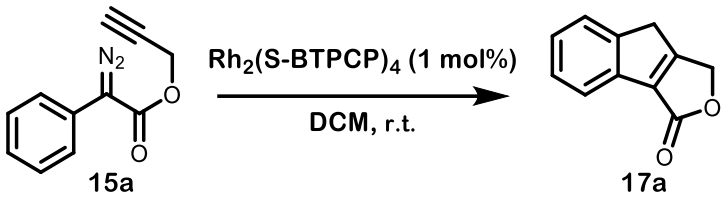

Scheme 8.19. General procedure for the rhodium-catalyzed 5-exo carbene/alkyne metathesis tandem reaction.

To an oven-dried Schlenk flask containing diazo compound **15a** (18.6 mg, 0.093 mmol) in anhydrous dichloromethane (2 mL), a solution of Rh_2(S-BTPCP)$_4$ (1.6 mg, 0.0009 mmol) in dichloromethane (1 mL) was added dropwise under a nitrogen atmosphere. The mixture was stirred for 1.5 hours (TLC monitoring). The solvent was then removed under reduced pressure and the crude reaction mixture was purified by column chromatography on silica gel (hexanes/EtOAc from95:5 to 85:15) to afford compound **17a** (11.6 mg, 72% yield) as a colorless solid.

MW ($C_{11}H_8O_2$): 172.18 g/mol; **Rf:** 0.23 (hexanes/EtOAc 7:3). **MP (ºC):** 161 -163. IR **(ATR) ν (cm^{-1}):** 2932, 1738, 1369, 972, 776. **^{1}H NMR ($CDCl_3$, 400 MHz):** δ_H 7.73 (d, 1H, J = 8.4 Hz), 7.52 (d, 1H, J = 7.5 Hz), 7.38 (t, 1H, J = 7.5 Hz), 7.31 (td, 1H, J = 7.5, 1.3 Hz), 5.19 (s, 2H), 3.70 (s, 2H). **^{13}C{H} NMR ($CDCl_3$, 101 MHz):** δ_C 172.1, 167.7, 146.6, 137.8, 135.0, 127.5, 126.6, 125.0, 121.1, 70.1, 35.4. **HRMS (ESI) m/z:** $[M+Na]^+$ calcd. for $C_{11}H_8O_2Na$ 195.0417; Found 195.0420.

References

1. Ei-ichi, N., Transition Metal-Catalyzed Organometallic Reactions that Have Revolutionized Organic Synthesis. *Bulletin of the Chemical Society of Japan* **2007,** *80* (2), 233-257.

2. de Frémont, P.; Marion, N.; Nolan, S. P., Carbenes: Synthesis, properties, and organometallic chemistry. *Coordination Chemistry Reviews* **2009,** *253* (7), 862-892.

3. Hermann, M., Ueber die bei der technischen Gewinnung des Broms beobachtete flüchtige Bromverbindung. *Justus Liebigs Annalen der Chemie* **1855,** *95* (2), 211-225.

4. Nef, J. U., Ueber das zweiwerthige Kohlenstoffatom. (Vierte Abhandlung.) Die Chemie des Methylens. *Justus Liebigs Annalen der Chemie* **1897,** *298* (2-3), 202-374.

5. Buchner, E.; Feldmann, L., Diazoessigester und Toluol. *Berichte der deutschen chemischen Gesellschaft* **1903,** *36* (3), 3509-3517.

6. Buchner, E.; Geronimus, J., Ueber trans-Phenyltrimethylencarbonsäure. *Berichte der deutschen chemischen Gesellschaft* **1903,** *36* (4), 3782-3786.

7. Doering, W. v. E.; Knox, L. H., Synthesis of Substituted Tropolones. *Journal of the American Chemical Society* **1953,** *75* (2), 297-303.

8. von E. Doering, W.; Hoffmann, A. K., The Addition of Dichlorocarbene to Olefins. *Journal of the American Chemical Society* **1954,** *76* (23), 6162-6165.

9. Arduengo, A. J., III; Harlow, R. L.; Kline, M., A stable crystalline carbene. *Journal of the American Chemical Society* **1991,** *113* (1), 361-363.

10. Tschugajeff, L.; Skanawy-Grigorjewa, M.; Posnjak, A.; Skanawy-Grigorjewa, M., Über Die Hydrazin-Carbylamin-Komplexe des Platins. *Zeitschrift für anorganische und allgemeine Chemie* **1925,** *148* (1), 37-42.

11. Rouschias, G.; Shaw, B. L., A revised structure for Chugaev's salt $[PtC_8H_{15}N_6]Cl$. *Journal of the Chemical Society D: Chemical Communications* **1970,** (3), 183-183.

12. Fischer, E. O.; Maasböl, A., On the Existence of a Tungsten Carbonyl Carbene Complex. *Angewandte Chemie International Edition in English* **1964,** *3* (8), 580-581.

13. a) Vyboishchikov, S. F.; Frenking, G., Structure and Bonding of Low-Valent (Fischer-Type) and High-Valent (Schrock-Type) Transition Metal Carbene Complexes. *Chemistry – A European Journal* **1998,** *4* (8), 1428-1438; b) Frenking, G.; Solà, M.; Vyboishchikov, S. F., Chemical bonding in transition metal carbene complexes. *Journal of Organometallic Chemistry* **2005,** *690* (24), 6178-6204.

14. a) Davies, H. M. L.; Beckwith, R. E. J., Catalytic Enantioselective C−H Activation by Means of Metal−Carbenoid-Induced C−H Insertion. *Chemical Reviews* **2003,** *103* (8), 2861-2904; b) Davies, H. M. L.; Hedley, S. J., Intermolecular reactions of electron-rich heterocycles with copper and rhodium carbenoids. *Chemical Society Reviews* **2007,** *36* (7), 1109-1119.

15. Green, S. P.; Wheelhouse, K. M.; Payne, A. D.; Hallett, J. P.; Miller, P. W.; Bull, J. A., Thermal Stability and Explosive Hazard Assessment of Diazo Compounds and Diazo Transfer Reagents. *Organic Process Research & Development* **2020,** *24* (1), 67-84.

16. a) Wang, K.; Wang, J., Transition-Metal-Catalyzed Cross-Coupling with Non-Diazo Carbene Precursors. *Synlett* **2019,** *30* (05), 542-551; b) Jia, M.; Ma, S., New Approaches to the Synthesis of Metal Carbenes. *Angewandte Chemie International Edition* **2016,** *55* (32), 9134-9166.

17. Xia, Y.; Wang, J., N-Tosylhydrazones: versatile synthons in the construction of cyclic compounds. *Chemical Society Reviews* **2017,** *46* (8), 2306-2362; Liu, Z.; Sivaguru, P.; Zanoni, G.; Bi, X., N-

Triftosylhydrazones: A New Chapter for Diazo-Based Carbene Chemistry. *Accounts of Chemical Research* **2022,** *55* (12), 1763-1781.

18. Bisag, G. D.; Ruggieri, S.; Fochi, M.; Bernardi, L., Sulfoxonium ylides: simple compounds with chameleonic reactivity. *Organic & Biomolecular Chemistry* **2020,** *18* (43), 8793-8809.

19.Kumar, S.; Borkar, V.; Mujahid, M.; Nunewar, S.; Kanchupalli, V., Iodonium ylides: an emerging and alternative carbene precursor for C–H functionalizations. *Organic & Biomolecular Chemistry* **2023,** *21* (1), 24-38.

20. Akter, M.; Rupa, K.; Anbarasan, P., 1,2,3-Triazole and Its Analogues: New Surrogates for Diazo Compounds. *Chemical Reviews* **2022,** *122* (15), 13108-13205.

21. a) Mato, M.; García-Morales, C.; Echavarren, A. M., Generation of Gold(I) Carbenes by Retro-Buchner Reaction: From Cyclopropanes to Natural Products Synthesis. *ChemCatChem* **2019,** *11* (1), 53-72; b) Armengol-Relats, H.; Mato, M.; Escofet, I.; Echavarren, A. M., Assembling Complex Structures through Cascade and Cycloaddition Processes via Non-Acceptor Gold or Rhodium Carbenes. *Synthesis* **2021,** *53* (21), 3991-4003.

22. Wang, T.; Hashmi, A. S. K., 1,2-Migrations onto Gold Carbene Centers. *Chemical Reviews* **2021,** *121* (14), 8948-8978.

23. Miege, F.; Meyer, C.; Cossy, J., When cyclopropenes meet gold catalysts. *Beilstein Journal of Organic Chemistry* **2011,** *7*, 717-734; Zhu, Z.-B.; Wei, Y.; Shi, M., Recent developments of cyclopropene chemistry. *Chemical Society Reviews* **2011,** *40* (11), 5534-5563.

24. Leftin, J. H.; Gil-Av, E., Metal-catalyzed stereospecific ring-opening of 1,2-dialkyl-3-carbomethoxycyclopropenes. *Tetrahedron Letters* **1972,** *13* (32), 3368-3370.

25. Binger, P.; McMeeking, J., Codimerization of 3,3-Dimethylcyclopropene with Ethylenecarboxylic Esters at Nickel(0) Catalysts. *Angewandte Chemie International Edition in English* **1974,** *13* (7), 466-467.

26. Binger, P.; Brinkmann, A., Cyclische Ketone aus 3,3-Dimethyl-1-cyclopropen und Kohlenmonoxid durch katalysierte Cotrimerisation. *Chemische Berichte* **1978,** *111* (7), 2689-2695.

27. Salomon, R. G.; Salomon, M. F.; Heyne, T. R., Vinylcyclopropanation of olefins with vinyldiazomethane. *The Journal of Organic Chemistry* **1975,** *40* (6), 756-760.

28. Davies, H. M. L.; Clark, D. M.; Smith, T. K., [3 + 4] Cycloaddition reactions of vinyl carbenoids with furans. *Tetrahedron Letters* **1985,** *26* (46), 5659-5662.

29. Davies, H. M. L.; Clark, D. M.; Alligood, D. B.; Eiband, G. R., Mechanistic aspects of formal [3 + 4] cycloadditions between vinylcarbenoids and furans. *Tetrahedron* **1987,** *43* (19), 4265-4270.

30. Davies, H. M. L., Tandem cyclopropanation/cope rearrangement: a general method for the construction of seven-membered rings. *Tetrahedron* **1993,** *49* (24), 5203-5223.

31. Davies, H. M. L.; Smith, H. D.; Korkor, O., Tandem cyclopropanation/Cope rearrangement sequence. Stereospecific [3 + 4] cycloaddition reaction of vinylcarbenoids with cyclopentadiene. *Tetrahedron Letters* **1987,** *28* (17), 1853-1856.

32. Wulff, W. D.; Yang, D. C.; Murray, C. K., [2 + 1]- Versus [4 + 2]-cycloadditions of Fischer carbene complexes with 1,3-dienes. Evidence for a zwitterionic intermediate in a cyclopropanation reaction. *Journal of the American Chemical Society* **1988,** *110* (8), 2653-2655.

33. Cantrell, W. R., Jr.; Davies, H. M. L., Stereoselective convergent synthesis of hydroazulenes via an intermolecular cyclopropanation/Cope rearrangement. *The Journal of Organic Chemistry* **1991,** *56* (2), 723-727.

34. a) Davies, H. M. L.; Oldenburg, C. E. M.; McAfee, M. J.; Nordahl, J. G.; Henretta, J. P.; Romines, K. R., Novel approach to seven-membered rings by the intramolecular tandem cyclopropanation/cope rearrangement sequence. *Tetrahedron Letters* **1988,** *29* (9), 975-978; b) Davies, H. M. L.; McAfee, M. J.; Oldenburg, C. E. M., Scope and stereochemistry of the tandem intramolecular cyclopropanation/Cope rearrangement sequence. *The Journal of Organic Chemistry* **1989,** *54* (4), 930-936.

35. Davies, H. M. L.; Young, W. B.; Smith, H. D., Novel entry to the tropane system by reaction of rhodium(II) acetate stabilized vinylcarbenoids with pyrroles. *Tetrahedron Letters* **1989,** *30* (35), 4653-4656.

36. Davies, H. M. L.; Matasi, J. J.; Ahmed, G., Divergent Pathways in the Intramolecular Reactions between Rhodium-Stabilized Vinylcarbenoids and Pyrroles: Construction of Fused Tropanes and 7-Azabicyclo[4.2.0]octadienes. *The Journal of Organic Chemistry* **1996,** *61* (7), 2305-2313.

37. a) Cheng, Q.-Q.; Deng, Y.; Lankelma, M.; Doyle, M. P., Cycloaddition reactions of enoldiazo compounds. *Chemical Society Reviews* **2017,** *46* (17), 5425-5443; b) Marichev, K. O.; Doyle, M. P., Catalytic asymmetric cycloaddition reactions of enoldiazo compounds. *Organic & Biomolecular Chemistry* **2019,** *17* (17), 4183-4195.

38. Davies, H. M. L.; Peng, Z.-Q.; Houser, J. H., Asymmetric synthesis of 1,4-cycloheptadienes and bicyclo[3.2.1]octa-2,6-dienes by rhodium(II) N-(p-(tert-butyl)phenylsulfonyl)prolinate catalyzed reactions between vinyldiazomethanes and dienes. *Tetrahedron Letters* **1994,** *35* (48), 8939-8942.

39. Reddy, R. P.; Davies, H. M. L., Asymmetric Synthesis of Tropanes by Rhodium-Catalyzed [4 + 3] Cycloaddition. *Journal of the American Chemical Society* **2007,** *129* (34), 10312-10313.

40. Doyle, M. P.; Hu, W.; Timmons, D. J., Highly Stereoselective Syntheses of Five- and Seven-Membered Ring Heterocycles from Ylides Generated by Catalytic Reactions of Styryldiazoacetates with Aldehydes and Imines. *Organic Letters* **2001,** *3* (23), 3741-3744.

41. Xu, X.; Hu, W.-H.; Zavalij, P. Y.; Doyle, M. P., Divergent Outcomes of Carbene Transfer Reactions from Dirhodium- and Copper-Based Catalysts Separately or in Combination. *Angewandte Chemie International Edition* **2011,** *50* (47), 11152-11155.

42. Xu, X.; Wang, X.; Zavalij, P. Y.; Doyle, M. P., Straightforward Access to the [3.2.2]Nonatriene Structural Framework via Intramolecular Cyclopropenation/Buchner Reaction/Cope Rearrangement Cascade. *Organic Letters* **2015,** *17* (4), 790-793.

43. Davies, H. M. L.; Smith, H. D.; Hu, B.; Klenzak, S. M.; Hegner, F. J., Divergent reaction pathways between rhodium(II)-stabilized vinylcarbenoids and benzenes. *The Journal of Organic Chemistry* **1992,** *57* (25), 6900-6903.

44. Qin, C.; Boyarskikh, V.; Hansen, J. H.; Hardcastle, K. I.; Musaev, D. G.; Davies, H. M. L., D2-Symmetric Dirhodium Catalyst Derived from a 1,2,2-Triarylcyclopropanecarboxylate Ligand: Design, Synthesis and Application. *Journal of the American Chemical Society* **2011,** *133* (47), 19198-19204.

45. Guzmán, P. E.; Lian, Y.; Davies, H. M. L., Reversal of the Regiochemistry in the Rhodium-Catalyzed [4+3] Cycloaddition between Vinyldiazoacetates and Dienes. *Angewandte Chemie International Edition* **2014,** *53* (48), 13083-13087.

46. Shapiro, N. D.; Toste, F. D., Synthesis of Azepines by a Gold-Catalyzed Intermolecular [4 + 3]-Annulation. *Journal of the American Chemical Society* **2008,** *130* (29), 9244-9245.

47. Gung, B. W.; Bailey, L. N.; Wonser, J., Gold-catalyzed intermolecular [4C+3C] cycloaddition reactions. *Tetrahedron Letters* **2010,** *51* (17), 2251-2253.

48. Garayalde, D.; Krüger, K.; Nevado, C., Gold-Catalyzed Cyclopenta- and Cycloheptannulation Cascades: A Stereocontrolled Approach to the Scaffold of Frondosins A and B. *Angewandte Chemie International Edition* **2011,** *50* (4), 911-915.

49. Yang, J.-M.; Tang, X.-Y.; Shi, M., Gold(I)-Catalyzed Intramolecular Cycloisomerization of Propargylic Esters with Furan Rings. *Chemistry – A European Journal* **2015,** *21* (12), 4534-4540.

50. a) Shu, D.; Song, W.; Li, X.; Tang, W., Rhodium- and Platinum-Catalyzed [4+3] Cycloaddition with Concomitant Indole Annulation: Synthesis of Cyclohepta[b]indoles. *Angewandte Chemie International Edition* **2013,** *52* (11), 3237-3240; b) Kusama, H.; Sogo, H.; Saito, K.; Suga, T.; Iwasawa, N., Construction of Cyclohepta[b]indoles via Platinum-Catalyzed Intermolecular Formal [4+3]-Cycloaddition Reaction of α,β-Unsaturated Carbene Complex Intermediates with Siloxydienes. *Synlett* **2013,** *24* (11), 1364-1370.

51. Drew, M. A.; Arndt, S.; Richardson, C.; Rudolph, M.; Hashmi, A. S. K.; Hyland, C. J. T., Divergent gold-catalysed reactions of cyclopropenylmethyl sulfonamides with tethered heteroaromatics. *Chemical Communications* **2019,** *55* (93), 13971-13974.

52. Wu, R.; Chen, Y.; Zhu, S., Rh(II)-Catalyzed Enynal Cycloisomerization for the Generation of Vinyl Carbene: Divergent Access to Polycyclic Heterocycles. *ACS Catalysis* **2023,** *13* (1), 132-140.

53. a) Wu, R.; Lu, J.; Cao, T.; Ma, J.; Chen, K.; Zhu, S., Enantioselective Rh(II)-Catalyzed Desymmetric Cycloisomerization of Diynes: Constructing Furan-Fused Dihydropiperidines with an Alkyne-Substituted Aza-Quaternary Stereocenter. *Journal of the American Chemical Society* **2021,** *143* (36), 14916-14925; b) Wu, R.; Chen, K.; Ma, J.; Yu, Z.-X.; Zhu, S., Synergy of activating substrate and introducing C-H···O interaction to achieve Rh_2(II)-catalyzed asymmetric cycloisomerization of 1,n-enynes. *Science China Chemistry* **2020,** *63* (9), 1230-1239; c) Wang, C.; Wu, R.; Chen, K.; Zhu, S., Enantioselective Synthesis of Biscyclopropanes Using Alkynes as Dicarbene Equivalents. *Angewandte Chemie International Edition* **2023,** *62* (29), e202305864; d) Qiu, S.; Gao, X.; Zhu, S., Dirhodium(ii)-catalysed cycloisomerization of azaenyne: rapid assembly of centrally and axially chiral isoindazole frameworks. *Chemical Science* **2021,** *12* (41), 13730-13736.

54. Brewbaker, J. L.; Hart, H., Cyclization of 3-diazoalkenes to pyrazoles. *Journal of the American Chemical Society* **1969,** *91* (3), 711-715.

55. Fang, Z.; Ma, Y.; Liu, S.; Bai, H.; Li, S.; Ning, Y.; Zanoni, G.; Liu, Z., Silver-catalyzed [4 + 3] cycloaddition of 1,3-dienes with alkenyl-N-triftosylhydrazones: a practical approach to 1,4-cycloheptadienes. *Organic Chemistry Frontiers* **2022,** *9* (16), 4426-4434.

56. Liu, Z.; Yang, Y.; Jiang, X.; Song, Q.; Zanoni, G.; Liu, S.; Bi, X., Dearomative [4 + 3] cycloaddition of furans with vinyl-N-triftosylhydrazones by silver catalysis: stereoselective access to oxa-bridged seven-membered bicycles. *Organic Chemistry Frontiers* **2022,** *9* (9), 2444-2452.

57. Davies, H. M. L.; Clark, T. J.; Church, L. A., Stereoselective cyclopropanations with vinylcarbenoids. *Tetrahedron Letters* **1989,** *30* (38), 5057-5060.

58. Davies, H. M. L.; Hu, B., Highly stereoselective [3 + 2] annulations by cyclopropanation of vinyl ethers with rhodium(II)-stabilized vinylcarbenoids followed by a formally forbidden 1,3-sigmatropic rearrangement. *The Journal of Organic Chemistry* **1992,** *57* (11), 3186-3190.

59. a) Davies, H. M. L.; Hutcheson, D. K., Enantioselective synthesis of vinylcyclopropanes by rhodium(II) catalyzed decomposition of vinyldiazomethanes in the presence of alkenes. *Tetrahedron Letters* **1993,** *34* (45), 7243-7246; b) Davies, H. M. L.; Kong, N.; Churchill, M. R., Asymmetric Synthesis of Cyclopentenes by [3 + 2] Annulations between Vinylcarbenoids and Vinyl Ethers. *The Journal of Organic Chemistry* **1998,** *63* (19), 6586-6589.

60. a) Miki, K.; Ohe, K.; Uemura, S., A new ruthenium-catalyzed cyclopropanation of alkenes using propargylic acetates as a precursor of vinylcarbenoids. *Tetrahedron Letters* **2003,** *44* (10), 2019-2022; b) Miki, K.; Ohe, K.; Uemura, S., Ruthenium-Catalyzed Cyclopropanation of Alkenes Using Propargylic Carboxylates as Precursors of Vinylcarbenoids. *The Journal of Organic Chemistry* **2003,** *68* (22), 8505-8513.

61. Johansson, M. J.; Gorin, D. J.; Staben, S. T.; Toste, F. D., Gold(I)-Catalyzed Stereoselective Olefin Cyclopropanation. *Journal of the American Chemical Society* **2005,** *127* (51), 18002-18003.

62. Miege, F.; Meyer, C.; Cossy, J., Synthesis of 3-Oxa- and 3-Azabicyclo[4.1.0]heptanes by Gold-Catalyzed Cycloisomerization of Cyclopropenes. *Organic Letters* **2010,** *12* (18), 4144-4147.

63. Miege, F.; Meyer, C.; Cossy, J., Gold(I)-Catalysed Cycloisomerisation of 1,6-Cyclopropene-enes. *Chemistry – A European Journal* **2012,** *18* (25), 7810-7822.

64. Miege, F.; Meyer, C.; Cossy, J., Rhodium-Catalyzed Cycloisomerization Involving Cyclopropenes: Efficient Stereoselective Synthesis of Medium-Sized Heterocyclic Scaffolds. *Angewandte Chemie International Edition* **2011,** *50* (26), 5932-5937.

65. Yang, Y.; Liu, Z.; Song, Q.; Sivaguru, P.; Zanoni, G.; Wang, K.; Bi, Q.; Bi, X., The merger of vinyl-N-triftosylhydrazones and silver catalysis to enable stereoselective vinylcyclopropanation of alkenes. *Chem Catalysis* **2022,** *2* (3), 563-577.

66. Herlé, B.; Holstein, P. M.; Echavarren, A. M., Stereoselective cis-Vinylcyclopropanation via a Gold(I)-Catalyzed Retro-Buchner Reaction under Mild Conditions. *ACS Catalysis* **2017,** *7* (5), 3668-3675.

67. Mato, M.; Herlé, B.; Echavarren, A. M., Cyclopropanation by Gold- or Zinc-Catalyzed Retro-Buchner Reaction at Room Temperature. *Organic Letters* **2018,** *20* (14), 4341-4345.

68. Mato, M.; Echavarren, A. M., Donor Rhodium Carbenes by Retro-Buchner Reaction. *Angewandte Chemie International Edition* **2019,** *58* (7), 2088-2092.

69. a) Hamaguchi, M.; Matsubara, H.; Nagai, T., Reaction of vinylcarbenoids with aldehydes: formation of vinylcarbonyl ylides followed by ring closure to oxiranes and dihydrofurans. *Tetrahedron Letters* **2000,** *41* (9), 1457-1460; b) Hamaguchi, M.; Matsubara, H.; Nagai, T., Reaction of Vinylcarbenoids with Benzaldehydes: Formation of Vinylcarbonyl Ylides Followed by Ring Closure to Oxiranes and Dihydrofurans. *The Journal of Organic Chemistry* **2001,** *66* (16), 5395-5404.

70. Hamaguchi, M.; Funakoshi, N.; Oshima, T., Reaction of vinylcarbenoids with thioketones: formation of vinylthiocarbonyl ylides followed by ring closure to thiiranes and dihydrothiophenes. *Tetrahedron Letters* **1999,** *40* (46), 8117-8120.

71. Aggarwal, V. K.; Alonso, E.; Bae, I.; Hynd, G.; Lydon, K. M.; Palmer, M. J.; Patel, M.; Porcelloni, M.; Richardson, J.; Stenson, R. A.; Studley, J. R.; Vasse, J.-L.; Winn, C. L., A New Protocol for the In Situ

Generation of Aromatic, Heteroaromatic, and Unsaturated Diazo Compounds and Its Application in Catalytic and Asymmetric Epoxidation of Carbonyl Compounds. Extensive Studies To Map Out Scope and Limitations, and Rationalization of Diastereo- and Enantioselectivities. *Journal of the American Chemical Society* **2003,** *125* (36), 10926-10940.

72. Lin, X.; Pu, M.; Sang, X.; Li, S.; Liu, X.; Wu, Y.-D.; Feng, X., Asymmetric Catalytic (2+1) Cycloaddition of Thioketones to Synthesize Tetrasubstituted Thiiranes. *Angewandte Chemie International Edition* **2022,** *61* (19), e202201151.

73. Briones, J. F.; Hansen, J.; Hardcastle, K. I.; Autschbach, J.; Davies, H. M. L., Highly Enantioselective Rh_2(S-DOSP)$_4$-Catalyzed Cyclopropenation of Alkynes with Styryldiazoacetates. *Journal of the American Chemical Society* **2010,** *132* (48), 17211-17215.

74. Briones, J. F.; Davies, H. M. L., Rh_2(S-PTAD)$_4$-catalyzed asymmetric cyclopropenation of aryl alkynes. *Tetrahedron* **2011,** *67* (24), 4313-4317.

75. Wang, Z.; Xu, G.; Tang, S.; Shao, Y.; Sun, J., Catalyst-Controlled Selective Alkylation/Cyclopropanation of Indoles with Vinyl Diazoesters. *Organic Letters* **2019,** *21* (20), 8488-8491.

76. Fang, R.; Yang, L.; Zhou, L.; Kirillov, A. M.; Yang, L., Carbocation versus Carbene Controlled Chemoselectivity: DFT Study on Gold- and Silver-Catalyzed Alkylation/Cyclopropanation of Indoles with Vinyl Diazoesters. *Organic Letters* **2020,** *22* (10), 4043-4048.

77. Ross, R. J.; Jeyaseelan, R.; Lautens, M., Rhodium-Catalyzed Intermolecular Cyclopropanation of Benzofurans, Indoles, and Alkenes via Cyclopropene Ring Opening. *Organic Letters* **2020,** *22* (12), 4838-4843.

78. Guo, P.; Sun, W.; Liu, Y.; Li, Y.-X.; Loh, T.-P.; Jiang, Y., Stereoselective Synthesis of Vinylcyclopropa[b]indolines via a Rh-Migration Strategy. *Organic Letters* **2020,** *22* (15), 5978-5983.

79. Davies, H. M. L.; Hu, B., Regioselective [3 + 2] annulations with rhodium(ii)-stabilized vinylcarbenoids. *Tetrahedron Letters* **1992,** *33* (4), 455-456.

80. Davies, H. M. L.; Xiang, B.; Kong, N.; Stafford, D. G., Catalytic Asymmetric Synthesis of Highly Functionalized Cyclopentenes by a [3 + 2] Cycloaddition. *Journal of the American Chemical Society* **2001,** *123* (30), 7461-7462.

81. Smith, A. G.; Davies, H. M. L., Rhodium-Catalyzed Enantioselective Vinylogous Addition of Enol Ethers to Vinyldiazoacetates. *Journal of the American Chemical Society* **2012,** *134* (44), 18241-18244.

82. Briones, J. F.; Davies, H. M. L., Enantioselective Gold(I)-Catalyzed Vinylogous [3 + 2] Cycloaddition between Vinyldiazoacetates and Enol Ethers. *Journal of the American Chemical Society* **2013,** *135* (36), 13314-13317.

83. López, E.; Lonzi, G.; López, L. A., Synthesis of Functionalized Cyclopentene Derivatives through Gold-Catalyzed Reaction of Stabilized Vinyldiazo Compounds and Styrenes. *Synthesis* **2017,** *49* (19), 4461-4468.

84. Yamamoto, K.; López, E.; Barrio, P.; Borge, J.; López, L. A., Gold-Catalyzed [3+2] Carbocycloaddition Reaction of Pinacol Alkenylboronates: Stereospecific Synthesis of Boryl-Functionalized Cyclopentene Derivatives. *Chemistry – A European Journal* **2020,** *26* (31), 6999-7003.

85. Yang, W.; Yang, Z.; Chen, L.; Lu, Y.; Zhang, C.; Su, Z.; Liu, X.; Feng, X., Chiral nickel(II) complex catalyzed asymmetric (3 + 2) cycloaddition of α-diazo pyrazoleamides with 2-siloxy-1-alkenes. *Chinese Chemical Letters* **2023,** *34* (4), 107791.

86. Saito, K.; Sogou, H.; Suga, T.; Kusama, H.; Iwasawa, N., Platinum(II)-Catalyzed Generation and [3+2] Cycloaddition Reaction of α,β-Unsaturated Carbene Complex Intermediates for the Preparation of Polycyclic Compounds. *Journal of the American Chemical Society* **2011,** *133* (4), 689-691.

87. Liu, T.; Han, L.; Liu, Y.; Zhang, D.; Li, W.-Z., Theoretical investigation on the Pt(II)-catalyzed [3+2] cycloaddition reactions of propargyl ether derivatives with n-butyl vinyl ether. *Computational and Theoretical Chemistry* **2012,** *992*, 97-102.

88. Rettenmeier, E.; Schuster, A. M.; Rudolph, M.; Rominger, F.; Gade, C. A.; Hashmi, A. S. K., Gold Catalysis: Highly Functionalized Cyclopentadienes Prepared by Intermolecular Cyclization of Ynamides and Propargylic Carboxylates. *Angewandte Chemie International Edition* **2013,** *52* (22), 5880-5884.

89. Cheng, X.; Zhu, L.; Lin, M.; Chen, J.; Huang, X., Rapid access to cyclopentadiene derivatives through gold-catalyzed cycloisomerization of ynamides with cyclopropenes by preferential activation of alkenes over alkynes. *Chemical Communications* **2017,** *53* (26), 3745-3748.

90. López, E.; Lonzi, G.; González, J.; López, L. A., Gold-catalyzed intermolecular formal (3+2) cycloaddition of stabilized vinyldiazo derivatives and electronically unbiased allenes. *Chemical Communications* **2016,** *52* (60), 9398-9401.

91. López, E.; González, J.; López, L. A., Unusual Regioselectivity in the Gold(I)-Catalyzed [3+2] Carbocycloaddition Reaction of Vinyldiazo Compounds and N-Allenamides. *Advanced Synthesis & Catalysis* **2016,** *358* (9), 1428-1432.

92. Yin, X.; Mato, M.; Echavarren, A. M., Gold(I)-Catalyzed Synthesis of Indenes and Cyclopentadienes: Access to (±)-Laurokamurene B and the Skeletons of the Cycloaurenones and Dysiherbols. *Angewandte Chemie International Edition* **2017,** *56* (46), 14591-14595.

93. Lian, Y.; Davies, H. M. L., Rhodium-Catalyzed [3 + 2] Annulation of Indoles. *Journal of the American Chemical Society* **2010,** *132* (2), 440-441.

94. Jing, C.; Cheng, Q.-Q.; Deng, Y.; Arman, H.; Doyle, M. P., Highly Regio- and Enantioselective Formal [3 + 2]-Annulation of Indoles with Electrophilic Enol Carbene Intermediates. *Organic Letters* **2016,** *18* (18), 4550-4553.

95. Shapiro, N. D.; Shi, Y.; Toste, F. D., Gold-Catalyzed [3+3]-Annulation of Azomethine Imines with Propargyl Esters. *Journal of the American Chemical Society* **2009,** *131* (33), 11654-11655.

96. Qian, Y.; Zavalij, P. J.; Hu, W.; Doyle, M. P., Bicyclic Pyrazolidinone Derivatives from Diastereoselective Catalytic [3 + 3]-Cycloaddition Reactions of Enoldiazoacetates with Azomethine Imines. *Organic Letters* **2013,** *15* (7), 1564-1567.

97. Zhang, Y.; Yang, Y.; Zhao, J.; Xue, Y., Mechanism and Diastereoselectivity of [3+3] Cycloaddition between Enol Diazoacetate and Azomethine Imine Catalyzed by Dirhodium Tetracarboxylate: A Theoretical Study. *European Journal of Organic Chemistry* **2018,** *2018* (24), 3086-3094.

98. Yang, W.; Wang, T.; Yu, Y.; Shi, S.; Zhang, T.; Hashmi, A. S. K., Nitrones as Trapping Reagents of α,β-Unsaturated Carbene Intermediates – [1,2]Oxazino[5,4-b]indoles by a Platinum- Catalyzed Intermolecular [3+3] Cycloaddition. *Advanced Synthesis & Catalysis* **2013,** *355* (8), 1523-1528.

99. Wang, X.; Xu, X.; Zavalij, P. Y.; Doyle, M. P., Asymmeric Formal [3 + 3]-Cycloaddition Reactions of Nitrones with Electrophilic Vinylcarbene Intermediates. *Journal of the American Chemical Society* **2011,** *133* (41), 16402-16405.

100. Xu, X.; Zavalij, P. Y.; Doyle, M. P., Highly Enantioselective Dearomatizing Formal [3+3] Cycloaddition Reactions of N-Acyliminopyridinium Ylides with Electrophilic Enol Carbene Intermediates. *Angewandte Chemie International Edition* **2013,** *52* (48), 12664-12668.

101. Xu, X.; Zavalij, P. Y.; Doyle, M. P., Catalytic Asymmetric Syntheses of Quinolizidines by Dirhodium-Catalyzed Dearomatization of Isoquinolinium/Pyridinium Methylides–The Role of Catalyst and Carbene Source. *Journal of the American Chemical Society* **2013,** *135* (33), 12439-12447.

102. Li, S.-J.; Fang, D.-C., DFT Studies on the Dirhodium-Catalyzed [3 + 2] and [3 + 3] Cycloaddition Reactions of Enol Diazoacetates with Isoquinolinium Methylide: Mechanism, Selectivity, and Ligand Effect. *Organometallics* **2018,** *37* (9), 1373-1380.

103. Chen, S.-Y.; Zeng, Y.-F.; Zou, W.-X.; Shen, D.-T.; Zheng, Y.-C.; Song, J.-L.; Zhang, S.-S., Divergent Synthesis of Tetrasubstituted Phenols via [3 + 3] Cycloaddition Reaction of Vinyl Sulfoxonnium Ylides with Cyclopropenones. *Organic Letters* **2023,** *25* (23), 4286-4291.

104. Deng, Y.; Massey, L. A.; Zavalij, P. Y.; Doyle, M. P., Catalytic Asymmetric [3+1]-Cycloaddition Reaction of Ylides with Electrophilic Metallo-enolcarbene Intermediates. *Angewandte Chemie International Edition* **2017,** *56* (26), 7479-7483.

105. Marichev, K. O.; Wang, K.; Dong, K.; Greco, N.; Massey, L. A.; Deng, Y.; Arman, H.; Doyle, M. P., Synthesis of Chiral Tetrasubstituted Azetidines from Donor–Acceptor Azetines via Asymmetric Copper(I)-Catalyzed Imido-Ylide [3+1]-Cycloaddition with Metallo-Enolcarbenes. *Angewandte Chemie International Edition* **2019,** *58* (45), 16188-16192.

106. Marichev, K. O.; Dong, K.; Massey, L. A.; Deng, Y.; De Angelis, L.; Wang, K.; Arman, H.; Doyle, M. P., Chiral donor–acceptor azetines as powerful reactants for synthesis of amino acid derivatives. *Nature Communications* **2019,** *10* (1), 5328.

107. Lee, D. J.; Ko, D.; Yoo, E. J., Rhodium(II)-Catalyzed Cycloaddition Reactions of Non-classical 1,5-Dipoles for the Formation of Eight-Membered Heterocycles. *Angewandte Chemie International Edition* **2015,** *54* (46), 13715-13718.

108. Baek, S.-y.; Lee, J. Y.; Ko, D.; Baik, M.-H.; Yoo, E. J., Rationally Designing Regiodivergent Dipolar Cycloadditions: Frontier Orbitals Show How To Switch between [5 + 3] and [4 + 2] Cycloadditions. *ACS Catalysis* **2018,** *8* (7), 6353-6361.

109. Chupakhin, E. G.; Kantin, G. P.; Dar'in, D. V.; Krasavin, M., Convenient preparation of (E)-3-arylidene-4-diazopyrrolidine-2,5-diones in array format. *Mendeleev Communications* **2021,** *31* (1), 36-38.

110. Inyutina, A.; Dar'in, D.; Kantin, G.; Krasavin, M., Tricyclic 2-benzazepines obtained via an unexpected cyclization involving nitrilium ylides. *Organic & Biomolecular Chemistry* **2021,** *19* (23), 5068-5071.

111. Inyutina, A.; Kantin, G.; Dar′in, D.; Krasavin, M., Diastereoselective Formal [5+2] Cycloaddition of Diazo Arylidene Succinimides-Derived Rhodium Carbenes and Aldehydes: A Route to 2-Benzoxepines. *The Journal of Organic Chemistry* **2021,** *86* (19), 13673-13683.

112. Vepreva, A.; Kantin, G.; Krasavin, M.; Dar'in, D., A General Way to Spiro-Annulated 2-Benzoxepines via $Rh_2(esp)_2$-Catalyzed [5+2] Cycloaddition of Diazo Arylidene Succinimides to Ketones. *Synthesis* **2022,** *54* (22), 5128-5138.

113. He, Y.; Huang, Z.; Wu, K.; Ma, J.; Zhou, Y.-G.; Yu, Z., Recent advances in transition-metal-catalyzed carbene insertion to C–H bonds. *Chemical Society Reviews* **2022,** *51* (7), 2759-2852.

114. a) Müller, P.; Pautex, N.; Doyle, M. P.; Bagheri, V., Rh(II)-Catalyzed Isomerizations of Cyclopropenes Evidence for Rh(II)-Complexed Vinylcarbene Intermediates. *Helvetica Chimica Acta* **1990,** *73* (5), 1233-1241; b) Müller, P.; Gränicher, C., Structural Effects on the RhII-Catalyzed Rearrangement of Cyclopropenes. *Helvetica Chimica Acta* **1993,** *76* (1), 521-534; Müller, P.; Gränicher, C., Selectivity in Rhodium(II)-Catalyzed Rearrangements of cycloprop-2-ene-1-carboxylates. *Helvetica Chimica Acta* **1995,** *78* (1), 129-144.

115. Davies, H. M. L.; Mark Hodges, L.; Matasi, J. J.; Hansen, T.; Stafford, D. G., Effect of carbenoid structure on the reactivity of rhodium-stabilized carbenoids. *Tetrahedron Letters* **1998,** *39* (25), 4417-4420.

116. Davies, H. M. L.; Stafford, D. G.; Hansen, T., Catalytic Asymmetric Synthesis of Diarylacetates and 4,4-Diarylbutanoates. A Formal Asymmetric Synthesis of (+)-Sertraline. *Organic Letters* **1999,** *1* (2), 233-236.

117. Hansen, J. H.; Gregg, T. M.; Ovalles, S. R.; Lian, Y.; Autschbach, J.; Davies, H. M. L., On the Mechanism and Selectivity of the Combined C−H Activation/Cope Rearrangement. *Journal of the American Chemical Society* **2011,** *133* (13), 5076-5085.

118. Davies, H. M. L.; Dai, X., Chapter 11 Total syntheses of natural products using the combine C-H activation/cope rearrangement as the key step. In *Strategies and Tactics in Organic Synthesis*, Harmata, M., Ed. Academic Press: 2008; Vol. 7, pp 383-407.

119. a) Davies, H. M. L.; Morton, D., Guiding principles for site selective and stereoselective intermolecular C–H functionalization by donor/acceptor rhodium carbenes. *Chemical Society Reviews* **2011,** *40* (4), 1857-1869; b) Davies, H. M. L.; Lian, Y., The Combined C–H Functionalization/Cope Rearrangement: Discovery and Applications in Organic Synthesis. *Accounts of Chemical Research* **2012,** *45* (6), 923-935.

120. Ma, B.; Liu, L.; Zhang, J., Gold-Catalyzed Site-Selective C−H Bond Functionalization with Diazo Compounds. *Asian Journal of Organic Chemistry* **2018,** *7* (10), 2015-2025.

121. Lovely, C. J.; Flores, J. A.; Meng, X.; Dias, H. V. R., Silver-Catalyzed C-H Insertion Reactions with Donor-Acceptor Diazoacetates. *Synlett* **2009,** *2009* (01), 129-132.

122. Yang, Y.; Liu, S.; Li, S.; Liu, Z.; Liao, P.; Sivaguru, P.; Lu, Y.; Gao, J.; Bi, X., Site-Selective C−H Allylation of Alkanes: Facile Access to Allylic Quaternary sp3-Carbon Centers. *Angewandte Chemie International Edition* **2023,** *62* (4), e202214519.

123. Archambeau, A.; Miege, F.; Meyer, C.; Cossy, J., Highly Efficient Stereoselective Catalytic Csp^3-H Insertions with Donor Rhodium Carbenoids Generated from Cyclopropenes. *Angewandte Chemie International Edition* **2012,** *51* (46), 11540-11544.

124. Xu, X.; Deng, Y.; Yim, D. N.; Zavalij, P. Y.; Doyle, M. P., Enantioselective cis-β-lactam synthesis by intramolecular C–H functionalization from enoldiazoacetamides and derivative donor–acceptor cyclopropenes. *Chemical Science* **2015,** *6* (4), 2196-2201.

125. Fürstner, A., Trans-Hydrogenation, gem-Hydrogenation, and trans-Hydrometalation of Alkynes: An Interim Report on an Unorthodox Reactivity Paradigm. *Journal of the American Chemical Society* **2019,** *141* (1), 11-24.

126. Peil, S.; Gutiérrez González, A.; Leutzsch, M.; Fürstner, A., C–H Insertion via Ruthenium Catalyzed gem-Hydrogenation of 1,3-Enynes. *Journal of the American Chemical Society* **2022,** *144* (9), 4158-4167.

127. Bhunia, S.; Liu, R.-S., Gold-Catalyzed 1,3-Addition of a sp^3-Hybridized C−H Bond to Alkenylcarbenoid Intermediate. *Journal of the American Chemical Society* **2008,** *130* (49), 16488-16489.

128. Padwa, A.; Blacklock, T. J.; Loza, R., Mechanistic aspects of the silver(I)-promoted rearrangement of cyclopropene derivatives. *The Journal of Organic Chemistry* **1982,** *47* (19), 3712-3721.

129. a) Li, C.; Zeng, Y.; Wang, J., Au-catalyzed isomerization of cyclopropenes: a novel approach to indene derivatives. *Tetrahedron Letters* **2009,** *50* (24), 2956-2959; b) Zhu, Z.-B.; Shi, M., Gold(I)-Catalyzed Cycloisomerization of Arylvinylcyclopropenes: An Efficient Synthetic Protocol for the Construction of Indene Skeletons. *Chemistry – A European Journal* **2008,** *14* (33), 10219-10222.

130. Zhu, Z.-B.; Shi, M., Palladium(II) Acetate Catalyzed Tandem Cycloisomerization and Oxidation of Arylvinylcyclopropenes Using p-Benzoquinone as Oxidant and Pro-nucleophile. *Organic Letters* **2009,** *11* (22), 5278-5281.

131. Shao, L.-X.; Zhang, Y.-P.; Qi, M.-H.; Shi, M., Lewis Acid Catalyzed Rearrangement of Vinylcyclopropenes for the Construction of Naphthalene and Indene Skeletons. *Organic Letters* **2007,** *9* (1), 117-120.

132. Bhanu Prasad, B. A.; Yoshimoto, F. K.; Sarpong, R., Pt-Catalyzed Pentannulations from In Situ Generated Metallo−Carbenoids Utilizing Propargylic Esters. *Journal of the American Chemical Society* **2005,** *127* (36), 12468-12469.

133. Lian, Y.; Davies, H. M. L., Rhodium Carbenoid Approach for Introduction of 4-Substituted (Z)-Pent-2-enoates into Sterically Encumbered Pyrroles and Indoles. *Organic Letters* **2010,** *12* (5), 924-927.

134. Lian, Y.; Davies, H. M. L., Rh2(S-biTISP)2-Catalyzed Asymmetric Functionalization of Indoles and Pyrroles with Vinylcarbenoids. *Organic Letters* **2012,** *14* (7), 1934-1937.

135. Barluenga, J.; Lonzi, G.; Tomás, M.; López, L. A., Reactivity of Stabilized Vinyl Diazo Derivatives toward Unsaturated Hydrocarbons: Regioselective Gold-Catalyzed Carbon–Carbon Bond Formation. *Chemistry – A European Journal* **2013,** *19* (5), 1573-1576.

136. López, E.; Lonzi, G.; López, L. A., Gold-Catalyzed C–H Bond Functionalization of Metallocenes: Synthesis of Densely Functionalized Ferrocene Derivatives. *Organometallics* **2014,** *33* (21), 5924-5927.

137. Zhu, D.-X.; Xia, H.; Liu, J.-G.; Chung, L. W.; Xu, M.-H., Regiospecific and Enantioselective Arylvinylcarbene Insertion of a C–H Bond of Aniline Derivatives Enabled by a Rh(I)-Diene Catalyst. *Journal of the American Chemical Society* **2021,** *143* (6), 2608-2619.

138. Zhu, D.-X.; Liu, J.-G.; Xu, M.-H., Stereodivergent Synthesis of Enantioenriched 2,3-Disubstituted Dihydrobenzofurans via a One-Pot C–H Functionalization/Oxa-Michael Addition Cascade. *Journal of the American Chemical Society* **2021,** *143* (23), 8583-8589.

139. a) Wang, T.-Y.; Chen, X.-X.; Zhu, D.-X.; Chung, L. W.; Xu, M.-H., Rhodium(I) Carbene-Promoted Enantioselective C−H Functionalization of Simple Unprotected Indoles, Pyrroles and Heteroanalogues: New Mechanistic Insights. *Angewandte Chemie International Edition* **2022,** *61* (34), e202207008; b) Zhu, D.-X.; Xu, M.-H., Rhodium(I)-Catalyzed Direct Enantioselective C–H Functionalization of Indoles. *The Journal of Organic Chemistry* **2023,** *88* (12), 7844-7848.

140. Gillingham, D.; Fei, N., Catalytic X–H insertion reactions based on carbenoids. *Chemical Society Reviews* **2013,** *42* (12), 4918-4931.

141. Landais, Y.; Planchenault, D.; Weber, V., Rhodium(II)-vinylcarbenoid insertion into the Si・H bond. A new stereospecific synthesis of allylsilanes. *Tetrahedron Letters* **1994,** *35* (51), 9549-9552.

142. Davies, H. M. L.; Hansen, T.; Rutberg, J.; Bruzinski, P. R., Rhodium(II) (S)-N-(arylsulfonyl)prolinate catalyzed asymmetric insertions of vinyl- and phenylcarbenoids into the Si-H bond. *Tetrahedron Letters* **1997,** *38* (10), 1741-1744.

143. Davies, H. M. L.; Yokota, Y., Regiochemistry of molybdenum-catalyzed O–H insertions of vinylcarbenoids. *Tetrahedron Letters* **2000,** *41* (25), 4851-4854.

144. Sevryugina, Y.; Weaver, B.; Hansen, J.; Thompson, J.; Davies, H. M. L.; Petrukhina, M. A., Influence of Electron-Deficient Ruthenium(I) Carbonyl Carboxylates on the Vinylogous Reactivity of Metal Carbenoids. *Organometallics* **2008,** *27* (8), 1750-1757.

145. Yue, Y.; Wang, Y.; Hu, W., Regioselectivity in Lewis acids catalyzed X–H (O, S, N) insertions of methyl styryldiazoacetate with benzyl alcohol, benzyl thiol, and aniline. *Tetrahedron Letters* **2007,** *48* (23), 3975-3977.

146. Hansen, J. H.; Davies, H. M. L., Vinylogous reactivity of silver(I) vinylcarbenoids. *Chemical Science* **2011,** *2* (3), 457-461.

147. Ueda, J.; Harada, S.; Nakayama, H.; Nemoto, T., Silver-catalyzed regioselective hydroamination of alkenyl diazoacetates to synthesize γ-amino acid equivalents. *Organic & Biomolecular Chemistry* **2018,** *16* (25), 4675-4682.

148. Xu, G.; Liu, K.; Dai, Z.; Sun, J., Gold/silver-catalyzed controllable regioselective vinylcarbene insertion into O–H bonds. *Organic & Biomolecular Chemistry* **2017,** *15* (11), 2345-2348.

149. Huang, D.; Xu, G.; Peng, S.; Sun, J., Gold-catalyzed highly regio- and enantioselective vinylcarbene insertion into O–H bonds of 2-pyridones. *Chemical Communications* **2017,** *53* (22), 3197-3200.

150. a) Bauer, J. T.; Hadfield, M. S.; Lee, A.-L., Gold catalysed reactions with cyclopropenes. *Chemical Communications* **2008,** (47), 6405-6407; b) Hadfield, M. S.; Bauer, J. T.; Glen, P. E.; Lee, A.-L., Gold(i)-catalysed alcohol additions to cyclopropenes. *Organic & Biomolecular Chemistry* **2010,** *8* (18), 4090-4095.

151. Phan, D. T. H.; Dong, V. M., Silver-catalyzed ring-opening of cyclopropenes: preparation of tertiary α-branched allylic amines. *Tetrahedron* **2013,** *69* (27), 5726-5731.

152. Mata, S.; López, L. A.; Vicente, R., Zinc-Catalyzed Synthesis of Allylsilanes by Si−H Bond Insertion of Vinyl Carbenoids Generated from Cyclopropenes. *Angewandte Chemie International Edition* **2017,** *56* (27), 7930-7934.

153. Mata, S.; López, L. A.; Vicente, R., Synthesis of Bifunctional Allylic Compounds by Using Cyclopropenes as Functionalized Allyl Equivalents. *Angewandte Chemie International Edition* **2018,** *57* (35), 11422-11426.

154. Wu, Y.; Song, Q.; Xia, Y.; Ning, Y.; Sivaguru, P.; Bi, X., Silver-catalyzed vinylcarbene insertion into Si–H bonds with vinyl N-triftosylhydrazones leading to allylsilanes. *Organic Chemistry Frontiers* **2023,** *10* (18), 4588-4592.

155. Zhao, X.; Wang, G.; Hashmi, A. S. K., Carbene B−H Insertion Reactions for C−B Bond Formation. *ChemCatChem* **2021,** *13* (20), 4299-4312.

156. Drikermann, D.; Mößel, R. S.; Al-Jammal, W. K.; Vilotijevic, I., Synthesis of Allylboranes via Cu(I)-Catalyzed B–H Insertion of Vinyldiazoacetates into Phosphine‐Borane Adducts. *Organic Letters* **2020,** *22* (3), 1091-1095.

157. Huang, M.-Y.; Zhao, Y.-T.; Chai, H.; Zhang, C.-D.; Zhu, S.-F., Copper-Catalyzed Ring-Opening/Borylation of Cyclopropenes. *CCS Chemistry* **2021,** *4* (4), 1232-1237.

158. Huang, M.-Y.; Zhao, Y.-T.; Zhang, C.-D.; Zhu, S.-F., Highly Regio-, Stereo-, and Enantioselective Copper-Catalyzed B−H Bond Insertion of α-Silylcarbenes: Efficient Access to Chiral Allylic gem-Silylboranes. *Angewandte Chemie International Edition* **2022,** *61* (26), e202203343.

159. a) Pei, C.; Zhang, C.; Qian, Y.; Xu, X., Catalytic carbene/alkyne metathesis (CAM): a versatile strategy for alkyne bifunctionalization. *Organic & Biomolecular Chemistry* **2018,** *16* (45), 8677-8685; b) Torres, Ò.; Pla-Quintana, A., The rich reactivity of transition metal carbenes with alkynes. *Tetrahedron Letters* **2016,** *57* (35), 3881-3891.

160. Dötz, K. H., Synthesis of the Naphthol Skeleton from Pentacarbonyl-[methoxy(phenyl)carbene]chromium (O) and Tolan. *Angewandte Chemie International Edition in English* **1975,** *14* (9), 644-645.

161. Bera, T.; Pandey, K.; Ali, R., The Dötz Benzannulation Reaction: A Booming Methodology for Natural Product Synthesis. *ChemistrySelect* **2020,** *5* (17), 5239-5267.

162. a) Wulff, W. D.; Kaesler, R. W., Cyclobutanone formation via in situ generated vinyl ketene complexes of chromium. *Organometallics* **1985,** *4* (8), 1461-1463; b) Parlier, A.; Rudler, H.; Platzer, N.; Fontanille, M.; Soum, A., Carbene complexes in organic synthesis: a new tungstacarbene-promoted alkyne insertion–olefin cyclopropanation reaction. *Journal of the Chemical Society, Dalton Transactions* **1987,** (5), 1041-1049; c) Korkowski, P. F.; Hoye, T. R.; Rydberg, D. B., Fischer carbene-mediated conversions of enynes to bi- and tricyclic cyclopropane-containing carbon skeletons. *Journal of the American Chemical Society* **1988,** *110* (8), 2676-2678; d) Hoye, T. R.; Rehberg, G. M., Reactions of $(CO)_5Cr{:}C(Me)N(CH_2CH_2)_2$ with enynes: mechanistic insight and synthetic value of changing a carbene donor group from alkoxy to dialkylamino. *Organometallics* **1989,** *8* (8), 2070-2071.

163. Padwa, A.; Krumpe, K. E.; Zhi, L., Cycloalkenone formation by the intramolecular addition of a α-diazoketone to an acetylenic pi-bond. *Tetrahedron Letters* **1989,** *30* (20), 2633-2636.

164. Hoye, T. R.; Dinsmore, C. J.; Johnson, D. S.; Korkowski, P. F., Alkyne insertion reactions of metal-carbenes derived from enynyl-.alpha.-diazoketones [$R'CN_2COCR_2CH_2C.tplbond.C(CH_2)n\text{-}_2CH{:}CH_2$]. *The Journal of Organic Chemistry* **1990,** *55* (15), 4518-4520.

165. a) Hoye, T. R.; Dinsmore, C. J., Double (internal/external) alkyne insertion reactions of α-diazoketones. *Tetrahedron Letters* **1991,** *32* (31), 3755-3758; b) Padwa, A.; Austin, D. J.; Xu, S. L., Rhodium (II) catalyzed cyclizations of α-diazo substituted alkynes. A new mode of reaction. *Tetrahedron Letters* **1991,** *32* (33), 4103-4106; c) Hoye, T. R.; Dinsmore, C. J., Rhodium(II) acetate catalyzed alkyne insertion reactions of .alpha.-diazo ketones: mechanistic inferences. *Journal of the American Chemical Society* **1991,** *113* (11), 4343-4345; d) Padwa, A.; Austin, D. J.; Chiacchio, U.; Kassir, J. M.; Rescifina, A.; Xu, S. L., Rearrangement of o-alkynyl substituted α-diazoacetophenones. Conversion to β-naphthols via arylketene intermediates. *Tetrahedron Letters* **1991,** *32* (42), 5923-5926; e) Padwa, A.; Austin, D. J.; Gareau, Y.; Kassir, J. M.; Xu, S. L., Rearrangement of alkynyl and vinyl carbenoids via the rhodium(II)-catalyzed cyclization reaction of .alpha.-diazo ketones. *Journal of the American Chemical Society* **1993,** *115* (7), 2637-2647; f) Padwa, A.; Kassir, J. M.; Xu, S. L., Cyclization Reactions of Rhodium Carbene Complexes. Effect of Composition and Oxidation State of the Metal. *The Journal of Organic Chemistry* **1997,** *62* (6), 1642-1652.

166. Padwa, A.; Krumpe, K. E.; Gareau, Y.; Chiacchio, U., Rhodium(II)-catalyzed cyclization reactions of alkynyl-substituted .alpha.-diazo ketones. *The Journal of Organic Chemistry* **1991,** *56* (7), 2523-2530.

167. a) Padwa, A.; Chiacchio, U.; Garreau, Y.; Kassir, J. M.; Krumpe, K. E.; Schoffstall, A. M., Generation of vinylcarbenes by the intramolecular addition of .alpha.-diazo ketones to acetylenes. *The Journal of Organic Chemistry* **1990,** *55* (2), 414-416; b) Mueller, P. H.; Kassir, J. M.; A. Semones, M.; Weingarten, M. D.; Padwa, A., Rhodium carbenoid mediated cyclizations. Intramolecular cyclopropanation and C-H insertion reactions derived from type II o-alkynyl substituted α-diazoacetophenones. *Tetrahedron Letters* **1993,** *34* (27), 4285-4288.

168. Kinder, F. R.; Padwa, A., Preparation of oxygenated heterocycles via the cyclization reaction of α-diazo substituted alkynes. *Tetrahedron Letters* **1990,** *31* (47), 6835-6838.

169. Padwa, A.; Weingarten, M. D., Rhodium(II)-Catalyzed Carbocyclization Reaction of α-Diazo Carbonyls with Tethered Unsaturation. *The Journal of Organic Chemistry* **2000,** *65* (12), 3722-3732.

170. a) Jansone-Popova, S.; May, J. A., Synthesis of Bridged Polycyclic Ring Systems via Carbene Cascades Terminating in C–H Bond Insertion. *Journal of the American Chemical Society* **2012,** *134* (43), 17877-17880; b) Jansone-Popova, S.; Le, P. Q.; May, J. A., Carbene cascades for the formation of bridged polycyclic rings. *Tetrahedron* **2014,** *70* (27), 4118-4127.

171. Le, P. Q.; May, J. A., Hydrazone-Initiated Carbene/Alkyne Cascades to Form Polycyclic Products: Ring-Fused Cyclopropenes as Mechanistic Intermediates. *Journal of the American Chemical Society* **2015,** *137* (38), 12219-12222.

172. Chen, P.-A.; Setthakarn, K.; May, J. A., A Binaphthyl-Based Scaffold for a Chiral Dirhodium(II) Biscarboxylate Ligand with α-Quaternary Carbon Centers. *ACS Catalysis* **2017,** *7* (9), 6155-6161.

173. Dong, K.; Pei, C.; Zeng, Q.; Wei, H.; Doyle, M. P.; Xu, X., Selective C(sp3)–H Bond Insertion in Carbene/Alkyne Metathesis Reactions. Enantioselective Construction of Dihydroindoles. *ACS Catalysis* **2018,** *8* (10), 9543-9549.

174. Torres, Ò.; Parella, T.; Solà, M.; Roglans, A.; Pla-Quintana, A., Enantioselective Rhodium(I) Donor Carbenoid-Mediated Cascade Triggered by a Base-Free Decomposition of Arylsulfonyl Hydrazones. *Chemistry – A European Journal* **2015,** *21* (45), 16240-16245.

175. Torres, Ò.; Roglans, A.; Pla-Quintana, A., An Enantioselective Cascade Cyclopropanation Reaction Catalyzed by Rhodium(I): Asymmetric Synthesis of Vinylcyclopropanes. *Advanced Synthesis & Catalysis* **2016,** *358* (22), 3512-3516.

176. Torres, Ò.; Solà, M.; Roglans, A.; Pla-Quintana, A., Unusual reactivity of rhodium carbenes with allenes: an efficient asymmetric synthesis of methylenetetrahydropyran scaffolds. *Chemical Communications* **2017,** *53* (71), 9922-9925.

177. Qiu, H.; Deng, Y.; Marichev, K. O.; Doyle, M. P., Diverse Pathways in Catalytic Reactions of Propargyl Aryldiazoacetates: Selectivity between Three Reaction Sites. *The Journal of Organic Chemistry* **2017,** *82* (3), 1584-1590.

178. Zeng, Q.; Dong, K.; Huang, J.; Qiu, L.; Xu, X., Copper-catalyzed carbene/alkyne metathesis terminated with the Buchner reaction: synthesis of dihydrocyclohepta[b]indoles. *Organic & Biomolecular Chemistry* **2019,** *17* (9), 2326-2330.

179. Yao, R.; Rong, G.; Yan, B.; Qiu, L.; Xu, X., Dual-Functionalization of Alkynes via Copper-Catalyzed Carbene/Alkyne Metathesis: A Direct Access to the 4-Carboxyl Quinolines. *ACS Catalysis* **2016,** *6* (2), 1024-1027.

180. Zheng, Y.; Mao, J.; Weng, Y.; Zhang, X.; Xu, X., Cyclopentadiene Construction via Rh-Catalyzed Carbene/Alkyne Metathesis Terminated with Intramolecular Formal [3 + 2] Cycloaddition. *Organic Letters* **2015,** *17* (22), 5638-5641.

181. Wang, X.; Zhou, Y.; Qiu, L.; Yao, R.; Zheng, Y.; Zhang, C.; Bao, X.; Xu, X., Enantioselective Carbene Cascade: An Effective Approach to Cyclopentadienes and Applications in Diels–Alder Reactions. *Advanced Synthesis & Catalysis* **2016,** *358* (10), 1571-1576.

182. Jia, S.; Dong, G.; Ao, C.; Jiang, X.; Hu, W., Rhodium-Catalyzed Formal C–O Insertion in Carbene/Alkyne Metathesis Reactions: Synthesis of 3-Substituted 3H-Indol-3-ols. *Organic Letters* **2019,** *21* (11), 4322-4326.

183. Li, X.; Sheng, H.; Song, Q., Rhodium-Catalyzed Intramolecular Cyclization to Synthesize 2-Aminobenzofurans via Carbene Metathesis Reactions. *Organic Letters* **2023,** *25* (12), 2113-2117.

184. a) Le Paih, J.; Dérien, S.; Özdemir, I.; Dixneuf, P. H., Catalytic Double Addition of Diazo Compounds to Alkynes: Synthesis of Functional Conjugated Dienes. *Journal of the American Chemical Society* **2000,** *122* (30), 7400-7401; b) Paih, J. L.; Bray, C. V.-L.; Dérien, S.; Dixneuf, P. H., Ruthenium-Catalyzed Synthesis of Functional Conjugated Dienes via Addition of Two Carbene Units to Alkynes. *Journal of the American Chemical Society* **2010,** *132* (21), 7391-7397.

185. Monnier, F.; Castillo, D.; Dérien, S.; Toupet, L.; Dixneuf, P. H., Addition of Diazoalkanes to Enynes Promoted by a Ruthenium Catalyst: Simple Synthesis of Alkenyl Bicyclo[3.1.0]hexane Derivatives. *Angewandte Chemie International Edition* **2003,** *42* (44), 5474-5477.

186. a) Eckert, M.; Monnier, F.; Shchetnikov, G. T.; Titanyuk, I. D.; Osipov, S. N.; Toupet, L.; Dérien, S.; Dixneuf, P. H., Tandem Catalytic Carbene Addition/Bicyclization of Enynes. One-Step Synthesis of Fluorinated Bicyclic Amino Esters by Ruthenium Catalysis. *Organic Letters* **2005,** *7* (17), 3741-3743; b) Monnier, F.; Vovard-Le Bray, C.; Castillo, D.; Aubert, V.; Dérien, S.; Dixneuf, P. H.; Toupet, L.; Ienco, A.; Mealli, C., Selective Ruthenium-Catalyzed Transformations of Enynes with Diazoalkanes into Alkenylbicyclo[3.1.0]hexanes. *Journal of the American Chemical Society* **2007,** *129* (18), 6037-6049; c) Eckert, M.; Moulin, S.; Monnier, F.; Titanyuk, I. D.; Osipov, S. N.; Roisnel, T.; Dérien, S.; Dixneuf, P. H., Ruthenium-Catalysed Synthesis of Fluorinated Bicyclic Amino Esters through Tandem Carbene Addition/Cyclopropanation of Enynes. *Chemistry – A European Journal* **2011,** *17* (34), 9456-9462; d) Moulin, S.; Roisnel, T.; Dérien, S., One-Step Ruthenium-Catalysed Transformation of 1,7-Enynes into Strained Bicyclic Amino Esters. *European Journal of Organic Chemistry* **2016,** *2016* (25), 4311-4314; e) Bray, C. V.-L.; Klein, H.; Dixneuf, P. H.; Macé, A.; Berrée, F.; Carboni, B.; Dérien, S., One-Step Synthesis of Strained Bicyclic Carboxylic and Boronic Amino Esters via Ruthenium-Catalysed Tandem Carbene Addition/Cyclopropanation of Enynes. *Advanced Synthesis & Catalysis* **2012,** *354* (10), 1919-1925.

187. Huang, J.; Hu, X.; Chen, F.; Gui, J.; Zeng, W., Rhodium(I)-catalyzed vinylation/[2 + 1] carbocyclization of 1,6-enynes with α-diazocarbonyl compounds. *Organic & Biomolecular Chemistry* **2019,** *17* (29), 7042-7054.

188. Vovard-Le Bray, C.; Dérien, S.; Dixneuf, P. H.; Murakami, M., A Direct Synthesis of Alkenyl Alkylidene Bicyclo[3.1.0]hexane Derivatives via Ruthenium(II)-Catalysed Bicyclisation of Allenynes. *Synlett* **2008,** *2008* (02), 193-196.

189. Cambeiro, F.; López, S.; Varela, J. A.; Saá, C., Cyclization by Catalytic Ruthenium Carbene Insertion into C-H Bonds. *Angewandte Chemie International Edition* **2012,** *51* (3), 723-727.

190. Cambeiro, F.; López, S.; Varela, J. A.; Saá, C., Vinyl Dihydropyrans and Dihydrooxazines: Cyclizations of Catalytic Ruthenium Carbenes Derived from Alkynals and Alkynones. *Angewandte Chemie International Edition* **2014,** *53* (23), 5959-5963.

191. Padín, D.; Cambeiro, F.; Fañanás-Mastral, M.; Varela, J. A.; Saá, C., [2 + 1] Cycloaddition of Catalytic Ruthenium Vinyl Carbenes: A Stereoselective Controlled Access to (Z)- and (E)-Vinyl Epoxypyrrolidines. *ACS Catalysis* **2017,** *7* (2), 992-996.

192. Padín, D.; Varela, J. A.; Saá, C., Ruthenium-Catalyzed Tandem Carbene/Alkyne Metathesis/N–H Insertion: Synthesis of Benzofused Six-Membered Azaheterocycles. *Organic Letters* **2020,** *22* (7), 2621-2625.

193. González-Rodríguez, C.; Suárez, J. R.; Varela, J. A.; Saá, C., Nucleophilic Addition of Amines to Ruthenium Carbenes: ortho-(Alkynyloxy)benzylamine Cyclizations towards 1,3-Benzoxazines. *Angewandte Chemie International Edition* **2015,** *54* (9), 2724-2728.

194. Carmen, E.; Maria, D. D.; Santiago, V., Nitrile Ylides: Generation, Properties and Synthetic Applications. *Current Organic Chemistry* **2007,** *11* (9), 741-772.

195. Huisgen, R.; Stangl, H.; Sturm, H. J.; Wagenhofer, H., 1,3-Dipolar Additions with Nitrile Ylides. *Angewandte Chemie International Edition in English* **1962,** *1* (1), 50.

196. a) Padwa, A.; Smolanoff, J.; Tremper, A., Photochemical transformations of small ring heterocyclic systems. LXV. Intramolecular cycloaddition reactions of vinyl-substituted 2H-azirines. *Journal of the American Chemical Society* **1975,** *97* (16), 4682-4691; b) Motion, K. R.; Robertson, I. R.; Sharp, J. T.; Walkinshaw, M. D., Reactions of diene-conjugated 1,3-dipolar intermediates: the formation of cyclopropa[c]isoquinolines from benzonitrile o-alkenylbenzyl ylides and their rearrangements to benzazepines. *Journal of the Chemical Society, Perkin Transactions 1* **1992,** (13), 1709-1719.

197. Weintraub, R. A.; Wang, X., Recent Developments in Isoindole Chemistry. *Synthesis* **2022,** *55* (04), 519-546.

198. Jeppsson, F.; Eketjäll, S.; Janson, J.; Karlström, S.; Gustavsson, S.; Olsson, L.-L.; Radesäter, A.-C.; Ploeger, B.; Cebers, G.; Kolmodin, K.; Swahn, B.-M.; von Berg, S.; Bueters, T.; Fälting, J., Discovery of AZD3839, a Potent and Selective BACE1 Inhibitor Clinical Candidate for the Treatment of Alzheimer Disease. *Journal of Biological Chemistry* **2012,** *287* (49), 41245-41257.

199. Frisch, M. J.; Trucks, G. W.; Schlegel, H. B.; Scuseria, G. E.; Robb, M. A.; Cheeseman, J. R.; Scalmani, G.; Barone, V.; Petersson, G. A.; Nakatsuji, H.; Li, X.; Caricato, M.; Marenich, A. V.; Bloino, J.; Janesko, B. G.; Gomperts, R.; Mennucci, B.; Hratchian, H. P.; Ortiz, J. V.; Izmaylov, A. F.; Sonnenberg, J. L.; Williams; Ding, F.; Lipparini, F.; Egidi, F.; Goings, J.; Peng, B.; Petrone, A.; Henderson, T.; Ranasinghe, D.; Zakrzewski, V. G.; Gao, J.; Rega, N.; Zheng, G.; Liang, W.; Hada, M.; Ehara, M.; Toyota, K.; Fukuda, R.; Hasegawa, J.; Ishida, M.; Nakajima, T.; Honda, Y.; Kitao, O.; Nakai, H.; Vreven, T.; Throssell, K.; Montgomery Jr., J. A.; Peralta, J. E.; Ogliaro, F.; Bearpark, M. J.; Heyd, J. J.; Brothers, E. N.; Kudin, K. N.; Staroverov, V. N.; Keith, T. A.; Kobayashi, R.; Normand, J.; Raghavachari, K.; Rendell, A. P.; Burant, J. C.; Iyengar, S. S.; Tomasi, J.; Cossi, M.; Millam, J. M.; Klene, M.; Adamo, C.; Cammi, R.; Ochterski, J. W.; Martin, R. L.; Morokuma, K.; Farkas, O.; Foresman, J. B.; Fox, D. J. *Gaussian 16 Rev. C.01*, Wallingford, CT, 2016.

200. Dong, K.; Fan, X.; Pei, C.; Zheng, Y.; Chang, S.; Cai, J.; Qiu, L.; Yu, Z.-X.; Xu, X., Transient-axial-chirality controlled asymmetric rhodium-carbene Csp^2-H functionalization for the synthesis of chiral fluorenes. *Nature Communications* **2020,** *11* (1), 2363.

201. Zhu, D.; Cao, T.; Chen, K.; Zhu, S., Rh_2(II)-catalyzed enantioselective intramolecular Büchner reaction and aromatic substitution of donor–donor carbenes. *Chemical Science* **2022,** *13* (7), 1992-2000.

202. Hong, K.; Zhou, Y.; Yuan, H.; Zhang, Z.; Huang, J.; Dong, S.; Hu, W.; Yu, Z.-X.; Xu, X., Catalytic 4-exo-dig carbocyclization for the construction of furan-fused cyclobutanones and synthetic applications. *Nature Communications* **2023,** *14* (1), 6378.

203. Fabian, W. M. F.; Kappe, C. O.; Bakulev, V. A., Ab Initio and Density Functional Calculations on the Pericyclic vs Pseudopericyclic Mode of Conjugated Nitrile Ylide 1,5-Electrocyclizations. *The Journal of Organic Chemistry* **2000,** *65* (1), 47-53.

204. Acuña-Parés, F.; Codolà, Z.; Costas, M.; Luis, J. M.; Lloret-Fillol, J., Unraveling the Mechanism of Water Oxidation Catalyzed by Nonheme Iron Complexes. *Chemistry – A European Journal* **2014,** *20* (19), 5696-5707.

205. a) Kozuch, S.; Shaik, S., Kinetic-Quantum Chemical Model for Catalytic Cycles: The Haber−Bosch Process and the Effect of Reagent Concentration. *The Journal of Physical Chemistry A* **2008,** *112* (26), 6032-6041; b) Kozuch, S.; Shaik, S., How to Conceptualize Catalytic Cycles? The Energetic Span Model. *Accounts of Chemical Research* **2011,** *44* (2), 101-110.

206. Muñoz-Molina, J. M.; Belderrain, T. R.; Pérez, P. J., Trispyrazolylborate coinage metals complexes: Structural features and catalytic transformations. *Coordination Chemistry Reviews* **2019,** *390*, 171-189.

207. a) Caballero, A.; Despagnet-Ayoub, E.; Mar Díaz-Requejo, M.; Díaz-Rodríguez, A.; González-Núñez, M. E.; Mello, R.; Muñoz, B. K.; Ojo, W.-S.; Asensio, G.; Etienne, M.; Pérez, P. J., Silver-Catalyzed C-C Bond Formation Between Methane and Ethyl Diazoacetate in Supercritical CO2. *Science* **2011,** *332* (6031), 835-838; b) Besora, M.; Olmos, A.; Gava, R.; Noverges, B.; Asensio, G.; Caballero, A.; Maseras, F.; Pérez, P. J., A Quantitative Model for Alkane Nucleophilicity Based on C−H Bond Structural/Topological Descriptors. *Angewandte Chemie International Edition* **2020,** *59* (8), 3112-3116; c) Gava, R.; Ballestín, P.; Prieto, A.; Caballero, A.; Pérez, P. J., Methane functionalization in water with micellar catalysis. *Chemical Communications* **2019,** *55* (75), 11243-11246; d) Matamoros-Recio, A.; Alonso-Rueda, E.; Borrego, E.; Caballero, A.; Pérez, P. J.; Martín-Santamaría, S., Molecular Dynamic Simulations of Aqueous Micellar Organometallic Catalysis: Methane Functionalization as a Case Study. *Angewandte Chemie International Edition* **2023,** e202314773.

208. Olmos, A.; Gava, R.; Noverges, B.; Bellezza, D.; Jacob, K.; Besora, M.; Sameera, W. M. C.; Etienne, M.; Maseras, F.; Asensio, G.; Caballero, A.; Pérez, P. J., Measuring the Relative Reactivity of the Carbon–Hydrogen Bonds of Alkanes as Nucleophiles. *Angewandte Chemie International Edition* **2018,** *57* (42), 13848-13852.

209. Álvarez, M.; Molina, F.; Pérez, P. J., Carbene-Controlled Regioselective Functionalization of Linear Alkanes under Silver Catalysis. *Journal of the American Chemical Society* **2022,** *144* (51), 23275-23279.

210. Padín, D.; Varela, J. A.; Saá, C., Cp*RuCl-Vinyl Carbenes: Two Faces and the Bifunctional Role in Catalytic Processes. *Chemistry – A European Journal* **2020,** *26* (33), 7470-7478.

211. Zhang, Y.; Yang, Y.; Xue, Y., Insights into C–O insertion in a carbene/alkyne metathesis cascade reaction catalyzed by $Rh_2(OAc)_4$: a DFT study. *Catalysis Science & Technology* **2020,** *10* (16), 5513-5524.

212. Zhang, C.; Hong, K.; Pei, C.; Zhou, S.; Hu, W.; Hashmi, A. S. K.; Xu, X., Gold(I)-catalyzed intramolecular cyclization/intermolecular cycloaddition cascade as a fast track to polycarbocycles and mechanistic insights. *Nature Communications* **2021,** *12* (1), 1182.

213. Zhang, C.; Hong, K.; Dong, S.; Pei, C.; Zhang, X.; He, C.; Hu, W.; Xu, X., Gold(I)-Catalyzed Aromatization: Expeditious Synthesis of Polyfunctionalized Naphthalenes. *iScience* **2019,** *21*, 499-508.

214. Hashmi, A. S. K.; Schuster, A. M.; Gaillard, S.; Cavallo, L.; Poater, A.; Nolan, S. P., Selectivity Switch in the Synthesis of Vinylgold(I) Intermediates. *Organometallics* **2011,** *30* (22), 6328-6337.

215. Cleary, S. E.; Li, X.; Yang, L.-C.; Houk, K. N.; Hong, X.; Brewer, M., Reactivity Profiles of Diazo Amides, Esters, and Ketones in Transition-Metal-Free C–H Insertion Reactions. *Journal of the American Chemical Society* **2019,** *141* (8), 3558-3565.

216. a) Nakamura, E.; Yoshikai, N.; Yamanaka, M., Mechanism of C−H Bond Activation/C−C Bond Formation Reaction between Diazo Compound and Alkane Catalyzed by Dirhodium Tetracarboxylate. *Journal of the American Chemical Society* **2002,** *124* (24), 7181-7192; b) Laconsay, C. J.; Pla-Quintana, A.; Tantillo, D. J., Effects of Axial Solvent Coordination to Dirhodium Complexes on the Reactivity and Selectivity in C–H Insertion Reactions: A Computational Study. *Organometallics* **2021,** *40* (24), 4120-4132; c) Flores, J. A.; Komine, N.; Pal, K.; Pinter, B.; Pink, M.; Chen, C.-H.; Caulton, K. G.; Mindiola, D. J., Silver(I)-Catalyzed Insertion of Carbene into Alkane C–H Bonds and the Origin of the Special Challenge of Methane Activation Using DFT as a Mechanistic Probe. *ACS Catalysis* **2012,** *2* (10), 2066-2078; d) Braga, A. A. C.; Maseras, F.; Urbano, J.; Caballero, A.; Díaz-Requejo, M. M.; Pérez, P. J., Mechanism of Alkane C−H Bond Activation by Copper and Silver Homoscorpionate Complexes. *Organometallics* **2006,** *25* (22), 5292-5300.

217. a) Lamb, K. N.; Squitieri, R. A.; Chintala, S. R.; Kwong, A. J.; Balmond, E. I.; Soldi, C.; Dmitrenko, O.; Castiñeira Reis, M.; Chung, R.; Addison, J. B.; Fettinger, J. C.; Hein, J. E.; Tantillo, D. J.; Fox, J. M.; Shaw, J. T., Synthesis of Benzodihydrofurans by Asymmetric C−H Insertion Reactions of Donor/Donor Rhodium Carbenes. *Chemistry – A European Journal* **2017,** *23* (49), 11843-11855; b) Dishman, S. N.; Laconsay, C. J.; Fettinger, J. C.; Tantillo, D. J.; Shaw, J. T., Divergent stereochemical outcomes in the insertion of donor/donor carbenes into the C–H bonds of stereogenic centers. *Chemical Science* **2022,** *13* (4), 1030-1036.

218. Fukuto, J. M.; Jensen, F. R., Mechanisms of SE2 reactions: emphasis on organotin compounds. *Accounts of Chemical Research* **1983,** *16* (5), 177-184.

219. a) Poater, A.; Cosenza, B.; Correa, A.; Giudice, S.; Ragone, F.; Scarano, V.; Cavallo, L., SambVca: A Web Application for the Calculation of the Buried Volume of N-Heterocyclic Carbene Ligands. *European Journal of Inorganic Chemistry* **2009,** *2009* (13), 1759-1766; b) Falivene, L.; Cao, Z.; Petta, A.; Serra, L.; Poater, A.; Oliva, R.; Scarano, V.; Cavallo, L., Towards the online computer-aided design of catalytic pockets. *Nature Chemistry* **2019,** *11* (10), 872-879.

220. Kim, J.; Ohk, Y.; Park, S. H.; Jung, Y.; Chang, S., Intramolecular Aromatic Carbenoid Insertion of Biaryldiazoacetates for the Regioselective Synthesis of Fluorenes. *Chemistry – An Asian Journal* **2011,** *6* (8), 2040-2047.

221. a) Li, Z.; Gao, H.-X., Theoretical study on the mechanism of Ag-catalyzed synthesis of 3-alkylideneoxindoles from N-aryl-α-diazoamides: a Lewis acid or Ag-carbene pathway? *Organic & Biomolecular*

Chemistry **2012,** *10* (31), 6294-6298; b) Liu, Y.; Yu, Z.; Zhang, J. Z.; Liu, L.; Xia, F.; Zhang, J., Origins of unique gold-catalysed chemo- and site-selective C–H functionalization of phenols with diazo compounds. *Chemical Science* **2016,** *7* (3), 1988-1995; c) Fructos, M. R.; Besora, M.; Braga, A. A. C.; Díaz-Requejo, M. M.; Maseras, F.; Pérez, P. J., Mechanistic Studies on Gold-Catalyzed Direct Arene C–H Bond Functionalization by Carbene Insertion: The Coinage-Metal Effect. *Organometallics* **2017,** *36* (1), 172-179; d) Postils, V.; Rodríguez, M.; Sabenya, G.; Conde, A.; Díaz-Requejo, M. M.; Pérez, P. J.; Costas, M.; Solà, M.; Luis, J. M., Mechanism of the Selective Fe-Catalyzed Arene Carbon–Hydrogen Bond Functionalization. *ACS Catalysis* **2018,** *8* (5), 4313-4322.

222. Hussong, M. W.; Hoffmeister, W. T.; Rominger, F.; Straub, B. F., Copper and Silver Carbene Complexes without Heteroatom-Stabilization: Structure, Spectroscopy, and Relativistic Effects. *Angewandte Chemie International Edition* **2015,** *54* (35), 10331-10335.

223. Tskhovrebov, A. G.; Goddard, R.; Fürstner, A., Two Amphoteric Silver Carbene Clusters. *Angewandte Chemie International Edition* **2018,** *57* (27), 8089-8094.

224. Álvarez, M.; Besora, M.; Molina, F.; Maseras, F.; Belderrain, T. R.; Pérez, P. J., Two Copper-Carbenes from One Diazo Compound. *Journal of the American Chemical Society* **2021,** *143* (12), 4837-4843.

225. Shu, C.; Shi, C.-Y.; Sun, Q.; Zhou, B.; Li, T.-Y.; He, Q.; Lu, X.; Liu, R.-S.; Ye, L.-W., Generation of Endocyclic Vinyl Carbene Complexes via Gold-Catalyzed Oxidative Cyclization of Terminal Diynes: Toward Naphthoquinones and Carbazolequinones. *ACS Catalysis* **2019,** *9* (2), 1019-1025.

226. Hoye, T. R.; Dinsmore, C. J., Tandem alkyne insertion and allyl sulfonium ylide rearrangement of γ,δ-alkynyl-α′-diazoketones. *Tetrahedron Letters* **1992,** *33* (2), 169-172.

227. Padwa, A.; Krumpe, K. E.; Kassir, J. M., Rhodium carbenoid mediated cyclizations of o-alkynyl-substituted .alpha.-diazoacetophenones. *The Journal of Organic Chemistry* **1992,** *57* (18), 4940-4948.

228. Gettwert, V.; Krebs, F.; Maas, G., Intramolecular Copper- and Rhodium-Mediated Carbenoid Reactions of α-(Propargyloxy)silyl-α-diazoacetates. *European Journal of Organic Chemistry* **1999,** *1999* (5), 1213-1221.

229. a) Praveen Rao, P. N.; Amini, M.; Li, H.; Habeeb, A. G.; Knaus, E. E., Design, Synthesis, and Biological Evaluation of 6-Substituted-3-(4-methanesulfonylphenyl)-4-phenylpyran-2-ones: A Novel Class of Diarylheterocyclic Selective Cyclooxygenase-2 Inhibitors. *Journal of Medicinal Chemistry* **2003,** *46* (23), 4872-4882; b) Fairlamb, I. J. S.; Marrison, L. R.; Dickinson, J. M.; Lu, F.-J.; Schmidt, J. P., 2-Pyrones possessing antimicrobial and cytotoxic activities. *Bioorganic & Medicinal Chemistry* **2004,** *12* (15), 4285-4299; c) Thaisrivongs, S.; Janakiraman, M. N.; Chong, K.-T.; Tomich, P. K.; Dolak, L. A.; Turner, S. R.; Strohbach, J. W.; Lynn, J. C.; Horng, M.-M.; Hinshaw, R. R.; Watenpaugh, K. D., Structure-Based Design of Novel HIV Protease Inhibitors: Sulfonamide-Containing 4-Hydroxycoumarins and 4-Hydroxy-2-pyrones as Potent Non-Peptidic Inhibitors. *Journal of Medicinal Chemistry* **1996,** *39* (12), 2400-2410; d) Turner, S. R.; Strohbach, J. W.; Tommasi, R. A.; Aristoff, P. A.; Johnson, P. D.; Skulnick, H. I.; Dolak, L. A.; Seest, E. P.; Tomich, P. K.; Bohanon, M. J.; Horng, M.-M.; Lynn, J. C.; Chong, K.-T.; Hinshaw, R. R.; Watenpaugh, K. D.; Janakiraman, M. N.; Thaisrivongs, S., Tipranavir (PNU-140690): A Potent, Orally Bioavailable Nonpeptidic HIV Protease Inhibitor of the 5,6-Dihydro-4-hydroxy-2-pyrone Sulfonamide Class. *Journal of Medicinal Chemistry* **1998,** *41* (18), 3467-3476.

230. a) Zhang, C.; Sun, Q.; Rudolph, M.; Rominger, F.; Hashmi, A. S. K., Gold-Catalyzed Regiodivergent Annulations of Diazo-Alkynes Controlled by $Et_3N(HF)_3$. *ACS Catalysis* **2021,** *11* (24), 15203-15211; b) Zhang,

C.; Hong, K.; Dong, S.; Liu, M.; Rudolph, M.; Dietl, M. C.; Yin, J.; Hashmi, A. S. K.; Xu, X., Generation and Utility of Cyclic Dienyl Gold Carbene Intermediates. *ACS Catalysis* **2023,** *13* (7), 4646-4655.

231. Zeng, Q.; Dong, K.; Huang, J.; Qiu, L.; Xu, X., Copper-catalyzed carbene/alkyne metathesis terminated with the Buchner reaction: Synthesis of dihydrocyclohepta[b] indoles. *Organic and Biomolecular Chemistry* **2019,** *17* (9), 2326-2330.

232. Ambler, B. R.; Peddi, S.; Altman, R. A., Ligand-Controlled Regioselective Copper-Catalyzed Trifluoromethylation To Generate (Trifluoromethyl)allenes. *Organic Letters* **2015,** *17* (10), 2506-2509.

233. Bao, M.; Qian, Y.; Su, H.; Wu, B.; Qiu, L.; Hu, W.; Xu, X., Gold(I)-Catalyzed and H2O-Mediated Carbene Cascade Reaction of Propargyl Diazoacetates: Furan Synthesis and Mechanistic Insights. *Organic Letters* **2018,** *20* (17), 5332-5335.

234. Han, H.; Zhang, T.; Yang, S.-D.; Lan, Y.; Xia, J.-B., Palladium-Catalyzed Enantioselective C–H Aminocarbonylation: Synthesis of Chiral Isoquinolinones. *Organic Letters* **2019,** *21* (6), 1749-1754.

235. Li, H.; Petersen, J. L.; Wang, K. K., Cascade Cyclizations via N,4-Didehydro-2-(phenylamino)pyridine Biradicals/Zwitterions Generated from Enyne−Carbodiimides. *The Journal of Organic Chemistry* **2003,** *68* (14), 5512-5518.

236. Chen, Y.; Cho, C.-H.; Shi, F.; Larock, R. C., Synthesis of 3-Sulfenyl- and 3-Selenylindoles by the Pd/Cu-Catalyzed Coupling of N,N-Dialkyl-2-iodoanilines and Terminal Alkynes, Followed by n-Bu4NI-Induced Electrophilic Cyclization. *The Journal of Organic Chemistry* **2009,** *74* (17), 6802-6811.

237. Yao, B.; Wang, Q.; Zhu, J., Palladium(II)-Catalyzed Intramolecular Diamination of Alkynes under Aerobic Oxidative Conditions: Catalytic Turnover of an Iodide Ion. *Angewandte Chemie International Edition* **2012,** *51* (21), 5170-5174.

238. Song, H.; Liu, Y.; Wang, Q., Cascade Electrophilic Iodocyclization: Efficient Preparation of 4-Iodomethyl Substituted Tetrahydro-β-carbolines and Formal Synthesis of Oxopropaline G. *Organic Letters* **2013,** *15* (13), 3274-3277.

239. Ohmura, T.; Yagi, K.; Torigoe, T.; Suginome, M., Intramolecular Addition of a Dimethylamino C(sp3)–H Bond across C–C Triple Bonds Using IrCl(DTBM-SEGPHOS)(ethylene) Catalyst: Synthesis of Indoles from 2-Alkynyl-N-methylanilines. *Synthesis* **2021,** *53* (17), 3057-3064.

240. Rodriguez, J. M.; Nevola, L.; Ross, N. T.; Lee, G.-i.; Hamilton, A. D., Synthetic Inhibitors of Extended Helix–Protein Interactions Based on a Biphenyl 4,4′-Dicarboxamide Scaffold. *ChemBioChem* **2009,** *10* (5), 829-833.

241. Chen, Z.; Liang, P.; Xu, F.; Deng, Z.; Long, L.; Luo, G.; Ye, M., Metal-Free Aminothiation of Alkynes: Three-Component Tandem Annulation toward Indolizine Thiones from 2-Alkylpyridines, Ynals, and Elemental Sulfur. *The Journal of Organic Chemistry* **2019,** *84* (19), 12639-12647.

242. Guo, H.; Zhang, Q.; Pan, W.; Yang, H.; Pei, K.; Zhai, J.; Li, T.; Wang, Z.; Wang, Y.; Yin, Y., One-pot Synthesis of Substituted Pyrazoles from Propargyl Alcohols via Cyclocondensation of in situ-Generated α-Iodo Enones/Enals and Hydrazine Hydrate. *Asian Journal of Organic Chemistry* **2021,** *10* (8), 2231-2237.

243. Bao, M.; Wang, X.; Qiu, L.; Hu, W.; Hong Chan, P. W.; Xu, X., Gold-Catalyzed 1,2-Acyloxy Migration/Coupling Cascade of Propargyl Diazoacetates: Synthesis of Isomycin Derivatives. *Organic Letters* **2019,** *21* (6), 1813-1817.

244. Navale, B. S.; Laha, D.; Banerjee, S.; Vanka, K.; Bhat, R. G., Highly Site-Selective Direct C–H Bond Functionalization of Unactivated Arenes with Propargyl α-Aryl-α-diazoacetates via Scandium Catalysis. *The Journal of Organic Chemistry* **2022,** *87* (21), 13583-13597.

245. Qiu, H.; Arman, H.; Hu, W.; Doyle, M. P., Intramolecular cycloaddition/rearrangement cascade from gold(iii)-catalysed reactions of propargyl aryldiazoesters with cinnamyl imines. *Chemical Communications* **2018,** *54* (91), 12828-12831.

246. Huang, J.; Li, L.; Chen, H.; Xiao, T.; He, Y.; Zhou, L., Synthesis of 3-Aryl-2-pyrones by Palladium-Catalyzed Cross-Coupling of Aryl Iodides with Cyclic Vinyldiazo Ester. *The Journal of Organic Chemistry* **2017,** *82* (17), 9204-9209.

247. Yang, Q.-L.; Xing, Y.-K.; Wang, X.-Y.; Ma, H.-X.; Weng, X.-J.; Yang, X.; Guo, H.-M.; Mei, T.-S., Electrochemistry-Enabled Ir-Catalyzed Vinylic C–H Functionalization. *Journal of the American Chemical Society* **2019,** *141* (48), 18970-18976.

248. Padwa, A.; Kinder, F. R., Rhodium(II)-catalyzed cyclization of 2-alkynyl 2-diazo-3-oxobutanoates as a method for synthesizing substituted furans. *The Journal of Organic Chemistry* **1993,** *58* (1), 21-28.